ANNUAL REPORT 2000

INFN

Laboratori Nazionali del Gran Sasso

Annual Report 2000

Contents

The Gran Sasso National Laboratory

The Gran Sasso National Laboratory (LNGS) is one of four INFN national laboratories. It is the largest underground laboratory in the world for experiments in particle and nuclear astrophysics and it is used as a world-wide facility by scientists (presently 636 in number) from 19 countries.
Its location is between to the towns of L'Aquila and Teramo, about 120 km from Rome. The underground facilities are near the ten kilometres long freeway tunnel crossing the Gran Sasso mountain. They consist of three large experimental halls, each about 100 m long, 20 m wide and 20 m high and service tunnels for a total volume of about 180,000 cubic metres. The average 1400 m rock coverage gives a reduction factor of one million in the cosmic ray flux; moreover the neutron flux is particularly low due to the smallness of the Uranium and Thorium content of the dolomite rocks of the mountain.
The mission of the Laboratory is to host experiments that require a low background environment in the field of particle and nuclear astrophysics.

The Laboratory hosts experiments in other disciplines too, mainly geology and biology, that can profit of its characteristics and of its infrastructures.
Main research topics of the present program are: solar neutrinos physics, neutrino oscillations with solar neutrinos, neutrino oscillations with atmospheric neutrinos, neutrino oscillations with a beam from CERN (CNGS program), neutrinos from stellar collapses, double beta decays (search for Majorana electron-neutrino mass), dark matter search, nuclear reactions of astrophysical interest, high energy cosmic rays, search for exotics (monopoles, wimps, etc.).
A complementary facility at Campo Imperatore at 2,000 m height on the mountain hosted an extensive air shower experiment (EAS-TOP) aimed toward the study of the cosmic radiation especially around the "knee" of the energy spectrum both in its own and in coincidence with two large underground detectors, LVD and MACRO. The EAS-TOP experiment has completed its data collecting runs in May 2000 and the facility has been decomissioned during the summer.
Solar neutrino physics is one of the main research sector of the laboratory. The GALLEX experiment, completed in 1997, has already given fundamental results in particle physics and astrophysics, proving that thermonuclear fusion is the mechanism producing the energy in the Sun and showing a relevant deficit in the solar neutrino flux at low energy. It is extremely difficult now, after the GALLEX results, to avoid the conclusion that neutrinos oscillate, and as a consequence have non zero masses. If confirmed, this will be the first evidence of physics beyond the standard theory. GNO has improved the technique to continue the research for a long period, gradually improving the resolution. The data of the first series of runs has been published, confirming the GALLEX results and reducing

the systematic uncertainty to 5.3%.
The results of GALLEX and of the other solar neutrino experiments in the world (Homestake, Kamiokande and Superkamiokande, SAGE) indicate that the flux of electron-neutrino from the Be chain might be substantially different from the predictions of the theory and, as a consequence, particularly sensitive to new physics. Borexino is dedicated mainly to the measure of the Be line component of the solar neutrino spectrum. In the year 2000 the construction of the main detector and of its ancillary facilities has substantially advanced, the test facility CTF2 is now ready to run for a series of tests. The filling of the detector is foreseen for the end of the year 2001.
The present solar models are based on data and extrapolations; in particular the thermonuclear cross sections of the involved reactions are not measured in the relevant energy range but rather extrapolated from higher energies.
The direct measurements are made very difficult by the very low values of the cross sections. A pilot experiment, using a 50 kV accelerator, LUNA, was designed primarily to study the reaction ^{3}He(^{3}He,2p)^{4}He in the energy relevant for the reactions in the sun. Based on the success of the project a new 400 kV accelerator has been built and installed in Gran Sasso (LUNA2). The new facility, now operative, will provide the possibility to measure several key reactions of the main stellar cycles down to very low energies.
If electron-neutrinos are massive, part of (or all) their mass might be of the Majorana type; in this case some well defined nuclides would decay through the neutrino-less double beta channel. The Laboratory hosts experiments searching for these very rare decays, employing different and complementary techniques.
The Heidelberg-Moscow experiment with a sensitive mass of 11 kg of enriched ^{76}Ge is the most sensitive experiment in the world; the Mibeta experiment has produced an array of 20 thermal detectors, based on TeO_2 crystals (340 g natural tellurium each). Both experiments regularly ran continuously during 2000, improving their sensitivity. They give presently the best and the second best upper limit on the electron-neutrino mass (if Majorana) in the world. A new experiment, CUORICINO, using the MIBETA, but improved, technique was able to start a test run with 20 TeO_2 bolometers (750 g natural tellurium each). When completed it will consist of 100 bolometers, a sensitive mass an order of magnitude larger than MIBETA.
A further experiment DBA is searching for two-neutrino and neutrino-less double beta decay in ^{100}Mo employing a liquid Argon proportional chamber. The experiment has been completed in the year 2000.
From astronomical observations, we know that our Galaxy contains matter, globally ten times more than normal matter, that does not emit light. It is called dark matter, for this reason, but its nature is unknown. Very probably not yet discovered elementary particles constitute a large, or even the dominant, fraction of dark matter. These particle should be massive, with masses of the order of several tens to hundreds of the proton mass, and should interact only weakly with ordinary matter; on the contrary they would already been observed. They are collectively called WIMPs (Weakly Interacting Massive Particles). The search for WIMPs is very difficult and requires a very low background environment (one must work deep underground) and the development of advanced background reduction techniques. The search is going on in many experiments world wide. At Gran Sasso three experiments, using different techniques, are active.

DAMA employs NaI crystals to detect the WIMPs by means of the flash of light produced in the detector by an Iodine nucleus recoiling after having been hit by a WIMP, a very rare phenomenon. To distinguish these events from the background, DAMA searches for an annual modulation of the rate, a behaviour that has several aspects that are peculiar of the searched effect and not of the main backgrounds. With its about 100 kg sensitive mass DAMA is the most sensitive experiment world wide. Data corresponding to a two-year continuos run (4-years overall) have been published in January 2000. They show evidence of the annual modulation signal, with all the expected characteristics at four standard deviations significance. The analysis of a further your of data is progressing. To further proceed, DAMA is working on an improved detector, that, in particular, will have 250 kg sensitive mass.

CRESST searches for WIMPs with a cryogenic technique, looking for a, very tiny, temperature increase in the detector, due to the energy deposited by nuclei hit by the WIMPs. To this aim the detector is kept at a very low temperature, 15 mK. During 2000 the experiment continued in the still necessary R&D, with major progress in the understanding of the backgrounds. A full experiment, CRESST2, has been proposed, based on the detection of both heath and of light. The new detector facility is being built in hall A, while the old one will be decommissioned in year 2001.

HDMS uses Ge crystals to search for WIMPs, namely a crystal were the WIMP interaction takes place, fully surrounded by a second crystal that acts as an active screen from the background. A prototype detector was installed in March 1998 and took successfully data for 15 month, until July 1999. Based on this experience, the final set up started data taking in August 2000.

MACRO is a very large multi-purpose experiment, that continuously collected data for several years. It has steadily improved the limits on monopoles flux, well below the Parker bound and it is producing many interesting results on cosmic rays physics. Particularly relevant are the muons originated by muon-neutrino interactions from below, in other words from neutrinos produced in the atmosphere that have crossed a large fraction of the earth and interacted in the rock under the detector or in the detector itself. Evidence for muon-neutrino oscillations has been reported, confirming the results of the SuperKamiokande experiment in Japan. Further analysis, with increasing statistics and systematic accuracy, have been performed in 2000. The experiment has completed its extremely successful life in December 2000.

LVD has completed the construction of the apparatus with a sensitive mass of 1000 t and improved its efficiency with an up-time in 2000 of 99.3%. The experiment would collect a few hundred events from a supernova explosion in the centre of the Galaxy. Interesting data on the penetrating component of the cosmic rays are continuously collected.

ICARUS is a general purpose detector. It was proposed in 1985 based on the novel concept of the liquid Argon time-projection chamber. A first important step was the construction of a 3 t prototype that was used for the necessary R&D program, completed in 1993. The following years have been spent to develop the techniques suitable for industrial production of large scale detectors. A first 600 t module, proposed in 1995 and approved and funded in 1996, is presently being constructed in Pavia. The construction of the first semi-module was close to be completed by the end of year 2000. A ten cubic metre prototype, industrially built with the same techniques of the 600 t unit, has been

transferred at Gran Sasso in an experimental hall and performed a series of tests.
Experiments in geology.
GIGS is a laser interferometer for geophysical purposes operating since 1994. The main results obtained so far are: 1) the recording of co-seismic steps during local earthquakes in 1994, 2) the recording of swarms of slow earthquakes, more than 180 in total, after 1997. A new scale law between the seismic moment and the rise time of the slow quakes has been established. A very interesting statistical, not causal, correlation between slow and normal quake sequences has been observed. During 1999 the group further analysed the 1997 data; till October 1999 the spectrometer worked in an equal arm configuration. In 1999 a new interferometer was built and from October 1999 two independent interferometers are at work.
A dedicated instrumental set-up continued during 2000 its systematic monitoring of the deformation phenomena in the rocks.
The PULEX-2 is a biology experiment exploits the unique low radiation characteristics of the Laboratory. Mammalian cells were cultured in parallel at LNGS underground laboratory, were a cell culture facility has been set up on purpose, and at the ISS in Rome, in the presence of standard background, both for up to about 360 generations; checks for the onset of metabolic changes and for sensitivity to genotoxic damage caused by different agents were periodically performed.
A few first generation experiments at the Gran Sasso Laboratory are approaching their closure and we are defining now the scientific program for the next period on the basis of several experimental proposals in various stages of preparation.
Experiments in underground laboratories, mainly GALLEX and Superkamiokande have, for the first time, shown evidence for physics beyond the Standard Theory. In particular neutrinos seem to have non-zero masses and lepton numbers seem not to be conserved. Gran Sasso Laboratory has a great opportunity to give further revolutionary contributions to the knowledge of the basic forces of nature. In particular the problem of neutrino masses will be tackled. We must definitively confirm the oscillation phenomenon, we must establish the states amongst which oscillations take place, we must measure the masses and the mixing parameters.
Experiments on a neutrino beam produced at CERN and aimed to detectors at Gran Sasso. In December 1999 the CERN Council approved the CNGS (CERN Neutrinos to Gran Sasso), the program to build the beam, that will be ready in 2005; a major step forward. In parallel, two proposals for appearance experiments have been submitted. One of these, OPERA, is based on emulsion techniques. During 2000 the Collaboration submitted a full proposal that has been discussed and recommended for approval, with a number of milestones, both by the Gran Sasso and CERN Scientific Committees. The project appears now to be fully funded and has been approved by INFN in January 2001. The "NOE" part of the ICANOE proposal has withdrawn, while the ICARUS part is proceeding as already mentioned.
Next generation atmospheric neutrinos experiments. A specific proposal, MONOLITH, was submitted to the Laboratory; during 2000 a series of tests and simulation studies was performed and a first proposal submitted to the Laboratory and discussed.
Solar neutrino spectroscopy experiments. LENS is a proposal for a real time, flavour sensitive experiment sensitive down to the fusion neutrinos, aiming to a final clarification

of the solar neutrino problem and to the measurement of the oscillation parameters. A series of R&D studies have been performed progressing towards the understanding of the techniques.
Next generation searches for Majorana neutrino mass. Several proposals, in various stages of elaboration, have been submitted. One of them, CUORICINO, has been mentioned. Given the success of the tests phases of CUORICINO an experiment aiming to an increase of a further order magnitude in sensitive mass, CUORE, is under study by a large international collaboration. Another proposal, GENIUS, aims to 1000 kg detector of enriched Ge. These proposals aim to reach a sensitivity to electron-neutrino mass dawn to 10-50 meV.
All the services and the personnel of the lab have been engaged in the planning of the next phases of activity ranging from the decommissioning of some large experiments, to the preparation of the infrastructures needed for the next experiments and to the rigorous definition of the safety rules, procedures and infrastructures.

Gran Sasso, February 2001.

The Director of the Laboratory
Prof. Alessandro Bettini

BOREXINO. Solar Neutrino Physics

H. Back[n], M. Balata[b], A. de Bari[e], T. Beau[o], A. de Bellefon[o], G. Bellini[a], J. Benziger[c], S. Bonetti[a], A. Brigatti[a], C. Buck[j], B. Caccianiga[a], L. Cadonati[d], F.P. Calaprice[d], G. Cecchet,[e], M. Chen,[r], L. Cser,[k], O. Dadoune[o], M. Deutsch[f], A. Di Credico[b], G. Di Pietro[a], R. Dossi[a], R. Eiseistein[d], F. Elisei[g], A. Etenko[s], F. von Feilitzsch[h], R. Fernholz[d], R. Ford[b], B. Freudiger[j], C. Galbiati[d], A. Garagiola[a], F. Gatti[i], S. Gazzana[b], M.G. Giammarchi[a], D. Giugni[a], T. Goldbrunner[h], A. Golubchikov[a], A. Goretti[a], C. Hagner[n], T. Hagner[h], W. Hampel[j], J. Handt[j], B. Harding[d], F.X. Hartmann[a], R. von Hentig[h], G. Heusser[j], M. Hult[p], A. Ianni,[d], J. Jochum,[h], E. Kellner[h], S. Kidner[d], J. Kiko[j], T. Kirsten[j], D. Kiss[k], M. Koehler[p], G. Korga[a], Y. Kozlov[s], G. Korschinek[h], H. de Kerret[o], D. Kryn[o], V. Lagomarsino[i], P. LaMarche[d], M. Laubenstein[b], F. Loeser[d], P. Lombardi[a], I. Machulin[s], S. Magni[a], S. Malvezzi[a], I. Manno[k], J. Maneira[a], G. Manuzio[i], G. Marx[k], A. Martemianov[b], F. Masetti[g], U. Mazzucato[g], K. McCarty[d], E. Meroni[a], L. Miramonti[a], P. Musico[i], H. Neder[j], M. Neff[b], L. Niedermeier[h], S. Nisi[b], L. Oberauer[h], M. Obolensky[o], F. Ortica[g], M. Pallavicini[i], L. Papp[a], S. Parmeggiano[a], R. Parsells[d], A. Pocar[d], L. Perasso[i], A. Perotti[e], G. Pieri[a], R.S. Raghavan[l], G. Ranucci[a], W. Rau[j], A. Razeto[i], E. Resconi,[i], A. Sabelnikov[s], P. Saggese[a], C. Salvo,[i], R. Scardaoni[a], S. Schönert[j], K.H. Schubeck[h], T. Shutt[d], M. Skorokhvatov[s], H. Simgen[j], O. Smirnov[m], A. Sonnenschein[d], A. Sotnikov[m], S. Sukhotin[s], V. Tarasenkov[s], R. Tartaglia,[b], G. Testera[i], D. Vignaud[o], B. Vogelaar[n], S. Vitale[i], V. Vyrodov[s], R. Walls[d], W. Wojcik[q], Y. Zakharov[j], O. Zaimidoroga[m], G. Zuzel[q]

[a]Dip. di Fisica dell'Università and Infn Milano - Italy
[b]Laboratori Nazionali del Gras Sasso, Assergi (Aq) - Italy
[c]Dep.t of Chemical Engineering, Princeton University - NJ USA
[d]Dep.t of Physics, Princeton University - NJ USA
[e]Dip. di Fisica dell'Università and Infn Pavia - Italy
[f]Dep.t of Physics, Massachusetts Institute of Technology - MA USA
[g]Dip. di Chimica dell'Università and Infn Perugia - Italy
[h]Technische Universität München - Germany
[i]Dip. di Fisica dell'Università and Infn Genova - Italy
[j]Max Planck Inst. für Kernphysik, Heidelberg - Germany
[k]KFKI-RMKI Research Institute for Particle & Nuclear Physics, Budapest - Hungary
[l]Bell Laboratories, Lucent Technologies, Murray Hill - NJ USA
[m]J.I.N.R. Dubna - Russia
[n]Dep.t of Physics, Virginia Polytechnic Institute - VA USA
[o]Laboratoire de Physique Corpusculaire et Cosmologie, Paris - France
[p]I.R.M.M. - EURATOM, Geel - Belgium
[q]Institute of Physics, Jagellonian University, Kracov - Poland
[r]Dept. of Physics, Queen's University, Ontario - Canada
[s]RRC Kurchatov Institute, Moscow - Russia

Abstract

The Borexino project is converging and the detector is planned to start the data taking in spring 2002. We summarize here the status of the construction and assembling of the Detector and the main achievements obtained in these years of technical developments. Finally we up to date the role we expect for Borexino in the present physics frame.

1 Introduction

Borexino is the first real time experiment which plans to study the low energy (sub-MeV) solar neutrinos. The main experimental goal is the study of the 0.862 MeV ^{7}Be solar neutrino line through the neutrino-electron elastic scattering. The maximum energy of the recoiling electron is 664 KeV and the experimental design threshold is at 250 KeV.
The main problem of a real time experiment with a so low energy threshold is the natural radioactivity which is omnipresent in any environment and in any material. As a consequence an intense R&D program has been carried out in the last ten years to develop methods for selecting very low radioactivity materials and/or purify them. An effort in this field has to be accompanied by an equally hard research in the field of the detection system and measurement of ultralow radioactivity levels.
The development of purification methods has been focused on the liquid aromatic compounds, which are used as solvent for the liquid scintillators. Four main methods have been developed and tested: distillation, water extraction, stripping with ultrapure N_2, solid gel column (Si gel, Al gel). In this field records has been achieved by the Collaboration as for example: 10^{-16}-10^{-17} (g of contaminants/g of material) for ^{232}Th and ^{238}U family; few microBq of ^{222}Rn in gases and liquids.
In addition the organic liquid selected by the collaboration on the basis of the optical qualities of the product and of the old age of the underground layers used for the crude oil, shows a ^{14}C presence not exceeding 10^{-18} in its ratio to ^{12}C.
For the measurements of these ultralow radioactivity levels the Borexino Collaboration developed new detectors and new methods, in addition to use the more classic systems. Thus, in addition to Ge underground detectors installed in Rn free environment, Inductively Coupled Plasma Mass Spectometer, Atomic Absortion Spectroscopy etc..., a special detector at ton level, the Counting Test Facility (CTF), has been constructed on purpose and installed in the underground Laboratory at Gran Sasso. A high sensitivity Neutron Activation (NAA) has also been developed.
In all these fields many records have been achieved. The sensitivities reached are summarized below and correspond to the lowest radioactivity levels obtained by the Borexino Collaboration, in preparation of the experiment:
- 10^{-10} g/g for ^{238}U and ^{232}Th, $\sim 10^{-8}$ g/g for ^{226}Ra, $\sim 10^{-5}$ for ^{nat}K, few tenth of mBq/kg for ^{60}Co, have been achieved with a Ge detector in measuring construction materials as the stainless steel, metal and plastic gaskets, products for PMT sealing, etc...;
- 10 μBq/m^2 for Rn emanation, 0.1 mBq/m^3 for Rn activity concentration in water and 1 mBq/m^3 for Ra, below 1 mBq/m^3 in the Nitrogen used for scintillator purification are the records achieved in the Rn measurements;

- few 10^{-15} g/g for ^{238}U, ^{232}Th, ^{40}K have been reached with the ICMPS in measuring the shielding water;
- few ppt for ^{238}U and ^{232}Th have been obtained in the Nylon measurements;
- few 10^{-16} for ^{238}U, ^{232}Th and $\sim 10^{-18}$ for $^{14}C/^{12}C$ are measured in the Counting Test Facility for the scintillator (Pseudocumene(PC));
- 10^{-13} - 10^{-14} g/g for Au, Ba, Ce, Co, Cr, Cs, Ga, Hg, In, Mo, Rb; less than few 10^{-15} g/g for Cd, Sb, Ta, W; 10^{-16} - 10^{-17} g/g for La, Lu, Re, Sc, Th; less than $1x10^{-17}$ g/g for U, have been reached by means of the Neutron Activation followed by a β-γ coincidence analysis selection applied to the scintillators (PC and PXE).

These results, many of them achieved for the first time, were a mandatory step which had to be achieved to proceed with Borexino.
The radiopurity quoted above has been obtained using plants constructed and installed for the CTF; the same methods are adopted of course in the Borexino auxiliary plants.
For what concern the Rn the quoted results are the achievements of the Borexino plants, already installed and tested.
The CTF was in addition an important bench mark for testing and studying various solutions for the Borexino detector [1] [2] [3] [4]. It is now running again after an upgrading (see below).

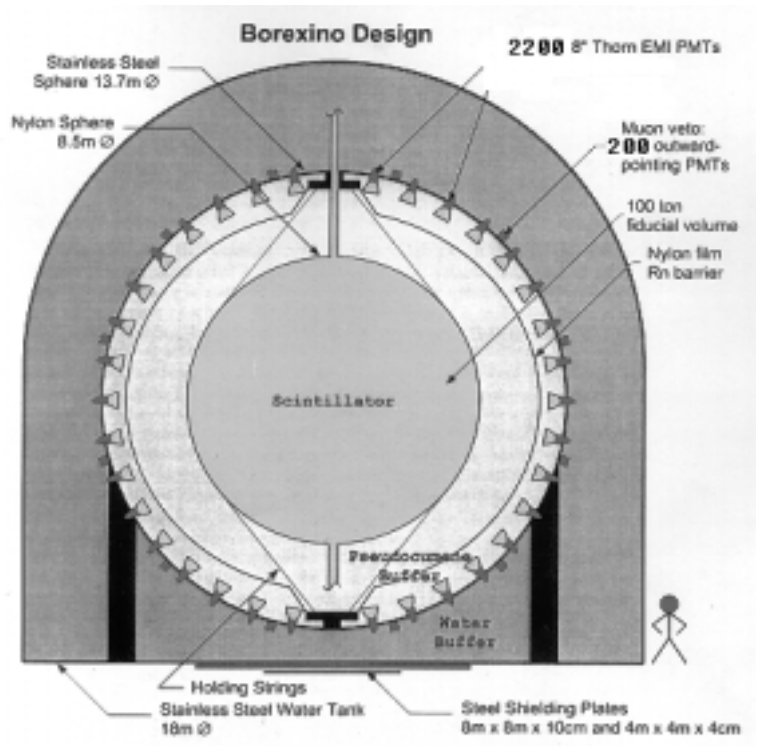

Figure 1: Schematic view of the Borexino detector.

2 The Borexino Detector

Borexino is an unsegmented liquid detector featuring 300 tonnes of well shielded ultrapure scintillator viewed by 2200 photomultipliers (fig. 1). The detector core is a transparent spherical vessel (Nylon Sphere, 100μm thick), 8.5 m of diameter, filled with 300 tonnes of liquid scintillator and surrounded by 1000 tonnes of high-purity buffer liquid. The scintillator mixture is PC and PPO (1.5 g/l) as a fluor, while the buffer liquid will be PC alone (with the addition of a light quencher, the DMP). The photomultipliers are supported by the Stainless Steel Sphere (SSS), which also separates the inner part of the detector from the external shielding, provided by 2400 tonnes of pure water (water buffer).
An additional containment vessel (Nylon film Radon barrier) is interposed between the scintillator Nylon Sphere and the photomultipliers, with the goal of reducing Radon diffusion towards the internal part of the detector.
The outer water shield is instrumented with 200 outward-pointing photomultipliers serving as a veto for penetrating muons, the only significant remaining cosmic ray background at the Gran Sasso depth (about 3500 meters of water equivalent). In addition the 2200 photomultipliers are equipped with light concentrators so that they see light only from the Nylon Sphere region, while the remaining 400 PMT's are sensitive to light originated in the whole volume of the Stainless Steel Sphere. This design greatly increases the capability of the system to identify muons crossing the PC buffer (and not the scintillator).
The BOREXINO design is based on the concept of a graded shield of progressively lower intrinsic radioactivity as one approaches the sensitive volume of the detector; this culminates in the use of 200 tonnes of the low background scintillator to shield the 100 tonnes innermost Fiducial Volume. In these conditions, the ultimate background will be dominated by the intrinsic contamination of the scintillator, while all backgrounds from the construction materials and external shieldings are negligible.
BOREXINO also features several external systems and apparatuses conceived to purify the experimental fluids (water, nitrogen and scintillator) and to keep clean conditions during the installation of the Detector (clean rooms).

3 Status of the project

After a long period of R&D, which includes also the CTF runs, the construction of the Borexino detector started in 1997. The activity of construction and installation have been devided in 6 areas; the detector itself (Area 1), the auxiliary plants (Area 2), the read-out from the phototubes to the on-line computer (Area 4), the quality control (Area 5); the software (Area 6); the facility in Hall C (Area 3).
The detector is now installed at 75%: Water Tank, Stainless-Steel Sphere, internal scaffoldings, air control in the sphere, clean-rooms, etc... are installed. Special care is now devoted to the internal precision cleaning of the sphere.
The cables are installed at 70% and we are starting the PMT installation.
The phototubes are manifactured by ETL with a special glass with reduced radioactivity and are in assembling phase, coupling them with the mechanics, sealing, mounting support, etc.... They are in final test phase, cleaning in clean rooms, coupling with the

optical concentrators in the Hall di Montaggio. Their preparation and mounting in the sphere is planned at a rate of 300/month.
The read-out electronics is completed and already installed in the Counting Room at the third floor of the Big Building, which houses the Rn measurement systems at the second floor, the main clean room in the first floor and the air control engines together with a cable handling system (Torrino) on the roof. The electronics is now in tuning phase and its operation mode is tested with the DAQ code, also in test phase.
A large clean room, installed for the construction of the Nylon Vessels (Inner Containment Vessel and Ra barrier), is now running with a plant that reduces substantially the Rn content, which could contaminate the surface of the Nylon via implantation on it of its daughters. The first Vessels (A) are now under construction and their test in the Borexino Sphere with a full water filling is expected to be done at the end of August 2001. The second and definitive Vessels (B) are also in construction phase and they will be finalized after the test of the Vessels A and eventually replaced to them. Special care is devoted to the leak check of the final Nylon Containment Vessel before and after the installation in Borexino, before the filling with PC.
A big effort is now devoted also to the auxiliary plants:
- the Storage Area has been installed and it is now in the precision cleaning phase;
- the Solid Column and the Scintillator handling for CTF and partly for Borexino is running (Module 0), even if the final column has not been installed yet;
- the distillation, water extraction, N_2 stripping system are close to be completed and part of them is in test phase;
- the interconnection among the various purification systems, Storage Area, Borexino and CTF Detectors is just now in installation phase in the hall C;
- the filling stations for Borexino are designed and their realization is waiting for the NSF funding;
- the PPO and DMP handling systems are in tender phase;
- the N_2 distribution plant, both for the normal Nitrogen ($\sim$ few mBq/m^3 of Rn containt) and for high purity line (less than 1μBq/m^3) are normally functioning.
The procurement of the Pseudocumene (PC), the solvent of the scintillator, is organized with the choosen supplier Enichem, which produces it at Sarroch (Sardinia). Four electropolished, high level components, precisely cleaned Isotanks have been prepared, which will shuttle between Sarroch and the underground hall C to keep the time of the esposition time of the Pseudocumene (PC) to the cosmic rays, from the production time to the underground storage below 24 hours. A special loading station is in costruction phase at the Sarroch plant to allow the PC loading on the Isotanks in N_2 atmosphere, without any contact with the air and via well treated stainless steel lines (pickled and passivated). The optical properties of the PC are tested in Sarroch before its loading and shipping to Gran Sasso.
The PPO is already procured and stored underground, while for DMP the Collaboration is still looking for the best producer, on the basis of its radioactivity content.
The problem of a Storage for the Buffer PC in case of need of empty out the Borexino detector is adressed and a candidate solution has been found.
The offline codes (full simulation of the signal and the background events, tracking, reconstruction) are working since few years. They are a development of the codes used in the

CTF data analysis and which have shown good performances and reliability. In addition Geant 4, developed by CERN, has been adapted to the Borexino needs.
The complex program of calibrations of the detector consists of: continous monitoring of the PMT by means of a system of optical fibers guiding a laser light; tests with various sources which will be inserted close to the external surface of the Stainless Steel Sphere and within the Inner containment Vessel, continuous tests of the optical properties of the Buffer PC via laser light. The equipment for the calibrations is ready at 90% and it will be installed together with the PMT's.
The upgraded version of CTF (CTF2) is now starting its running. The program includes: tests of batches of PC as received from Sarroch, after storage and circulation in the Storage Area, after purification in the purification systems, tested separately. The Collaboration plans to fill Borexino with a scintillator tested to be already at radioactivity levels acceptable for the Borexino purposes.
The safety matter has been adressed very seriously by the Borexino Collaboration since the beginning. First the detector has been calculated to withstand to a possible hearthquake with an acceleration horizontal and vertical of 0.3 g, well over the 0.15 g demanded by the italian law. All the plants are analyzed for their "intrinsic safety" and are equipped with various fire estinguishing plants and alarms. A full HAZOP analysis is now under way: it is carried out for the plants and for the procedures adopted in the various operations.
The final filling of Borexino is scheduled by the end of the year 2001 and the starting run in the late spring 2002.

4 The expected impact of Borexino on the Neutrino Physics

We refer to the present status of the study of the Solar Neutrinos in the frame of the oscillation hypothesis. The regions still allowed for the oscillation hypothesis in a plot δm^2 vs $\sin^2\theta$ are four, as it is well known: three for the MSW hypothesis (Small Mixing Angle- SMA, Large Mixing Angle-LMA, LOW) and one for the Vacuum oscillation hypothesis (Figs. 2a, 2b). These regions are the results of the fit on the Solar Standard Model (BP2000) and on the data of the Homestake, Gallium, and Kamiokande experiments. The recent results obtained by Superkamiokande indicate a larger probability for the LMA and LOW region with respect to the SMA and Vacuum regions.
The contribution of the Borexino data to the solution of the Neutrino oscillation problem will be based upon:
- Determination of the total Neutrino flux in the electron scattered energy range: 0.250-0.800 MeV. The rates expected in Borexino with 100 tonnes of fiducial volume are the following: 55 events/d if the Standard Solar Model (BP 2000) previsions should be realistic, 31 ev/d if the LMA solution should be valid, 12 ev/d for the SMA solution, 29 ev/d in the LOW solution, and finally 26 ev/d for the Vacuum hypothesis with a large range of fluctuation. The 80% of the events are due to the ^{7}Be source neutrinos. These rates have to be compared with an expected background of $\sim$ 15 ev/d. It is clear that a small rate could be in favour to the SMA solution, while a high rate should disfavour it.
- Seasonal Modulation. The Seasonal variations can be due to two origins: the eccentricity

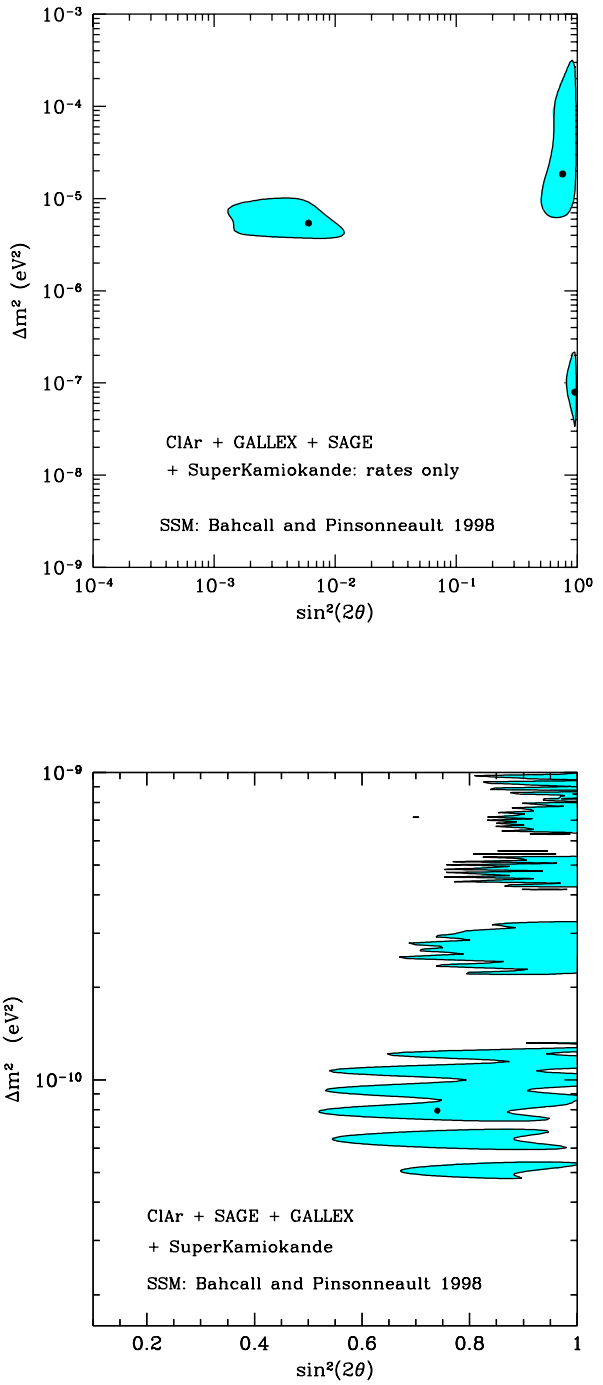

Figure 2: a) Allowed regions in the Δm^2-$\sin^2\theta$ parameter space in the MSW oscillation hypothesis; b) Allowed regions in the Δm^2-$\sin^2\theta$ parameter space in the vacuum oscillation hypothesis.

of the Earth orbit with respect to the Sun (geometrical modulation) and to the possible Vacuum solution. The geometrical modulation produces an effect of about 7% and can be well detected by Borexino, reproducing its typical $1/R^2$ behaviour with a C.L. at 5σ in three years of data taking. For the modulations due the Vacuum oscillations Borexino is almost unique due the monochromaticity of the ^{7}Be line. The Vacuum oscillation can produce a seasonal modulation varying of a factor up to $\sim$4 along the year. A Fourier analysis applied to the simulated Borexino data following the Vacuum oscillation hypothesis shows that the Borexino sensitivity is very high on a wide δm^2 range.
- Zenith Angle Distribution and day/night difference. The matter regeneration in passing through the Earth during the night is particularly enhanced in the LOW region and Borexino is well positioned to explore it because the by far largest variation occurs just at the energy of the ^{7}Be neutrinos. The difference in rate in the sub-MeV region can reach a factor two between day and night.
- Low Energy Spectral Shape of ^{8}B neutrinos. A general characteristic of the energy dependence of flavour conversion by the MSW effect is a gradual decrease in flavour survival, and stronger observable effects, towards low energies, producing an increasing distorsion of the spectral shape of the ^{8}B signal towards the low end of the spectrum. The ^{8}B energy spectrum has been already well measured by Kamiokande, SK and now in SNO with a lower energy threshold at about 6 MeV. The lower energy sensitivity of Borexino allows to explore the spectrum over few MeV with a rate ranging between 0.2-0.45 ev/d depending on the difference scenarios.
In conclusion the recent developments in the neutrino physics scenario have in some way strengthened the role of Borexino in this field.

5 List of articles

1. G. Alimonti et al.

   Light propagation in a large volume liquid scintillator.

   Nuclear Instr. and Methods A 440 (2000) 360.

2. G.Ranucci

   An analytical approach to the description of absorption and reemission effects in large scintillation counters.

   Nuclear Instr. and Methods A 440 (2000) 388.

3. B.Caccianiga, M.Giammarchi

   Neutrinoless Double Beta Decay with Xe-136 in BOREXINO and the BOREXINO Counting Test Facility (CTF)

   Astroparticle Physics Vol. 14(2000)15.

4. G. Bellini et al.

   High sensitivity quest for Majorana neutrino mass with the BOREXINO counting test facility.

Physics Letters B (493) 216.

5. Borexino collaboration

   Science and Technology of BOREXINO: a real-time Detector for Low Energy Solar Neutrinos. hep-ex/0012030. Accepted for publication on Astroparticle Physics.

6 List of Presentations

1. **Bormio2000** B. Caccianiga, *The Solar Neutrino Puzzle: a strong indication for new physics*, XXXVIII International Winter meeting on nuclear physics, Bormio, 24-28 January 2000.

2. **CSNP** G. Bellini, *The Borexino project and fundamental achievements in the very low radioactivity techniques*, Columbia (North Carolina), March 2000.

3. **CIPANP2000** J.C. Maneira, *Status of the Borexino solar neutrino experiment*, VII Conference on the Intersections of Particle and Nuclear Physics, Quebec City, Canada, May 2000.

4. **Sudbury2000** G. Ranucci, *Borexino*, Neutrino 2000 International Conference, Sudbury (Canada), June 2000.

5. **LowNu 2000 (Sudbury)** G. Testera, *Detecting low energy solar neutrinos in Borexino*, Neutrino 2000 International Conference, Sudbury (Canada), June 2000.

6. **Verbier2000** L. Oberauer, *Status of the BOREXINO Solar Neutrino Experiment*, Conference on Cosmology and Particle Physics, Verbier (Switzerland), July 2000.

7. **LowNu 2000 (Tokio)** M.G. Giammarchi, *Borexino*, International Workshop on Low Energy Solar Neutrinos, Tokyo, December 2000.

8. **LowNu 2000 (Tokio)** R. von Hentig, *A very high sensitivity Neutron Activation Analysis*, International Workshop on Low Energy Solar Neutrinos, Tokyo, December 2000.

9. **LowNu 2000 (Tokio)** M. Laubenstein, *Radon background reduction and material selection*, International Workshop on Low Energy Solar Neutrinos, Tokyo, December 2000.

10. **MG2000** B. Caccianiga, *Status and perspectives of the Borexino experiment*, IX Marcel Grossmann Meeting, Roma, 2-8 luglio 2000.

11. **NOW2000** E. Meroni, *Borexino and its Physycs*, Europhysics Neutrino Oscillation Workshop, Otranto, 9-16 settembre 2000.

12. **NOW2000** M. Laubenstein, *Experimental Techniques for the Low Energy Neutrino experiments*, Europhysics Neutrino Oscillation Workshop, Otranto, 9-16 settembre 2000.

13. **Faro2000** J. Maneira, *Radon background reduction and Material selection*, III International meeting on new Worlds in Astroparticle Physics, Faro, Portogallo.

References

[1] G. Alimonti et al. (BOREXINO Collaboration). A Large Scale Low Background Liquid Scintillation Detector: the Counting Test Facility at Gran Sasso, Nuclear Instruments and Methods, A406 (1998) 411.

[2] G. Alimonti et al. (BOREXINO Collaboration). Ultralow background measurements in a large volume underground detector, Astroparticle Physics, 8 (1998) 141.

[3] G. Alimonti et al. (BOREXINO Collaboration). Measurements of the ^{14}C abundance in a low-background liquid scintillator, Phys. Lett. B, 422 (1998) 349.

[4] G. Alimonti et al. (BOREXINO Collaboration). Light propagation in a large volume liquid scintillator. Nuclear Instr. and Methods A 440 (2000) 360.

CRESST. Dark Matter Search

M. Bruckmayer[a], C. Bucci[d], S. Cooper[c], C. Cozzini[a],
P. Di Stefano[a], F. von Feilitzsch[b], T. Frank[a], D. Hauff[a],
T. Jagemann[b], J. Jochum[b], R. Keeling[c], H. Kraus[c],
J. Marchese[c], F. Pröbst[a], Y. Ramachers[c], J. Schnagl[b],
W. Seidel[a*], I. Sergeyev[a], M. Stark[b], L. Stodolsky[a], H. Wulandari[b]

[a] Max–Planck–Institute für Physik,
Föhringer Ring 6, D-80805 Munich, Germany
[b] Technische Universität München,
Physik Department E15, D-85748 Garching, Germany
[c] Oxford University, NAPL, Keble Road, Oxford OX1 3RH, UK
[d] Laboratori Nazionali del Gran Sasso, INFN, 67010 Assergi (AQ), Italy
[*] Spokesman of the collaboration

Abstract

We present the current status as well as future developments for the CRESST (Cryogenic Rare Event Search using Superconducting Thermometers) experiment, aiming at the direct detection of WIMP dark matter. After describing the extensive test-phase to acquire a complete control over all experimental parameters of the setup, we show first results of the measurements using Sapphire calorimeters as absorbers, being particularly sensitive to light WIMPs.

1 Introduction

The goal of the CRESST project is the direct detection of elementary particle dark matter and the elucidation of its nature. The search for Dark Matter and the understanding of its nature remains one of the central and most fascinating problems of our time in physics, astronomy and cosmology. There is strong evidence for it on all scales, ranging from dwarf galaxies, through spiral galaxies like our own, to large scale structures [1].

Particle physics provides some well motivated candidates of which the lightest supersymmetric particle (LSP) is the favourite one. The extension of the standard model of elementary particles physics to the minimal supersymmetric standard model (MSSM) offers the LSP as a Dark Matter candidate in the form of a neutralino, a superposition of neutral particles arising in the theory, fulfilling all necessary requirements like e.g. stability and weak interaction cross sections with 'ordinary' baryonic matter. Indeed,

supersymmetric models contain many parameters and many assumptions and by relaxing few simplifying assumptions one can find candidates for particle dark matter in a wide mass range [2]. Generically, particle dark matter candidates, being neutral, stable and weakly interacting, are called WIMPs (weakly interacting massive particles) and are to be distinguished from proposals involving very light quanta such as axions. WIMPs are expected to interact with baryonic matter by elastic scattering on nuclei and all direct detection experiments have focused on this possibility.

Conventional methods for direct detection rely on the ionization or scintillation caused by the recoiling nucleus. This leads to certain limitations connected with the relatively high energy involved in producing an ionization and with the sharply decreasing efficiency of ionization by slow nuclei. Cryogenic detectors use much lower energy excitations, such as phonons, and while conventional methods are probably close to their limits, cryogenic technology can still make great improvements. Since the principal physical effect of a WIMP nuclear recoil is the generation of phonons, cryogenic calorimeters are well suited for WIMP detection.

The detectors developed by the CRESST collaboration consist of a dielectric target–crystal with a small superconducting film evaporated onto the surface. When this film is held at a temperature in the middle of its superconducting to normal conducting phase transition, it functions as a highly sensitive thermometer. The detectors presently employed in Gran Sasso use tungsten films and sapphire absorbers, running near 15 mK [3, 4]. The technique can also be applied to a variety of other materials [5]. The small change in temperature of the superconducting film resulting from an energy deposit in the target leads to a relatively large change in the films resistance. This change in resistance is then measured with a SQUID.

2 Present status of CRESST

The central part of the CRESST installation at the LNGS is the cryostat. The cryostat design separates the detectors in the "cold box" from the dilution refrigerator by a long "cold finger", with internal cold lead shielding, blocking the line–of–sight to the detectors. The cold box is constructed entirely of low background materials. It is surrounded by shielding consisting of 14 cm copper (inner shield) and 20 cm of lead (outer shield). The volume for the detector chamber of about 30 litres is large enough to use much larger total detector masses in the future. The cold box and shielding are installed in a measured class 100 clean room area. For servicing, the top of the cryostat can be accessed from the first floor outside the clean room.

The installation was completed at Gran Sasso in 1997 and a series of detector tests were made in the prototype cold box during 1998. The purpose of the prototype cold box was to test the mechanical and cryogenic performance of the design and to provide a reasonably shielded environment for completing the development of the 262 g sapphire detectors. As can be expected in such a complicated setup, the first runs showed that several details needed improvement: Vibrations caused by the needle valve of the dilution refrigerator's 1K pot needed to be eliminated by installing a fixed impedance; the design of the detector holders has been improved to reduce the vibration effect of the boiling of

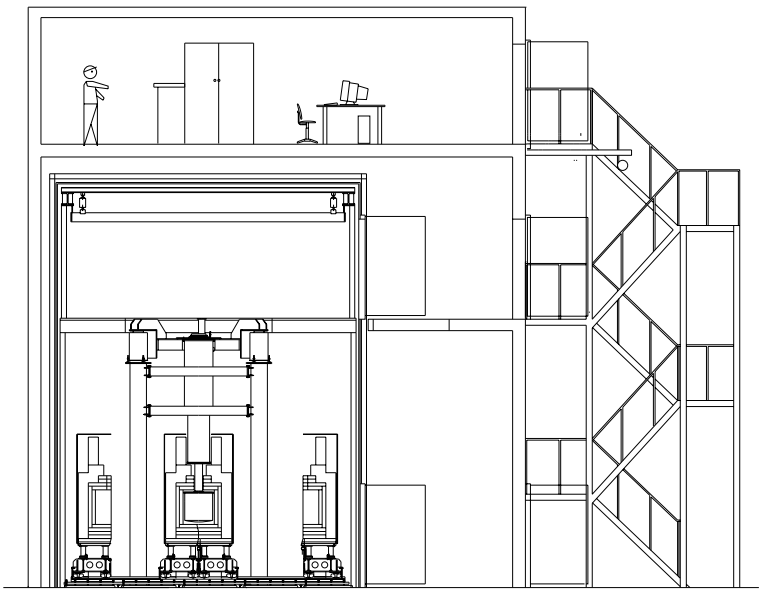

Figure 1: Cross section of CRESST building in Hall B.

the liquid nitrogen; the slow heat release due to enclosed H_2 in the copper of some new components was eliminated by selecting low background copper without that problem.

To allow monitoring the longterm stability in a search for dark matter we have developed tungsten thermometers with attached electrical heaters. A periodical injection of heater pulses corresponding to different energies in the detector crystal allows to monitor the stability and efficiency of the detector performance. Important performance examples for monitoring are the energy calibration or possible deviations from linearity in the detector response function.

At the end of this testing periods we had four 262 g sapphire detectors which achieved energy resolutions in the range of 200 eV (FWHM) at 1.5 keV [6]. The best detector reached a resolution of 133 eV at 1.5 keV [7]. As mentioned above, these tests were made in the prototype cold box, which was made of the right type of copper but which had been exposed at the surface for many years to cosmic rays and had been activated correspondingly. In addition, no attempt has been undertaken to remove surface contaminations. In order to replace it at the first opportunity, detector tests were stopped in spring 1998 and efforts concentrated on preparing the new cold box.

The new low background cold box was made using copper which had been stored underground since production and between machining steps. After machining the surface of each piece was cleaned by electro-polishing and subsequent rinsing with high purity water. The pieces were then stored in a gas–tight container made of polyethylene and flushed with nitrogen.

During 1999, a series of measurements with four 262 g sapphire detectors under low background conditions was performed in the new cold box. The typical measured rate was of the order of a few 10^3 counts per day kg and keV below 20 keV, comparable to, and to lower energies even stronger than the count rate in a calibration run. In fact, it

was far higher than any expectation. A series of tests to find the reason for this behaviour has subsequently been launched.

First, we excluded the possibility of radioactivity as the reason for this enormous rate. The detectors are mounted facing each other with no material in between. The practically complete absence of any events in true time coincidence between any pair of detectors excludes γ-emitters in the crystals and surrounding materials and surface contaminations of the crystals with β-emitters. Also β-emitters within the crystals were excluded by the shape of the spectrum. Moreover, the rate had a non-Poissonian character in time, which cannot be caused by radioactivity. Although the pulse shapes of the events were indistinguishable to real events from calibration runs the rate showed irregular 'bursts' (high count rates in short time intervals) which also contained only consistent pulse shapes, so radioactivity as a reason was excluded despite the pulse shapes of events.

In subsequent runs the detectors have been insulated from external vibrations by mounting them on a spring–suspended platform (horizontal and vertical resonance frequencies of 1.5 Hz and 3 Hz). These steps lead to an immunity of the base line signal against vibrations in tests where external vibrations were applied to the cryostat. Nevertheless, the rate did not decrease. This lead us to exclude external vibrations as the origin of the background.

In a further run we were investigating the possibility that electromagnetic interferences with a too short duration to be seen directly by the SQUID might heat the tungsten thermometer and cause thermal signals with a shape very similar to particle pulses like observed. A modification of the readout circuit of one detector in order to suppress the possible heating effect made the system completely immune to any external electromagnetic interference created for test purposes inside the Faraday cage. However, the background rate did not decrease and we excluded interferences as the source of our background.

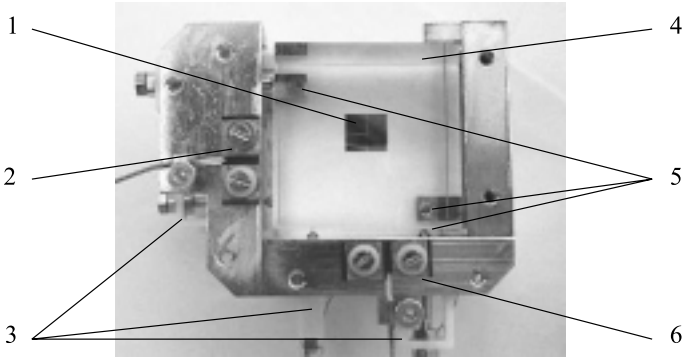

Figure 2: Picture of a sapphire 262g crystal. (1) Tungsten thermometer, (2) holder pads with screw contacts for connecting to the heater circuit, (3) plastic springs, (4) sapphire crystal, (5) sapphire balls, (6) holder pads with screw contacts for connecting to the SQUID read–out circuit.

The crucial tool to finally find this elusive source in 2000 turned out to be a special detector crystal, built as a diagnostic tool for our problem, the so called 'double detector'. A 262 g sapphire crystal has been prepared to carry two tungsten thermometers which were

read–out like two independent detectors. We found that the signals from both thermometers are strictly coincident in time with a constant ratio of the pulse heights and again with the same shape as particle pulses. Again the signals were not coincident with other detectors in the setup. This clearly demonstrated that all signals originate from energy depositions into the crystal, creating high frequency phonons in the sapphire crystals independent of read out circuits and external influences except from the immediate vicinity of the crystals. Therefore, the last remaining structural part, the supporting structure of the detectors, has been examined. In fact, it turned out that the sapphire balls, fixing the crystal in its holder, under pressure by Teflon springs caused micro-cracks in the sapphire crystals which release mechanical energy as they spread. In the course of a run this yields a gradually developing network of cracks which result in almost macroscopic scratches, visible under a microscope. So, the sapphire spheres have been replaced by small Delrin cylinders, thereby increasing slightly the contact area (now ring–like instead of point–like) and softening the contact of supporting structures and crystal.

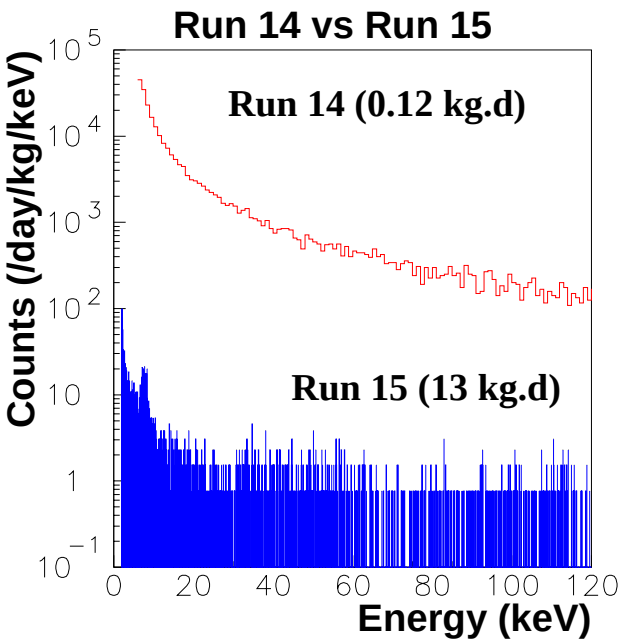

Figure 3: Typical energy spectrum before and after modifying the crystal support structure. Note the considerable decrease in count rate.

The final proof that we eliminated, finally, the reason for our high background can be inspected in Fig. 3 where we show the comparison of a high rate spectrum and a more recent background measurement. We are confident that we do not suffer anymore from non-radioactively induced background at least down to the level of background we currently achieve. Our current background level can be summarised as a drop in count rate by about three orders of magnitude down to about (1 - 2) counts/(day kg keV) above 10 keV for all detectors in the setup. The best crystal in terms of sensitivity to low energies achieved so far a conservative 100% efficiency threshold of 2 keV. Note that these 2 keV correspond to 2 keV nuclear recoil energy to be contrasted to ionization detectors

which would roughly (in case of Germanium) need a threshold of 300 eV in order to have the same low energy sensitivity for recoils [8]. These results can be compared to results from other groups [9] and clearly shows the improvement for this particular detection technique achieved so far.

We finished the year 2000 by conducting a special purpose calibration run. We mounted a very weak (about 0.15 Bq) Co57 source inside the cryostat. The source then shines directly on the bare sides of two sapphire crystals. This measurement will serve to calibrate especially the low energy part of the spectrum and provide us therefore with a cross check of the test pulser method for online calibration. Data analysis of that particular calibration is still in progress. The systematic uncertainties of the setup that can be precisely found out that way will help to finalise the analysis of the background data taken so far.

3 Outlook and conclusion

Cryogenic sapphire detectors for WIMP detection are particularly sensitive to low-mass WIMPs [2, 5]. Another important distinction to other direct detection experiments is their enhanced sensitivity for the spin–dependent interaction of WIMPs. In the light of recent work [10] which points out the importance of this long neglected interaction channel for WIMPs it turns out that the forthcoming results from the CRESST experiment using sapphire absorbers might become interesting not only as the crucial preparation phase for the CRESST phase II experiment [5, 11]. One interesting option to note for the future of CRESST using sapphire absorbers (or similarly sensitive, low threshold detectors) could be 'WIMP astronomy' in the sense of measuring the hypothetical solar WIMP population [12] and retrieving WIMP halo structure informations this way.

To summarise, the CRESST experiment succeeded to remove the enormous background rate resulting from a network of micro-cracks in the crystals developing due to an improper fixing of the crystals in their holders. Since this year our background is finally dominated by radioactive background sources. Their identity still has to be found out in order to remove them. A special purpose low energy calibration run from the end of this year will determine possible systematic uncertainties of the setup. First results on WIMP cross section limits will be prepared soon.

4 List of Publications

1. W. Seidel, in Proc. Third Int. Workshop on *Dark Matter in Astrophysics and Particle Physics (DARK2000)*, Heidelberg, Germany (IOP, Publ. Bristol, 2000), ed. H.V. Klapdor-Kleingrothaus

2. P. Di Stefano *et al.*, in Proc. Third Int. Workshop on *Identification of Dark Matter, IDM2000* York, UK (World Sci. Publ., 2000), ed. N.J.C. Spooner

3. Y. Ramachers *et al.*, in Proc. Third Int. Workshop on *Identification of Dark Matter, IDM2000* York, UK (World Sci. Publ., 2000), ed. N.J.C. Spooner

4. P. Di Stefano for the CRESST Coll., The CRESST Experiment: Recent Results and Prospects, To be published Proc. of *Conference on Cosmology and Particle Physics (CAPP 2000)*, Verbier, Switzerland, 17-28 Jul 2000; hep–ex/0011064

5. M. Bravin et al., Simultanous Measurement of Phonons and Scintillation Light for Active Background Rejection in the CRESST Experiment, Nucl. Instrum. Meth. A444:323-326,2000

6. M. Sisti et al., The CRESST Dark Matter Experiment: Status and Perspectives, Nucl. Instrum. Meth. A444:312-314,2000

7. J. Jochum et al., The CRESST Dark Matter Search, Nucl. Phys. Proc. Suppl. 87:70-73,2000

8. CRESST Collaboration (J. Jochum et al.), The CRESST Dark Matter Search, Phys. Atom. Nucl. 63:1242-1248,2000; hep-ex/0005003

9. O. Meier et al., Active Thermal Feedback for Massive Cryogenic Detectors, Nucl. Instrum. Meth. A444:350-352,2000

References

[1] N.J.C. Spooner, ed., Proc. Third Int. Workshop on *Identification of Dark Matter, IDM2000* (World Sci. Publ., 2000) York, UK

[2] A. Gabutti *et al.*, *Astropart. Phys.* **6**, 1 (1996); V.A. Bednyakov *et al.*, *Phys. Rev.* D **55**, 503 (1997)

[3] P. Colling *et al.*, *Nucl. Instrum. Methods* A **354**, 408 (1995)

[4] F. Pröbst *et al.*, *J. Low Temp. Phys.* **100**, 69 (1995)

[5] M. Bravin *et al.*, *Astropart. Phys.* **12**, 107 (1999)

[6] M. Sisti *et al.*, *Nucl. Instrum. Methods* A **444**, 312 (2000)

[7] O. Meier *et al.*, *Nucl. Instrum. Methods* A **444**, 350 (2000)

[8] L. Baudis *et al.*, *Nucl. Instrum. Methods* A **418**, 348 (1998)

[9] A. De Bellefon *et al.*, *Astropart. Phys.* **6**, 35 (1996); S. Cebrián *et al.*, *Preprint astro–ph/0004292*

[10] D. Tovey, R.J. Gaitskell, P. Gondolo, Y. Ramachers and L. Roszkowski, *Phys. Lett.* B **488**, 17 (2000); V.A. Bednyakov and H.V. Klapdor–Kleingrothaus, *Preprint hep–ph/0011233* and references therein

[11] P. Di Stefano *et al.*, in [1]

[12] T. Damour and L.M. Krauss, *Phys. Rev.* D **59**, 063509 (1999)

DAMA. Dark Matter Search

M. Amato[c], P. Belli[a], R. Bernabei[a], A. Bussolotti[a,*], F. Cappella[a,b], R. Cerulli[a], C.J. Dai[d], H. L. He[d], G. Ignesti[c], H.H. Kuang[d], F. Montecchia[a], F. Nozzoli[a,b], A. Incicchitti[c], A. Mattei[c,*], D. Prosperi[c]

in the neutron measurements: M.Angelone[e], P.Batistoni[e], M.Pillon[e]

in the search for other rare processes: V.V. Kobychev[f], O.A. Ponkratenko[f], V.I. Tretyak[f], Yu.G. Zdesenko[f]

[a]Dip. di Fisica, Universita' di Roma "Tor Vergata" and INFN, sez. Roma2, Italy; [b]Laboratorio Nazionale del Gran Sasso, INFN, Assergi(Aq), Italy; [c]Dip. di Fisica, Universita' di Roma "La Sapienza" and INFN, sez. Roma, Italy; [d]IHEP, Chinese Academy, P.O. Box 918/3, Beijing 100039, China; [e]ENEA - C. R. Frascati, P.O. Box 65, I-00044 Frascati, Italy; [f]Institute for Nuclear Research, 252650 Kiev, Ukraine;

* technical staff

Abstract

DAMA is searching for rare processes by developing and using several kinds of radiopure scintillators. The main running set-ups are: i) the $\simeq$ 100 kg NaI(Tl) set-up; ii) the $\simeq$ 6.5 kg ($\simeq$ 2 l volume) liquid Xenon (LXe) scintillator; iii) the R&D installation for tests on prototype detectors and for small scale experiments. Moreover, in the framework of devoted R&D for higher radiopure detectors and PMTs, sample measurements are regularly performed with the low background Ge detector of the DAMA experiment, which is operating deep underground since many years, and at Ispra. Works to increase the exposed mass up to $\simeq$ 250 kg of NaI(Tl) are in progress.

1 Introduction

DAMA is devoted to the search for rare processes by developing and using low radioactivity scintillators. Its main aim is the search for relic particles (WIMPs: Weakly Interacting Massive Particles) embedded in the galactic halo, whose existence has been pointed out both by experimental observations and by theoretical considerations. Thus, our solar system, which is moving with respect to the galactic system, is continuously hit by a WIMP

"wind". The quantitative study of this "wind" allows both to obtain information on the Universe evolution and to investigate Physics beyond the Standard Model.

The WIMPs are mainly searched for by elastic scattering on target nuclei, which constitute a scintillation detector. For this purpose, radiopure NaI(Tl), liquid Xenon and CaF_2(Eu) detectors are developed and used (main recent references are given in [1, 2, 3, 4, 5, 6, 7, 8, 9, 10, 11] and in the 2000 publication list quoted in the following). In particular, the $\simeq$ 100 kg NaI(Tl) set-up has been realized to investigate the so-called WIMP "annual modulation signature". This experiment, in fact, can effectively exploit such a signature because of its well known technology, of its high intrinsic radiopurity, of its mass and of its suitable control of the operational parameters. The relevance of performing experiments with a proper clear signature is evident.

An R&D activity to develop higher radiopure detectors is continuously carried out toward the creation of ultimate radiopure detectors as well as studies on their possible new applications. As a result of one of these efforts, the exposed target-detector mass of the NaI(Tl) set-up is in progress to be enlarged up to $\simeq$ 250 kg.

Finally, profitting of the radiopurity achieved in the whole set-ups, several searches for other rare processes are also performed, such as for: i) $\beta\beta$ processes; ii) charge-non-conserving (CNC) processes; iii) Pauli exclusion principle (PEP) violating processes; iv) nucleon instability; etc. Also in these cases competitive results have been obtained so far [12].

In the following the main DAMA activity during year 2000 are summarized.

2 The $\simeq$ 100 kg highly radiopure NaI(Tl) set-up

The main goal of the $\simeq$ 100 kg NaI(Tl) set-up is the search for WIMPs by the annual modulation signature.

The main parts of the experimental set-up are the NaI(Tl) detectors, the Cu box containing the detectors, the shield and the glove-box for calibrations. The detectors are enclosed in a sealed low radioactivity OFHC Cu box fluxed with HP N_2; the Cu box is maintained at small overpressure with respect to the environment, such as also the glove-box. All the used materials have been selected for low radioactivity by sample measurements with the Ge detector deep underground in the Gran Sasso National Laboratory (LNGS), with AAS and MS in the Rome University "La Sapienza" and in Ispra [8]. The whole set-up and its main performances have been discussed in ref. [8]. The experiment is taking data from single photoelectron threshold up to several MeV (being the optimization done for the lowest energy region: 2-20 keV); some additional triggers are also operative to achieve results on other topics.

During August/September 2000 a significant upgrading of this set-up has been carried out. In particular, the electronic chain from the pre-amplifiers (which are located outside the plexiglass box tightly enveloping the passive shield) up to the computer has been upgraded; a new electronic chain and DAQ have been installed. The data acquisition is now performed by a Digital UNIX-alpha; NIM, CAMAC and VXI standards are used.

The new VXI electronics has allowed to significantly simplify the electronic chain, in particular its analogic part. In fact, the multiplexer electronics, which handled in the previous configuration many lines on single CAMAC Lecroy transient digitizer, has been eliminated. At present each line has its own VXI transient digitizer, which in addition offers higher sampling frequency and larger bandwidth.

The data taking of a 6^{th} annual cycle has been started at fall of year 2000, while the data of the 5^{th} annual cycle are already at hand.

2.1 The search for the WIMP annual modulation signature and related studies

Since the Earth rotates around the Sun, which is moving with respect to the galactic system, it would be crossed by a larger WIMP flux in June (when its rotational velocity is summed to the one of the solar system with respect to the Galaxy) and by a smaller one in December (when the two velocities are subtracted). The fractional difference between the maximum and the minimum of the rate is of order of $\simeq 7\%$. Therefore, to select the modulated component of the signal, large mass apparata with suitable performances and control of operating conditions are necessary, such as the $\simeq 100$ kg highly radiopure NaI(Tl) DAMA set-up.

The annual modulation signature is very distinctive as we have discussed e.g. in ref. [5, 7, 8, 13] and in other publications during year 2000 (listed at end of this document). In fact, a WIMP-induced seasonal effect must simultaneously satisfy all the following requirements: the rate must contain a component modulated according to a cosine function (1) with one year period (2) and a phase that peaks around $\simeq 2^{nd}$ June (3); this modulation must only be found in a well-defined low energy range, where WIMP induced recoils can be present (4); it must apply to those events in which just one detector of many actually "fires" (single hit events), since the WIMP multi-scattering probability is negligible (5); the modulation amplitude in the region of maximal sensitivity must be $\lesssim 7\%$ (6). Only systematic effects able to fulfil these 6 requirements could fake this signature; therefore for some other effect to mimic such a signal is highly unlikely.

During year 2000 the data collected in two further annual cycles, DAMA/NaI-3 and DAMA/NaI-4 (total statistics 38475 kg·day) have been investigated. In particular, a cumulative analysis of all the available data, DAMA/NaI-1 to 4 (total statistics 57986 kg·day; see Table 1) has been carried out, properly accounting also for the physical constraint which arises from the measured upper limit on the recoil rate [3].

A model independent analysis

A model independent analysis of the data of the four annual cycles offers an immediate evidence of the presence of an annual modulation of the rate of the single hit events in the lowest energy interval (2–6 keV) as shown in Fig. 1. There each data point has been obtained from the raw rate measured in the corresponding time interval after subtracting the constant part.

The χ^2 test on the data of Fig. 1 disfavors the hypothesis of unmodulated behaviour (probability: $4 \cdot 10^{-4}$), while fitting these residuals with the function $A \cdot \cos\omega(t - t_0)$, one

Table 1: Released data sets.

Period	Statistics (kgday)
DAMA/NaI-1	4549
DAMA/NaI-2	14962
DAMA/NaI-3	22455
DAMA/NaI-4	16020
Total statistics	57986
+ DAMA/NaI-0	upper limit
	on recoils by PSD

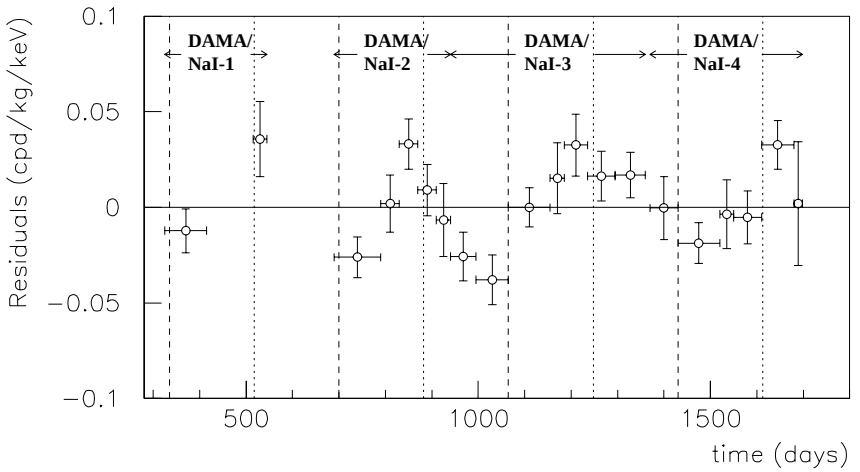

Figure 1: Model independent residual rate for single hit events, in the 2-6 keV cumulative energy interval, as a function of the time elapsed since January 1-st of the first year of data taking. The expected behaviour of a WIMP signal is a cosine function with minimum roughly at the dashed vertical lines and with maximum roughly at the dotted ones.

gets: i) for the period T = $\frac{2\pi}{\omega}$ = (1.00 ± 0.01) year when t_0 is fixed at the 152.5^{th} day of the year (corresponding to $\simeq$ 2 June); ii) for the phase t_0 = (144 ± 13) days, when T is fixed at 1 year. In the two cases A is: (0.022 ± 0.005) cpd/kg/keV and (0.023 ± 0.005) cpd/kg/keV, respectively. Similar results, but with slightly larger errors, are found in case all the parameters are kept free.

We have extensively discussed the results of the investigations of the known sources of possible systematics when releasing the data of each annual cycle; moreover, during year 2000 a dedicated paper has been released (*Eur. Phys. J. C18 (2000), 283-292*),

where in particular the data of the DAMA/NaI-3 and DAMA/NaI-4 running periods have been considered in quantitative evaluations. A relative systematic error, affecting the energy spectrum, of order of $\lesssim 10^{-3}$ is given by these investigations; moreover, no known systematic effect or side reaction able to mimic a WIMP induced effect has been found.

In conclusion, the result of the model independent approach, together with the result of the search for possible systematics able to mimic the WIMP annual modulation signature, allows to candidate a WIMP contribution to the measured rate independently on the nature and coupling with ordinary matter of the involved WIMP particle.

Model dependent analyses

To investigate the nature and coupling with ordinary matter of a possible candidate, an effective energy and time correlation analysis is necessary as well as a complete model framework[1].

At present the lightest supersymmetric particle named neutralino is considered the best candidate for WIMP; in supersymmetric theories both the squark and the Higgs bosons exchanges give contribution to the coherent (SI) part of the neutralino cross section, while the squark and the Z^0 exchanges give contribution to the spin dependent (SD) one.

Let us recall that the differential energy distribution of the recoil nuclei in WIMP-nucleus elastic scattering can be calculated [3, 14] by means of the differential cross section of the WIMP-nucleus elastic processes

$$\frac{d\sigma}{dE_R}(v, E_R) = \left(\frac{d\sigma}{dE_R}\right)_{SI} + \left(\frac{d\sigma}{dE_R}\right)_{SD} =$$

$$= \frac{2G_F^2 m_N}{\pi v^2}\{[Zg_p + (A-Z)g_n]^2 F_{SI}^2(E_R) + 8\frac{J+1}{J}(a_p < S_p > + a_n < S_n >)^2 F_{SD}^2(E_R)\} \quad (1)$$

where: G_F is the Fermi coupling constant; m_N is the nucleus mass; v is the WIMP velocity in the laboratory frame; E_R is the recoil energy; Z is the nuclear charge and A is the atomic number; $g_{p,n}$ ($a_{p,n}$) are the effective WIMP-nucleon couplings for SI (SD) interactions; $< S_{p,n} >$ are the mean values of the nucleon spin in the nucleus and J is the nuclear spin; $F_{SI}^2(E_R)$ and $F_{SD}^2(E_R)$ are the SI and SD form factors, respectively. Therefore, the differential cross section and, consequently, the expected energy distribution depends on the WIMP mass and on four unknown parameters of the theory: $g_{p,n}$ and $a_{p,n}$. A generalized SI WIMP-nucleon cross section can be written as $\sigma_{SI} = \frac{4}{\pi} G_F^2 m_{Wp}^2 g^2$; there the coupling g is a function of g_p and g_n and – in a first approximation – is independent on the used target nucleus since $\frac{Z}{A}$ can be considered nearly constant for the nuclei typically used in WIMP direct searches. As regards the SD interaction we have introduced the useful notations

$$\bar{a} = \sqrt{a_p^2 + a_n^2},$$

[1] A model framework is identified not only by the general astrophysical, nuclear and particle physics assumptions, but also by the set of values used for all the parameters needed in the model itself and in related quantities (for example WIMP local velocity (v_0), form factor parameters, etc.).

$$tg\theta = \frac{a_n}{a_p},$$
$$\sigma_{SD} = \frac{32}{\pi}\frac{3}{4}G_F^2 m_{Wp}^2 \bar{a}^2, \quad (2)$$

where σ_{SD} is a suitable SD WIMP-nucleon cross section.

In the following the results obtained by analysing the data in given model frameworks are summarized.

I. WIMPs with dominant SI interaction in a given model framework

Since often the spin-independent (SI) interaction with ordinary matter is assumed to be dominant for the neutralino, first model dependent analyses of the data have been performed by considering a candidate in this scenario, that is neglecting the term $\left(\frac{d\sigma}{dE_R}\right)_{SD}$ in eq. (1) [2].

A full energy and time correlation analysis – properly accounting for the physical constraint arising from the measured upper limit on recoils [3] – has been carried out in the framework of a given model for spin-independent coupled candidates with mass above 30 GeV. A standard maximum likelihood method[3] has been used. Following the usual procedure we build the y log-likelihood function, which depends on the experimental data and on the theoretical expectations; then, y is minimized and parameters' regions allowed at given confidence level are derived. Obviously, different model frameworks vary the expectations and, therefore, the cross section and mass values corresponding to the y minimum, that is also the allowed region at given C.L.. In particular, the inclusion of the uncertainties associated to every parameter in the model itself and/or in related quantities enlarges the allowed region as discussed e.g. in *Phys. Rev. D61, 023512 (2000)* for the particular case of the astrophysical velocities.

Also in the case considered here the minimization procedure has been repeated by varying v_0 from 170 km/s to 270 km/s to account for its present uncertainty. For example, in this model framework (*Phys. Lett. B480, 23 (2000)*) $m_W = (72^{+18}_{-15})$ GeV and $\xi\sigma_{SI} = (5.7 \pm 1.1) \cdot 10^{-6}$ pb correspond to the position of y minimum when $v_0 = 170$ km/s, while $m_W = (43^{+12}_{-9})$ GeV and $\xi\sigma_{SI} = (5.4 \pm 1.0) \cdot 10^{-6}$ pb when $v_0 = 220$ km/s. Fig. 2 shows the regions allowed at 3σ C.L. in that model framework, when: i) $v_0 = 220$ km/s (dotted contour); ii) the uncertainty on v_0 is taken into account (continuous contour); iii) possible bulk halo rotation is considered (dashed contour). No other uncertainties on the used parameters have been considered here (some of them have been included in the approach summarized in the next subsection).

In conclusion, the data collected over four annual cycles favour at 4 σ C.L. the presence of an annual modulation in the low energy experimental rate, while this effect investigated in terms of a WIMP candidate with dominant SI interaction and mass above 30 GeV, supports allowed WIMP masses up to 130 GeV (1 σ C.L.) and even up to 180 GeV (1 σ

[2]Note that the results of the data analyses summarized here and in the following are not restricted anyhow only to the neutralino case.

[3]Substantially the same results are obtained with other analysis approaches such as e.g. the Feldman and Cousins one.

C.L.) if possible dark halo rotation is included.

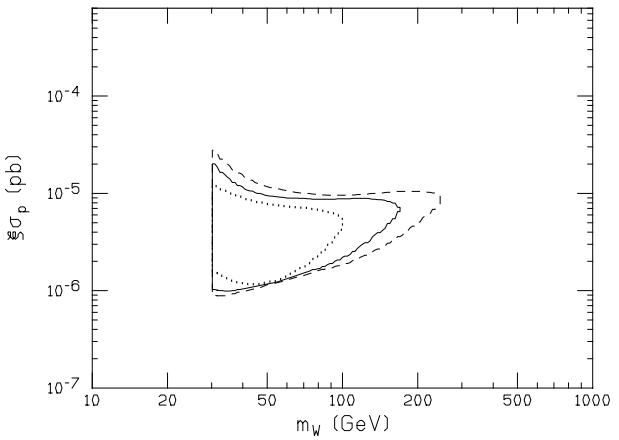

Figure 2: Regions allowed at 3σ C.L. on the plane $\xi\sigma_p$ ($\xi = \frac{\rho_{WIMP}}{0.3GeVcm^{-3}}$ and σ_p = WIMP scalar cross section on proton) versus m_W (WIMP mass) for a WIMP with dominant SI interaction in the considered model framework: i) for $v_0 = 220$ km/s (dotted contour); ii) when accounting for v_0 uncertainty (170 km/s $\leq v_0 \leq$ 270 km/s; continuous contour); iii) when considering also a possible bulk halo rotation as in ref. [12] (dashed contour). See text. The inclusion of present uncertainties on some nuclear and particle physics parameters would enlarge these regions (varying consequently the position of the minimum for the y log-likelihood function); full estimates are in progress. Note that here $\sigma_p = \sigma_{SI}$.

Theoretical implications of these results in terms of a neutralino with dominant SI interaction and mass above 30 GeV have been discussed in ref. [14, 15], while the case for an heavy neutrino of the fourth family has been considered in ref. [16].

II. WIMPs with mixed coupling in given model framework

The analysis of the data has been extended (see *ROM2F/2000-35*) considering the more general case of eq. (1), that is a WIMP having not only a spin-independent, but also a spin-dependent coupling different from zero, as it is also possible for the neutralino (see above).

Following the usual procedure we build the y log-likelihood function, which depends on the experimental data and on the theoretical expectations in the given model framework. Then, y has been minimized – properly accounting also for the physical constraint set by the measured upper limit on recoils [3] – and parameters' regions allowed at given confidence level have been obtained. In particular, the calculation has been performed by minimizing the y function with respect to the $\xi\sigma_{SI}$, $\xi\sigma_{SD}$ and m_W parameters for each given θ value. In the present framework the uncertainties on v_0 have been included; moreover, the uncertainties on the nuclear radius and the nuclear surface thickness parameter in the SI form factor, on the b parameter in the used SD form factor (see later) and on the measured quenching factors [3] have also been considered (see *ROM2F/2000-35*).

Fig. 3 shows slices (colored areas) for some m_W of the region allowed at 3 σ C.L. in the ($\xi\sigma_{SI}$, $\xi\sigma_{SD}$, m_W) space at fixed θ value. Four particular couplings are reported there:

i) $\theta = 0$ (a_n =0 and $a_p \neq 0$ or $|a_p| >> |a_n|$); ii) $\theta = \pi/4$ ($a_p = a_n$); iii) $\theta = \pi/2$ ($a_n \neq 0$ and $a_p = 0$ or $|a_n| >> |a_p|$); iv) $\theta = 2.435$ rad ($\frac{a_n}{a_p}$ = -0.85, pure Z^0 coupling). The case $a_p = -a_n$ is nearly similar to the case iv).

The dashed lines given for the case $m_W = 50$ GeV represent the limit curves calculated for $v_0 = 220$ km/s from the data of the DAMA liquid Xenon experiment [6]; regions above these dashed lines could be considered excluded at 90% C.L. Since the ^{129}Xe nucleus – on the contrary of the ^{23}Na and of the ^{127}I – has the neutron as odd nucleon, only the case $\theta \simeq \pi/2$ would be affected; similar results are obtained for all the other WIMP masses. However, we have to recall that, as widely known, the comparison of results achieved by different experiments – even more when different target nuclei and/or different techniques have been used – is affected by intrinsic uncertainties. We take this occasion to recall also that, moreover, no direct quantitative comparison can be performed between results obtained in direct and in indirect searches since it strongly depends on assumptions and on the considered model framework[4]. In particular, it does not exist a biunivocal correspondence between the observables in the two kinds of experiments: WIMP-nucleus elastic scattering cross section (direct detection case) and flux of muons from neutrinos (indirect detection case). In fact, elastic cross sections on proton spanning several orders of magnitude can give the same muon flux for different e.g. neutralino configurations and viceversa.

As already pointed out, when the SD contribution goes to zero (y axis), an interval not compatible with zero is obtained for $\xi\sigma_{SI}$ (see Fig. 3). Similarly, when the SI contribution goes to zero (x axis), finite values for the SD cross section are obtained. Large regions are allowed for mixed configurations also for $\xi\sigma_{SI} \lesssim 10^{-5}$ pb and $\xi\sigma_{SD} \lesssim 1$ pb; only in the particular case of $\theta = \frac{\pi}{2}$ (that is $a_p = 0$ and $a_n \neq 0$) $\xi\sigma_{SD}$ can increase up to $\simeq 10$ pb, since the ^{23}Na and ^{127}I nuclei have the proton as odd nucleon.

In our study we have also shown that: i) finite values can be allowed for $\xi\sigma_{SD}$ even when $\xi\sigma_{SI} \simeq 3{\cdot}10^{-6}$ pb as in the region allowed in the pure SI scenario considered above; ii) regions not compatible with zero in the $\xi\sigma_{SD}$ versus m_W plane are allowed even when $\xi\sigma_{SI}$ values much lower than those allowed in the dominant SI scenario previously summarized are considered; iii) minima of the y function with both $\xi\sigma_{SI}$ and $\xi\sigma_{SD}$ different from zero are present for some m_W and θ pairs; the related confidence level ranges between $\simeq 3\ \sigma$ and $\simeq 4\ \sigma$.

In conclusion, this analysis has shown that the DAMA data of the four annual cycles, analysed in terms of WIMP annual modulation signature, can also be compatible with a mixed scenario where both $\xi\sigma_{SI}$ and $\xi\sigma_{SD}$ are different from zero. The pure SD and pure SI cases in the model framework considered here are also implicitly given in Fig 3 for the quoted m_W and θ values.

Further investigations are in progress on model dependent analyses. As an example we recall that for the SD form factor an universal formulation is not possible since the internal degrees of the WIMP particle model (e.g. supersymmetry in case of neutralino) cannot be completely separated from the nuclear ones. In the calculations presented here we have adopted the SD form factors of ref. [17] estimated by considering the Nijmengen

[4]In addition, large uncertainties are present in the evaluation of the results of the indirect searches themselves.

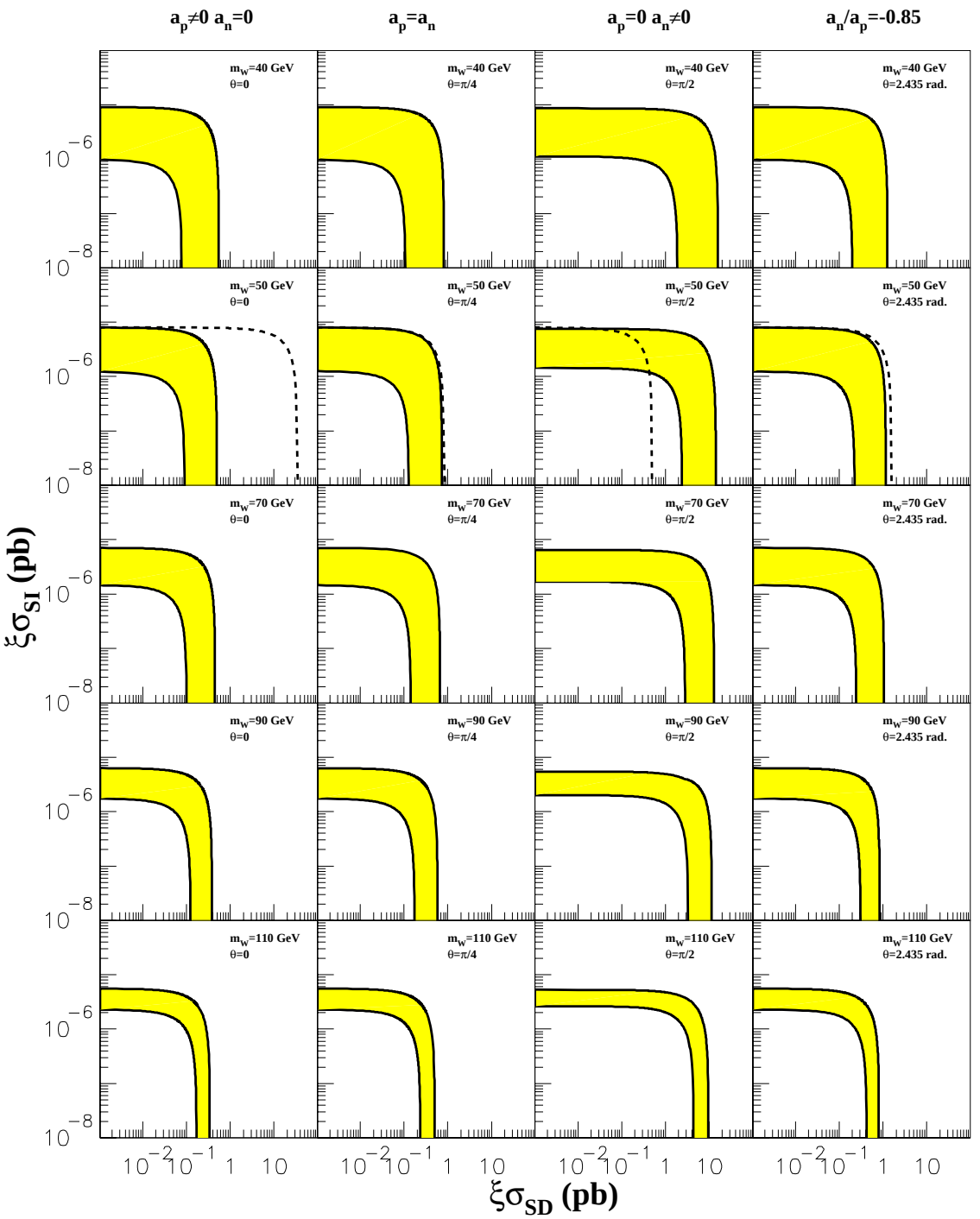

Figure 3: Slices (colored areas) for some m_W of the region allowed at 3 σ C.L. in the ($\xi\sigma_{SI}$, $\xi\sigma_{SD}$, m_W) space at fixed θ value. Four particular couplings are reported here: i) $\theta = 0$; ii) $\theta = \pi/4$ iii) $\theta = \pi/2$; iv) $\theta = 2.435$ rad (*ROM2F/2000-35*).

nucleon-nucleon potential. Other formulations are possible for SD form factors and can be considered.

2.1.1 Conclusion

Further investigations are in progress on model dependent analyses.
Moreover, the data of the 5^{th} annual cycle are already at hand, while – after a full upgrading of the electronics and of the data acquisition system – the set-up is now running to collect the data of a 6^{th} annual cycle.
Finally, the exposed mass will be increased in near future up to $\simeq$ 250 kg to achieve higher experimental sensitivity.

3 The LXe set-up

3.1 Introduction

The LXe detector has been filled up to August 2000 with Kr-free Xenon enriched at 99.5% in ^{129}Xe; the sensitive mass is $\simeq$ 6.5 kg. The vessel for the LXe is made by OFHC low radioactivity copper ($\leq$100 μBq/kg for U/Th and $\leq$310 μBq/kg for potassium). The scintillation light is collected by three EMI PMTs with MgF_2 windows, working in coincidence. The measured quantum efficiency for normal incidence has a flat behaviour around the LXe scintillation wavelength ($\simeq$ 175 nm); depending on the PMT, its value can range between 18% and 32%. The PMTs collect the scintillation light through three windows (3" in diameter) made of special cultured crystal quartz (total transmission of the LXe ultraviolet scintillation light $\approx$ 80%, including reflection losses). A low radioactivity copper shield inside the thermo-insulation vacuum cell surrounds the PMT-s; then, 2 cm of steel (insulation vessel thickness), $5-10$ cm of low radioactivity copper, 15 cm of low radioactivity lead, $\approx$1 mm of cadmium and $\approx$10 cm of polyethylene are used as outer hard shielding. The environmental Radon nearby the detector is removed by continuously flushing high purity Nitrogen gas in a plexiglass box (before in a Supronyl envelop) which tightly encloses the whole set-up and the hard shield. Each PMT is connected with a low noise preamplifier, whose outputs are fed to the data acquisition system. For every event the amplitudes of each single PMT pulse and the amplitude and shape of the sum pulse are recorded. The energy dependence of the detector resolution is: $\sigma/E = 0.056 + 1.19/\sqrt{E[keV]}$.

During year 2000 a significant upgrading of the whole set-up has been performed. In particular: i) a general maintenance of the vacuum and cooling system has been carried out to improve their performances; ii) a sealed plexiglass box has replaced the supronyl envelope where HP Nitrogen is continuously flushed; iii) the vacuum/filling/purification/recovery line has been simplified to improve its effectiveness; iv) a new automatised inert cold trap @194K has been installed; v) a new monitoring system of the cryogenic and working parameters has been realized for on-line remote control and set of general alarms; vi) the modifications of the filling line needed to install the container of Kr-free Xenon enriched in ^{136}Xe at $\simeq$ 68% have been realized. Now both the Xenon enriched in ^{129}Xe and in ^{136}Xe can alternatively access the vacuum/filling/purification/recovery line.

Preliminary measurements with the Xenon enriched in ^{136}Xe have been started.

Finally, during 2000 new results were achieved regarding the WIMP-^{129}Xe inelastic scattering, the electron stability and the nucleon and di-nucleon stability; they are summarized in the following.

3.2 New limits on WIMP-^{129}Xe inelastic scattering

A new measurement has been carried out on the direct detection of WIMP by investigating the WIMP-nucleus inelastic scattering, producing low-lying excited nuclear states [18, 19]. In this case, a possible WIMP signal can be identified by the presence of characteristic peaks in the measured energy spectrum as a result of the emission of successive deexcitation gammas from the excited nuclear states. [19]. Very few experimental

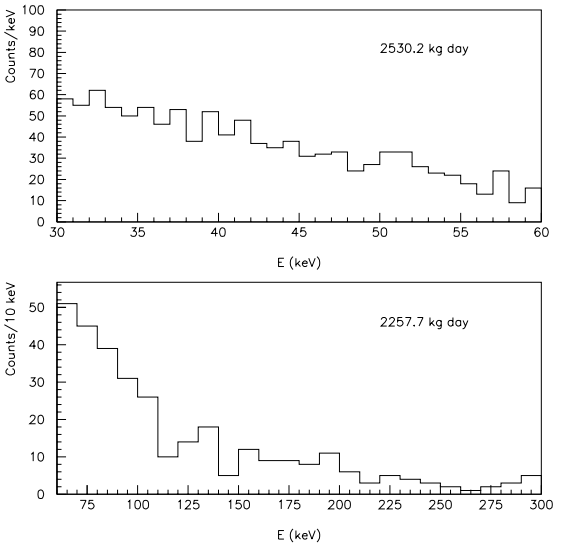

Figure 4: Measured energy distributions from 30 to 60 keV (2530.2 kg · day statistics) and from 60 to 300 keV (2257.7 kg · day statistics). The used energy bins and the statistics are marked on each plot.

attempts to exploit this technique have been performed so far [2, 20], since this experimental approach, offering in principle a good signature for WIMPs, requires e.g. very large exposures

In the present investigation, according to ref. [2], we have searched for the inelastic excitation of ^{129}Xe by Dark Matter particles considering only the deexcitation channel from the level at 39.58 keV, since the contribution from the isomeric state at 236.14 keV is strongly suppressed by the space factor as discussed in ref. [2]. The deexcitation from the 39.58 keV level can give rise to: a γ (7.5%), a K internal conversion (75%) and an L internal conversion (17.5%) [21]; therefore, for each WIMP event the measured energy is given by the sum of the energies of all the deexcitation products and of the recoil energy.

In Fig. 4 the measured energy distributions from 30 keV to 60 keV (2530.2 kg · day statistics) and from 60 to 300 keV (2257.7 kg · day statistics) are shown.

The inelastic processes involving the 39.58 keV level have been studied by estimating for each m_W the expected energy distribution. No evidence for this process at the reached level of sensitivity has been found; therefore exclusion plots have been derived, both for the case of model independent approach (σ_I^{as} vs m_W) [2] and for some model dependent ones (ρ_W vs m_W); σ_I^{as} is the asintotic point-like cross section for $v \to \infty$ and ρ_W is the WIMP local halo density. In particular, Fig. 5 gives model dependent exclusion plots for various candidates.

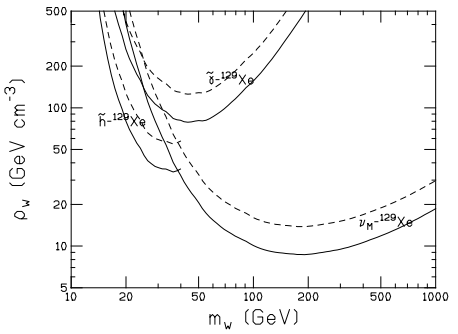

Figure 5: Limits (90% C.L.) on relic halo density for photino, higgsino and and ν_M as a function of the WIMP mass from the WIMP-^{129}Xe inelastic scattering (solid lines). The dashed lines are the previous limits of Ref. [4]. We recall that the halo density is expected to range between 0.2 and 0.7 GeV $\cdot$ cm^{-3}. For the used astrophysical and nuclear physics assumptions see the paper.

In conclusion, the present measurements have achieved an improvement of about a factor two on the excluded relic abundance for the considered heavy Majorana fermions from the study of inelastic processes with respect to those of our previous Ref. [2] within the same model framework.

3.3 New limits on the possible decay channel: $e^- \to \nu + \gamma$

The invariance of the QED Lagrangian, $\mathcal{L}_{QED}$, under U(1) local gauge transformations requires massless photons and exact charge conservation (CC) in accordance with the well known Weinberg theorem [22]. However, the possibility that CC can be broken in future unified theories has been discussed extensively in the literature [23]. To describe charge non-conservation phenomena, photons cannot be exactly massless and the Lagrangian must contain terms that destroy gauge invariance; moreover, the symmetry breaking can be either explicit or, alternatively, spontaneous.

Owing to its fundamental importance, experimental efforts to test CC both in the lepton and in the hadron sectors have continued since 1959 [24] until the present.

The new result we achieved during year 2000 is based on the approach where the electron decays (inside the sensitive volume of a given detector or from its surroundings) into a neutrino and a photon ($e^- \to \nu_e \gamma$) by searching for γ rays of $\approx$ 255.5 keV. For this purpose the energy distribution collected by the LXe set-up during about 347 days (a partial statistics was already analysed searching for WIMP-^{129}Xe inelastic scattering;

see above) has been analysed. The experimental spectrum of the LXe scintillator in the energy region $40-500$ keV with total statistics of 2257.7 kg·day is shown in Fig. 6, where the absence of the peak searched for around ≈ 255 keV is evident. Therefore these data have been used to set a bound on the probability of the electron decay in the considered channel. The obtained life time limit on the charge non-conserving (CNC) electron decay through the considered channel is: $\tau > 2.0(3.4) \cdot 10^{26}$ y at 90% (68%) C.L., one order of magnitude higher than the previous available best limit for that channel.

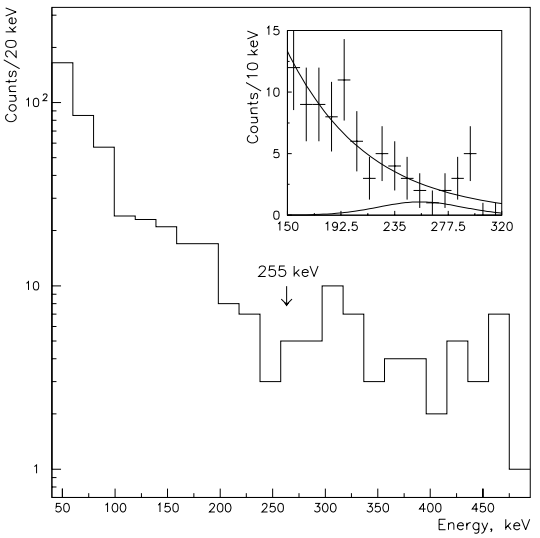

Figure 6: LXe energy spectrum in the region $40-500$ keV (total statistics: 2257.7 kg·day). In the inset the part of the spectrum in the energy region of interest here is shown in linear scale together with the fitting curve (dashed line) and excluded peak ($\tau = 2.0 \cdot 10^{26}$ y).

Currently there is no self-consistent and non-contradictory theory describing possible violations of the charge conservation and offering a method to suitably parametrize information given by the experimental life time limits. However, according to Bahcall [25], a suitable CNC parameter can be introduced by assuming that the weak interaction Lagrangian includes a small CNC part having the usual form, but with a neutrino replacing the electron in the lepton current: $\mathcal{L}_{CNC} = \frac{1}{2} e \varepsilon_{e\nu\gamma} \overline{\psi}_e \gamma_\mu (1-\gamma_5) \psi_\nu A^\mu +$ H.C., where the $\varepsilon_{e\nu\gamma}$ parameter gives a measure of the charge non-conservation. Our experimental limit leads to the bound $\varepsilon^2_{e\nu\gamma}(m_e/m_\gamma)^2 < 2.8(1.6) \cdot 10^{-51}$ at 90% (68%) C.L. This limit combined with the best laboratory limit on the photon mass: $m_\gamma < 2 \cdot 10^{-16}$ eV (established in an experiment with toroidal Cavendish balance [26]), yields the restrictions $\varepsilon^2_{e\nu\gamma} < 4.3(2.5) \cdot 10^{-94}$ at 90% (68%) C.L.

3.4 New limits on nucleon and di-nucleon decay into invisible channels

The data collected deep underground at the Gran Sasso National Laboratory of INFN by the $\simeq$ 6.5 kg DAMA liquid Xenon scintillator for a total 2257.7 kg×day statistics have also been analysed to search for nucleon and di-nucleon decays into invisible channels (decay to $\nu_i\overline{\nu}_i$ or to $\nu_i\overline{\nu}_i\nu_i$ or to $5\nu_i$, etc., with $i = e, \mu, \tau$) or disappearance.

The baryon (B) and lepton (L) numbers are absolutely conserved in the Standard Model due to unbroken global symmetry. However, the replacement of global symmetries by local, often spontaneously broken, gauge invariances is the mainstream in the development of the modern field theory. Consequently, most of the current grand unified theories – including those based on supersymmetry – predict violation of baryon and lepton numbers and, thus, the decay of protons and neutrons bounded in nuclei. The processes with $\Delta B = 1$, $\Delta B = 2$, $\Delta(B - L) = 0$, $\Delta(B - L) = 2$ have been discussed in literature (see e.g. [27] and references therein), while the disappearance of nucleon and di-nucleon into "nothing" has been addressed in [28] in relation with possible existence of extra timelike dimensions.

Nucleon instability has been searched for in many underground experiments with the help of massive detectors such as IMB, Fréjus, Kamiokande, SuperKamiokande and others. About eighty decay modes have been analyzed; however, no evidence for the nucleons decay has been found [29].

To achieve our result we exploit a new approach with respect to previous experiments. In fact, in result of N or NN decay (disappearance), one or two holes in the nuclear shells will be created, and – if the disappeared nucleons were not in the most external shell – the daughter nucleus will be in an excited state. In the subsequent deexcitation process this nucleus will emit γ quanta if the energy of excitation, E_{exc}, is lower than binding energy of the least bound proton or neutron. Otherwise, one or even few particles (p, n, α) will be emitted with practically 100% probability. As a result, parent (A, Z) nucleus could be transformed not only to an $(A - 1, Z)$ or to an $(A - 1, Z - 1)$ nucleus after the n or p decay (or to $(A - 2, Z)$, $(A - 2, Z - 1)$ and $(A - 2, Z - 2)$ after the nn, pn and pp decay) but as well to various nuclides with lower A and Z numbers. By searching for the deexcitation γ-rays we can gain in the branching ratio (probability to obtain a specific daughter product) which will be close to 1 (instead of e.g. Kamiokande's 2.7×10^{-5}) and – since the parent and daughter nuclei are located in the detector itself – in efficiency which will be also close to 1 (instead of e.g. the small Fréjus' efficiency to detect the neutrinos from the Earth).

We have considered only the N and NN decays on a few most external nuclear shells without subsequent emission of p or n. The list of such daughter nuclides which could be created in the LXe DAMA detector (filled with Kr-free Xenon enriched in ^{129}Xe at 99.5%) together with their characteristics is given in Table 2, where for completeness we take into consideration also the pn and pp decays with electric charge non-conservation.

The experimental spectrum of the LXe scintillator in the energy region 50–500 keV with total statistics 2257.7 kg×day is shown in Fig. 7. Comparing these experimental data with the calculated response functions (see *Phys. Lett. B493 (2000), 12*) we did not find evidence for the N or NN decays. Thus limits for probabilities of such processes

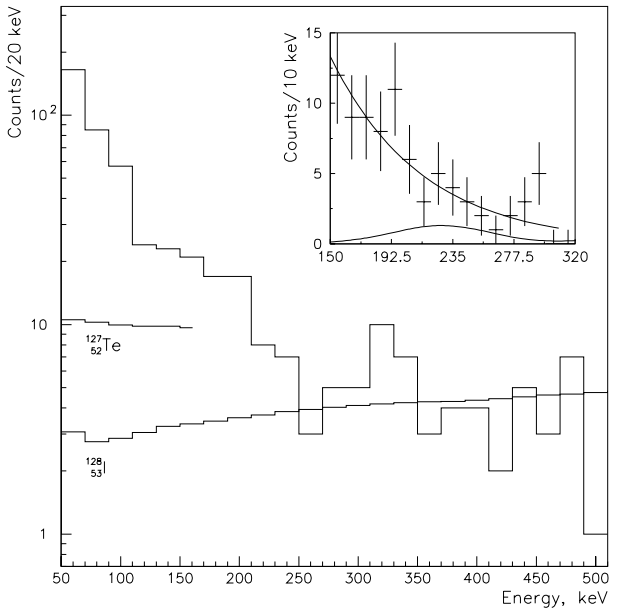

Figure 7: Energy distribution measured by the LXe detector in the 50–500 keV energy interval; the total statistics is 2257.7 kg×day (full histogram). The dotted line is the 90% C.L. excluded distribution for ^{127}Te decay ($\tau_{pp} = 5.5 \times 10^{23}$ yr); the dashed line is the exclusion for ^{128}I decay ($\tau_p = 1.9 \times 10^{24}$ yr). In the inset the 150–320 keV energy region is shown in linear scale together with the fitting curve (dotted line) and the excluded distribution for the ^{127}Xe decay ($\tau_{nn} = 1.2 \times 10^{25}$ yr).

Table 2: Processes of N and NN decays in the DAMA LXe detector, daughter nuclides and their characteristics. The energy release is given in MeV.

Initial nucleus	De-cay	Daughter nucleus, half-life, modes of decay and energy release		
$^{129}_{54}$Xe	n	$^{128}_{54}$Xe	stable	
	p	$^{128}_{53}$I	$T_{1/2}$=24.99 m	β^- 94% (Q=2.127); β^+, EC 6% (Q=1.258)
	nn	$^{127}_{54}$Xe	$T_{1/2}$=36.41 d	EC (Q=0.664)
	pn	$^{127}_{53}$I	stable	
	pp	$^{127}_{52}$Te	$T_{1/2}$=9.4 h	β^- (Q=0.694)

have been determined.

Using this approach (in which a decay of isotopes created after a nucleon or di-nucleon disappearance in parent nuclei is searched for) the new limits on the N and NN decay into invisible channels have been set: $\tau_p = 1.9 \times 10^{24}$ yr, $\tau_{nn} = 1.2 \times 10^{25}$ yr and $\tau_{pp} = 5.5 \times 10^{23}$ yr at 90% C.L. The latter values are the same or better than those previously established

by the Fréjus collaboration; in particular, the limits for the NN decay into $\nu_\tau\overline{\nu}_\tau$ are set for the first time.

4 R&D installation and developments

The set-up named "R&D", which is used for prototype tests and small scale experiments has been fully dismounted and reassembled with some upgrading in a new experimental site during year 2000. The new performances of the installation will allow to effectively realize, as planned, various small scale experiments in incoming years.

The data taking in the "R&D" installation has been re-started on fall 2000 testing various prototypes. Moreover, the preliminary works for new measurements with CaF_2(Eu) detectors have been preformed; the data taking is foreseen to start at beginning of 2001.

Various R&D developments to further improve low background set-ups and scintillators as well as new developments for higher radiopure PMTs are carried out. The related sample measurements are regularly carried out with the DAMA low background Ge detector running deep underground in the low background facility of the Gran Sasso Laboratory since several years.

Finally, the works needed to fulfil the present NaI(Tl) experiment up to $\simeq$ 250 kg of exposed mass are in progress.

5 Conclusions

All the DAMA activities are producing results; in particular, the $\simeq$ 100 kg NaI(Tl) set-up is investigating for a 6^{th} annual cycle the WIMP annual modulation signature. Moreover the LXe set-up is running filled with Xenon enriched in ^{136}Xe; the analysis of new data taken at ENEA - Neutron Generator during 2000 is in progress.

Some upgradings of the set-ups have been performed during year 2000 and others are in preparation.

Further data analyses and data taking to investigate other rare processes are also in progress.

Finally, works are in progress to build the $\simeq$ 250 kg NaI(Tl) set-up.

6 List of Publications during 2000

1. R. Bernabei, P. Belli, R. Cerulli, F. Montecchia, M. Amato, G. Ignesti, A. Incicchitti, D. Prosperi, C.J. Dai, H.L. He, H.H. Kuang, J.M. Ma: Dark Matter search with the DAMA experiments, Nucl.Phys. **B** (Proc. Sup.) **87** (2000), 67.

2. P. Belli, R. Bernabei, A. Bottino, F. Donato, N. Fornengo, D. Prosperi, S. Scopel: Extending the DAMA annual modulation region by inclusion of the uncertainties in astrophysical velocities, Phys. Rev. **D61** (2000), 023512.

3. P. Belli, R. Bernabei, C.J. Dai, G. Ignesti, A. Incicchitti, F. Montecchia, O.A. Ponkratenko, D. Prosperi, V.I. Tretyak, Yu.G. Zdesenko, Quest for electron decay $e^- \to \nu + \gamma$ with liquid Xenon scintillator, Phys. Rev. **D61** (2000), 117301.

4. R. Bernabei, P. Belli, R. Cerulli, F. Montecchia, M. Amato, G. Ignesti, A. Incicchitti, D. Prosperi, C.J. Dai, H.L. He, H.H. Kuang, J.M. Ma, Search for WIMP annual modulation signature: results from DAMA/NaI-3 and DAMA/NaI-4 and the global combined analysis, Phys. Lett. **B480** (2000), 23.

5. R. Bernabei, M. Amato, P. Belli, R. Cerulli, C.J. Dai, H.L. He, G. Ignesti, A. Incicchitti, H.H. Kuang, J.M. Ma, F. Montecchia, D. Prosperi, Recent DAMA Results, ROM2F/2000-15, to appear in the Proceed. of the Int. Workshop DM2000, Marina del Rey, February 2000.

6. R. Bernabei, P. Belli, R. Cerulli, F. Montecchia, M. Amato, G. Ignesti, A. Incicchitti, D. Prosperi, C.J. Dai, H.L. He, H.H. Kuang, J.M. Ma, Searching for signals from the dark Universe , to appear in the Proceed. of the Int. Workshop VULCANO2000, Vulcano, Italy, May 2000.

7. R. Bernabei, P. Belli, R. Cerulli, F. Montecchia, M. Amato, G. Ignesti, A. Incicchitti, D. Prosperi, C.J. Dai, H.L. He, H.H. Kuang, J.M. Ma, Searching for signals from the dark Universe by DAMA at Gran Sasso, to appear in the Proceed. of the Int. Workshop Neutrino2000, Sudbury, Canada, June 2000.

8. R. Bernabei, P. Belli, R. Cerulli, F. Montecchia, M. Amato, G. Ignesti, A. Incicchitti, D. Prosperi, C.J. Dai, H.L. He, H.H. Kuang, J.M. Ma, Searching for signals from the dark Universe , to appear in the Proceed. of the Int. Workshop NUCTH2000, Bologna, Italy, July 2000.

9. R. Bernabei, M. Amato, P.Belli, R. Cerulli, C.J. Dai, H.L. He, G. Ignesti, A. Incicchitti, H.H. Kuang, J.M. Ma, F. Montecchia, Recent results from the DAMA particle Dark Matter search, to appear in the Proceed. of the Int. Workshop CAPP-2000, Verbier, Suisse, July 2000

10. A. Bussolotti, A. Incicchitti, A. Mattei, Sistema di sicurezza e controllo dell'apparato DAMA a Xenon liquido, internal report ROM2F/2000-27.

11. P. Belli, A. Bussolotti, R. Cerulli, C.J. Dai, La nuova catena elettronica dell'apparato da $\simeq$ 100 kg di NaI(Tl) dell'esperimento DAMA, internal report ROM2F/2000-29.

12. R. Bernabei, P. Belli, R. Cerulli, F. Montecchia, M. Amato, G. Ignesti, A. Incicchitti, D. Prosperi, C.J. Dai, H.L. He, H.H. Kuang, J.M. Ma, Recent results on the search for signals from the dark Universe by the DAMA experiment, ROM2F/2000-32 to appear in the Proceed. of the Int. Workshop PIC20, Lisbona, Portugal, July 2000.

13. R. Bernabei, P. Belli, R. Cerulli, F. Montecchia, M. Amato, G. Ignesti, A. Incicchitti, D. Prosperi, C.J. Dai, H.L. He, H.H. Kuang, J.M. Ma, Dark Matter search by DAMA experiment, to appear in the Proceed. of the Ninth Marcel Grossmann Meeting, Rome, July 2000.

14. R. Bernabei, P. Belli, R. Cerulli, C. J. Dai, G. Ignesti, A. Incicchitti, F. Montecchia, D. Prosperi, Improved limits on WIMP-129Xe inelastic scattering, New Journal of Physics **2** (2000), 15.1-15.7 (http://www.njp.org/).

15. R. Bernabei, P. Belli, R. Cerulli, F. Montecchia, M. Amato, G. Ignesti, A. Incicchitti, D. Prosperi, C.J. Dai, H.L. He, H.H. Kuang, J.M. Ma, Results on the investigation of the WIMP annual modulation signature with the $\simeq$ 100 kg NaI(Tl) set-up, to appear in the Proceed. of the Int. Workshop IDM2000, York, UK, September 2000.

16. R. Bernabei, P. Belli, R. Cerulli, F. Montecchia, M. Amato, A. Incicchitti, D. Prosperi, C.J. Dai, LXe DAMA experiment: results and perspectives, to appear in the Proceed. of the Int. Workshop IDM2000, York, UK, September 2000.

17. R. Bernabei, M. Amato, P. Belli, R. Cerulli, C.J. Dai, V. Yu. Denisov, H.L. He, A. Incicchitti, H.H. Kuang, J.M. Ma, F. Montecchia, O.A. Ponkratenko, D. Prosperi, V.I. Tretyak, Yu.G. Zdesenko, Search for the nucleon and di-nucleon decay into invisible channels , Phys. Lett. **B493** (2000), 12.

18. R. Bernabei, P. Belli, R. Cerulli, F. Montecchia, M. Amato, G. Ignesti, A. Incicchitti, D. Prosperi, C.J. Dai, H.L. He, H.H. Kuang, J.M. Ma, On the investigation of possible systematics in WIMP annual modulation search, Eur. Phys. J. **C18** (2000), 283-292.

19. R. Bernabei, P. Belli, R. Cerulli, F. Montecchia, M. Amato, G. Ignesti, A. Incicchitti, D. Prosperi, C.J. Dai, H.L. He, H.H. Kuang, J.M. Ma, Particle Dark Matter search by DAMA at Gran Sasso, to appear on the Proceed. of the 20th Texas Symposium, Austin, USA, December 2000 (in preparation).

20. R. Bernabei, P. Belli, R. Cerulli, F. Montecchia, M. Amato, G. Ignesti, A. Incicchitti, D. Prosperi, C.J. Dai, H.L. He, H.H. Kuang, J.M. Ma, Investigating the DAMA annual modulation effect in a mixed coupling framework, ROM2F/2000-35, to appear as INFN on-line preprint on www.lngs.infn.it and submitted for publication.

References

[1] P. Belli et al., Il N. Cim. C19 (1996), 537.

[2] R. Bernabei et al., Phys. Lett. B387 (1996), 222; Phys. Lett. B389 (1996), 783.

[3] R. Bernabei et al., Phys. Lett. B389, (1996), 757.

[4] R. Bernabei et al., Astrop. Phys. 7 (1997),73.

[5] R. Bernabei et al., Phys. Lett. B424, (1998), 195.

[6] R. Bernabei et al., Phys. Lett. B436 (1998), 379.

[7] R. Bernabei et al., Phys. Lett. B450 (1999), 448.

[8] R.Bernabei et al., Il N. Cim. A112 (1999), 545.

[9] R. Bernabei et al., Phys. Rev. Lett. 83 (1999), 4918.

[10] R. Bernabei et al., Il N. Cim. A112 (1999), 1541.

[11] P. Belli et al., Nucl. Phys. B563 (1999), 97.

[12] P. Belli et al., Astrop. Phys. 5 (1996), 217; R. Bernabei et al., Il N. Cim. A110 (1997), 189; R. Bernabei et al., Phys. Lett. B408 (1997), 439; R. Bernabei et al., Il N. Cim. A111, 347 (1998) & Il N. Cim. A, oct. 1998; P. Belli et al., Astrop. Phys. 10 (1999), 115; P. Belli et al., Phys. Rev. C60 (1999), 065501; P. Belli et al., Phys. Lett. B460 (1999), 236; P. Belli et al., Phys. Lett. B465 (1999), 315; P. Belli et al., Phys. Rev. D61 (2000), 117301; R. Bernabei et al., Phys. Lett. B493 (2000), 12.

[13] P. Belli et al.: in the volume "3K-Cosmology", AIP pub., 65 (1999).

[14] A. Bottino et al., Phys. Lett. B402, 113 (1997); Phys. Lett. B423, 109 (1998); Phys. Rev. D59 (1999), 095004; Phys. Rev. D59 (1999), 095003; Astropart. Phys. 10 (1999), 203; Astropart. Phys. 13, 215 (2000); Phys. Rev. D62 (2000) 056006; Phys.Rev. D62 (2000) 056006; hep-ph/0010203; hep-ph/0012377.

[15] R.W. Arnowitt and P. Nath, Phys. Rev. D60 (1999), 044002; E. Gabrielli et al., hep-ph/0006266;

[16] D. Fargion et al., Pis'ma Zh. Eksp. Teor. Fiz. 68, (JETP Lett. 68, 685) (1998); Astropart. Phys. 12, 307 (2000).

[17] M.T. Ressell et al., Phys. Rev. C56, 535 (1997).

[18] M. W. Goodman and E. Witten, Phys. Rev. D31 (1985), 3059; L. Gonzales-Mestres and Peret-Gallix, pre-print LAPP-EXP-87-03 (1987).

[19] J. Ellis et al., Phys. Lett. B212 (1988), 375.

[20] K. Fushimi et al., Nucl. Phys. B35 (Proc. Supp.) (1994), 400.

[21] Table of the Isotopes, Lederer C.M. and Shirley V.S. eds, VII ed. (1978), John Wiley & sons inc.

[22] S. Weinberg, Phys. Rev. B135 (1964), 1049.

[23] L.B. Okun and Ya.B. Zeldovich, Phys. Lett. B78 (1978), 597; M.B. Voloshin and L.B. Okun, JETP Lett. 32 (1978), 145; R.N. Mohapatra, Phys. Rev. Lett. 59 (1987), 1510; L.B. Okun, Leptons and Quarks (North-Holland, Amsterdam, 1982), p. 181; L.B. Okun, Sov. Phys. Usp. 32 (1989), 543; Comments Nucl. Part. Phys. 19 (1989), 99; Phys. Rev. D **45**, No. 11 (1992) VI.10.

[24] G. Feinberg and M. Goldhaber, Proc. Nat. Acad. Sci. U.S.A. 45 (1959), 1301.

[25] J.N. Bahcall, Rev. Mod. Phys. 50 (1978), 881; "Neutrino Astrophysics", Cambridge University, Cambridge, 1993, p. 360.

[26] R. Lakes, Phys. Rev. Lett. 80 (1998), 1826.

[27] P. Langacker, Phys. Rep. 71 (1981) 185; M. Goldhaber, P. Langacker and R. Slansky, Science 210 (1980), 851; H.V. Klapdor-Kleingrothaus and A. Staudt, *Non-accelerator Particle Physics* (IoP, Bristol and Philadelphia, 1995).

[28] F.J. Yndurain, Phys. Lett. B 256 (1991), 15; G. Dvali, G. Gabadadze and G. Senjanovic, hep-ph/9910207.

[29] C. Caso et al. (Particle Data Group), *Review of Particle Physics*, Europ. Phys. J. C3 (1998), 1.

DBA. Search for double beta decay of ^{100}Mo with liquid argon ionization chamber.

V.D. Ashitkov[1], A.S. Barabash[1], S.G. Belogurov[1], G. Carugno[2], S.I. Konovalov[1], F.Massera[4], G. Puglierin[2], R.R. Saakyan[1,3], V.N. Stekhanov[1], V.I. Umatov[1],

[1]Institute of Theoretical and Experimental Physics, B. Cheremushkinskaya 25, 117259 Moscow, Russia

[2]Dipartimento di Fisica e INFN, Universita di Padova, via Marzolo 8, I-35131 Padova, Italy

[3]Laboratori Nazionali del Gran Sasso dell'INFN, I-67010 Assergi (L'Aquila), Italy

[4]INFN, Sezione di Bologna, 40126, via Berti Pichat, 6/2 (Bologna), Italy

Abstract

Using a liquid argon ionization chamber the $2\nu\beta\beta$ decay of ^{100}Mo was detected with its half-life of $[7.5 \pm 1.1(stat) \pm 1.5(syst)] \cdot 10^{18}$ y. The limits on half-lives for 0ν- and $0\nu\chi^0$-decays of ^{100}Mo were estimated as $9.3(5.0) \cdot 10^{21}$ y and $4.3(2.7) \cdot 10^{20}$ y respectively at 68(90)% CL. Available world data for the $2\nu\beta\beta$ decay of ^{100}Mo lead to the average "world" value of the half-life, $T_{1/2} = (8.0 \pm 0.7) \cdot 10^{18}$ y, that corresponds to the nuclear matrix element, $M_{GT} = 0.118 \pm 0.005$.

1 Introduction

Intensive research for the neutrinoless double beta decay is due to its connection with fundamental aspects of particle physics (see, for example, reviews [1, 2, 3]). The main interest in this process is certainly concerned with neutrino mass, because if the $0\nu\beta\beta$ decay were detected then according to the theory the mass of at least one neutrino must be nonzero and this mass is of the Majorana type.

At the moment only lower limits on half-lives ($T_{1/2}$) have been obtained experimentally. These limits are used to deduce upper limits on the Majorana neutrino mass, the right-handed current admixture parameter, the Majoron-Majorana neutrino coupling constant etc. However, uncertainties in nuclear matrix elements (NME) calculations do not allow reliable limits to be placed on these fundamental values. In this context the detection of $2\nu\beta\beta$ decay becomes of particular importance because information on experimental values of NME(2ν) for different nuclei enables a more accurate calculation of both NME(2ν) and NME(0ν). Besides that, more precise study of the 2ν decay mode is interesting from the

point of view of a search for a possible time variation of the weak interaction coupling constant [4, 5].

The nuclide ^{100}Mo is one of the most attractive for investigations of $\beta\beta$ decay. It has a large $\beta\beta$ transition energy, 3034 keV. In addition the transition $^{100}\mathrm{Mo}(0^+_{\mathrm{g.s.}}) - {}^{100}\mathrm{Ru}(0^+_{\mathrm{g.s.}})$ is characterized by the highest value of NME for both the 2ν decay mode (extracted from experiments, see ref.[6], for example) and the 0ν decay mode (as predicted by recent calculations [2, 7]). The study of $2\nu\beta\beta$ decay of ^{100}Mo may be useful for checking the low-lying-state dominance hypothesis [8, 9, 10]. As it was pointed out in [4, 5], ^{100}Mo is a good candidate for the geochemical $2\nu\beta\beta$ decay experiments. Follow-up comparison of the geochemical results with the results of the direct (counter) experiments will allow a conclusion on the variability of the weak interaction constant to be deduced (it is presented in detail in [4, 5]). In this connection the problem of measuring the half-life of the $2\nu\beta\beta$ decay of ^{100}Mo with a high accuracy assumes great importance. Up to date there are a few positive results for the $2\nu\beta\beta$ decay of ^{100}Mo [8-12]. The experimental values of the half-life are inside the interval from $[6.75^{+0.37(stat)}_{-0.42(stat)} \pm 0.68(syst)] \cdot 10^{18}$ y[15] to $11.5^{+3.0}_{-2.0} \cdot 10^{18}$ y[11].

This paper presents the results of a new independent detection of the $2\nu\beta\beta$ decay of ^{100}Mo obtained during year 2000 using a liquid ionization chamber at Gran Sasso underground laboratory. Besides that, the average "world" value of ^{100}Mo half-life and the corresponding NME for the $2\nu\beta\beta$ transition are given.

2 Experimental Procedure

The experiment is being carried out in the Gran Sasso Underground Laboratory (3500 m w.e. deep). The experimental setup consists of a liquid argon ionization chamber placed in passive shielding (15cm of lead) surrounded by a neutron shielding (see below), a gas system, electronics and a data acquisition system. The active detection portion of the chamber is composed of alternating circular planes of anodes and cathodes with screen grids placed between them. The cathodes are made of molybdenum foil approximately 50 mg/cm^2 thick. The chamber contains 14 cathodes, 15 anodes and 28 screening grids. The chamber has been assembled with eight cathodes containing enriched molybdenum (98.4% ^{100}Mo) and six cathodes with natural molybdenum (9.6% ^{100}Mo). Radioactive impurities of the Mo samples are less than 0.015 Bq/kg for ^{214}Bi, 0.0015 Bq/kg for ^{208}Tl and 0.04 Bq/kg for ^{234m}Pa.

Each anode is connected to a charge-sensitive preamplifier, followed by an amplifier and a flash ADC with the 50 ns sampling time. The energy resolution (FWHM) is 6% at an energy of 3 MeV. The trigger for data collection requires that at least one anode signal exceeds the threshold (0.8 MeV). Each trigger causes digitized signals from all anodes to be written to a data tape. Data processing is performed off-line. Two-electron events (events with two neighboring anode signals with a time difference of < 0.6 μs) are selected. The detection efficiency is calculated by Monte Carlo. The more detailed description of the experimental setup can be found in [16, 17, 18].

3 Results obtained in 2000

During the year 2000 DBA collaboration made a notable progress in the detector hardware upgrade as well as in data taking and analysis. The main development was the installation of the neutron passive shielding made up of 30 cm of water for neutron thermalization and 1cm of boron acid to capture thermal neutrons. A preliminary analysis shows that the shielding reduced the background at the high energy part of the spectrum (above 3.5 MeV) by roughly an order of magnitude. Two experimental runs were conducted in 2000, 708 hours with a baseline neutron shielding and 643 hours with an improved (in terms of screening tightness) neutron shielding.

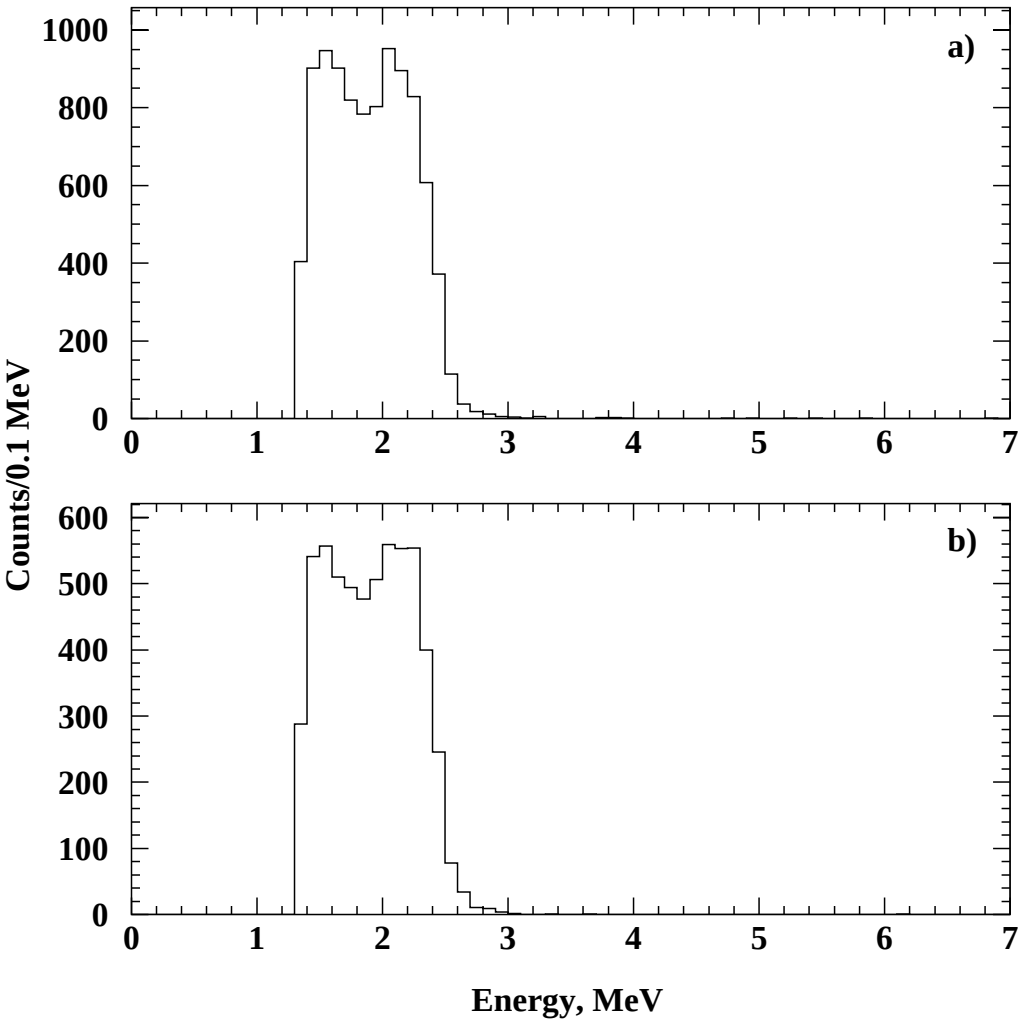

Figure 1: Energy spectra of two-electron events for (a) enriched (651.4 kg·h) and (b) natural (441.1 kg·h) molybdenum.

The results presented here were obtained with 137.8 g (313 hours of data taking) and 306 g (2063 hours of data taking) of enriched Mo. This corresponds to the run with the baseline neutron shielding summed up with previous years runs. The analysis of the data taken with the improved neutron shielding is under way. Fig. 1 shows the energy spectra of two-electron events for enriched (651.4 kg·h) and natural (441.1 kg·h) molybdenum. The threshold for the first electron is equal to 0.8 MeV, for second one is 0.5 MeV. Events from natural Mo cathodes are used for background estimation.

0ν-decay. To reduce the background the energy threshold for each electron of a pair has been selected to be 1 MeV. The energy range (2.8–3.1) MeV has been studied with an additional selection on signal shape. As a result 4 events in the enriched molybdenum and 4 events in the natural Mo (i.e. 5.9 events if recalculated for 651.4 kg·h) have been detected. Using the detection efficiency (6.9%) one can obtain the limit on the $0\nu\beta\beta$ decay of ^{100}Mo, $T_{1/2} > 9.3(5.0) \cdot 10^{21}$ y at 68%(90%) C.L.

$0\nu\chi^0$-decay. The energy interval of $2.3 - 3.0$ MeV has been investigated. 1165 events for the enriched Mo foils and 1157 events for the natural foils (recalculated for 651.4 kg·h) have been obtained. For the efficiency of 5.7% we have got the limit, $T_{1/2} > 4.3(2.7) \cdot 10^{20}$ y at 68%(90%) C.L.

2ν-decay. Events have been analyzed in the energy interval of $1.4 - 2.3$ MeV where the signal-to-background ratio is maximal. Background subtraction have led to the final value of the effect, 802 ± 122 events. Using the calculated detection efficiency of the $2\nu\beta\beta$ decay of ^{100}Mo (2.2%) one gets the half-life:

$$T_{1/2} = [7.5 \pm 1.1(stat) \pm 1.5(syst)] \cdot 10^{18} \text{ y}.$$

The systematic error is mainly due to the possible contributions of radioactive impurities in the foils. We consider this result as preliminary one. The analysis will be continued and we hope to decrease both statistical and systematic errors.

4 Discussion

Table 1: Experimental half-lives for the $2\nu\beta\beta$ decay of ^{100}Mo.

Year, reference	$T^{2\nu}_{1/2}$, $\times 10^{18}$ y
1991, /8/	$11.5^{+3.0}_{-2.0}$
1995, /10/	$9.5 \pm 0.4(stat) \pm 0.9(syst)$
1997, /11/	$7.6^{+2.2}_{-1.4}$
1997, /12/	$6.75^{+0.37(stat)}_{-0.42(stat)} \pm 0.68(syst)$
2000, present work	$7.5 \pm 1.1(stat) \pm 1.5(syst)$
Average	8.0 ± 0.7

Table 1 presents all the available positive experimental results on the half-life of ^{100}Mo. Only the preliminary result of M. Moe et al. [12] is not given because we use their

more precise final result [15]. The last line shows the average of the half-lives of all five experiments. The average estimate has been performed according to the usual technique of calculation of the average value with different variances (see, for example, [19]) summing up the statistical and systematic errors in quadrature.

Using the phase factor $G = 8.9 \cdot 10^{-18}$ y^{-1} (for $g_A = 1.25$) [6] and our average "world" half-life one can get NME (2ν) for the transition of ^{100}Mo($0^+_{g.s.}$) - ^{100}Ru($0^+_{g.s.}$), $M_{GT} = (0.23 \pm 0.01)$ MeV^{-1} or $M_{GT} = (0.118 \pm 0.005)$ (scaled by the electron rest mass).

The analysis of the data obtained with the improved neutron passive shielding is currently under way. It may improve sensitivity to $0\nu\beta\beta$ process by reducing the background in the 0ν energy range. In addition, it may bring sensitivity to the content of ^{42}Ar in atmosphere [21] up to a record level of $(3-5) \cdot 10^{-21}$ g/g.

5 Acknowledgements

We would like to thank M. Balata for providing the liquid nitrogen system and fruitful discussions. We are also very grateful to L. Marelli, B. Romualdi, A. Rotilio and E. Tatananni for frequent technical support. The portion of this work was supported by the INFN (Italy) and the Russian Foundation for Basic Research under grant 97-02-17344.

6 Publications and Conferences

1. Barabash A.S., "Search for double beta decay of ^{100}Mo with liquid argon ionization chamber", *Carolina Symposium on Neutrino Physics, March 10-12, 2000 (Columbia, USA).*

2. Barabash A.S., "Search for double beta decay of ^{100}Mo with liquid argon ionization chamber", *International Workshop on NONACCELERATOR NEW PHYSICS (NANPINO), July 19-22, 2000 (Dubna, Russia).*

3. Barabash A.S., "Limit on ^{222}Rn content in liquid argon", *International Workshop "Radon Background in Rare-Event Experiments", June 14, 2000 (Sudbery, Canada).*

References

[1] Klapdor-Kleingrothaus H.V., and Staudt A., *Non-accelerator Particle Physics*, IOP Publ., 1994.

[2] Faessler A., and Simkovic F.,*J. Phys. G*, 1998, vol. 24, p. 2139.

[3] Klapdor-Kleingrothaus H.V.,*Proc. 5-th Int. WEIN Symp. "Physics Beyond the Standard Model"*, Herczeg P. *et al.*, Eds., Singapore: World Sci., 1999, p. 275.

[4] Barabash A.S., *JETP Lett.*, 1998, vol. 68, p. 1.

[5] Barabash A.S., *Eur. Phys. J. A*, 2000, vol. 8, p. 137.

[6] Suhonen J., and Civitarese O., *Phys. Rep.*, 1998, vol. 300, p. 123.

[7] Simkovic F., *et al., Phys. Rev. C*, 1999, vol. 60, p. 055502.

[8] Abad J. *et al. Ann. Fis. A*, 1984, vol. 80, p. 9.

[9] Civitarese O., and Suhonen J., *Nucl. Phys. A*, 1999, vol. 653, p. 321.

[10] Semenov S.V. *et al., Phys. At. Nucl.*, 2000, vol. 63, p. 1196

[11] Ejiri H. *et al., Phys. Lett. B*, 1991, vol. 258, p. 17.

[12] Elliot S.R., Hahn A.A., and Moe M.K.,*J. Phys. G*, 1991, vol. 17, p. S145.

[13] Dassie D. *et al., Phys. Rev. D*, 1995, vol. 51, p. 2090.

[14] Alston-Garnjost M. *et al., Phys. Rev. C*, 1997, vol. 55, p. 474.

[15] De Silva A. *et al., Phys. Rev. C*, 1997, vol. 56, p. 2451.

[16] Ashitkov V.D. *et al., Phys. At. Nucl.*, 1998, vol. 61, p. 910.

[17] Ashitkov V.D. *et al., Nucl.Phys. B* (Proc. Suppl.), 1999, vol. 70, p. 233.

[18] Ashitkov V.D. *et al., Phys. At. Nucl.*, 1999, vol. 62, p. 2044.

[19] Groom. D.E. *et al., Eur. Phys. J. C*, 2000, vol. 15, p. 1.

[20] Ejiri H. *et al., Nucl. Phys. A*, 1996, vol. 611, p. 85.

[21] Ashitkov V.D. *et al., Nucl. Instr. Meth.*, 1998, A416, p. 179.

EAS-TOP. Cosmic Ray Experiment

M. Aglietta[a,b], B. Alessandro[b], P. Antonioli[c], F. Arneodo[d], L. Bergamasco[b,e], M. Bertaina[b,e], C. Castagnoli[a,b], A. Castellina[a,b], A. Chiavassa[b,e], G. Cini Castagnoli[b,e], B. D'Ettorre Piazzoli[f], G. Di Sciascio[f], W. Fulgione[a,b], P. Galeotti[b,e], P.L. Ghia[a,b], M. Iacovacci[f], G. Mannocchi[a,b], C. Morello[a,b], G. Navarra[b,e], O. Saavedra[b,e], G. C. Trinchero[a,b], P. Vallania[a,b], S. Vernetto[a,b], C. Vigorito[b,e], S. Valchierotti[b,e]

[a] Istituto di Cosmo-Geofisica del CNR, Torino, Italy
[b] Istituto Nazionale di Fisica Nucleare, Sezione di Torino, Italy
[c] Istituto Nazionale di Fisica Nucleare, Sezione di Bologna, Italy
[d] Istituto Nazionale di Fisica Nucleare, LNGS, Assergi, L'Aquila, Italy
[e] Dipartimento di Fisica Generale dell'Università di Torino, Italy
[f] Dipartimento di Scienze Fisiche dell' Università and INFN, Sezione di Napoli, Italy

Abstract

The EAS-TOP array (Campo Imperatore, 2000 m a.s.l., 30^0 with respect to the vertical of the underground Gran Sasso Laboratories) has operated with:

- the e.m. detector: 35 modules of scintillators, 10 m^2 each, fully efficient for $N_e > 10^5$;
- the muon-hadron detector: 140 m^2 calorimeter with 9 layers of 13 cm iron absorbers and streamer tubes as active elements, operating for hadron calorimetry at $E_h > 50$ GeV, and for muon counting at $E_\mu > 1$ GeV;
- the Cherenkov light detector: 8 telescopes with tracking capabilities equipped with imaging photomultipliers and wide angle optics;
- three radio antennas for EAS radio emission measurements;
- moreover it operated in coincidence with the underground MACRO and LVD muon detectors ($E_\mu > 1.3$ TeV; full area $A_\mu^{TeV} \approx 1000$ m^2).

The array has been in operation, in different configurations, between 1989 and May 2000 (decommissioning time).

1 Aim of the experiment

The aim of the EAS-TOP experiment is the study of cosmic rays (under different aspects and with different methodologies) in the energy range $10^{13}-10^{16}$ eV, through the detection of Extensive Air Showers. The range includes the region of the "knee" of the primary spectrum that has been investigated in different EAS components: e.m., hadron, Cherenkov

light, GeV and TeV muons (exploiting the unique possibility of surface and deep underground measurements, which is essential for debugging the "interaction-composition-fluctuation" problem in the understanding of EAS data, through the interpretation of a subset of individual events).

To construct the experimental knowledge of cosmic radiation in the quoted energy range, i.e. between the direct measurements, and the "giant" EAS arrays, other aspects have been investigated, i.e.: the γ-ray primaries (diffuse, transients, candidate sources), the anisotropies, the phenomenology and the physics of penetrating showers, the EAS phenomenology, the local atmospheric effects on the shower development, and some features of hadronic interactions at ultra high energies, relevant for the interpretation, and the extrapolation to higher energies of the models elaborated from the accelerator data.

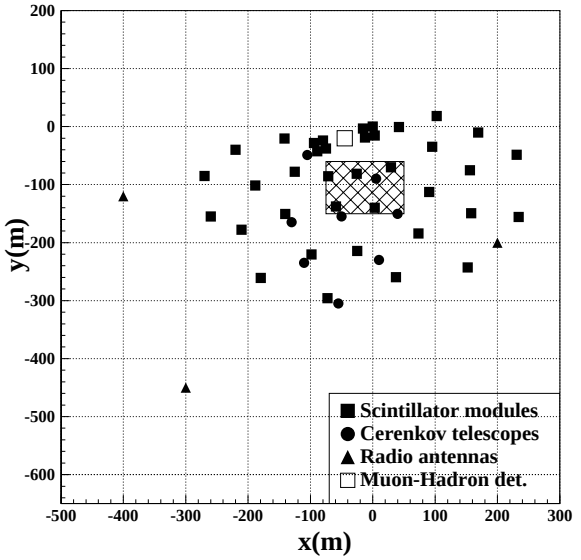

Figure 1: *The EAS-TOP array. The shaded area shows the core location region used for the shower size spectrum measurement.*

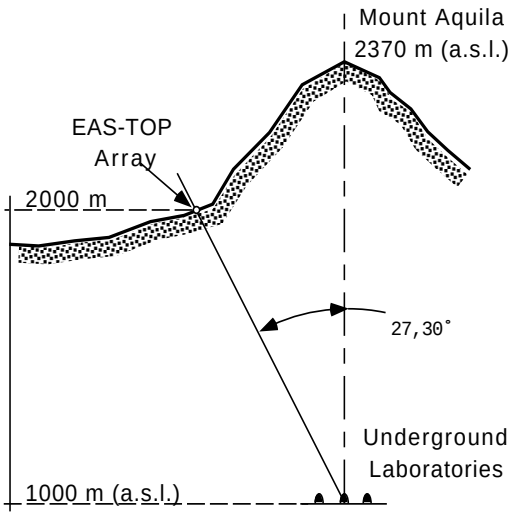

Figure 2: *The EAS-TOP array location with respect to the underground Gran Sasso laboratories.*

The basic detector configuration described in the Abstract (and shown in figs. 1 and 2 together with the array location with respect to the underground Gran Sasso Laboratories) has been implemented in time: a) to improve the response to very inclined showers, with vertical scintillators in eight modules, and two vertical walls made of streamer tubes at the North and South sides of the calorimeter; b) for muon counting, with 130 m^2 scintillator detectors distributed in the field, shielded with 30 cm of iron absorber; c) to test the "Time Track Compatibilty" method for reconstructing the EAS longitudinal profile, with 40 m^2 RPC positioned below the bottom layer, for muon timing measurements [1]; d) to increase the statistics of high energy events observed in C.l., with five QUASAR-370 photomultipliers, in cooperation with the TUNKA group of Institute for Nuclear Physics

[1] *Collaboration with: M. Ambrosio, C. Aramo, G. Battistoni, R. Fonte, A. Grillo.*

of Moscow State University [2].

In year 2000, i.e. the period covered by the present report, the array has been operated up to May 10, and then dismounted (operation completed on July 10).

From the point of view of the analysis, most attention has been given to completing the statistics on the different items (some data require the full statistics to obtain significant physical interpretation), and crossing the information on the different observables to check the interpretation itself.

The experiment results from a collaboration between INFN and CNR (Istituto di Cosmo-Geofisica, Torino).

2 Results

We will summarize in the following the main results reported by EAS-TOP, with particular attention to the activity performed in year 2000. The main aspects of specific items have already been reviewed in previous issues of these reports, as e.g.: the knee data and the studies of HAS in 1999, the high energy interaction data in p-N collisions (p-Air total inelastic cross section at $\sqrt{s} \approx 2$ TeV, and large P_t jet production cross section at $\sqrt{s} \approx 500$ GeV) in 1998, the studies of the anisotropies in 1996, and different aspects of the gamma-ray searches in different issues.

2.1 The studies of the *knee*

We remind here the first observation reported by EAS-TOP of the dependence of the value of shower size at the knee (N_e^k) on the atmospheric depth (i.e. zenith angle), proving that the observed spectral break is a real effect characterized by a primary mass and energy, of the knee in the muon number (N_μ^k), and of the consistent relation between the N_e and N_μ spectra below and above the knee.

In figs. 3 and 4 the size spectrum and the $N_e - \rho_\mu^{200m}$ relation around the knee (in vertical direction), providing information on the primary composition, are shown. The data of fig. 4 confirm the reported observation through the $N_e - N_\mu$ relation of a composition becoming heavier at the knee (see the 1999 Report). Such data are obtained on a wider energy range with respect to the previous ones and at constant core distance (i.e. without using a muon lateral distribution function). The comparison is performed with a different interacion model (QGSJET in spite of HDPM, always in the CORSIKA frame). It is thus shown that the result is stable, and does not depend on some peculiarity of the data treatment or choice of hadronic interaction model. The amount of the effect is still somehow dependent on the interaction model used, and for such reason too, the tests of interaction models through different observables have to be as stringent as possible.

The statistics has been improved in year 2000, including the full data set and the final data are being compared with the simulations. The full statistics of the coincidences of the full array (including Cherenkov light data, and the coincidences with the underground detectors) are now available, and are being processed and compared with the results of

[2] *Collaboration with: E.E. Korosteleva, L.A. Kuzmichev, B.K. Lubsandorjev, V.V. Prosin.*

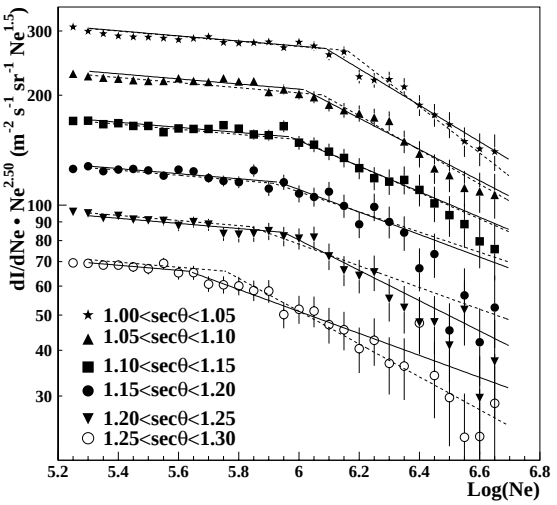

Figure 3: *Differential shower size spectra measured at different zenith angles (i.e. atmospheric depths), showing the knee position, and its shift with zenith angle.*

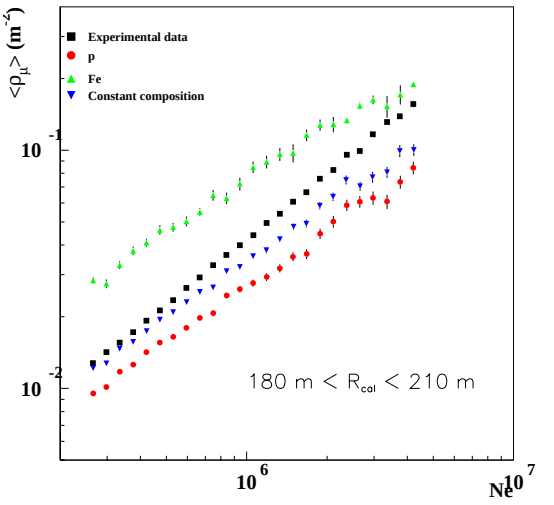

Figure 4: *The experimental relation $\rho_\mu(200m)$ vs Ne compared with the expectations from pure iron and proton primary compositions and a mixed constant one (CORSIKA-QGSJET).*

the simulations (some results have been discussed at the *"Giornate di studio su Fisica delle Particelle, Astrofisica e Cosmologia"* organized by INFN at LNGS).

2.2 Wide angle Cherenkov light measurements

The wide angle Cherenkov light detector based on five QUASAR-370 photomultipliers installed on five telescopes has been operating for about 110 hours in good atmospheric conditions in the last two years, at energy threshold $E_{th}^C \approx 300$ TeV. The surface of each photomultiplier is 0.1 m^2, and the full opening angle 45 degrees.

The e.m. detector data are used to localize the core position also for the Cherenkov light (C.l.) reconstruction. The common analysis is performed on the basis of the shower size (Ne), arrival zenith angle (θ), C.l. photon density at 100 m from the EAS core (Q100), and slope of the C.l. lateral distribution (Ro). As interesting examples of the data obtained from the correlated analysis, in figs. 5 and 6, the mean C.l. lateral distribution function reconstructed for $< E_0 > = 2.7$ PeV, and the absorption curve of the shower size of showers at energy: $10^{3.2} < E_0 < 10^{3.6}$ TeV are shown. The experimental data are compared with a few events simulated with the CORSIKA-QGSJET code. The primary energy is determined from the C.l. data ($Log(E_0) = Log(Q100) + 1.25(sec\theta - 0.92)^2$), and the atmospheric depth from the EAS zenith angle. As a first step these data show that the phenomenology on which the analysis is based, and the response of the detector are understood and agree with the expectations. The analysis is in progress. [3]

[3] *The work has been supported by INTAS under grant 96-0526 (coordinator A.M. Hillas); a comunica-*

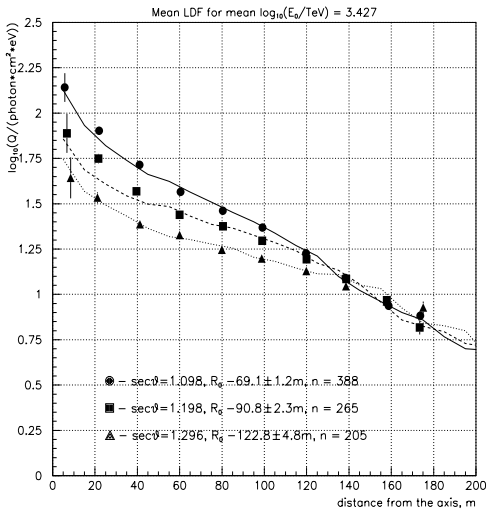

Figure 5: *The mean Cherenkov light lateral distribution measured at different atmospheric depths and compared with the results of the simulation performed with the CORSIKA code (QGSJET) for three events with the same primary energy.*

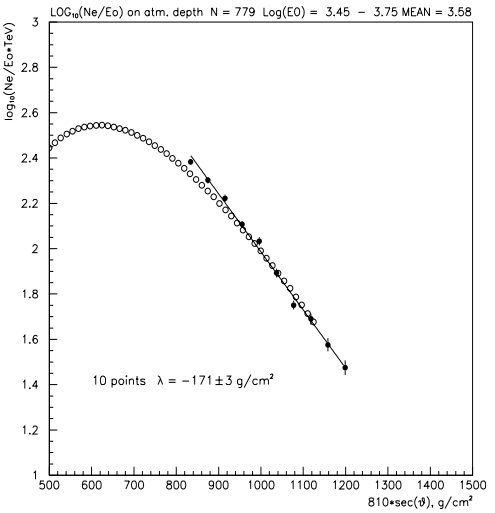

Figure 6: *EAS absorption curve obtained from the combined Cherenkov and e.m. data, compared with the longitudinal development of a shower simulated with the CORSIKA code.*

2.3 The hadron spectrum at 820 gcm^{-2}

Inside the EAS-TOP calorimeter, a set of (80×80) cm^2 scintillators is lodged below two absorber layers; each of them is centered on a pad and discriminated at the level of 30 particles, corresponding to an energy threshold of about 30 GeV. Their logical OR defines the "local hadron trigger", its frequency being $f_h \simeq 0.06$ Hz.

An event is accepted as a hadron if : a) the cascade crosses at least three consecutive planes of the calorimeter, including the one positioned immediately below the scintillator and excluding the uppermost unshielded one; b) the maximum energy is recorded on the pad belonging to the "column" formed by the pads below the triggering scintillator on all the three planes.

The total charge induced on the 8 inner planes, each over the area of (3×3) pads corresponding to the scintillator position, is measured and then converted to the equivalent number of vertical particles by means of periodical calibration runs using a single muon trigger (pressure and temperature dependence of the induced charge are corrected for).

The energy calibration has been obtained by simulating the detector response by means of a Monte Carlo based on the Geant code.

From a total of about 10^6 triggers, 40832 survived the reconstruction and selection criteria and were classified as hadrons, either single or in showers, in a total observation

tion has been presented at the 17th European Cosmic Ray Symposium (Lodz, 2000).

time of 615 d. The angular aperture is defined by the trigger conditions; using the Monte Carlo simulation, the effective collection area $A(E,\theta)$ has been calculated. The trigger efficiency is higher than 80% above 200 GeV for vertical incidence and is less than 10% for $\theta = 30^o$.
The measured number of events in each energy bin is given by (T = obs. time):

$$n_{ev}^{mis}(E, E+\Delta E) = \int_0^{\Omega} \int_E^{E+\Delta E} S(E,\theta) T A(E,\theta) d\Omega dE \tag{1}$$

The hadron intensity at angle θ, with respect to the one for vertical incidence, is:

$$S(E,\theta) = S_{vert}(E) exp(-\frac{x(\theta) - x_{vert}}{\Lambda(E)}) \tag{2}$$

$\Lambda(E)$ is the attenuation length obtained through simulations. Assuming a power law spectrum inside each energy bin to get the mean value $\overline{E}$, the vertical flux is thus:

$$S_{vert}(\overline{E}, x_{vert}) = \frac{n_{ev}^{mis}(\overline{E})}{2\pi T \overline{E}^{\gamma} \int\int E^{-\gamma} exp(-\frac{x(\theta)-x_{vert}}{\Lambda(E)}) A_{eff}(E,\theta) sin\theta d\theta dE} \tag{3}$$

The effect of the whole reconstruction and calibration procedure has been studied by means of a simulation of primary protons, with a power law energy spectrum with $\gamma = 2.7$ and input angular distribution as calculated for residual protons at the experimental depth in the range $0^\circ - 40^\circ$. Such analysis led to a correction in the low energy region.

Mean Hadron Energy (GeV)	E_0 **(GeV)**	E_1 **(GeV)**	**Hadron Number**	S_{had} $(m^2 ssr GeV)^{-1}$	$\sigma(S_{had})$ $(m^2 s\ sr\ GeV)^{-1}$
41	32	56	10222	$.12\ 10^{-2}$	$.12\ 10^{-4}$
73	56	100	12875	$.27\ 10^{-3}$	$.24\ 10^{-5}$
129	100	178	9506	$.60\ 10^{-4}$	$.63\ 10^{-6}$
229	178	316	4930	$.14\ 10^{-4}$	$.21\ 10^{-6}$
408	316	562	2174	$.29\ 10^{-5}$	$.66\ 10^{-7}$
726	562	1000	802	$.47\ 10^{-6}$	$.18\ 10^{-7}$
1290	1000	1778	299	$.92\ 10^{-7}$	$.56\ 10^{-8}$
2295	1778	3162	119	$.17\ 10^{-7}$	$.16\ 10^{-8}$
4081	3162	5623	44	$.26\ 10^{-8}$	$.46\ 10^{-9}$
7257	5623	10000	23	$.84\ 10^{-9}$	$.18\ 10^{-9}$
12904	10000	17783	12	$.14\ 10^{-9}$	$.49\ 10^{-10}$
22945	17783	31623	3	$.90\ 10^{-10}$	$.52\ 10^{-10}$

Table 1: *The all hadron flux at* 820 *g cm*$^{-2}$ *as measured by EAS-TOP.*

The experimental all hadron flux at the atmospheric depth of $x_{vert} = 820$ g cm^{-2}, resulting from the average of three "columns", is plotted in table 1, and shown in Fig.7, together with the same spectrum observed by KASCADE at sea level (we want essentially to discuss here the experimental datum, and its derivation).

The overhall fit in the energy range 30 GeV - 30 TeV gives:

$$S(E) = (2.25 \pm 0.20)\ 10^{-7}(\frac{E}{1000\ GeV})^{(-2.79\pm0.06)}\ m^{-2}s^{-1}sr^{-1}GeV^{-1} \qquad (4)$$

(where a 15% systematic uncertainty on the absolute value has further to be added).

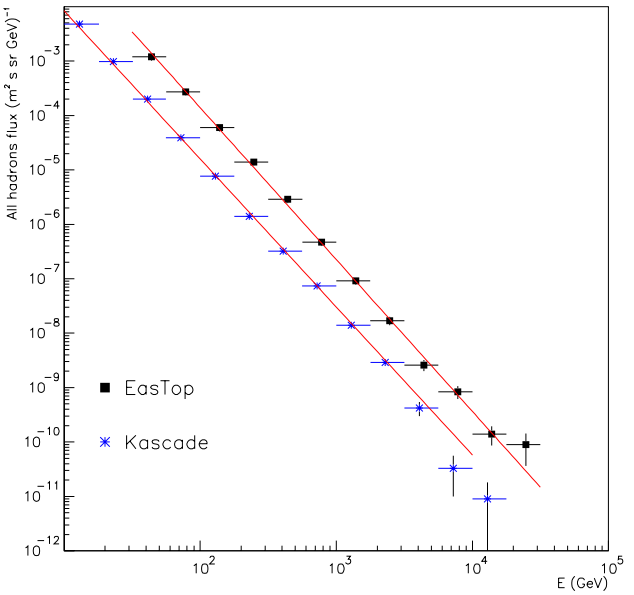

Figure 7: *The single hadron spectrum at* 820 $g\ cm^{-2}$ *as measured by EAS-TOP, compared with the KASCADE data at sea level.*

The error bars shown in the plot are statistical only. The systematic uncertainties have been evaluated by investigating:
a) the fluxes obtained with the different columns triggered by each scintillator, leading to a maximum uncertainty $\frac{\sigma_S}{S} \simeq 15\%$;
b) the acceptance uncertainty, $\frac{\Delta A(E,\theta)}{A(E,\theta)}$, which equals 20% at 100 GeV and goes down to 7% in the TeV region;
c) the uncertainty due to the angular distribution of hadrons which reflects in the attenuation length used to evaluate the flux, leading to $\frac{\sigma_S}{S} \simeq 7\%$ around 1 TeV;
d) the uncertainty in the energy determination due to the whole procedure (calibration, simulation and reconstruction), which can be estimated by comparing the results from the test run with the CERN e^+ beam. In the energy region up to the particle density compatible to a hadron energy $\simeq 650\ GeV$, $\frac{\Delta N}{N} \simeq 2.6\%$; for a power law spectrum with slope $\gamma = 2.7$, the corresponding flux uncertainty is $\frac{\sigma_S}{S} \simeq 7\%$.

2.4 Gamma-ray Astronomy

Upper limits to the gamma-ray flux in primaries, from the galactic disk, the gamma-ray sources observed at lower energies, and possibly related to the gamma-ray bursts observed by satellites have already been reported and discussed.

A search for possible transient gamma-ray sources (both unpredicted, through a sky-survey of the northern hemisphere, and candidate ones) at $E_\gamma \geq 5 \cdot 10^{13}$ eV has been completed in year 2000 through the correlation of the BAKSAN and EAS-TOP data. The independent fluctuations of the two arrays counting rates are well understood in terms of poissonian statistics, up to very large significance values ($S > 5$ s.d.). This shows that the contributions due to instrumental effects are negligible, and sets a firm base to the search for transients and the joint analysis. The correlated data also behave following statistical fluctuations. The absence of nonstatistical excesses as a result of the survey over the visible sky ($19° < \delta < 69°$) leads to upper limits to the number of bursts of transient emission, n_γ. For the declination band corresponding to the zenith, at 90% c.l., we have: $n_\gamma/(\Omega \cdot t) < 12/(\mathrm{yr \cdot sr})$, with flux $\Phi_\gamma(E_\gamma > 5 \cdot 10^{13}\ \mathrm{eV}) > 2.0 \cdot 10^{-11}$ cm^{-2} s^{-1} and duration Δt$<$ 8 hrs.

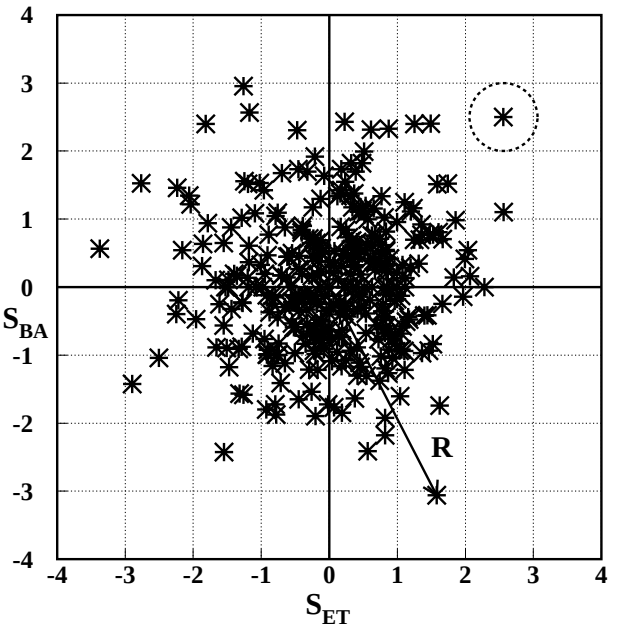

Figure 8: *Plot of daily correlated excesses in EAS-TOP (S_{ET}) and BAKSAN (S_{BA}) in 349 daily transits of Markarian 421. The largest excess discussed in the text is shown.*

Three sources, Crab Nebula, Markarian 421 and Markarian 501 (established at TeV energies through the observation of atmospheric Cherenkov light detectors) have been investigated. No significant excesses have been detected from any of them; at 90% c.l., the typical obtained upper limits (for the Crab Nebula, and Markarian 501) are: $n_\gamma/t <$ 10.5/yr with $\Phi_\gamma(E_\gamma > 6. \cdot 10^{13}\ \mathrm{eV}) > 1.4 \cdot 10^{-11}$ cm^{-2} s^{-1} and Δt$<$ 5.5 hrs.

Slightly peculiar is the case of Markarian 421 for which the second most significant BAKSAN excess (S_{BA} = 2.5 s.d., recorded on 15th January 1994) coincides with the EAS-TOP largest one (S_{ET} = 2.6 s.d.) (this event is demonstrated in Fig. 8). If we take into account its peculiar location in the uppermost tails of both distributions, we obtain, following Rayleigh statistics, from the integration of $F(R)$ for $S_{ET} > 2.6$ and $S_{BA} > 2.5$, an expected chance imitation rate $n_{ch} = 0.01$, so that it is worthwhile to point it out. This, if not due to a statistical fluctuation, would show that the gamma-ray spectrum of AGNs, during flaring activity, extends up to primary energies $E_\gamma \approx 5 \cdot 10^{13}$ eV (with $\Phi_\gamma = (1 \div 2) \cdot 10^{-11}$ cm^{-2} s^{-1}), with no significant absorption on infrared photons in the intergalactic space at such energies up to the distance of Mrk 421 (z=0.031).

A paper has been published in Astroparticle Physics.

2.5 The search for γ-ray bursts with Cherenkov light

A method for searching for γ-ray bursts at VHE has been developed, by looking for short duration time variations in the counting rate of the C.l. detectors while oriented in the direction corresponding to the events recorded in the underground detectors. The two wide angle detectors located on each telescope are used. Each of them is realized with 7 photomultipliers (d = 6.8 cm each) on the focal plane of a parabolic mirror (0.5 m^2, 40 cm focal length) for a total f.o.v. of 0.16 sr, the f.o.v. of each individual photomultiplier being 2.3 10^{-2} sr.

The Cherenkov events are identified by the coincidence, in a time window of 30 nsec, between any two photomultipliers having the same geometrical position on the focal plane of the two mirrors of the same telescope. The trigger threshold is $N_{phe}^{th} = 200$ photoelectrons/PM corrisponding to $E_0^{th} \approx 10$ TeV; the trigger rate is about 5 Hz/telescope.

The aim of the analysis is to point out possible excesses with time duration $\Delta t \leq 1$ s in the counting rate of the Cherenkov events detected by corresponding PMs. The search for coincidences of the same couple of corresponding PMs on two different telescopes has been performed for all the excesses having $P < 10^{-4}$. In 47 hours of observing time 1 of such events has been observed against 0.24 expected from statistical fluctuations. From the absence of significant counting rate excesses in a total exposure time of 7.52 h sr the derived upper limit to the photon flux at 90% c.l. is:
$\Phi_\gamma(> 10$ TeV$) < 1.2\ 10^{-8}$ ph cm^{-2} for $\Delta t \leq 1$ s and rate $N < 3.2$ events d^{-1} sr^{-1}.
The corresponding upper limit to the energy fluence is:
$\Phi_E(> 10\text{TeV}) \leq\ 2.4\ 10^{-7}$erg cm^{-2}.

This result is compared to other experimental data in fig. 9. The measurement, extended to the full data set, due to the wider acceptance of the detector with respect to the imaging ones, while being more limited on the fluence limit (see fig. 9), will provide an improvement on the maximum event rate (N).

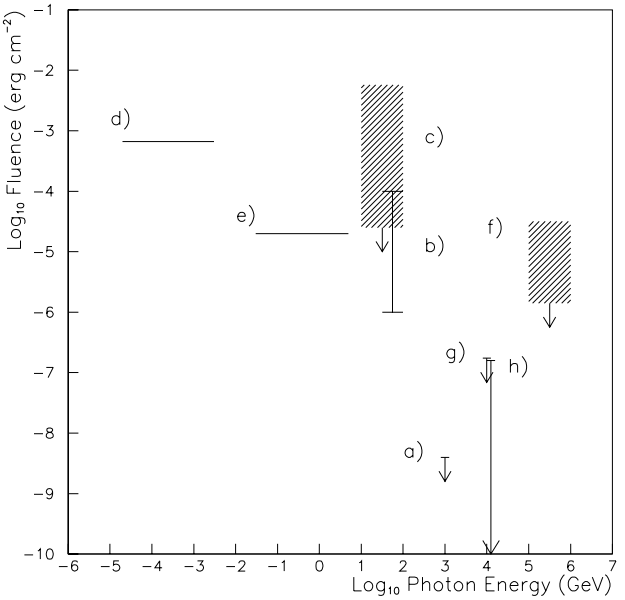

Figure 9: Upper limit to the energy fluence obtained by the EAS-TOP Cherenkov array (g) compared with the results of other experiments: (a) upper limit set by the WHIPPLE telescope; (b) range of fluences reported by MILAGRITO during GRB 970417a; (c) upper limits obtained by EAS-TOP scintillator array at 10-100 GeV during 45 BATSE bursts; (d,e) fluences measured by BATSE and EGRET, respectively, during GRB 940217; (f) upper limits obtained by EAS-TOP scintillator array at 100-1000 TeV during 56 BATSE bursts; (h) range of upper limits obtained by the HEGRA arrays.

3 Collaborators and Institutions

M. Aglietta, B. Alessandro, V.V. Alexeenko, P. Antonioli, F. Arneodo, V.S. Berezinsky, L. Bergamasco, M. Bertaina, A. Campos Fauth, A. Castellina, C. Castagnoli, A. Chiavassa, G. Cini Castagnoli, B. D'Ettorre Piazzoli, G. Di Sciascio, W. Fulgione, P. Galeotti, A. Gazizov, P. L. Ghia, R. Granella, M. Iacovacci, E.E. Korosteleva, L.B. Konstantinovich, L.A. Kuzmichev, A.S. Lidvansky, A. Lima de Godoi, B.K. Lubsandorzhiev, G. Mannocchi, C. Melagrana, N. Mengotti Silva, C. Morello, G. Navarra [4], H. Nogima, L. Periale, P. Picchi, V.V. Prosin, L. Riccati, O. Saavedra, M. Serio, G. C. Trinchero, A. Turtelli, P. Vallania, S. Vernetto, C.Vigorito, S. Valchierotti
Technical staff: G. Giuliani, A. Giuliano, F. Gomez, G. Pirali
Istituto Nazionale di Fisica Nucleare, Sezione di Torino, Torino, Italy
Istituto di Cosmo-Geofisica del CNR, Torino, Italy
Dipartimento di Fisica Generale dell' Università di Torino, Torino, Italy
INFN, Laboratori Nazionali del Gran Sasso, Assergi (AQ), Italy
Dipartimento di Scienze Fisiche dell' Università and INFN, Napoli, Italy

[4] *spokesperson*

Istituto Nazionale di Fisica Nucleare, Sezione di Bologna, Bologna, Italy
Instituto di Fisica, Universidade Estadual, de Campinas, Campinas (SP), Brazil
Institute of Physics, National Academy of Sciences of Belarus, Minsk, Belarus
Institute for Nuclear Research, Russian Academy of Sciences, Moscow, Russia
Institute for Nuclear Physics, Moscow State University, Moscow, Russia
Universidade de Sao Paulo, Sao Paulo (SP), Brazil

4 List of Publications

1. "Study of the cosmic ray primary spectrum at $10^{15} < E_0 < 10^{16}$ eV with the EAS-TOP array"
   Nuclear Physics B, **85**, 318 (2000)

2. "Search for $E_\gamma > 5.10^{13}$ eV γ-ray transients through the BAKSAN and EAS-TOP correlated data"
   Baksan and EAS-TOP Collaborations
   Astroparticle Physics, **14**, 189 (2000)

3. "Search for Gamma Ray Bursts at $E_0 \approx 10^{13}$ eV"
   SIF Conference Proceedings, **68**, 7 (2000)

4. "Measurement of the hadron energy spectrum at mountain altitude by EAS-TOP"
   SIF Conference Proceedings, **68**, 11 (2000)

5. "Cosmic Rays Physics around the knee of the primary spectrum"
   SIF Conference Proceedings, **68**, 15 (2000)

6. "Study of UHE cosmic neutrinos through horizontal extensive air showers"
   in "Neutrino Mixing", World Scientific, 163 (2000)

GNO. Gallium Neutrino Observatory

M. Altmann[a], M. Balata[b], P. Belli[c], E. Bellotti[d], R. Bernabei[c], E. Burkert[e], C. Cattadori[d], G. Cerichelli[f], R. Cerulli[c], M. Chiarini[e], M. Cribier[g], S. d'Angelo[c], G. Del Re[f], K. Ebert[h], F. von Feilitzsch[a], N. Ferrari[b], W. Hampel[e], J. Handt[e], E. Henrich[h], G. Heusser[e], J. Kiko[e], T. Kirsten[e], T. Lachenmaier[a], J. Lanfranchi[a], M. Laubenstein[b], D. Motta[d,e], H. Richter[e], W. Rau[e], S. Wänninger[a], M. Wojcik[i], L. Zanotti[d]

[a] Physik Department E15, Technische Universität München (TUM), James-Franck Straße, D-85748 Garching b. München, Germany

[b] INFN, Laboratori Nazionali del Gran Sasso (LNGS), S.S. 17/bis Km 18+910, I-67010 L'Aquila - Italy

[c] Dip. di Fisica, Universitá di Roma "Tor Vergata" and INFN, Sez. Roma II, Via della Ricerca Scientifica, I-00133 Roma - Italy

[d] Dip. di Fisica, Universitá di Milano "Bicocca", and INFN Sez. Milano, Via Emanueli, I-20126 Milano - Italy

[e] Max-Plank-Institut für Kernphysik (MPIK), P.O.B. 103980, D-69029 Heidelberg - Germany

[f] Dip. di Ingegneria Chimica e Materiali, Universitá dell'Aquila, Localita' Monteluco di Roio, L'Aquila - Italy

[g] DAPNIA/Service de Physique de Particules, CE Saclay, F-91191 Gif-sur-Yvette Cedex - France

[h] Institut für Technische Chemie, Forschungszentrum Karlsruhe (FZK), Postfach 3640, D-76021 Karlsruhe, Germany

[i] Instytut Fisyki, Uniwersitet Jagiellonski, ul. Reymonta 4, PL-30059 Krakow - Poland

Abstract

GNO (Gallium Neutrino Observatory) is monitoring the low energy solar neutrino flux with a 30 tons gallium detector at LNGS. During the year 2000, 12 solar runs and 5 blank runs have been successfully done; in total 30 solar runs (corresponding to $\approx$ 850 days of live time) have been accumulated since spring 1998 when GNO started the data taking. The result of the first 19 solar runs (GNO-I) is: 65.8 $^{+10.2}_{-9.6}$ (stat.) $^{+3.4}_{-3.6}$ (sys.) SNU. The combined result from both GNO-I and GALLEX (I-IV) together is 74.1 $\pm$5.4 (stat.) $^{+4.0}_{-4.2}$ (sys.) SNU. The various activities performed during 2000 and the R&D in progress are also reported.

1 Introduction

The gallium solar neutrino experiment at Laboratori Nazionali del Gran Sasso detects solar neutrinos via the reaction $^{71}Ga\,(\nu_e, e\,)^{71}Ge$, which has a threshold of 233 keV. The detector is sensitive mainly to pp-neutrinos (53% of the interaction rate according to the standard solar model [1]), with smaller contributions to the signal from ^{7}Be ν (27%), ^{8}B ν (12%), and CNO ν (8%).

The target consists of 101 tons of a $GaCl_3$ solution in water and HCl, containing 30.3 tons of natural gallium; this amount corresponds to $\sim 10^{29}\,^{71}Ga$ nuclei.

The ^{71}Ge atoms produced by solar neutrinos (at a rate of about 0.7 per day, one half of the amount predicted by solar models) are extracted from the gallium tank every 4 weeks [2] and introduced in low-background gas proportional counters [3] as germane gas (GeH_4). The decay of ^{71}Ge (e.c., τ=16.5 days) produces a signal in the counters consisting of a point-like ionization at 10.4 keV, or 1.1 keV. The signal is recorded by fast digitizers to allow background reduction by pulse shape analysis. The solar neutrino interaction rate on ^{71}Ga is deduced from the number of ^{71}Ge atoms observed. For a complete description of the experimental procedure see [4].

The gallium detector was operated between 1991 and 1997 by the GALLEX collaboration: 65 'solar runs' were performed. The solar neutrino capture rate on ^{71}Ga was measured with a global uncertainty of 10 % as: 77.5 $\pm$ 6.2 (stat.) $^{+4.3}_{-4.7}(sys.)$ SNU [1] (1σ) [4]. This result has important physical implications both for astrophysics and for particle physics (for discussion see for example [5]).

After maintenance of the chemical plants and renovation of the DAQ and electronics, a new series of measurements was started in April 1998, within the GNO (Gallium Neutrino Observatory) project [6]. The experiment is presently running with 30 tons of gallium (GNO30). The goals of GNO are:
- measurement of the interaction rate of low energy solar neutrinos on gallium, with an accuracy of 4-5% (half of the error achieved in GALLEX);
- monitoring of the neutrino flux over a complete solar cycle.

The importance of these goals is evident when one considers that the only experiments sensitive to the main component of the solar neutrino flux (the pp neutrinos) which can operate in the next decade are those based on the use of gallium. The ^8B neutrino flux has been measured with high accuracy by the Superkamiokande experiment; the ^7Be ν flux is

[1] 1 SNU (Solar Neutrino Unit) = 10^{-36} captures per second and per absorber nucleus

going to be directly measured by the Borexino and Kamland experiments. Therefore, the achievement of a good precision in the measurement of the neutrino interaction rate on gallium represents a unique possibility to probe the pp component in the solar neutrino flux within a few percent.

In section 2 we discuss the GNO solar neutrino observations and the results obtained from the first 19 GNO extractions (GNO-I, 574 days of live time). In section 3 we report the experimental activity carried on during 2000; In section 4 we describe several items of the R&D activity in progress.

2 Results on solar neutrino observations

GNO started solar neutrino observations in May 1998: the complete list of runs is reported in Table 1. 12 solar runs and 5 blank runs were successfully performed in the year 2000. At the beginning of January 2001, counting is completed for 25 solar runs; other 5 solar runs are still counting.

Data from the first 19 GNO solar runs (GNO-I, from May 1998 until January 2000) have been evaluated.

Pulses with amplitudes compatible with L and K captures (corresponding respectively to 1.1 and 10.4 keV) are selected according to their shape. Genuine ^{71}Ge decays give a characteristic signal on the fast digitizer; they produce a point-like ionization in the counting gas: the recorded pulses are fast compared to most background events. For the pulse shape discrimnation we use a one parameter cut. We consider the rise-time (RT) from 8% to 60% of the pulse amplitude. RT is required to be less than about 40-45 ns, depending on the specific counter and gas mixture. The cut has a high efficiency for ^{71}Ge signals ($\geq$ 95%) and rejects most background. The remaining backgrounds in the acceptance windows are then rejected on the basis of the time momenta of the pulses (maximum likelihood analysis).

In figure 2 we show in the E-RT plane the counts observed in the GNO solar runs: in fig 2(b) are plotted all the counts detected during the first two ^{71}Ge halflifes (0-33 days) after start of counting; fig. 2(c) shows all counts detected in the time window 100-133 days; fig. 2(a) shows, for comparison, the ^{71}Ge signal observed in a counter calibration (see section 3.2). Notice the excess counts due to ^{71}Ge decays in plot (b), compared to plot (c).

The result of the maximum likelihood analysis identifies a total of 90 decaying ^{71}Ge atoms that were observed during 574 days of neutrino exposure in solar runs SR1-SR19. The corresponding ν interaction rate for GNO-I is 65.8 $^{+10.2}_{-9.6}$ (stat.) $^{+3.4}_{-3.6}$ (sys.) SNU [7]. The combined result for GALLEX and GNO-I (65+19=84 solar runs) is 74.1 $\pm$5.4 (stat.) $^{+4.0}_{-4.2}$ (sys.) SNU [7]. The overall error is 9 %. Results from the single solar runs are plotted in Figure 1 as a function of the extraction time both for GALLEX and for GNO-I.

For further information on the GNO-I results, their interpretation, data analysis, and a discussion of the systematic of the experiment see reference [7].

Table 1: Summary of GNO runs performed between April 1998 and January 2001. For each extraction the following data are reported: extraction label; extraction type (SR=Solar Run, BL=BLank); extraction date, referred to the end of the extraction; exposure time in days; counter type and number used for ^{71}Ge counting (Fe=Iron cathode, Si=Silicon cathode, FC=Iron shaped cathode, SC=Silicon shaped cathode); counting time; chemical yield (tank to counter), measured by non-radioactive Ge carrier. Status at 09-Jan-2001.

Extraction	Type	Date	Exposure (days)	Counter	Counting time (days) (09-Jan-2001)	Chemical yield (%)
A1	-	23-apr-98		Fe-112	-	94.2
A2	-	20-may-98	28	Si-106	-	96.1
A3	SR1	17-jun-98	28	SC-138	179.6	96.1
A4	SR2	22-jul-98	35	Fe-118	173.5	93.5
A5	SR3	26-aug-98	35	Si-114	162.3	95.1
A6	SR4	23-sep-98	28	Si-113	138.3	97.9
A7	SR5	21-oct-98	28	FC-093	137.7	94.6
A8	SR6	18-nov-98	28	Si-108	166.5	94.5
A9	SR7	16-dec-98	28	SC-136	180.6	94.4
A10	SR8	12-jan-99	28	FC-102	179.4	96.4
A11	SR9	09-feb-99	28	SC-135	194.7	95.8
A12	-	10-mar-99	28	-	-	Ge lost
A13	SR10	14-apr-99	35	SC-139	187.4	94.6
A14	SR11	19-may-99	35	Fe-039	180.4	96.3
A15	SR12	16-jun-99	28	Fe-112	179.4	95.7
A16	SR13	28-jul-99	42	SC-136	165.8	94.4
A17	SR14	25-aug-99	28	FC-093	167.6	96.0
A18	SR15	22-sep-99	28	FC-102	165.6	97.1
A19	SR16	20-oct-99	28	Si-113	165.4	95.7
A20	SR17	17-nov-99	28	SC-139	166.5	95.6
A21	SR18	14-dec-99	27	Fe-039	166.6	94.7
A22	SR19	13-jan-00	29	Si-106	166.5	91.5
A23	BL1	14-jan-00	1	SC-138	164.5	96.0
A24	SR20	09-feb-00	27	Si-108	164.6	91.2
A25	SR21	08-mar-00	28	FC-093	167.8	94.8
A26	SR22	05-apr-00	28	FC-174	166.6	97.7
A27	BL2	06-apr-00	1	FC-102	165.5	95.1
A28	SR23	03-may-00	27	SC-136	167.8	94.7
A29	SR24	31-may-00	28	Fe-039	165.8	93.0
A30	-	28-jun-00	28	SC-139	HV unstable	98.1
A31	BL3	29-jun-00	1	FC-126	164.1	93.9
A32	SR25	26-jul-00	27	Si-106	167.7	93.9
A33	SR26	23-aug-00	28	SC-138	139.6	94.1
A34	SR27	20-sep-00	28	Si-108	111.6	97.2
A35	BL4	21-sep-00	1	FC-093	110.6	96.2
A36	SR28	18-oct-00	27	FC-174	83.6	95.4
A37	SR29	15-nov-00	28	FC-102	55.5	93.9
A38	SR30	13-dec-00	28	SC-136	27.4	98.1
A39	BL5	14-dec-00	1	Fe-039	26.3	95.0

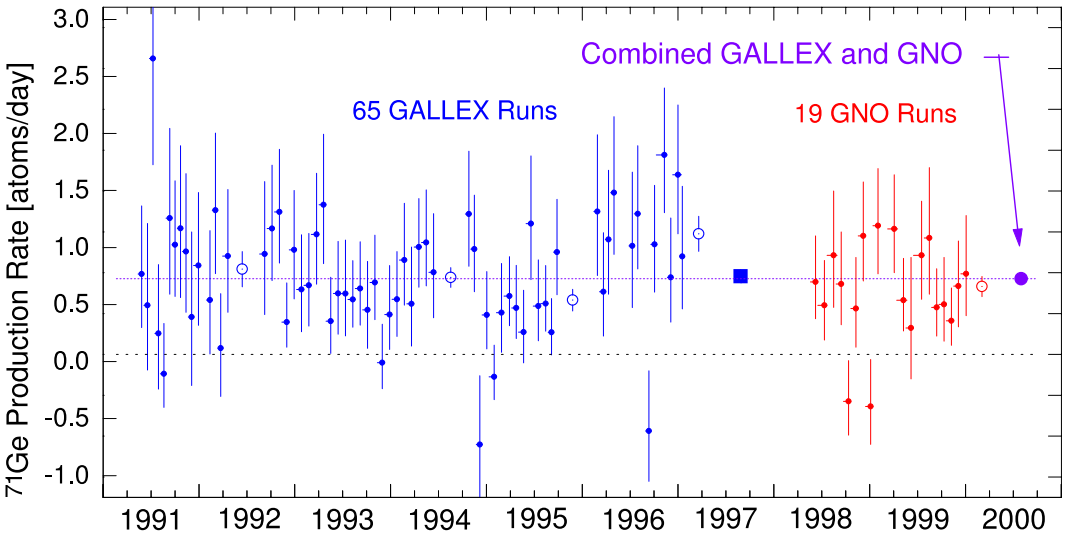

Figure 1: Measured solar neutrino capture rate (atoms/day) in the single 65 GALLEX solar runs, and in GNO solar runs SR1-SR19 (GNO-I). A signal of 100 SNU corresponds to a production rate of 0.90 ^{71}Ge atoms per day inside the 30 tons gallium tank.

3 Experimental activity during 2000

3.1 Extraction system and synthesis line

During 2000 the following activities were performed at the extraction and synthesis plants:
-maintenance of the main building itself: care of the structure, of the electrical plant, water distribution piping etc;
-maintenance of gallium tank, absorber plant, auxiliary plants;
-maintenance of the building safety equipment: building ventilation system, tank leak sensor; HCl leak detector;
-preparation and carrying out of 18 extractions, see table 1;
-46 kg of highly pure HCl were added to the 53 m^3 of the gallium solution (about 3 Kg of HCl are removed during each run for extracting the ^{71}Ge);
-Atomic absorption analysis has been carried out for each run to control the extraction yield;
-in collaboration with the L'Aquila University Chem. Eng. department several tests were performed, to further study the behaviour of the Ge during absorption in the columns and during the acidification.

3.2 Electronics and DAQ system

The improvement on the electronics set-up as compared with the GALLEX one was described in the previous LNGS annual reports [8] [9]. During 2000 the counting system was upgraded to 16 independent lines. All HV modules have been changed, leading to a rms noise figure of few mV namely a S/N$_{electronics}$ of 300 and 40 respectively in the K and

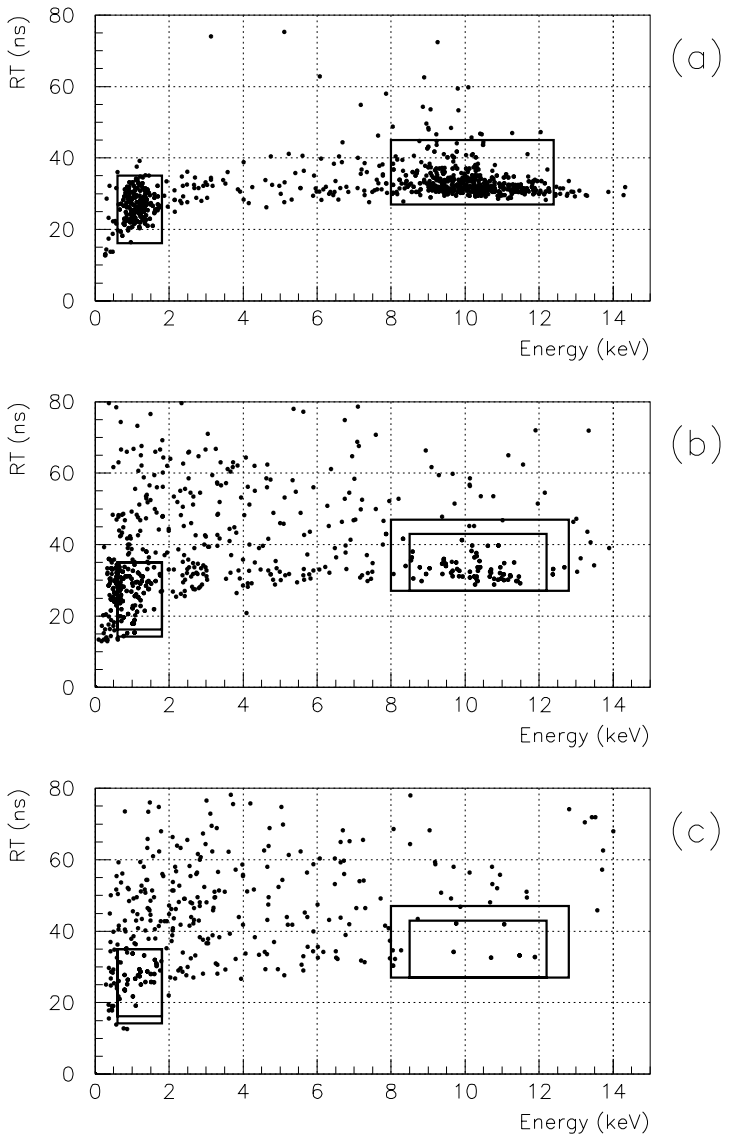

Figure 2: Scatter plot energy vs rise-time: (a) ^{71}Ge calibration, (b) counts detected in the GNO solar runs SR1-SR32 during the first 2 ^{71}Ge meanlifes after start of counting (c) all counts detected in the time window 100-133 days after the start of counting. The boxes represent the L fast window (energy around 1.1 keV) and the K fast window (energy around 10.4 keV), where the ^{71}Ge signal concentrates. Notice the excess counts due to ^{71}Ge decays in plot (b), compared to plot (c). The excess counts attributed to ^{71}Ge are evaluated by a maximum likelihood analysis of the time momenta of each event inside the selection windows.

L regions. The anticoincidence NaI installed in the lead tank has been recovered [10]; the 8 counter positions on this active side are now ready to host counters if needed.

3.3 ^{71}Ge calibrations

In order to determine the efficiencies of the pulse shape algorithms applied in the data analysis, two counters were filled with ^{71}Ge. The sample was prepared by neutron irradiation of a Ge chip (about 60 mg) at the TUM reactor (December 1999); the activated Ge was sent to Heidelberg where it was dissolved, diluted, converted to GeH_4 and inserted into two counters (Fe043 and Si119): counting has been carried out in the same conditions (shielding, electronics and DAQ) as for solar run counters. The efficiency used for the RT cuts was determined within 1.5 %, and is used for the analysis of solar runs[7].

3.4 Radon test

The experience with GALLEX has shown that a few Rn atoms are sometimes introduced in the counters during the synthesis and counter filling operations. The decays of Rn and its daughters can produce events which simulate real ^{71}Ge events, and are concentrated in the first days of counting (the half-life of ^{222}Rn is 3.83 days). A 'Rn cut' is introduced in the data analysis, by defining a dead time for each detected Rn decay chain (see [11] for details). The efficiency of this cut was evaluated in GALLEX to be (91 $\pm$ 5)%, and the uncertainty on that number represents a relevant component of the systematic error in the experiment ($\approx$ 1.5 %, see [7]). A Rn test started in 1999 to further improve the characterization and understanding of Rn events and to decrease the systematic uncertainty due to the Rn cut. A Ra source was introduced in a proportional counter, releasing few Rn atoms per day in the counter gas; in fact one needs a low Rn activity (of the order of 4-5 Rn chains per day) in order not to overlap different chains, disentangle the single decays in the chain, and collect a large statistic. The decay of the Rn atoms and its daughters is recorded with the same electronics and DAQ used for standard runs; the measurement is going on since one year. The analysis of the data acquired allows a good understanding of the Rn chain events; in particular we managed to extract the E-RT (energy-rise-time) distribution for α particles, β particles and recoil nuclei (see figure 3). Concerning the determination of the Rn cut efficiency, preliminary results are in agreement with the previous GALLEX estimates, but the expected uncertainty should decrease to 3 % or less; the corresponding systematic error on the neutrino interaction rate will be less then 1 %.

4 R&D in progress

4.1 Data analysis

Data analysis is carried on with the energy-rise-time method described in section 3; a more sophisticated pulse-shape analysis based on fitting the whole pulse rather than the rise-time only is under study. Each pulse is fitted with the typical point-like ionization pulse (reconstructed from the X-ray counter calibration, see [9]) convoluted with a charge collection function. The width of the collection function is proportional to the spreading

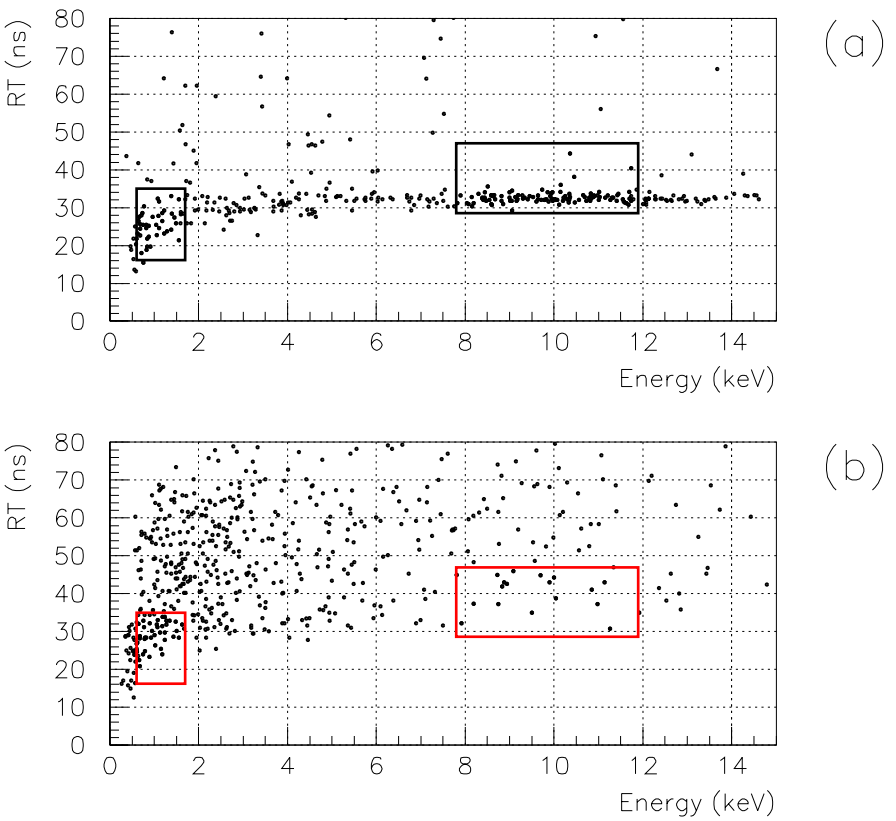

Figure 3: Energy vs rise-time plot for Rn calibration: (a) events due to recoil Pb nuclei in the α decay $^{218}Po \rightarrow ^{214}Pb$ transition; (b) events due to β particles in the $^{214}Pb \rightarrow ^{214}Bi$ β decay. For the interpretation of the distributions see the text.

of the primary charge inside the counter gas. Cuts can be defined on several parameters of the charge collection function. The possibility to employ a neural network defined on the fitted pulse parameters is also under study.

4.2 Developement of new detectors

Proportional counters developed for GALLEX [3] are used in GNO to detect the ^{71}Ge decay; they have been optimized to have an extreme low background, typically 1 count/10 days, in the relevant parameter regions, and have shown to be very easy to use and reliable instruments. Even if it is an ambitious program, the collaboration aims to improve the ^{71}Ge detection technique. The goal is to lower the systematic error on the counting efficiency, and if possible the energy resolution and the fraction of fully contained events, of course without a degradation of the S/N ratio. Beside the developement of new proportional counters at MPI Heidelberg (see [8]), the collaboration is working on two other techniques:

1. Cryogenic detectors

   At TUM a project is ongoing to test the feasibility of low temperature calorimeters as detectors for measuring the ^{71}Ge-decay [12]. With such detectors the ^{71}Ge extracted from the gallium tank together with the non-radioactive Germanium, is converted to GeH_4, and then thermally deposited on a substrate, which is then put in a cryostat to work as a thermal detector. During 1999 a detector with a 4π geometry was built and operated at TUM to detect a ^{71}Ge activity. The Ge layer was deposited on a sapphire crystal (lower detector); a second sapphire substrate (upper detector) recovers the X-rays eventually produced by the ^{71}Ge decay, and escaping the Ge layer from above. The ^{71}Ge calibration showed that the detector can work with the expected energy resolution and counting efficiency, which is near 98%. To meet the goals set by the experimental procedure of GNO some modifications in the 4π-detector design still have to be carried out to meet the goals set by the experimental procedure of GNO. The time window between extraction and measurement being very small due to the short half-time of ^{71}Ge ($T_{1/2}$ = 11,43d). First steps have been taken to develop a detector concept comprising the possibility of independently performing the chemical deposition of germanium via CVD (= chemical vapour deposition) onto a piece of superconducting foil, for instance Niobium and, in a second step, of integrating it via glueing in the detection apparatus itself. First measurements showed promising results, and are to be continued intensively in the next few months. Another crucial point for the implementation of a cryogenic detection concept in GNO is the deposition efficiency of the Germane gas (GeH_4) onto the cryogenic detector. Great efforts have been made to increase the efficiency of this CVD process: By means of very localized heating, using a miniaturized deposition chamber, reducing the volumes during the process and by increasing gas transfer efficiencies, the overall efficiency of the Ge deposition onto the surface of a cryogenic detector was significantly improved from first $\sim$1% to 70% and in a second step to $\sim$91%. The efficiency was determined using several independent methods of which the NAA (= Neutron Activation Analysis) proved to be the most

accurate one. The present efficiency of this CVD process being in the range of GNO's chemical extraction efficiency, further steps can now be taken towards a prototype run at the Gran Sasso Laboratory.

In order to show the feasibility of "Cryo-GNO" and to prepare the prototype phase at LNGS, a new dilution refrigerator has been set up in the Underground Laboratory (15 m.w.e) of the "Beschleunigerlaboratorium/Maier-Leibnitz-Laboratorium" in Garching.

2. Hybrid counters

   The idea is to merge a proportional miniaturized straw tube with a solid state device surrounding it with a 4π geometry: the straw tube, filled with a light gas mixture, will deserve the detection of 1 (or 10) keV Auger electrons and 1 keV X rays, while the 9 or 10 keV X rays will be detected in the sourrounding solid state device; the coincidence of the devices (35% probability for counter dimensions similar to the actual ones), will be a clear tagging of the event. This integrated detector need to be operated at LN temperature to have a few percent energy resolution in the solid state device.

4.3 Neutrino source

The gallium detector was calibrated two times (in 1994 and in 1995) with a man-made electron-neutrino source with known intensity [13]. A very intense (≈ 2 MCi) ^{51}Cr ν source was prepared for the calibrations at the Siloe reactor in Grenoble (France) and transported to LNGS after irradiation. ^{51}Cr is an isotope ideal for the calibration of the gallium detector: it has a meanlife of 40 days, and it emits neutrinos with two monochromatic lines at 750 keV (90 %) and 430 keV (10 %). The ratio R between the measured ^{71}Ge production rate and the expected production rate as deduced from the known source activity is $R = 0.93 \pm 0.08$ [14]. This proofs the absence of any unknown systematic errors are at a level of less than 10 %. The collaboration is evaluating the feasibility of a new source experiment, with the aim of measuring as accurately as possible the ν ^{71}Ga cross section at energies corresponding to those of the ^{7}Be solar ν.

Contacts have been started with the Research Institute of Atomic Reactors (RIAR) at Dimitrovgrad (Russia), for the evaluation of feasibility and costs of irradiation of the enriched Cr samples previously used in GALLEX.

5 Conclusions

The gallium detector at LNGS is monitoring low energy solar neutrinos since May 1991 with 30 tons of natural gallium. From the 65 GALLEX solar runs plus the 19 GNO I solar runs, the solar neutrino interaction rate on gallium has been measured with an overall accuracy of $\sim 9\%$. Data taking is going on regularely with four-week-exposure runs, with the aim to reach an accuracy of the order of 5%, and to study possible time dependences of the signal at 10-15 % level.

6 Acknowledgemnts

We would like to acknowledge Keith Rowley for his precious help in the synthesis work and the LNGS and other collaborating institute staffs, for the support continuously given for the conduction of the GNO experiment.

7 List of Publications

1. GNO collaboration, "GNO progress report for 1999", LNGS annual Report 1999, 57-68., GNO report n.12
2. M. Altmann et al., "Cryogenic detectors: a promising option for GNO?", Nucl.Inst.Meth. A444 (2000) 96-99, GNO report n.13
3. GNO collaboration, "GNO solar neutrino observations: results for GNO I", Phys.Lett. B490 (2000) 16-26., GNO report n.14

8 List of Conference Presentations

1. E. Bellotti, "First results from GNO", XIX International Conference on Neutrino Physics and Astrophysics Sudbury (Canada), June 14-21 2000.
2. T. Kirsten, "^{51}Cr and ^{75}Se neutrino sources", LowNu Workshop on Solar Neutrinos below 1 MeV, Sudbury (Canada), June 14-21 2000.
3. C. Cattadori "Solar neutrino results from GNO", XXX International Conference on High Energy Physics, Osaka (Japan), July 27 - August 2, 2000.
4. N. Ferrari, "GNO and its performances", Europhysics Neutrino Oscillation Workshop, Conca Specchiulla (Otranto), September 9-16 2000.
5. N. Ferrari, "GNO status and future perspectives", Low energy solar neutrino Workshop, Tokyo (Japan), December 4-5 2000.

References

[1] J.N. Bahcall, Phys. Rept. 333 (2000) 47-62; S. Turck-Chiéze et al, Nucl. Phys. (Proc. Suppl.) 87 (2000) 162-171; V. Castellani et al., Nucl. Phys. (Proc. Suppl.) 70 (1999) 301-314.

[2] E.Henrich, K.H.Ebert, Angew. Chemie Int. Ed. (Engl.) 31 (1992) 1283; E.Henrich et al., 'GALLEX, a challange for chemistry', Proc. IV Int'l. Solar Neutrino Conf., ed. W.Hampel, MPI Kernph., Heidelberg (1997) 151-162.

[3] R. Wink et al. Nucl. Inst. and Meth. A329 (1993) 541.

[4] GALLEX collaboration, Phys.Lett. B285 (1992) 376; Phys.Lett. B314 (1993) 445; Phys.Lett. B327 (1994) 377; Phys.Lett. B342 (1995) 440; Phys.Lett. B357 (1995) 237; Phys.Lett. B388 (1996) 384, Phys.Lett. B447 (1999) 127.

[5] T.Kirsten, Rev.Mod.Phys., 71 (1999) 1213-1232.

[6] E.Bellotti et al., GNO collaboration, LNGS report INFN/AE-96-27.

[7] GNO collaboration, Phys Lett. B 490 (2000) 16-26.

[8] GNO collaboration, LNGS annual report 1998, pag. 55-69.

[9] GNO collaboration, LNGS annual report 1999, pag. 57-68.

[10] G. Heusser, 'Characteristics of the GALLEX Spectrometer', Trends in Astroparticle Physics', ed. P. Ch. Bosetti, (1994) p.33, Teubner, Leipzig.

[11] H.Lalla, 'Zeitabhängiger Untergrund im GALLEX- Sonnenneutrino-Experiment', thesis, Ruprecht-Karls-Universität Heidelberg (1993).

[12] M.Altmann et al., Nucl.Inst.Meth. A444 (2000) 96-99.

[13] M. Cribier et al., Nucl. Inst. and Meth. A 378 (1996) 233-250.

[14] GALLEX collaboration, Phys Lett. B 436 (1998) 158.

HDMS. Dark Matter Search

H.V. Klapdor-Kleingrothaus*, A. Dietz, G. Heusser, St. Kolb,
I.V. Krivosheina, B. Majorovits, H. Strecker

* Spokesman of the Collaboration

Abstract

The Heidelberg Dark Matter Search (HDMS) is an experiment designed for the search for WIMP dark matter. It is using a special configuration of Ge detectors, to efficiently reduce the background in the low-energy region below 100 keV. The latest results from this experiment are discussed. The results from the prototype detector which was running from March 1998 until July 1999 in the Gran Sasso underground laboratory are summarized. The final setup started taking data in Gran Sasso in August 2000. The performance of the final detector setup is discussed.

1 Introduction

Weakly Interacting Massive Particles (WIMPs) are leading candidates for the dominant form of matter in our Galaxy. These relic particles from an early phase of the Universe arise independently from cosmological considerations in supersymmetric particle physics theories as neutralinos - the lightest supersymmetric particles.

Direct WIMP detection experiments exploit the elastic WIMP scattering off nuclei in a terrestrial detector [1]. However, detecting WIMPs is not a simple task. Their interaction with matter is very feeble ($\sigma \leq \sigma_{weak}$) and predicted rates in supersymmetric models range from 10 to 10^{-5} events per kilogram detector material and day [2, 3, 4, 5, 6] (see also Fig. 1). Moreover, for WIMP masses between a few GeV and 1 TeV, the energy deposited by the recoil nucleus is less then 100 keV. Thus, in order to be able to detect a WIMP, an experiment with a low-energy threshold and an extremely low radioactive background is required. Since the reward would be no less than discovering the dark matter in the Universe, a huge effort is put into direct detection experiments. More than 20 experiments are running at present and even more are planned for the future (for recent reviews see [7, 8, 9]).

2 Description of the experiment

In direct detection experiments looking for WIMPs one of the main goals is the reduction of background events since the sensitivity of experiments roughly scales with the obtained background level.

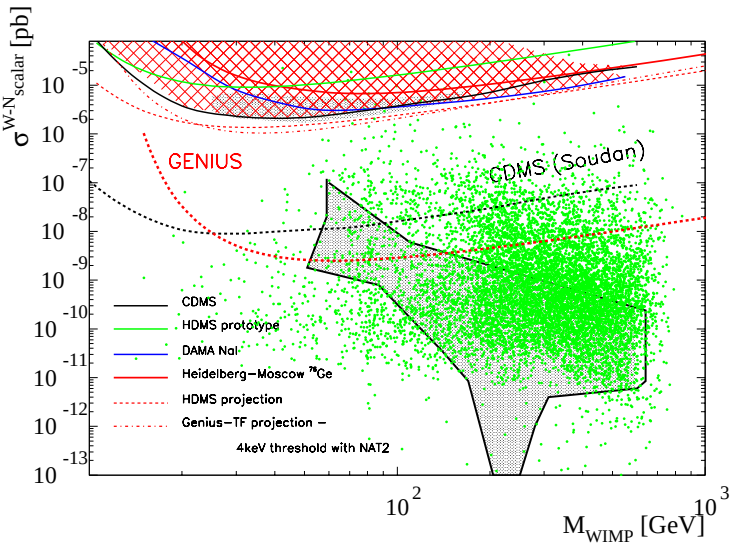

Figure 1: Exclusion plot of the scalar WIMP-nucleon elastic scattering cross section as a function of the WIMP mass. Plotted are excluded areas from the presently most sensitive direct detection experiments (hatched area, DAMA [10], CDMS [11], Heidelberg-Moscow [12], HDMS prototype[13] and some projections for experiments running or being presently under construction (HDMS [13], Genius TF [14]). The extrapolated sensitivities of future experiments (GENIUS [15], CDMS at Soudan [11]) are also shown. The scatter plot corresponds to predictions from theoretical considerations of the MSSM [6]. The small shaded area represents the 2σ evidence region from the DAMA experiment [16]. The large shaded area corresponds to calculations in the mSUGRA-inspired framework of the MSSM, with universality relations for the parameters at GUT scale [17] (Figure taken from [6]).

The Heidelberg-Dark-Matter-Search experiment (HDMS) uses the idea to operate two HPGe-detectors in a special configuration [18, 19] (see figure 2). A small (possibly enriched) detector is placed inside a bigger well type detector. The outer HPGe crystal acts both, as an active and as a passive shield: If an event is detected within both, inner and outer detector, it can be considered as a background event since for WIMPs it is extremely unlikely to scatter twice within such a short distance. Simulations have shown that for an optimal geometry a reduction in background by up to a factor of 20 can be achieved for the inner detector [19]. Furthermore the outer detector serves as a passive shield against external radioactivity for the inner detector. The design has the advantage that only extremely radio-pure material is in the direct vicinity of the inner detector since HPGe is one of the cleanest materials with respect to radiopurity that can presently be produced.

Table 1:
Technical data of the prototype detector of the HDMS experiment (from [20]).

Property	Inner Detector	Outer Detector
Crystal Type	p–type	n–type
Mass [g]	202	2111
Active Volume [cm^3]	37	383
Crystal diameter [mm]	35.2	84.4
Crystal length [mm]	40.3	86.2
Operation Bias [V]	+2500	-1500
Energy resolution FWHM (1332 keV) [keV]	1.87	4.45
Energy threshold [keV]	2.5	7.5

3 The prototype detector

A prototype detector with the mentioned special design was built by EG&G Ortec. Three of the four contacts of the detector were unfortunately soldered, thus resulting in radioactively contaminated material being close to the HPGe-crystals. The FETs which are the first preamplifier elements were placed 20 cm away from the crystal holder system being already outside the first 10 cm copper shield. This reduces the influence of the FET impurities onto the measurement to a negligible level. Both inner and outer crystals were made out of natural zone-refined high purity germanium. The most important properties of the detector are shown in table 1.

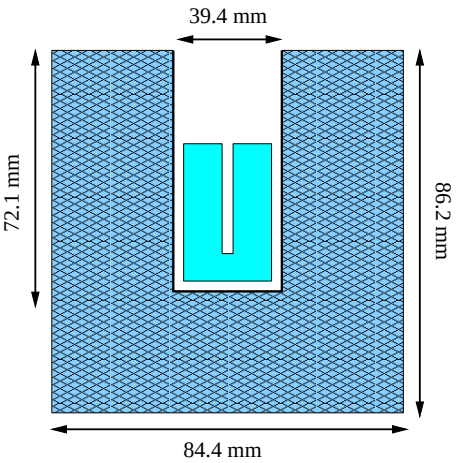

Figure 2: Schematic view of the HDMS detector configuration. All events which are seen in both the inner and the outer Ge-detector can be considered as background events, not resulting from a WIMP-nucleon recoil.

Property	Inner Detector prototype	Outer Detector prototype	Inner Detector ^{73}Ge	Outer Detector final setup
Threshold	(2.0±0.2)keV	(7.5±0.2)keV	(2.0±0.2)keV	(7.5±0.2)keV
Energy res.				
at zero keV	(1.06±0.30)keV	(3.04±0.10)keV	(0.76±0.05) keV	(2.82±0.06) keV
extrapol.				
at zero keV	(0.92±0.01)keV	(3.34±0.01)keV	(0.83±0.01)keV	(2.91±0.04) keV
correction				
at 81 keV	(1.15±0.03)keV		(0.95±0.03) keV	
at 344 keV		(3.62±0.03)keV		(3.03±0.03)keV
at 1408 keV		(4.55±0.03)keV		(4.46±0.02)keV

Table 2: Energy resolutions for different energies and thresholds of the two detector configurations, prototype setup and final setup.

3.1 The anti-coincidence and the crosstalk

Due to the special concentric design, the spatial separation between the two detectors is very small. This gives rise to pick-up signals. If one of the detectors sees an event, a cross talk signal is induced in the other one.

Recording spectra of calibration sources with the list mode allows to visualize this pick-up signal (see Fig. 6). The anti-coincidence cut between the two detectors to recognize multiple scattered background events can only be applied, if the cross talk is eliminated. This cut is made by defining all events as background events, in which an energy deposition is seen in both detectors above the energy threshold of the proper detector.

It was shown that the cross talk is linear with energy and stable over time and can be corrected for off-line [20]. Once the correction is made, the anti-coincidence can be applied. The suppression factor for compton scattered events is about a factor of four for the inner detector in the relevant energy region for WIMP dark matter search (below 50 keV, see Fig. 3). Note, however, that in the sum spectrum the peaks resulting from the X-rays do not vanish through the anti-coincidence cut, since they result from the internal contamination of the HPGe-crystals with cosmogenically produced isotopes.

3.2 Measurements at the Gran Sasso underground laboratory

The HDMS prototype detector was installed at the LNGS in March 1998 and successfully took data for approximately 15 months until July 1999 with a total life time of 362.91 days [13].

The time stability of the energy resolution, threshold and calibration parameters (slope and intercept of energy calibration) has been checked elsewhere [13, 21]. The measured energy resolutions and thresholds of the detectors are listed in Tab. 2. They correspond to standard values for detectors of this size.

The individual typical duration of a run was about 23 hours. The experiment was stopped daily and the most important detector parameters like leakage current and mean count rates were checked. No substantial fluctuations were recorded. For a detailed

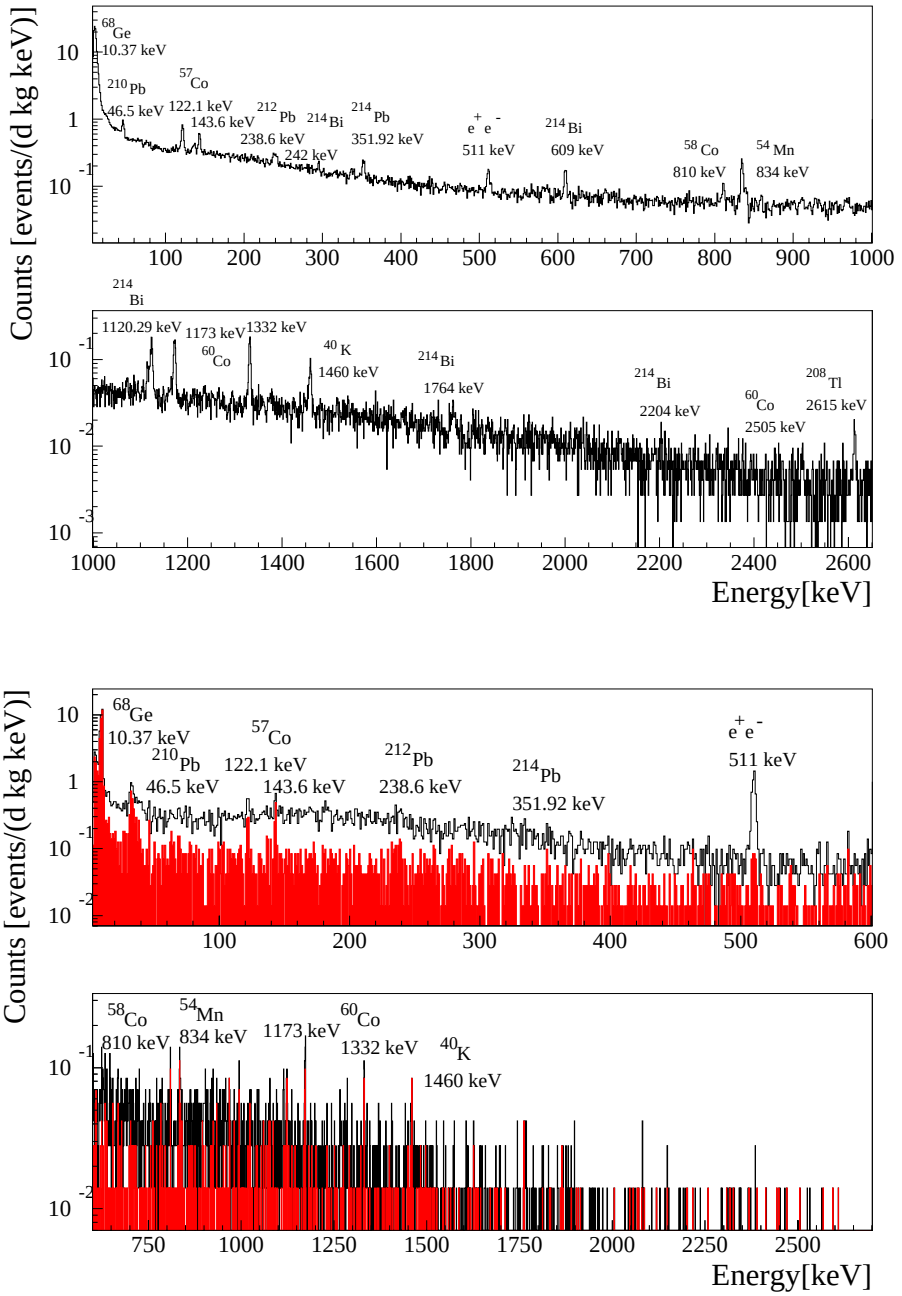

Figure 3: Spectra of the HDMS detectors of the prototype setup after a total measuring time of 362.91 days. Upper two panels: outer detector; lower two panels: inner detector; The open histogram denotes the overall spectrum, the filled histogram corresponds to the spectrum after the anti-coincidence cut with the outer detector (from [13]).

discussion of the time behavior of the prototype see [13, 21].

3.3 Results from the prototype detector

After the individual runs were calibrated and corrected for the crosstalk, they were added to provide the sum spectra. From the sum spectrum of the inner detector (after the anti-coincidence cut) the limits on WIMP dark matter can be extracted.

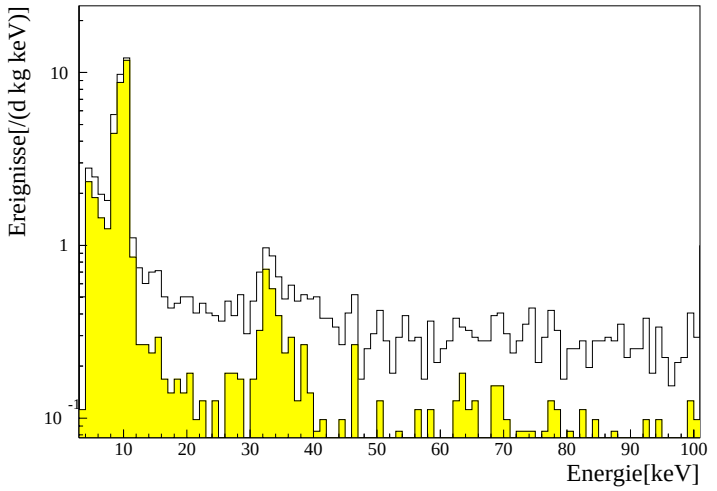

Figure 4: Low-energy spectrum of the inner, naturl Ge detecor before and after (open and solid histograms, respectively) the anti coincidence is applied with the outer Ge detector. The internal, low-energy x rays, as well as the structure centered at 32 keV are not removed by the anti-coincidence.

3.3.1 The sum spectra

The spectra of the full time measurement for both detectors are shown in figure 3.

The most prominent structures in the outer detector mainly result from the U/Th decay chains, primordial ^{40}K and some cosmogenic isotopes. Clearly visible is a smeared out structure at approximately 5 MeV, indicating the presence of a α-contamination within the detector cap.

Although the statistics of the inner detector is lower, some structures can already be identified. The most obvious structure is a peak at 10.37 keV resulting from the decay of ^{68}Ge. Also here some peaks resulting from the U/Th decay chains and other cosmogenic isotopes can be identified. Note also the existence of a peak at 46.5 keV indicating the presence of a ^{210}Pb contamination. The structure visible at 32.5 keV is slightly smeared out having a full width of half maximum of 2.0 keV (compare to the energy resolution at 300 keV: 1.15 keV). The origin of this structure could not yet be identified.

After the anti-coincidence cut the count rate of the inner detector undergoes a reduction of a factor of 4.3 in the energy region above 40 keV (see Fig. 4 for the sum spectrum in the low-energy region before and after the anti-coincidence cut). The peak at 10.37 keV is, as expected, not affected by the anti-coincidence since the decays of ^{68}Ge take place

Table 3: Number of counts per 1 keV energy bin after an exposure of 9.9 kg d.

Bin [keV]	Counts/keV	Bin [keV]	Counts/keV
2-3	1	25-26	1
3-4	2	26-27	1
4-5	7	28-29	3
5-6	6	29-30	0
6-7	11	30-31	0
7-8	8	31-32	0
8-9	12	32-33	1
9-10	38	33-34	3
10-11	37	34-35	4
11-12	1	35-36	4
12-13	1	36-37	1
13-14	1	37-38	1
14-15	2	38-39	3
15-16	1	39-40	2
16-17	0	40-41	1
17-18	1	41-42	0
18-19	0	42-43	2
19-20	3	43-44	1
20-21	1	44-45	0
21-22	0	45-46	0
22-23	0	46-47	1
23-24	0	47-48	0
24-25	1	48-49	2

within the detector itself thus leading to full energy deposition in one detector only. The structure at 32.5 keV does not vanish after the cut either.

3.3.2 Dark Matter limits

Since many cosmogenic isotopes have half lifes below 300 days, typically the count rate in low-level detectors decreases considerably after one year of storage underground.

For this reason only the last 49 days, corresponding to 9.9 kg d of measurement for the inner detector was used for the evaluation of the HDMS prototype data. Table 3 shows the number of counts per 1 keV energy bin after an exposure of 9.9 kg d (from [13]). The procedure of extracting limits on WIMP dark matter from the obtained spectrum follows the method described in [12]. The background index in the energy region between 2 keV and 30 keV was 0.5 counts/(kg keV d). No further background subtraction was applied, i.e. the raw spectrum was used for the analysis, without cutting out the prominent x-ray structures around 10 keV or the peak at 32.5 keV.

The resulting upper limit is shown in the exclusion plot in figure 5. Already with the prototype detector the limit could be considerably improved with respect to the Heidelberg–Moscow $\beta\beta$ experiment in the WIMP Mass region below 40 GeV. This is due to the

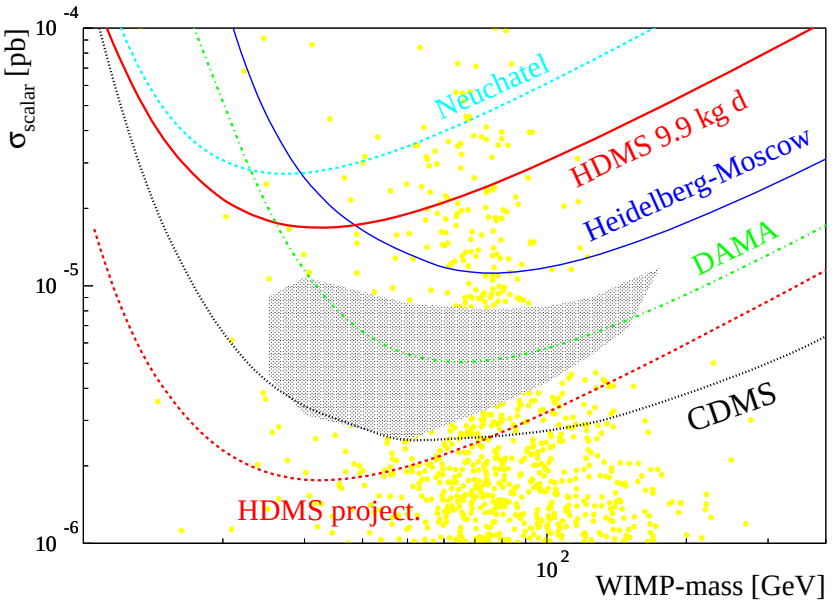

Figure 5: Exclusion plot for the presently most sensitive WIMP dark matter direct search experiments. It is visible that for low WIMP masses the HDMS prototype experiment is already now more sensitive than the Heidelberg–Moscow $\beta\beta$ experiment. Also shown are the present limits from the DAMA experiment [10], the CDMS experiment [11] and the Neuchatel experiment [22] (the latter not corrected for its known overestimation of its sensitivity by a factor of $\sim$3).

fact that an energy threshold of 2 keV has been obtained for this measurement (compare to 9 keV threshold of the Heidelberg–Moscow $\beta\beta$ experiment [12]).

4 The final HDMS setup: first results

The detector discussed so far was in many senses only a prototype. The basic goal of this setup was to prove the feasibility of the anti-coincidence technique.

For the final setup some important changes have been made. These will be discussed in the following, before discussing the detector performance.

4.1 Construction of the ^{73}Ge inner crystal

In low-level setups it is essential to avoid any materials with radio contamination.

As has been shown in considerations and simulations of the background spectrum measured with the HDMS prototype detector [13, 24], the main background components seem to result from the following sources:

- Contamination of the natural HPGe inner crystal with cosmogenically produced isotopes, especially ^{68}Ge (10.37 keV peak).

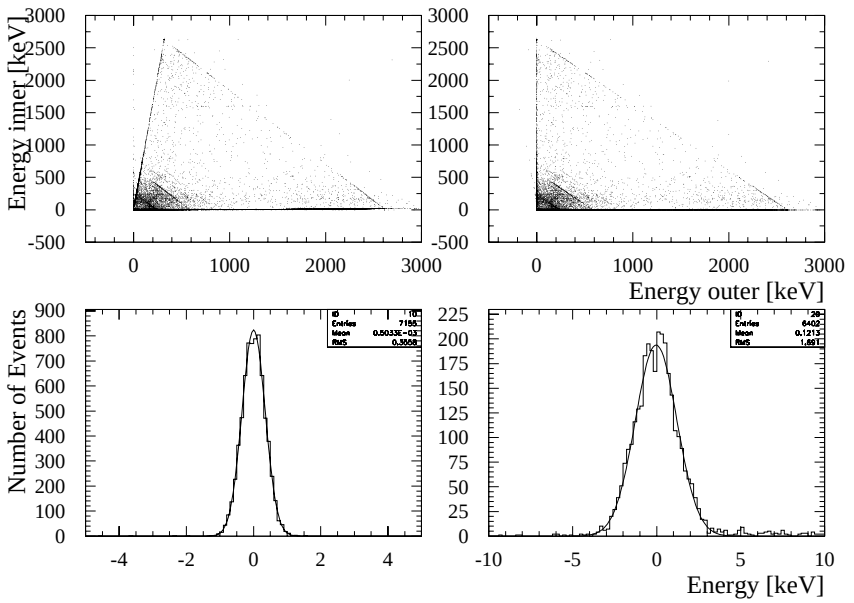

Figure 6: Upper panel: Scatter plot of ^{228}Th calibration measurement. Each dot corresponds to one event. The y- and x-axis display the energy deposited in the inner- and outer detector, respectively. Left: Before the correction for pick-up signals the zero energy axes have a non-zero slope. Right: After the correction the zero energy axes correspond to the y- and x- axes. Lower panel: Projection of the zero energy axis onto the energy axis of the second detector. For good correction the distribution of the events has to be Gaussian around zero. Left: Projection onto energy axis of the inner detector. The FWHM of the peak is (0.81±0.01) keV. Right: Same as left for the outer detector. The FWHM is (2.91±0.03) keV.

- Soldering tin used for contacting of the detectors (α-peak at 5 MeV).
- U/Th contamination of the crystal holder system which was built out of copper provided by EG&G Ortec (now Perkin Elmer).

To further reduce the background of the final setup with respect to the prototype detector, changes were done at the identified background sources. The following modifications were done for the final installation of the HDMS detector with respect to the prototype one (see [23]):

- The inner detector has been replaced by a crystal grown out of HPGe material enriched in ^{73}Ge. This has the effect that the mother isotope of cosmogenic ^{68}Ge production, ^{70}Ge (^{70}Ge(n,t)^{68}Ge), is deenriched by up to a factor of 50. Thus the decay of ^{68}Ge will be suppressed by this factor with respect to a natural HPGe crystal.
- The contacts of the HPGe crystals were pinched in order to avoid the use of soldering tin inside the detector cap.

- The crystal holder system has been replaced. The new material is from the same sample as the material used in the Heidelberg–Moscow $\beta\beta$ experiment, which is known to be very clean.

This detector system was installed at Perkin Elmer (formerly EG&G Ortec), Oak Ridge, Tennessee, USA, and shipped to Heidelberg, where some test measurements were made, before installation in its final location. Some of the important parameters will be discussed in the next section.

4.2 Basic parameters from measurements at Gran Sasso

After checking the stability of the detector system in the Low Level Laboratory in Heidelberg, the detector was transported to the Gran Sasso Underground Laboratory in Italy. It was installed in its low-level surrounding, shielded by 10 cm low activity electro-polished copper followed by an outer subsequent 20 cm Boliden lead layer. A 15 cm thick borated polyethylene shield against neutrons completes the setup.

The energy resolutions obtained from calibration measurements for inner and outer detector are shown, together with the old reference values, in table 1. Apparently the performance of both detectors could be slightly improved with respect to the prototype.

The behaviour of the pick-up signal of the new setup is shown in figure 6.

Once the correction for crosstalk has been made, it is possible to obtain the zero energy resolution of the detector. The pick-up events of a detector follow a Gaussian distribution around the zero energy axis. Thus, if the correction is good, the projection of all zero events of the first detector onto the energy axis of the second detector yields a peak at 0 keV with proper Gaussian shape. The width of the peak corresponds to the zero energy resolution of the second detector. This is seen for the inner and outer crystals in the lower left and right panel of figure 6, respectively. The resolutions are (0.81±0.01) keV for the inner and (2.91±0.03) keV for the outer detector. This is in good agreement with the extrapolated zero energy resolution from the calibration measurement which yields (0.76±0.05) keV and (2.82±0.06) keV for the inner and outer detector, respectively (see also table 1). Again it is apparent that an improvement has been achieved for both detectors with respect to the prototype.

The basic parameters denoting a stable detector performance have been checked regularly. Each week an energy calibration is made using standard ^{133}Ba and ^{152}Eu-^{228}Th sources. The energy resolution remained stable over time slightly around 1 keV for the inner detector below 400 keV.

5 Conclusion

The prototype detector of the HDMS experiment successfully took data at LNGS over a period of about 15 months. Most of the background sources (with exception of the 32 keV structure in the inner detector) were identified. The background reduction factor in the inner detector through anti-coincidence is about 4. The background in the low-energy region of the inner detector (with exception of the region still dominated by cosmogenic activities) is already comparable to the most sensitive dark matter search experiments.

For the final experimental setup, important changes were made. The crystal holder was replaced by a holder made of ultra low level copper, the soldering of the contacts was avoided, thus no soldering tin was used in the new setup and finally the inner crystal made of natural Germanium in the described prototype was replaced by an enriched ^{73}Ge crystal. In this way, the ^{70}Ge isotope (which is the mother isotope for ^{68}Ge production) is strongly de-enriched.

After a period of test measurements in the low-level laboratory in Heidelberg, the full scale experiment was installed at LNGS in August 2000. The energy threshold of the inner detector is unchanged at 2.0 keV and the energy resolution has slightly improved with respect to the prototype detector [23].

References

[1] M. W. Goodman and E. Witten, Phys. Rev. D **31**(1985)3059.

[2] G. Jungmann, M. Kamionkowski, K. Griest, Phys. Rep. **267**(1996)195

[3] V. Bednyakov, H.V. Klapdor–Kleingrothaus, S.G. Kovalenko, Y. Ramachers, Z. Phys. A **357**(1997)339

[4] Bottino et al., hep-ph/0001309.

[5] V. Bednyakov, H.V. Klapdor-Kleingrothaus, Phys. Rev D **62**(2000)043524 and hep-ph/9908427

[6] V. Bednyakov, H.V. Klapdor-Kleingrothaus, hep-ph/0011233

[7] H.V. Klapdor-Kleingrothausand Y. Ramachers, Euro. Phys. J. A **3**(1998)85

[8] L. Baudis and H.V. Klapdor-Kleingrothausin *Proc. of Beyond the Desert 1999*, ed. by H.V. Klapdor–Kleingrothaus, I.V. Krivosheina (IOP Bristol 2000), p.881

[9] Y. Ramachers, astro-ph/9911260 and in Proc. XI Rencontres de Blois, Frontiers of Matter, France, June 27 - July 3, 1999

[10] R. Bernabei et al., Nucl. Phys. B (Proc. Suppl) **70**(1998)79

[11] CDMS Collaboration, R. Abusaidi et al. Nucl. Inst. Meth. A **444**(2000)345, Phys. Rev. Lett. **84**(2000)5699 and astro-ph/0002471

[12] HEIDELBERG MOSCOW COLLABORATION, Phys. Rev. D **59**(1999)022001 and Preprint hep-ex/9811045

[13] L. Baudis, A. Dietz, B. Majorovits, F. Schwamm, H. Strecker, H.V. Klapdor-Kleingrothaus, Phys. Rev. D **63**(2000)022001, astro-ph/0008339

[14] L. Baudis, A. Dietz, G. Heusser, B. Majorovits, H. Strecker, H.V. Klapdor-Kleingrothaus, submitted for publication, hep-ex/0012022

[15] H.V. Klapdor-Kleingrothaus, L. Baudis, G. Heusser, B. Majorovits, H. Päs, 'GENIUS: a Supersensitive Germanium Detector System for Rare Events', Proposal, MPI-H-V26-1999, hep-ph/9910205 (1999) and in *Proc. of Beyond the Desert 1999*, ed. by H.V. Klapdor–Kleingrothaus, I.V. Krivosheina (IOP Bristol 2000), pp. 915-1014

[16] R. Bernabei et al., Nucl. Phys. B (Proc. Suppl),**70**(1998)79.

[17] J. Ellis et al., Phys. Lett. B **481**(2000)304 and hep-ph/0001002

[18] L. Baudis, J. Hellmig, H.V. Klapdor-Kleingrothaus, A. Müller, F. Petry, Y. Ramachers, Nucl. Inst. and Meth. A **385**(1997)265

[19] L. Baudis, J. Hellmig, H.V. Klapdor-Kleingrothaus, B. Majorovits, Y. Ramachers, H. Strecker, Internal Report, Proposal MPI H-V2-1998

[20] Y.A. Ramachers, PhD thesis, University of Heidelberg, 1998

[21] L. Baudis, PhD thesis, University of Heidelberg, 1999

[22] D. Reusser et al., Phys. Lett. B **255**(1991)143

[23] B. Majorovits, PhD thesis, University of Heidelberg, 2000

[24] F. Schwamm, diploma thesis, University of Heidelberg, 1999, unpublished

The Heidelberg-Moscow experiment on $\beta\beta$ decay

H.V. Klapdor-Kleingrothaus[a*], A. Dietz[a], G. Heusser[a], St. Kolb[a],
I.V. Krivosheina[a], B. Majorovits[a], H. Strecker[a],
V. Alexeev[b], A. Bakalyarov[b], A. Balysh[b], S.T. Belyaev[b],
V.I. Lebedev[b], S. Zhukov[b]

[a] Max-Planck Institut für Kernphysik, P.O. Box 103980, 69029 Heidelberg, Germany
[b] Russian Science Center, Kurchatov Institute, 123182 Moscow, Russia
[*] Spokesman of the Collaboration

Abstract

The latest results from the Heidelberg-Moscow experiment are presented. A new data analysis method based on Pulseform Analysis with neural networks has been developed. Applying this method to 37.24 kg y of data a lower limit on the half life of neutrinoless double beta decay of 2.1 (3.5) $\times 10^{25}$ y, 90%C.L. (68%C.L.) is derived. From this an upper bound on the effective Majorana Neutrino mass of $\langle m_\nu \rangle \leq 0.34$ eV (0.26 eV) can be inferred. The Heidelberg-Moscow Experiment is since eight years the most sensitive probe of the effective Majorana Neutrino mass worldwide.

1 Introduction

The question of a nonvanishing neutrino mass is still one of the most outstanding open problems in modern physics. Especially after the recent striking hints for neutrino oscillations from the Super-Kamiokande experiment it has become very important to verify these results independently. Neutrinoless double beta ($0\nu\beta\beta$) decay is one of the most promising tools for the search of a finite neutrino mass and some other physics beyond the standard model [1, 2]. Double beta decay experiments are indispensible to solve the problem of the structure of the neutrino mass matrix [3, 4]. Furthermore they seem to be the only possibility to distinguish between the Majorana- and the Dirac-nature of the neutrino. If $0\nu\beta\beta$-decay is observed neutrinos have to be of Majorana-type and have a finite mass.

Detector	ANG1	ANG2	ANG3	ANG4	ANG5
Total mass	0.980 kg	2.906 kg	2.446 kg	2.400 kg	2.781 kg
Active mass	0.920 kg	2.758 kg	2.324 kg	2.295 kg	2.666 kg
saturation voltage		3000 V	3200 V	2900 V	1900 V
working voltage	4000 V	4000 V	4000 V	2500 V	2500 V
FWHM at 1332 keV		1.98 keV	1.91 keV	1.97 keV	2.06 keV
enrichment in ^{76}Ge [%]	85.9±1.3	86.6±2.5	88.3±2.6	86.3±1.3	85.6±1.3

Table 1: Technical data of the enriched Germanium detectors (from [9]).

2 The setup of the Heidelberg–Moscow $\beta\beta$ experiment

The Heidelberg–Moscow $\beta\beta$ experiment is presently the most sensitive experiment looking for neutrinoless double beta decay [1, 2, 5, 6, 7]. It is making use of germanium detectors which are embedded into an extreme low level surroundings. In the final setup of the Heidelberg–Moscow $\beta\beta$ experiment [8] five HPGe detectors made out of crystals enriched to 86-88% with ^{76}Ge are operated in an ultra low-level background in the Gran Sasso underground laboratory in Italy. From non-observation of the neutrinoless double beta decay an upper limit on its half life can be extracted.

All the detectors were specially designed for their purpose, using only carefully selected low-level copper. Four of the detectors are shielded with 40 cm of low-level lead. The whole system is sealed inside a steal box which is flushed with gaseous nitrogen, in order to minimize the ^{222}Rn contamination in the direct surroundings of the detectors. The whole setup is surrounded by 20 cm of borated polyethylene plates to avoid the neutron influence on the detectors. On top of the construction a muon veto shield is installed which effectively recognizes any through-going muons.

The fifth detector is housed inside a separate box without neutron shield and without muon veto. The inner shielding material here is electrolytic low-level copper. The total active mass of the experiment with all detectors is 10.96 kg.

The experiment started it's operation in 1992 and has collected 55.91 kg y of data without Pulse Shape Analysis (PSA) and 37.24 kg y with PSA (since 1995) so far.

The most important parameters for the single HPGe crystals are listed in table 1.

The very high sensitivity of the Heidelberg–Moscow $\beta\beta$ experiment with respect to other experimental approaches is based on the following facts:

- With 10.96 kg active detector mass using enriched ^{76}Ge the source strength of this experiment is the highest one in operation.
- The experiment is housed in a very clean surroundings, resulting in a very efficient background reduction.
- Detector and source are identical, resulting in a very high detection efficiency close to 100%, and at the same time in a very good energy resolution.

- The use of Pulse Shape Analysis (PSA) leads to a further efficient background reduction.

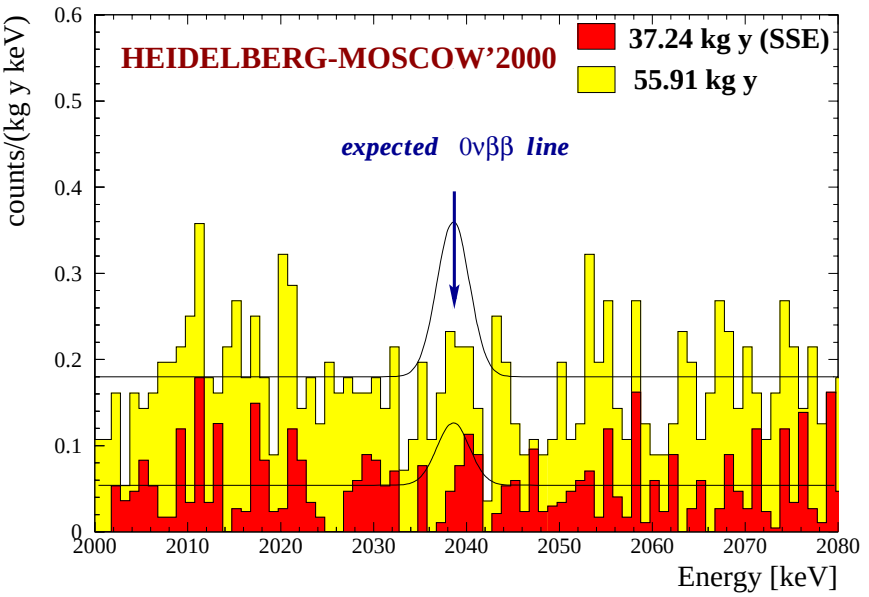

Figure 1: Heidelberg-Moscow experiment: energy spectrum in the range between 2000 keV and 2080 keV, where the peak from neutrinoless double beta decay is expected. The open histogram denotes the overall sum spectrum without PSA after 55.91 kg y of measurement (since 1992). The filled histogram corresponds to the SSE data after 37.24 kg y. Shown are also the excluded (90%C.L.) peak areas from the two spectra.

2.1 The pulse shape analysis used so far

Since 1995 an additional background reduction has been achieved through the use of Digital Pulseshape Analysis (PSA). Due to the fact that the shape of the detected pulse is dependent on the type of interaction, a distinction between multiple scattered Compton events and single interaction events (as $0\nu\beta\beta$-decay) is possible. A $0\nu\beta\beta$-decay event would appear as a Single Site Event (SSE), since the mean free path of the two electrons emitted by the decay is smaller than the time resolution of the detector allows to distinguish due to the low drift velocities of the electron-hole pairs. This means that Multiple Site Events (MSE) in the energy region of $0\nu\beta\beta$-decay can be regarded as background.

To distinguish between the two interaction types a one-parameter method was developed at that time, based on the fact that the time structure of the pulse shapes in Germanium detectors are mainly dependent on the locations of the various events of a count within the HPGe-crystal. For MSE's one expects a broader pulse in time than for SSE's since the initial locations of the electron-hole pairs are distributed over a larger area of the crystal and the overall detection time therefore increases. Like this a reduction of

the background by a factor of three in the area of the expected signal could be reached [9, 10, 11].

2.2 Pulseshape analysis using neural networks

A large amount of information is neglected with the pulse shape discrimination method used so far, since only one parameter serves as the distinguishing criterium. Furthermore the method relies on a statistical correction of the measured SSE pulses since the efficiency of the method is with 70% substantially smaller than 100%, resulting in a loss of information about the single events. For this reason we developed a new method based on neural networks to use as much information as possible from the recorded pulse shapes.

Neural networks are nowadays used in a wide variety of applications like pattern-, image- and videoimage-recognition. Since in the case of PSA the discrimination technique relies on a pattern recognition process, it seemed consequent to base a new PSA-technique on this method. In contrast to the old method, where only one parameter was used as the distinguishing criterium, all the information obtained by the measurement about the time structure of the pulse is fed to the neural networks in order to distinguish between SSE's and MSE's.

The network has to be configured in order to be able to distinguish reasonably between two types of input patterns. This is mostly done by a sort of training process, the backpropagation procedure. If one has a library of input patterns, these can be passed to the network. After the input pattern has been applied and the output has been calculated, the connections between the neurons are adjusted according to the generalized delta rule (see [12] for a detailed description of neural networks). After a certain number of these training procedures the network 'learns' the characteristic patterns of the types of input information and the output of the network results in a value close to zero for a pattern of type A) and in a value close to one for a pattern of type B).

In the new analysis the networks were trained using 40.000 pulses for each detector. An efficiency of $\sim$80 % for classifying the pulse correctly could be reached, to be compared to 70% of the earlier used method. For a detailed description of the use of neural networks in the data analysis see [13].

3 The new limit

Data analysis of the present spectrum (Fig. 1) using the new method with neural networks yield the following results [14].

In figure 1 the resulting energy spectrum in the range between 2000 keV and 2080 keV is shown. The number of expected background events in the three sigma region around the awaited peak is 20.18 ± 1.62. The number of measured events in the same energy interval is 16.19. Since there are less events observed than expected, the limit is obtained following the suggestion of [15], to set the number of observed events equal to the number of expected events in this case. Thus 8.65 (5.08) events can be excluded with 90% C.L. (68% C.L.) to be due to neutrinoless double beta decay.

The corresponding spectrum with the excluded area (90 % C.L.) is shown in figure 1.

For the half life of $0\nu\beta\beta$ decay the following lower limit can be given:

$$T_{1/2}^{0\nu\beta\beta} \geq 2.1 \times 10^{25} \text{ yr} \quad 90\% C.L. \tag{1}$$

$$T_{1/2}^{0\nu\beta\beta} \geq 3.5 \times 10^{25} \text{ yr} \quad 68\% C.L. \tag{2}$$

If the real number of measured events is taken, a better limit is resulting from the analysis. In this case 6.21 (3.39) events could be excluded with 90 % C.L. (68 % C.L.) to be caused by neutrinoless double beta decay.

This would result in a limit on the half life of:

$$T_{1/2}^{0\nu\beta\beta} \geq 2.9 \times 10^{25} \text{ yr} \quad 90\% C.L. \tag{3}$$

$$T_{1/2}^{0\nu\beta\beta} \geq 5.2 \times 10^{25} \text{ yr} \quad 68\% C.L., \tag{4}$$

however it should be taken with some care as it is based on a dip in the measured spectrum.

Taking the conservative limit, following [15], using the matrix elements from [16], the lower limit on the half life of $0\nu\beta\beta$ can be converted into an upper limit for the effective Majorana neutrino mass:

$$\langle \mathrm{m}_\nu \rangle \leq 0.34 \ eV \quad 90\% \ C.L. \tag{5}$$

$$\langle \mathrm{m}_\nu \rangle \leq 0.26 \ eV \quad 68\% \ C.L. \tag{6}$$

Analysis of the data with the 'old' pulse shape discrimination method [9] yields practically an identical result.

4 Conclusions

The Heidelberg-Moscow Experiment, which is taking data since 1992, is presently and since eight years the most sensitive experiment to neutrinoless double beta decay worldwide. Since 1995 a PSA method is used, which effectively reduces the background in the interesting energy region around the Q-value of the double beta decay of ^{76}Ge at 2038.5 kev by a factor of approximately three. A new method based on neural networks has been developed. This method increases the efficiency of correct pulse recognition to 80%. It has been applied to 37.24 kg y of experimental data, resulting in a lower limit on the neutrinoless double beta decay of $\mathrm{T}_{1/2} > 2.1\ (3.5) \times 10^{25}$ y, 90%C.L. (68%C.L.). From this an upper limit on the effective Majorana Neutrino Mass of $\langle \mathrm{m}_\nu \rangle \leq 0.34$ eV (0.26 eV) can be inferred.

Fig. 2 shows a comparison of this result with the other most sensitive double beta experiments, and their future potential. The latter will not allow to reach the present Heidelberg-Moscow limit.

Fig. 3 shows the expectations for the effective Majorana neutrino mass from the present experimental status of all existing neutrino oscillation experiments in the presently experimentally favored neutrino mass models (from [3, 4, 20]). It is seen that with the

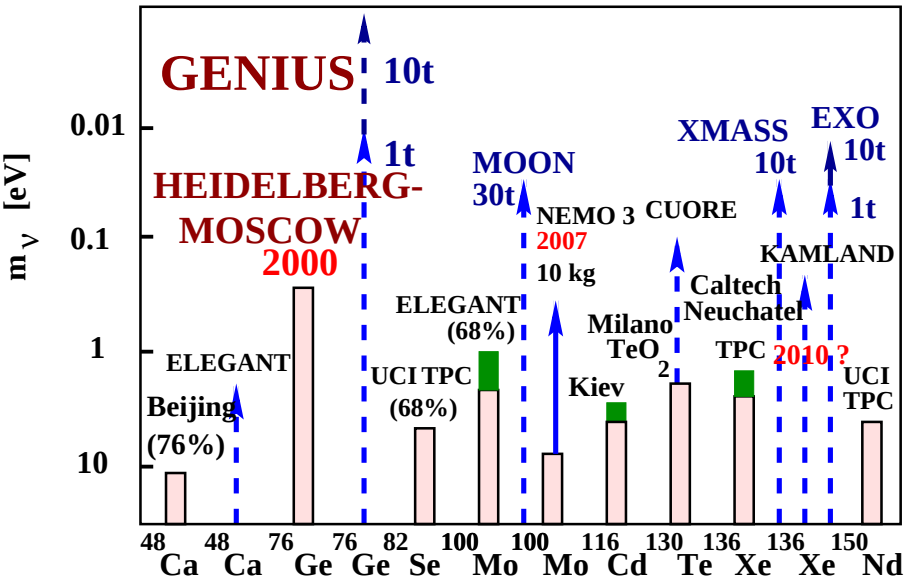

Figure 2: Present situation, 2000, and expectations for the future, of the most promising $\beta\beta$-experiments. Light parts of the bars: present status; dark parts: expectations for running experiments; solid and dashed lines: experiments under construction and proposed experiments, respectively.

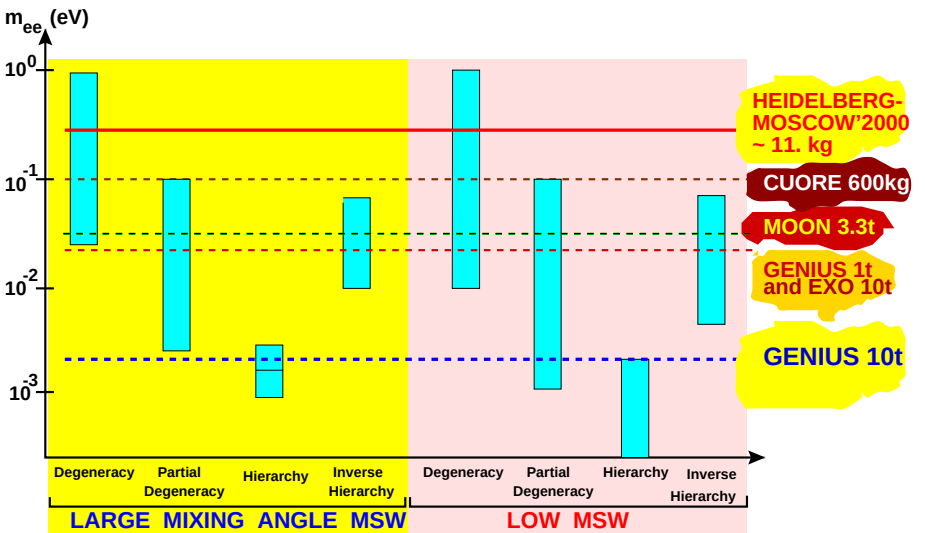

Figure 3: Values of $\langle m_\nu \rangle$ expected from present neutrino oscillation experiments in different neutrino mass schemes. The expectations are compared with the present neutrino mass limit *obtained* from the Heidelberg-Moscow experiment as well as with the *expected* sensitivities for the CUORE[17], MOON[18], EXO[19] proposals and the 1 and 10 ton GENIUS proposal (see [1], from [4]) .

sensitivity of the Heidelberg-Moscow experiment double beta decay just starts to probe the first models. It has been shown recently that it excludes for example the small angle MSW solution of the solar neutrino problem in degenerate scenarios, if neutrinos are considered as hot dark matter in the universe [21, 22, 23, 24].

A fundamental conclusion from Fig. 3 is that the range of $\langle m_\nu \rangle$ accessible by the method of double beta decay in future experiments, exploiting it to its ultimate limit, is covering essentially all neutrino mass scenarios allowed by present neutrino oscillation experiments. Thus nature is extremely generous to us, allowing $\beta\beta$-decay to give in future, with sufficiently sensitive experiments (GENIUS), a fundamental contribution to solving the structure of the neutrino mass matrix and in this way to particle physics.

References

[1] H.V. Klapdor-Kleingrothaus, *60 Years of Double Beta Decay - From Nuclear Physics to Beyond Standard Model Physics*, World Scientific, Singapore, 2000, 1300 p

[2] H.V. Klapdor-Kleingrothaus, Int. J. Mod. Phys. A **13**(1998)3953 and H.V. Klapdor-Kleingrothaus in Lepton and Baryon Number Violation, Proceedings of the First International Symposium on Lepton and Baryon Number Violation, Trento, 20-25 April 1998, editors H.V. Klapdor-Kleingrothaus and I.V. Krivosheina, IoP Bristol, 1999, page 251; H.V. Klapdor-Kleingrothaus, in Springer Tracts in Modern Physics **163**(2000)69-104.

[3] H.V. Klapdor-Kleingrothaus, H. Päs and Y. Smirnov, accepted for publication at Phys. Rev. D, hep-ph/0003219

[4] H.V. Klapdor-Kleingrothaus, H. Päs, in Proc. of the Third Int. Conference on Dark Matter in Astro– and Particle Physics (DARK2000) July 2000, Heidelberg, Eds. H.V. Klapdor–Kleingrothaus and B. Majorovits, Springer, Heidelberg, 2001

[5] H.V. Klapdor-Kleingrothaus, Proposal, Internal Report, MPI-H ,1987

[6] H.V. Klapdor-Kleingrothaus, In Proc. of NEUTRINO'96, Helsinki, June 1996, World Scientific, Singapore, 1997, pp. 317-341.

[7] Heidelberg-Moscow Collaboration., L. Baudis, A. Dietz, G. Heusser, H.V. Klapdor-Kleingrothaus, S Kolb, I. Krivosheina, B. Majorovits, V.F. Melnikov, H. Päs, F. Schwamm, H. Strecker, V. Alexeev, A. Bakalyarov, A. Balysh, S.T. Belyaev, V.I. Lebedev and S. Zhoukov, Phys. Rev. Lett. **83**(1999)41

[8] M. Guenther et al., Phys. Rev. D **55**(1997)54

[9] J. Hellmig and H.V. Klapdor-Kleingrothaus, Nucl. Inst. Meth. **455**(2000)638

[10] J. Hellmig, F. Petry and H.V. Klapdor-Kleingrothaus, Patent DE 19721323 A

[11] Heidelberg–Moscow Collaboration, L. Baudis, M. Guenther, J. Hellmig, G. Heusser, M. Hirsch, H.V. Klapdor-Kleingrothaus, S Kolb, H. Päs, Y. Ramachers, H. Strecker, M. Voellinger, A. Bakalyarov, A. Balysh, S.T. Belyaev, V.I. Lebedev and S. Zhoukov, Physics Letters B **407**(1997)219-224

[12] B. Kröse and P. van der Smagt, University of Amsterdam, *An Introduction to Neural Networks*, 1996, from http://www.robotic.dlr.de/Smagt/books/

[13] B. Majorovits and H.V. Klapdor-Kleingrothaus, Eur. Phys. J. **6**(1999)463

[14] B. Majorovits, PhD thesis, University of Heidelberg, 2000

[15] Particle Data Group (PDG 96), R.M. Barnett et al., Phys. Rev. D **54**(1996)1

[16] A. Staudt, K. Muto and H.V. Klapdor-Kleingrothaus, Europhys. Lett. **13**(1990)31

[17] E. Fiorini et al., Phys. Rep. **307**(1998)309

[18] H. Ejiri et al., nucl-ex/9911008, Phys. Rev. Lett. **85**(2000)2917-2920

[19] M. Danilov et al., Phys. Lett. B **480**(2000)12 and hep-ex/0002003

[20] H.V. Klapdor-Kleingrothaus, Proc. NOON 2000 - Internat. Workshop on 'NEUTRINO OSCILLATIONS AND THEIR ORIGIN', Tokyo, Dec. 2000, World Scientific, Singapore, 2001

[21] H. Georgi and S.L. Glashow, Phys. Rev. D **61**(2000)097301

[22] H. Minakata and O. Yasuda, Phys. Rev. D **56**(1997)1692 and H. Minakata, hep-ph/0004249

[23] O. Yasuda in *Proc. of Beyond the Desert 1999*, ed. by H.V. Klapdor–Kleingrothaus and I.V. Krivosheina (IOP Bristol 2000), p. 223

[24] J. Ellis and S. Lola, Phys. Lett. B **458**(1999)310 and hep-ph/9904279

ICARUS T600. Imaging Cosmic and Rare Underground Signals

F.Arneodo[a], B.Badełek[b], A.Badertscher[c], B.Baiboussinov[d], G.Battistoni[e], P.Benetti[f], E.Bernardini[a], A.Borio di Tigliole[f], R.Brunetti[f], A.Bueno[c], E.Calligarich[f], M.Campanelli[c], C.Carpanese[c], D.Cavalli[e], F.Cavanna[g], P.Cennini[h], S.Centro[d], A.Cesana[i], C.Chen[j], Y.Chen[j], D.Cline[k], A.Dabrowska[l], C. De Vecchi[f], R.Dolfini[f], A.Ferrari[e,h], A.Gigli Berzolari[f], I. Gil-Botella[c], D.Grech[m], P.Goudsmit[c], K.He[j], X.Huan[j], J.Holeczek[n], B.Jokisz[n], C.Juszczak[m], D.Kiełczewska[b], J.Kisiel[n], T.Kozłowski[o], J.Łagoda[b], Z.Li[j], F.Lu[j], J.Ma[j], M.Markiewicz[p], F.Mauri[f], D.Mazza[g], G.Meng[j], C.Montanari[f], M.Moszyński[o], S.Navas-Concha[c], G.P.Nurzia[g], S.Otwinowski[k], O.Palamara[a], D.Pascoli[d], J.Pasternak[m], L.Periale[q,r], S.Petrera[g], G.Piano Mortari[g], A.Piazzoli[f], P.Picchi[q,r], F.Pietropaolo[h,d], T.Rancati[e], A.Rappoldi[f], G.L.Raselli[f], J.Rico[c], E.Rondio[o], M.Rossella[f], C.Rossi[g], A.Rubbia[c], **C.Rubbia**[f,*], P.Sala[e], D.Scannicchio[f], Y.Seo[k], F.Sergiampietri[k,t], N.Sinanis[c], J.Sobczyk[m], J.Stepaniak[o], M.Stodulski[l], M.Szeptycka[o], M.Szleper[o], M.Terrani[i], S.Ventura[d], C.Vignoli[f], H.Wang[k], J.Woo[k], G.Xu[j], Z.Xu[j], M.Wójcik[s], A.Zalewska[l], C.Zhang[j], Q.Zhang[j], S.Zheng[j]. W.Zipper[n].

[a] INFN, Laboratori Nazionali del Gran Sasso, S.S. 17 bis Km 18+910, Assergi (AQ), Italy
[b] Institute of Experimental Physics, Warsaw University, Warszawa, Poland
[c] Inst. for Part. Phys. Eidgenössische Tech. Hochschule CH-8093 Zürich, Switzerland
[d] Dip.to di Fisica e INFN, Univ. di Padova, via Marzolo 8, Padova, Italy
[e] Dip.to di Fisica e INFN, Univ. di Milano, via Celoria 2, Milano, Italy
[f] Dip.to di Fisica e INFN, Univ. di Pavia, via Bassi 6, Pavia, Italy
[g] Dip.to di Fisica e INFN, Univ. di L'Aquila, via Vetoio, L'Aquila, Italy
[h] CERN, CH-1211, Geneva 23, Switzerland
[i] Dip.to di Ingegneria Nucleare, Univ. di Milano, via Celoria, Milano, Italy
[j] IHEP - Academia Sinica, 19 Yuquan Road, Beijing, People's Republic of China
[k] Dep.t of Physics, UCLA, Los Angeles, CA 90024, USA
[l] H.Niewodniczański Institute of Nuclear Physics, Kraków, Poland
[m] Institute of Physics, Wrocław University, Wrocław, Poland
[n] Institute of Physics, University of Silesia, Katowice, Poland
[o] A.Sołtan Institute for Nuclear Studies, Warszawa, Poland
[p] Faculty of Physics and Nuclear Techniques, Univ. of Mining and Metallurgy, Kraków, Poland
[q] ICGF del CNR, corso Fiume 4, e Dip.to di Fisica, Univ. di Torino, via Giuria 1, Torino, Italy
[r] INFN, Laboratori Nazionali di Frascati, Via E. Fermi 40, Frascati (Roma), Italy
[s] Institute of Physics, Jagellonian University, Kraków, Poland
[t] INFN, Sezione di Pisa, Via Livornese 1291, S. Piero a Grado (PI), Italy

[*] *Spokesman of the ICARUS Collaboration*

Abstract

The ICARUS T600 is a self-contained experimental programme, with significant physics potentialities, though with a strong connotation of technological development in view of the operability of a large mass liquid Argon "electronic bubble chamber" inside the Gran Sasso underground laboratory. Main physics issues are observations, with unique experimental features, of neutrinos from various sources and possibly of proton decay.

Fundamental achievement of the year 2000 is the completion of the detector construction.

A full test of the T600 experimental set-up, from the cryogenics and electronics performance up to detection of cosmic ray tracks, is now foreseen to take place in Pavia, during the first months of the year 2001.

A second important achievement of the ICARUS activity, during the year 2000, is represented by the successful long-term test run of a large scale prototype ($10m^3$ of LAr), operated for the first time at the Gran Sasso Laboratory: this test aimed to the detection and reconstruction of cosmic ray events and concluded the $R\&D$ programme of the Collaboration, opening the way for the T600 installation at the Laboratory Nazionali del Gran Sasso.

1 Introduction

The ICARUS T600 project [1] has been fully approved and financed during the years 1996-97. The construction started immediately after: the detector is now fully assembled and the external cryogenic plant is presently near completion. A full test of the experimental set-up has been foreseen, prior to its final installation at Gran Sasso. The test will take place in Pavia, and we expect to detect long tracks from cosmic muons by the first months of the year 2001.

The ICARUS T600 is a self-contained experimental programme, with significant physics potentialities, though with a strong connotation of technological development in view of the operability of a large mass liquid Argon "electronic bubble chamber" inside the Gran Sasso underground laboratory. It will give the proof that this technology we have been developing for many years has finally reached maturity. It is the necessary demonstrational premise for larger scale detector with a considerable experimental impact, commensurate with the potentialities of such a novel technology in which both high visual resolution and accurate calorimetry are combined. When successful, it will open the way to the observation of neutrinos from various sources and possibly of proton decay with unique features.

We report here the main outcomes from the activities of the year 2000: these will cover the ICARUS T600 construction (Mechanics, Cryogenics, Electronics), the development of the LAr scintillation light detection technique (finalised to the employment in the T600 experiment), and a report on a conclusive test of the ICARUS technology performed at LNGS, with a large scale (14 t of LAr mass) prototype. More details can be found in the ICARUS Web page [2].

2 The ICARUS T600 Detector

The construction of the T600 detector has been completed during 2000, in all its various components: after delivery of the cryostat (divided in two half-modules), mounting of the internal detector (wire chambers, field shaping system, monitors and probes) started immediately. In parallel, the electronics layout for the equipment of half of the total number of signal wires, corresponding to one half-module, has been realised. An important, additional component, the scintillation light detection system, has been developed and installed inside the detector. The external cryogenic set-up is being completed during the first weeks of 2001.

2.1 T600 Cryogenics and Internal detector Mechanics

The assembly of the first half-cryostat was completed in September 1999, see *LNGS Annual Report 1999* [3]. During the construction, all the welds were tested for helium tightness at the level of 10^{-6} mbar lt sec^{-1} by pumping vacuum into the aluminium honeycomb panels that constitute the cryostat walls. These panels, once assembled, are equivalent to vacuum tight boxes; the cryostat walls then define an independent volume that separates the inner LAr volume from the outside world. The pressure conditions inside the walls (which are independently regulated by means of a vacuum/pressurization system) determine the flow direction in case of small residual leaks. Keeping a low pressure

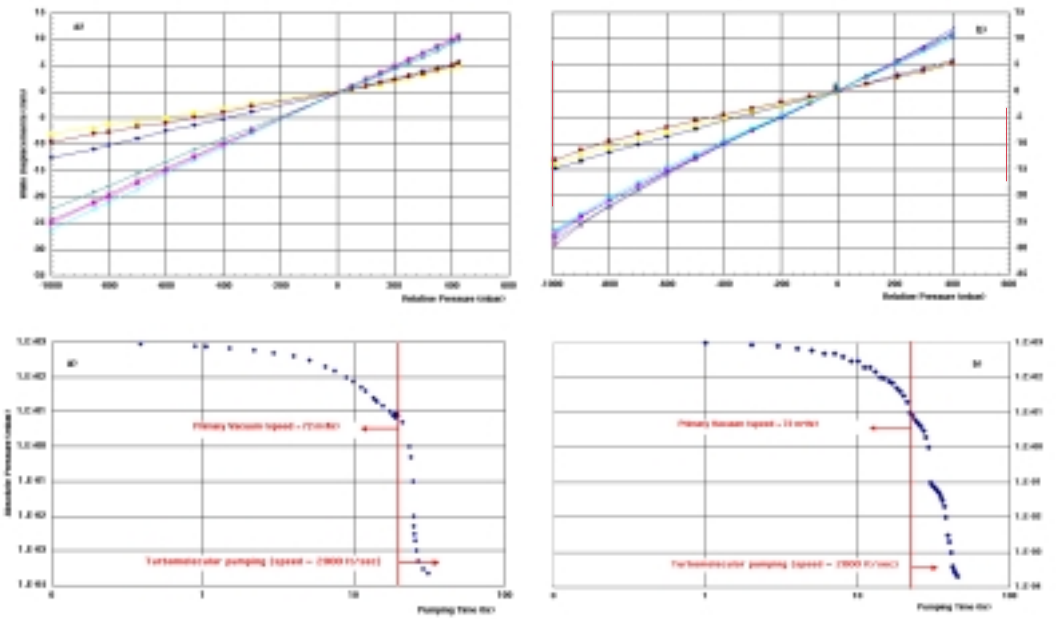

Figure 1: *Deformation and Vacuum curves for the first (a) and second (b) half-module. The two sets of deformation curves are relative to displacements of the vertical walls (less rigid, with higher deformation) and horizontal walls (shorter and reinforced by the structural elements for the chamber supports on the bottom part and for the flanges insertion on the top part).*

inside the walls inter-space, this provides therefore an additional degree of safety on the LAr purity. In February 2000, the full mechanical test of the first half-module was completed. The test procedure consisted of a series of vacuum/over-pressurization cycles at the maximum loads foreseen by the project. The panel deformations were almost perfectly linear over the full range of applied loads, the stresses on the outer skin were well within the elastic limit and in good agreement with finite elements analysis. The final vacuum reached after 30 hours of pumping in the main LAr volume was about 10^{-4} mbar, limited by water out-gassing from the cryostat walls (residual water coming from the final pickling of the internal cryostat surfaces), as shown in Fig. 1(a).

The first half-module was delivered in the assembly hall in Pavia at the end of February 2000 and the mounting of the T600 internal detector components started immediately after.

The assembly was performed in a 100,000 class clean room and made use of a suitable mechanical platform ("assembly island") to facilitate the assembly procedures.

The wire chambers' sustaining structure was mounted outside the cryostat, on the assembly island (see Fig. 2), and then moved inside the cryostat by means of dedicated rails, Fig. 3.

Figure 2: *Picture of the (second third of the) sustaining structure mounting on the assembly island outside the cryostat. The first third is already inside the cryostat.*

The alignment of the components of the whole structure has been carefully measured, using accurate optical theodolite devices. A satisfactory precision (of the order of 0.3 mm, that is the device precision limit) has been found. This result is important because the accuracy of the wire chamber event reconstruction capability, which depends on the exact distance between adjacent wires pairs and on the parallelism of the three wire planes,

rely entirely on the mechanical quality of the sustaining structure. Furthermore, the good quality of the mechanics assures that, during the cooling phase and at the cryogenic temperature (87 K), no stress is induced on the wires and everything remains in the required precision range.

In June 2000 the nearly 30,000 wires, forming the three wire planes of the first half-module, started to be positioned onto the sustaining frame. The wiring of the corresponding 832 modules (32 wires each) had been done months earlier, using a semi-automatic wiring table, and the positioning operation resulted to be very fast (of the order of 12 modules per hour). The wires mechanical tension was checked after mounting onto the frame. It was found to be satisfactory: the spread of the wire tension distribution was about $\sigma = 30$ g, for a nominal tension of 1,200 g).

Figure 3: *Picture of the whole internal detector sustaining structure inside the first half-cryostat.*

Also the scintillation light detection system, see Fig. 9, and all the slow control devices have been anchored to the sustaining structure.

From October 2000 to January 2001 the high voltage and field electrodes system (cathode, race tracks, high voltage feed- trough) have been mounted, see Fig. 4.

In parallel with the assembly of the first half-module internal detector, the cold body of the second half-module was assembled (March - July 2000), applying directly some mechanical modifications identified during the construction and test of the first one. The final test in vacuum was made in July 2000. No problems were found. As for the the first half-module, the panel's deformations during vacuum pumping were almost perfectly linear and the stresses on the outer skin were well within the elastic limit. The final vacuum, reached after 30 hours of pumping in the main LAr volume, was still 10^{-4} mbar, limited by water out-gassing from the cryostat walls, Fig. 1(b). The second half-module

Figure 4: *Picture of the electric field shaping electrodes (race tracks) mounting. In the middle of the cryostat the cathode is visible.*

was then delivered in the assembly hall in Pavia at the beginning of August 2000.

A major modification applied for the second half-module was the substitution of the cooling circuit (formerly constituted by a set of pipes embedded into the aluminium honeycomb panels) with an external screen surrounding the whole LAr container and made of preformed aluminium panels ($\sim$ 10 mm thick). This new solution adds to an easier (and non destructive) inspection capability, a much larger conductance that allows, in principle, a LN_2 circulation in two phases. This guarantees in turn an intrinsically stable temperature control and a lower consumption rate (due to a much lower mass circulation rate).

During the construction of the second half-module, the insulation around the external walls of the first half-module was assembled (obviously excluding the middle one, facing the second LAr container). The top part of the first container, that hosts all the exit ports and feedthroughs for the wire chambers readout and for all the internal instrumentation (Photomultipliers, LAr purity monitors, level and temperature probes, etc.) was also completely assembled with insulation, joints, carpentry, etc.., Fig. 5.

Installation of the external cooling screen and completion of the insulation assembly followed the delivery and positioning of the second half-module in the assembly hall.

All the external circuits for LN_2 and LAr, including the automatic control system, were also mounted. The LN_2 circulation pumps and the corresponding circuits have been doubled, compared to the original project, to guarantee continuous operation of the plant also in case of accidental failure of one of the cooling units or of the attached regulation devices[1].

[1]Actually this additional safety feature is motivated only by technical reasons. It doesn't add extra

Figure 5: *Top side of the T600 module during installation of the electronics racks.*

LAr circuits (main purifiers, liquid and gas recirculation systems) for the two half-modules were decoupled, in order to independently handle the purity in the two main containers. At present, all the circuits are completely installed, excluding those few parts connected to the front side of the module which is still open for the final assembly operations of the internal detector.

Finally, an external trigger system, for cosmic muons crossing the detector volume, has been realised with scintillator planes arranged with a suitable coincidence logic [4]. This system will provide additional trigger and T_0 signals, besides the internal trigger system with PMT's detecting scintillation light. The external trigger system will be used during the Pavia test run: detection of long muon tracks is necessary for an overall test of the detector performance and in particular for checking the DAQ system and its capability to correctly re-build the event topology from several sections of the wire chamber.

The first half-module is thus completed, including all electrical connections to the outside world. The front side of the cryostat is now being closed, allowing the start-up operations foreseen for the full test of the detector.

2.2 T600 Electronics and DAQ System

The main features of the ICARUS electronics set-up is described in [5] and [6].

During the year 2000 and following the data taking on the $10m^3$ module at LNGS (see 3.3), the final choice for the shaping configurations of the front-end amplifiers was confirmed and the production of the readout electronics was started. Before assembly of the electronic rack units, all the delivered boards were verified on a test station and accepted upon a noise level criterion (a maximum rms of 1.25 ADC counts over a 100

personnel safety, as the safety devices were already designed from the beginning to withstand the most extreme conditions.

μs window, with a null input capacitance) when hosted in a fully equipped analog crate. A total amount of ∼10,000 channels (over ∼55,000 needed for the T600 equipment) have so far been verified and seven rack units have been already installed on top of the T600 detector, in view of the forthcoming test in Pavia of the T600 first half-module.

The full set of wire connections through the flanges has been exhaustively checked, with reasonable *rms* noise levels below 1.6 *ADC* counts, achieved on all channels in working conditions.

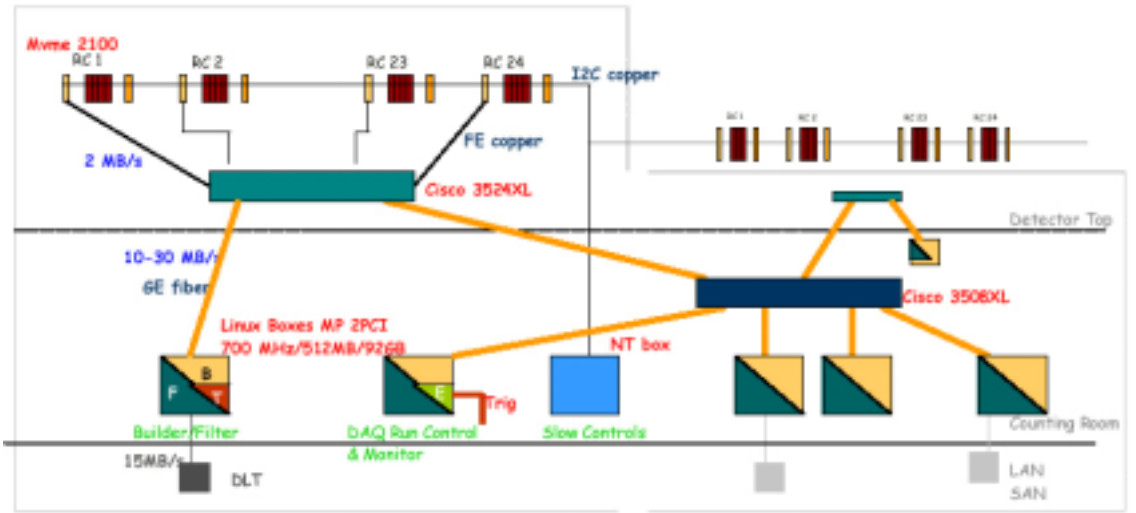

Figure 6: *Schematic view of the DAQ layout for the T600 test run.*

Every assembled rack unit hosts a custom designed rack monitor, which controls the working condition (temperature, power supplies, wire biasing HV distributions) and provides a small set of digital i/o channel. The remote sensing of the whole of the racks is done via an i2c-bus, and the collected status is available for slow control.

The data acquisition infrastructure laid down in Pavia follows the proposed layout [7], see Fig. 7. A fully interconnected gigabit switched network provides the building data paths from the front-end cpu's to the receiving workstations, which can behave in turn both as the building data merger and as event filtering/classifier before final storage. A single given machine will play the Event Manager role during the T600 test, to handle event building synchronised to the trigger facility. The achieved building rates on the preliminary DAQ test on the T600 fullfill the requirements (∼1 MB/s from each digital crate, merged to a single receiving workstation), allowing a full drift imaging DAQ running at 1 Hertz. The disk space installed on the workstation cluster (∼1 TB) will be enough to store the whole raw data sample expected for the T600 test run, allowing further optimisation and tuning of the "zero" suppression parameters and event filtering algorhytms to be run completely decoupled from the data taking.

2.3 LAr Scintillation light detection

A system to detect light from liquid argon scintillation has been implemented in the T600 first half-module. The system provides an effective method for absolute time measurement of events and a useful internal trigger signal.

The light produced by the liquid argon scintillation is a monochromatic radiation in the VUV spectrum with $\lambda = 128$ nm. The scintillation provides a high and prompt ($< 1\mu$s) photon emission, which is a function of the electric field in the drift volume. For typical electric field used in liquid argon TPCs (300÷500 V/cm), the photon production for mip muons is about $1 \div 2 \times 10^4$ MeV^{-1}. The attenuation length of the 128 nm light in LAr, as measured by the ICARUS collaboration, is about 0.9 m [8].

After an intense R&D study on the different methods and devices able to detect the LAr scintillation light, a system based on large-surface photomultiplier tubes (PMT) immersed directly in the LAr has been adopted.

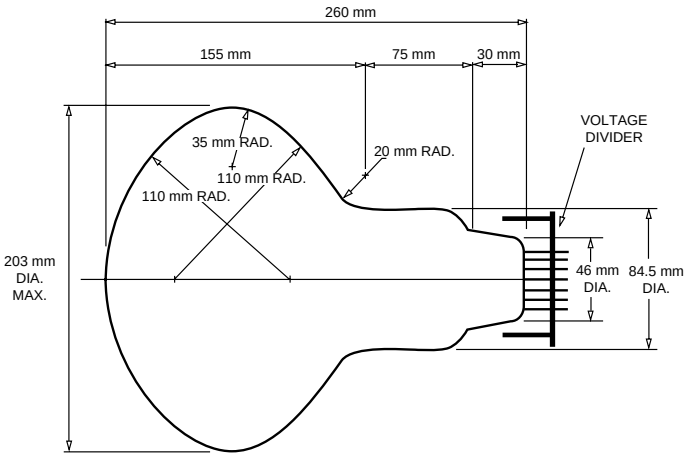

Figure 7: *The Electron Tubes Limited D727KFLB photomultiplier outline drawing.*

To this purpose the Electron Tubes D727KFLB photomultiplier has been chosen. This is a 200 mm (8") diameter hemispherical photomultiplier (see Fig. 6) with blue sensitive bialkali photocathode on a platinum underlayer especially designed to operate at low temperature. Thanks to the 12-stage dinode structure, the PMT typical gain is 5×10^7. Tests performed at the LAr temperature have proven that the window and the body of this PMT, realised in a single carrying glass structure without weldings, offer a good safety for what concerns possible breaks during the cooling phase of the system in the T600 detector. Moreover, possible variations of the PMT gain and noise down to 87 K do not affect the PMT sensitivity.

The PMTs have been made sensitive to the LAr VUV photons coating the glass window with a proper fluorescent wavelength shifter. To this purpose, by means of a monochromator, the global quantum efficiency (PMT+wavelength shifter) has been measured as a function of different coating density and materials, as shown in Fig. 8. Among other fluorescent wavelength converter, such as the sodium salicylate, the Tetraphenyl-Butadiene (TPB) shows a higher sensitivity in the wavelength region of the LAr scintillation light.

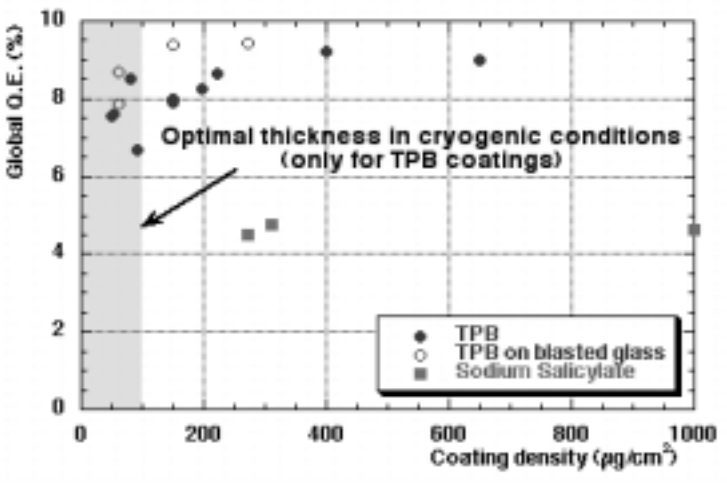

Figure 8: *Global quantum efficiency (PMT+wavelength shifter) as a function of different coating thickness and compounds.*

The coating of the PMT glass windows has been realised preparing a TPB solution in toluene and spraying it by means of a nebuliser. This method provides fine-grained and uniform layer of TPB all over the PMT surface. In order not to overcome coating instability, the layer thickness was maintained under 200 μg/cm^2. Moreover, the sand-blasting of the PMT glass windows makes the TPB coatings more adhesive and durable.

The number of photons reaching the photomultiplier surfaces has been computed taking into account:

- the internal geometry of the T600 detector;
- the design of the PMT system;
- the overall PMT quantum efficiency at the 128 nm light ($\approx 10\%$);
- the finite light attenuation length in LAr (≈ 0.9 m);
- the necessity to detect also those events for which the light production is low (i.e. 5 MeV solar neutrino interactions).

The results suggest the use of 60 PMTs per half-module placed in the region behind the wire planes. Though the complete set of PMTs is planned only for the T600 second half-module, the first has been supplied with 21 PMTs which allow a geometrical acceptance better than 60% of the TPC drift volume.

For each chamber a row of 9 PMTs has been mounted in the centre (with respect to the vertical) of the wire chamber sustaining structure, behind the wire planes, as shown in Fig. 9. The distance between two consecutive PMTs is 2 m. For test purposes, 3 additional non-aligned PMTs have been mounted in the second chamber.

For each PMT a single coaxial cable (RG316) is used to pick-up the current signal and to provide the device with the power supply. To this purpose the voltage divider

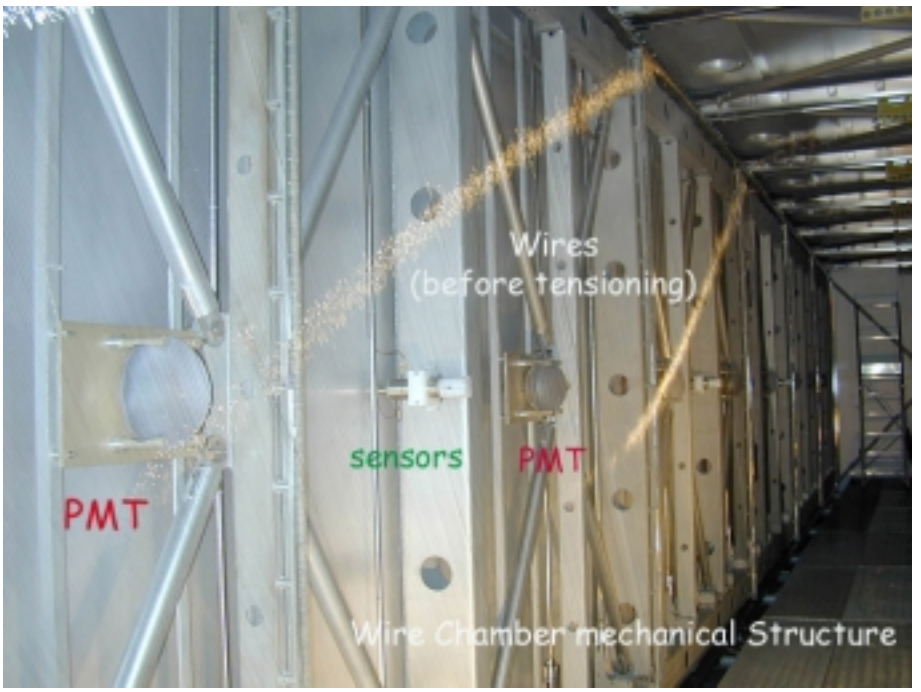

Figure 9: *PMT mounting inside the first half-module cryostat.*

have been welded directly on the PMT output leads. Before mounting, the complete chain (PMT + divider + cable) has been characterised both at cryogenic and at room temperature.

In Fig. 10 and 11, as example, two pictures showing the PMT assembling and its final mounting behind the three wires planes are presented.

3 The $10m^3$ module test at LNGS

On the way to the realization of the T600, a large prototype (14 t of LAr, usually indicated as the "$10m^3$ module") was built in 1997, in order to assess the major issues concerning cryogenics, internal detector mechanics and liquid Argon purification. The $10m^3$ prototype has undergone several cooling and filling tests in Pavia; this phase successfully ended in July 1999 [9]. The $10m^3$ was then dismounted and transported to LNGS, at the external facility *"Hall di Montaggio"* (see detail in Fig.12), for a further, conclusive test run. This phase aimed to a full test of the $10m^3$ as a detector module, i.e. to collect ionising events from the wire chamber and allow a complete exercise of event acquisition and full 3D reconstruction with the final electronic set-up, DAQ system and off-line codes.

In the next section we briefly report some of the main outcomes from the LNGS test run that has been performed during the first half of the year 2000. More information can be found in the ICARUS Web page [2].

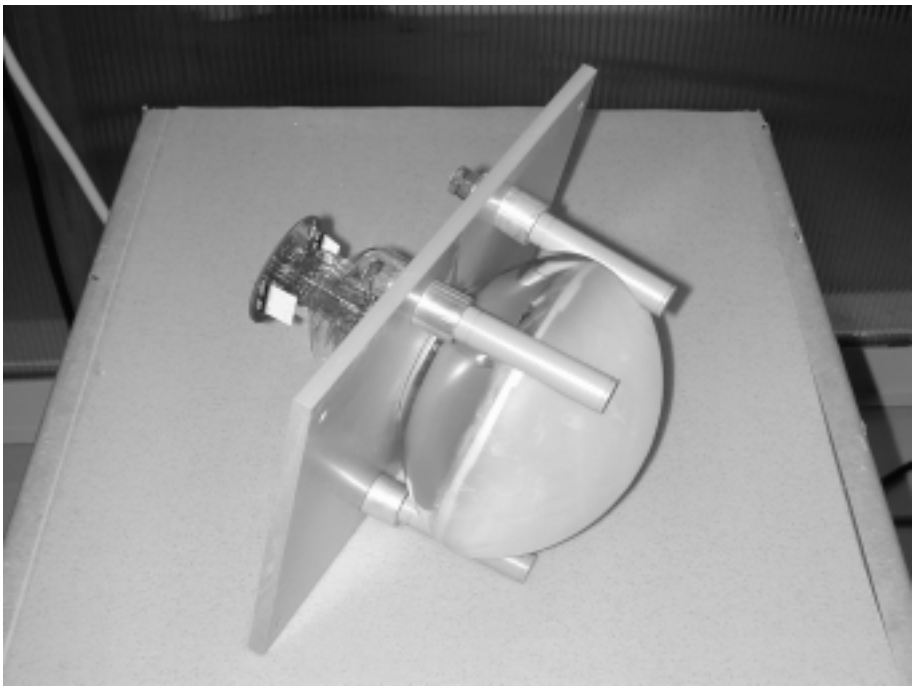

Figure 10: *Picture of a PMT final assembling. It is evident the TPB coat on the PMT glass window. The voltage divider has been mounted directly on the PMT outputs leeds. The sustaining structure has been properly designed in order to compensate the thermal stresses occurring during the cooling phase of the system.*

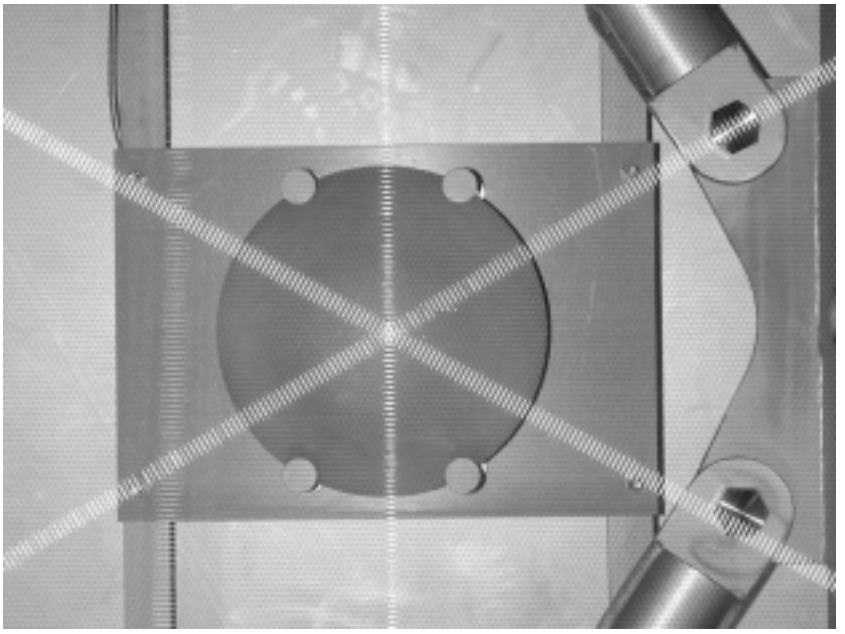

Figure 11: *Picture of a PMT in its final mounting behind the three wire planes.*

3.1 Module upgrade and start-up

The $10m^3$ module has already been described in details as reported in last *LNGS Annual Report* (1999) [3]. This module is exactly a "slice" of one half-module of the T600 detector, having the same cross-section (2.580 w $\times$ 3.890 h m^2) and the length reduced to 1 m (internal dimensions of the Al cryostat). External insulation, cooling system, purification system (in liquid phase and in gas phase) are one-to-one copy of the corresponding features actually in use with the T600 detector, see Fig. 12. The wire chamber also reproduces the geometry and all technical solutions of the T600 TPC, except for the dimensions, in order to fit the reduced volume of the $10m^3$ module, and for the number of wire planes, limited to two planes (with the wires of the first induction-plane oriented at 60^o angle respect to the collection-plane) instead of three planes (as in the T600 TPC). The sensitive volume is therefore of (3×2) m^2 $\times$ 0.35 m of drift length.

In order to transform the $10m^3$ from a test facility into a fully operational detector module a number of important modifications had to be performed [10]. Among these we mention: (1) the construction of the cathode and field shaping rings (race tracks), needed to establish a uniform electric field along the 0.35 m drift distance, perpendicular to the wire planes. (2) the installation of a HV feed-through; (3) the cable connection of each wire group to the corresponding signal feed-through (for a total number of 1856 wires); (4) the installation of two PMT's for scintillation light detection; (5) the installation of three "purity monitors" for electron lifetime measurement.

The detector upgrade and re-mounting took place during 1999 and is reported in details in [3].

A number of analog (V791-CAEN) [5] and digital (V789-CAEN) [6] electronic boards, from the first batch of the production series for the T600 module, have been connected to (part of) the available signal wires of the $10m^3$ TPC, see Fig. 12.

The start-up procedure began in January 2000: after air removal from the cryostat, with vacuum pumping down to $\sim 10^{-4}$ mbar and GAr flushing, we started the cooling-down phase, flushing the cooling circuits with gas N_2. After four days of precooling, we began operating the liquid N_2 pump. When inner temperatures dropped at $\sim -170^oC$, the LAr filling was started: this step was completed in about 35 hours.

The module was then ready for operations.

3.2 e-lifetime Measurements

The electron lifetime measured just after LAr filling was in the 100 μs range, according to expectations based on the residual leak rate (10^{-5} mbar/s).Then the LAr pump was turned on to enhance the LAr purity. In a few days an e^- lifetime in the millisecond range was reached. Without operating the GAr recirculation unit, a slow purity degradation is expected, due to residual internal outgassing. After stopping the pump we observed indeed this behaviour, Fig.13. The e^- lifetime was then easily restored by operating again the LAr pump. We repeated several times this cycle during the cryostat operation.

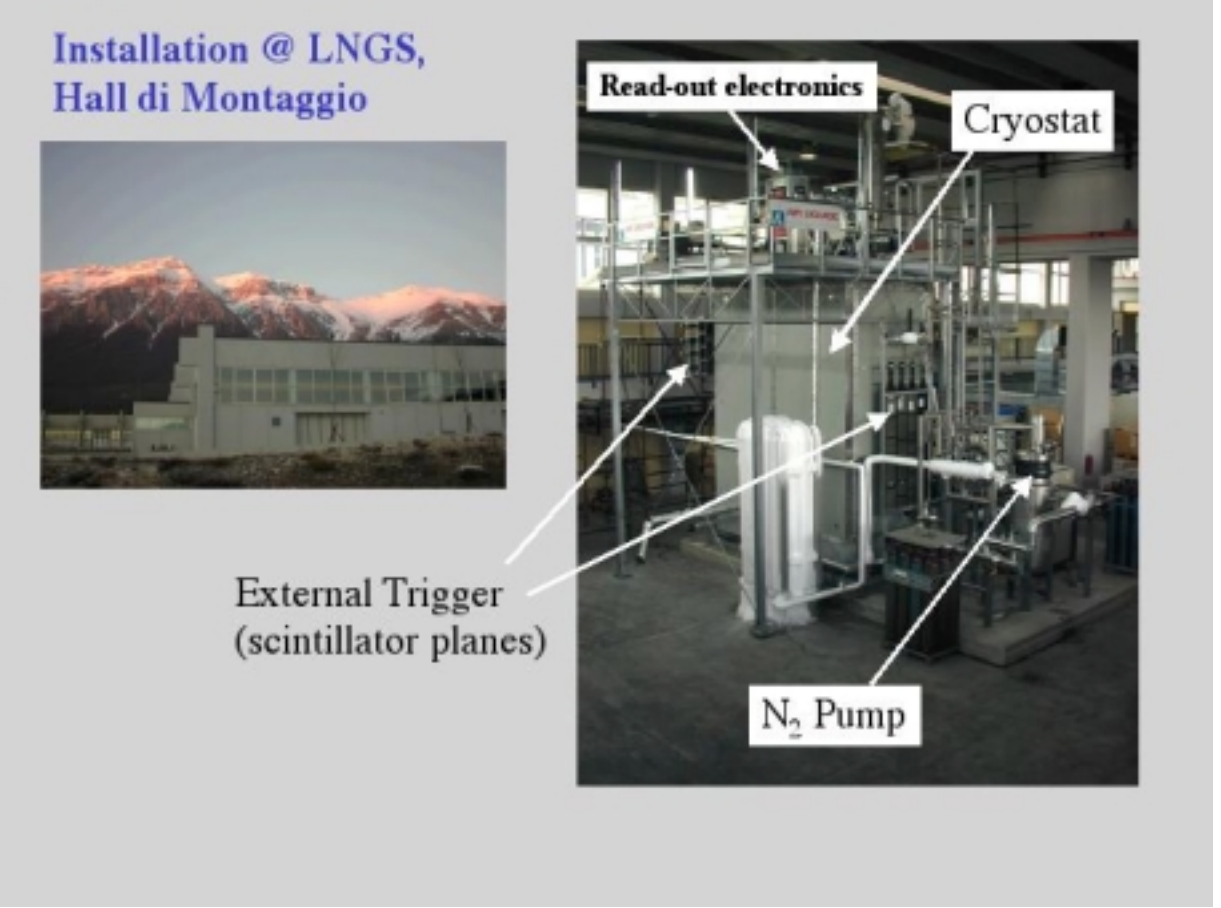

Figure 12: *The 10 m^3 module during the LNGS test run*

3.3 Events Collection and 3D reconstruction

In mid February 2000, a first group of 256 electronics channels was connected to a set of wires of the induction-plane, facing the cathode. We set the cathode high voltage to get the nominal field value of 300 V/cm, and the read-out wires to virtual ground. We began recording the first tracks of ionising particles, see Fig.14, and data taking continued for several weeks [2]. The trigger was provided either by the coincidence of an external system of scintillator planes (see Fig. 12), or by scintillation light collected with the two PMTs placed in the LAr volume.

In April 2000 we increased the number of readout channels up to 480 wires for both planes (for a total of 960 active wires). Together with the third coordinate from the drift time information, the signals from the two planes provide all necessary means for a complete 3D reconstruction of the recorded events (see below). In particular, a large sample of long muon tracks, up to about 3.5 m length, has been collected and several cosmic ray data runs were taken with various field intensities, up to 500 V/cm.

The last weeks of the LNGS run have been spent for further DAQ tests, exploiting the DAEDALUS chip features of the digital boards [6], in particular regarding the self-triggering capability of the detector, making use of a hit finding and zero suppression

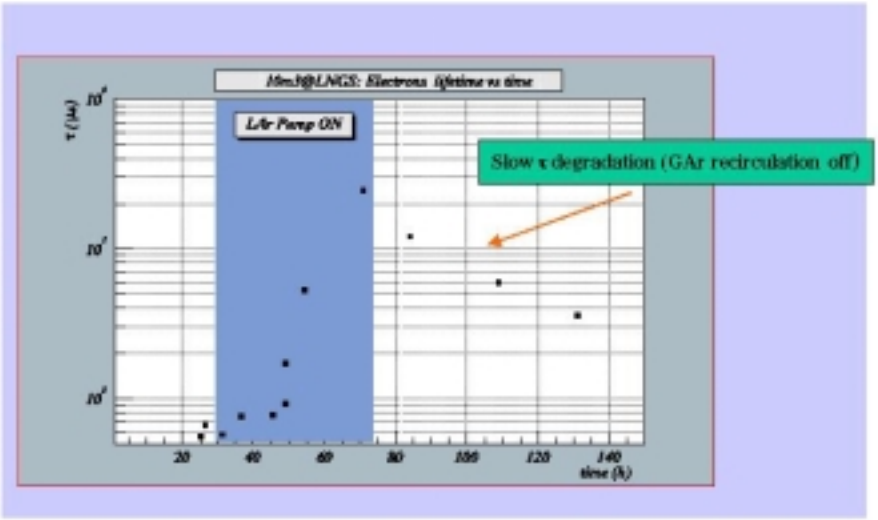

Figure 13: *Time evolution of the e-lifetime.*

algorithm.

The run was stopped in May 2000, after about 100 days of continuous operation.

The ICARUS readout system is structured as a multichannel waveform recorder that continuously stores charge informations collected by each sense wire during the drift of the electrons. Each wire is equipped with an integrating amplifier followed by a 10 bit *ADC* that samples the signal every 400 ns. The relevant information carried by the recorded waveforms are: peak time, that gives the track position inside the active volume; pulse height, which is proportional to the charge of the ionization track; rise time, that depends both on track angle and on distribution of the electron clouds during the drift. In the off-line analysis these parameters are extracted in two steps: first, the Regions Of Interest (ROI) of the signal (those containing some signal above the noise) in the recorded waveform are identified (filtering and hit finding procedures) and then, a signal extraction procedure is applied to determine the signal parameters. A study has been performed to optimise this hit finding algorithm, based on the signal and noise characteristics of the $10m^3$ data.

Analysing a sample of m.i.p. events, a signal to noise ratio of ~ 12 has been found, confirming the results previously obtained with a 50 l chamber at CERN, during a test dedicated to the electronics performance.

Combining the information from drift time and hits separately from each of the two wire planes, two 2D views for each event are normally obtained (one view for some of the collected events is shown in Fig.14). A 3D view of the event can be obtained by correlation of the two different planes signals (x and y coordinates) and drift time (z coordinate).

3D reconstruction algorithms have been developed using the single muon data collected during the $10m^3$ run. The muon tracking procedure consists of: a pattern recognition

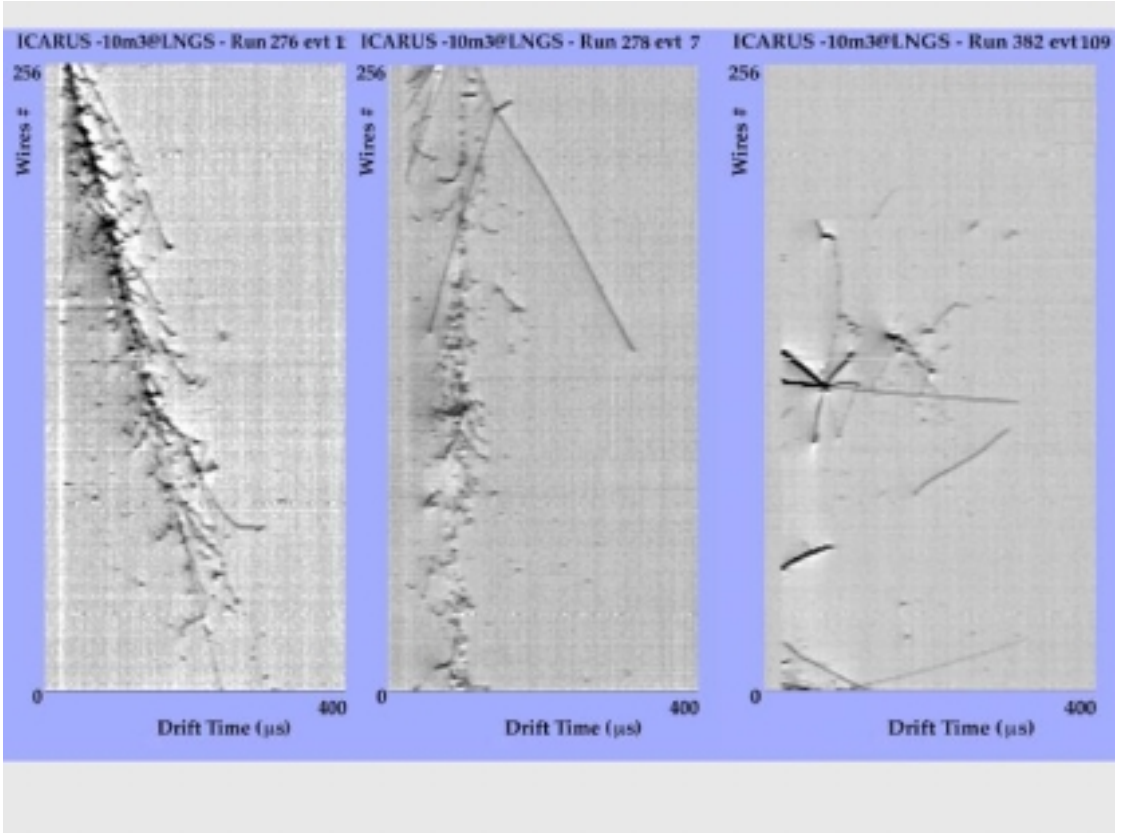

Figure 14: *Examples of Cosmic-ray events collected during the LNGS test.*

stage, based on the search for a set of aligned points amongst the hits selected by the hit finding algorithm, and a linear fit procedure through the aligned hits, to calculate track parameters in a 3D orthogonal reference frame.

In Fig.15 we show, as an example, the 3D reconstruction of a sample of single crossing muon events recorded in one run, triggered by the coincidence of the external system of scintillator planes.

Optimisation of the off-line code for calorimetric reconstruction of the energy deposition and particle identification is in progress.

4 Conclusions

The realization of the ICARUS T600 detector has been completed during the year 2000, with a final major effort of the whole Collaboration: all the components, from the internal detector mechanics to the cryogenics plant, from the electronics equipment of the signal wires to the DAQ system, have been assembled and individually tested.

A long-term run with a large ICARUS prototype, suitably upgraded to reproduce all features of the T600 detector and operated for the first time at the LNGS site during the first half of 2000, has successfully opened the way to the final installation of the T600 experiment in the Gran Sasso underground laboratory.

The installation of a VUV LAr scintillation light detection system in the T600 module

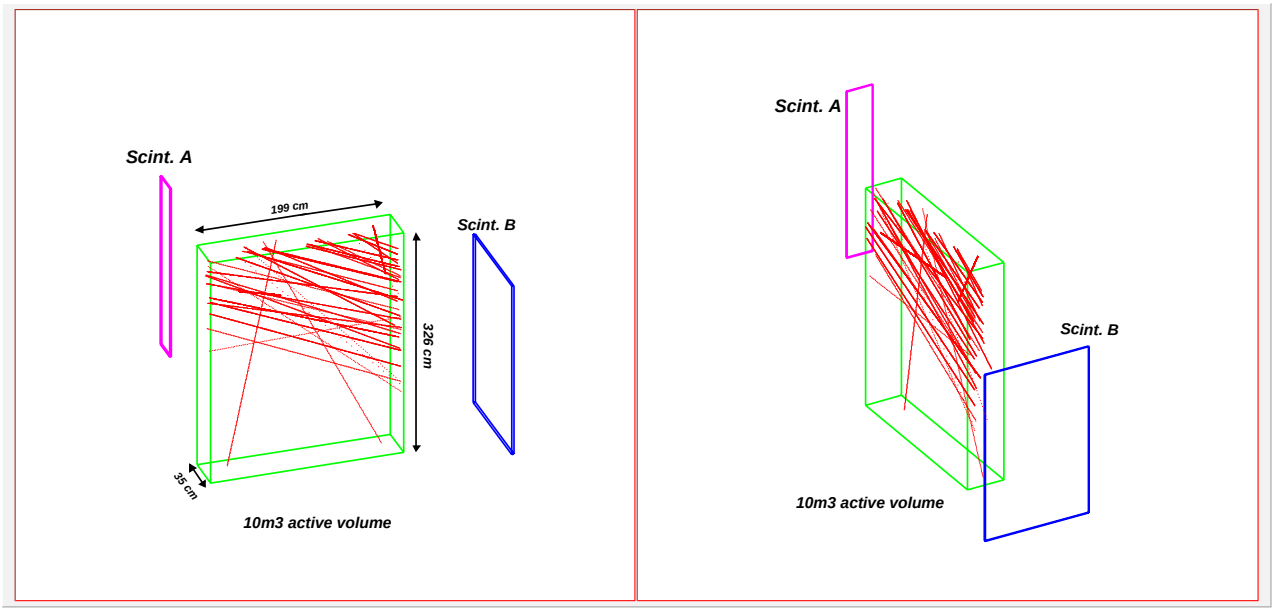

Figure 15: *3D reconstruction algorithm: sample of superimposed muon tracks crossing the* $10m^3$ *active volume (viewed from two different angles), identified by the linear fit procedure. The trigger is provided, in this case, by the external system of scintillator planes (also shown).*

is an important additional feature of the ICARUS technology, developed during the year 2000. Detection of scintillation light emitted during ionization processes provide the T_0 signal needed for a complete 3D event reconstruction and for self-trigger purposes, particularly important for low energy events detection.

A full test of the T600 experiment, from the cryogenics and electronics performance up to detection of cosmic ray tracks, is now foreseen to take place in Pavia, during the first months of the year 2001.

In parallel, a detailed overview of the physics issues and of the relevance of the T600 run at LNGS is being elaborated by the Collaboration. It will be addressed to the competent organisms in the next few months.

References

[1] ICARUS Collaboration, "A first 600 ton ICARUS detector installed at the Gran Sasso Laboratory", Addendum to Proposal by the ICARUS Collaboration, **LNGS - 95/10**, (1995).

[2] *http://www.aquila.infn.it/icarus.*

[3] **INFN-LNGS Annual Report (1999)**, *ICARUS*, 87.

[4] **ICARUS-TM-2000/05**, "An external trigger system for the ICARUS T600 test".

[5] S.Centro et al., "Low-Noise BiCMOS Front-End and Fast Analogue Multiplexer for Ionization Chamber", **Nucl. Instr. and Meth. A 409**, (1998), 300.

[6] C. Carpanese et al., "DAEDALUS: a hardware signal analyser for ICARUS", **Nucl. Instr. and Meth. A 409**, (1998), 294.

[7] **ICARUS-TM-2000/02**, "DAQ back-end hardware proposal".

[8] ICARUS Collaboration, "Detection of scintillation light in coincidence with ionizing tracks in a LAr TPC", **Nucl. Instr. and Meth. A 432**, (1999), 240

[9] **ICARUS-TM/99-09** (1999), "Report on performance evaluation of the ICARUS $10m^3$ prototype".

[10] **ICARUS-TM/99-05**, "Use of the ICARUS $10m^3$ module as a detector prototype"

5 List of Publications

List of the ICARUS publications during the year 2000:

1. ICARUS Collaboration, "First observation of 140 cm drift ionizing tracks in the ICARUS LAr TPC", **Nucl. Instr. and Meth. A 449**, (2000), 36.
2. ICARUS Collaboration, "Determination of through-going tracks' direction by means of delta-rays with the ICARUS LAr TPC", **Nucl. Instr. and Meth. A 449**, (2000), 42.
3. ICARUS Collaboration, "Scintillation Efficiency of nuclear recoil in Liquid Xenon", **Nucl. Instr. and Meth. A 449**, (2000), 147.
4. ICARUS Collaboration, "Study of Solar Neutrinos with the 600 ton liquid argon ICARUS detector", **Nucl. Instr. and Meth. A 455**, (2000), 378.
5. ICARUS Collaboration, "ICARUS 600 ton: a status report", Proceedings of the *"6th topical seminar on neutrino and astroparticle physics"*, S. Miniato (Italy, May 1999), **Nucl. Phys. Proc. Suppl. 85** (2000), 119.
6. ICARUS Collaboration, "Operation of a $10m^3$ ICARUS Detector Module", Proceedings of the *"Frontiers Detectors for Frontier Physics"* Conference, I.la d'Elba (Italy, May 2000), to be published in **Nucl. Instr. and Meth.** (Special Issue).
7. ICARUS Collaboration, "The ICARUS Liquid Argon Time Projection Chamber", Proceedings of the *"Imaging 2000"* Conference, Stockholm (Sweden, July 2000), to be published in **Nucl. Phys. Proc. Suppl.**.

LUNA and LUNA2. Laboratory for Underground Nuclear Astrophysics

R.Bonetti[1], C.Broggini[2], L.Campajola[3], C.Casella[1], P.Corvisiero[4], H.Costantini[4], A.D'Onofrio[5], A.Formicola[6], Z.Fülöp[7] G.Gervino[8], L.Gialanella[3], U.Greife[9], A.Guglielmetti[1], C.Gustavino[10], G.Gyürky[7] G.Imbriani[3,11], M.Junker[10], A.Lemut[4], B.Limata[3], A.Ordine[3], P.G.Prada Moroni[4], P.Prati[4], V.Roca[3], D.Rogalla[6], C.Rolfs[6], M.Romano[3], F.Schümann[6], O.Straniero[12], F.Strieder[6], E.Somorjai[7], F.Terrasi[5], H.P.Trautvetter[6], S.Zavatarelli[4]

[1] Università di Milano, Dipartimento Di Fisica and INFN, Milano, Italy
[2] INFN, Padova, Italy
[3] Università di Napoli, Dipartimento di Fisica and INFN, Napoli, Italy
[4] Università di Genova, Dipartimento di Fisica andINFN, Genova, Italy
[5] Dipartimento di Scienze Ambientali, Seconda Univerità di Napoli, Caserta, Italy
[6] Institut für Experimentalphysik III, Ruhr-Univerität Bochum, Germany
[7] ATOMKY, Debrecen, Hungary
[8] Politecnico di Torino, Dipartimento di Fisica and INFN, Torino, Italy
[9] Colorado School of Mines, Golden, USA
[10] Laboratori Nazionali del Gran Sasso, Assergi, Italy
[11] Osservatorio Astronomico di Capodimonte, Napoli, Italy
[12] Osservatorio Astronomico di Collurania, Teramo, Italy

Abstract

The underground accelerator facility LUNA installed at the Laboratori Nazionali del Gran Sasso offers unique possibilities for the studies of low cross section nuclear reactions. A new 400 kV accelerator has been installed in the underground laboratories in June 2000. The machine is actually under test in order to proove its capabilities. The new equipment includes also a BGO-4π-summing detector, a data aquisition system FAIR, a windowless gas target system and a beam calorimeter. The work on this equipment is in progress in order to investigate the D(p,γ)^{3}He

(old 50 kV accelerator), ^{14}N(p,γ)^{15}O (new 400 kV accelerator) nuclear reactions. Screening and stopping power measurements with the two reactions D(^{3}He,p)^{4}He and ^{3}He(d,p)^{4}He have also been performed at very low energies.

Introduction

An accurate knowledge of thermonuclear reaction rates is important in understanding the generation of energy, the luminosity of neutrinos, and the synthesis of elements in stars. Due to the Coulomb barrier (height E_C) of the entrance channel, the reaction cross section σ(E) drops nearly exponentially with decreasing energy E. Thus it becomes increasingly difficult to measure σ(E) and to deduce the astrophysical S(E) factor defined by the equation:

$$S(E) = \sigma(E) E \exp\left(31.29 Z_1 Z_2 \sqrt{\frac{\mu}{E}}\right) \quad (1)$$

In the equation (1) μ is the reduced mass in units of amu, Z_1 and Z_2 are the nuclear charges of the interacting particles in the entrance channel and E is the center of mass energy in units of keV. Although experimental techniques have improved significantly over the years to extend σ(E) measurements to lower energies, for a long time it has not been possible to measure S(E) within the thermal energy region in stars called the Gamow energy window. Its energy depends on the stellar temperature and lies far below the height of the Coulomb barrier. Instead, the observed σ(E) data at higher energies had to be extrapolated to thermal energies. As always in physics, such an extrapolation into the unknown can lead to considerable uncertainties [1].

The low-energy studies of thermonuclear reactions in a laboratory at the Earth's surface are hampered predominantly by the effects of cosmic rays in the detectors. Passive shielding provides a reduction of gammas and neutrons from the environment, but it produces at the same time an increase of gammas and neutrons due to the cosmic rays interactions in the shield itself. A 4π active shielding can only partially reduce the problem of cosmic rays background. The best solution is to install an accelerator facility in a laboratory deep underground. As a pilot project, a 50 kV accelerator facility has been installed in the Laboratori Nazionali del Gran Sasso (LNGS). The Laboratory for Underground Nuclear Astrophysics (LUNA) pilot project was designed primarily for a renewed study of the ^{3}He(^{3}He, 2p)^{4}He reaction (Q=12.86 MeV) in the energy range of the solar Gamow peak which has its maximum at 21.9 keV for a central star temperature of $T = 15.5 \cdot 10^6$ K. Based on the success of this project a new 400 kV machine has been installed underground at LNGS. The new facility will provide the possibility to measure several key reactions of the pp-chain, the CNO-cycle and the MgAl-cycle at extremely low energies [2].

1 The new 400 kV accelerator facility

In June 2000 the LUNA collaboration has installed a new 400 kV accelerator in the underground laboratories of LNGS. The accelerator has been constructed by High Voltage Engineering Europe B.V. (The Netherlands). After mounting the accelerator in the new

building at the exit of Hall A, the collaboration has started some tests in order to proove the specifications of the machine.

The terminal is located in a pressure vessel filled with 20 bar of a N_2 and CO_2 mixture. The high voltage is generated by an inline Cockroft Walton power supply. The RF ion source is mounted directly on the accelerator tube. After the accelerator tube, the only ion optical element is a 45° analyzing magnet, keeping the number of optical components to a minimum. Steering the beam properly on the target is done by this magnet and a magnetic Y-steerer. The system is as short as possible and only magnetic optical elements are used in order to maintain the important space charge compensation that is needed in order to prevent luminosity degradation. The use of a shortening rod guaranties a dynamic range of the machine which reaches from 400 kV to acceleration voltages lower than 50 kV. The high voltage ripple measured with a pickup plate is as low as ±4 V at 200 kV. The output current obtained at 400 kV is of 1 mA of H (75 % p and 25 % H_2) and of 500 μA (^{4}He).

Since in Nuclear Astrophisycs the nuclear cross sections drop exponentially with the energy it is very important to know exactly the energy of the beam impinging on the target. In consequence it is necessary to have a small energy spread and a precise knowledge of the beam energy.

To measure the energy spread of the beam a nuclear resonance method was applied. It consists in measuring some very narrow resonances whose width is very well known. We have choosen a resonance in $^{25}\mathrm{Mg(p,\gamma)^{26}Al}$ reaction at $E_b = 390$ keV and $^{23}\mathrm{Na(p,\gamma)^{24}Mg}$ reaction at $E_b = 309$ keV. Those resonances have a width less than 20 eV. The width essentially determines the sensitivity of the method. The energy of the beam impinging on the target was changed around the resonance energy making very small steps. For evaluating the relative reaction rate at different beam energies, a specific energy region of the gamma spectrum of the reaction has been choosen. As you can see in the figure (1) the gaussian curve that was obtained experimentally (solid curve) is larger than the one that would be obtained taking into account only the width of the resonance (dotted curve). From the experimental width of the gaussian curve it is therefore possible to determine the energy spread of the beam. For both reaction channels the energy spread measured with this method was found to be 76 eV.

The calibration of the beam energy is still in progress. For this purpose we are measuring the reaction channel $^{12}\mathrm{C(p,\gamma)^{13}N}$. The method makes use of the resulting capture gamma ray transition, whose intensity varies smoothly with beam energy and whose varying energy can be determined to high accuracy by comparison with precisely known energies of gamma rays from natural background gamma rays.

The cross sections measured in Nuclear Astrophysics are very low (1 fbar) and thus, since the runs can be very long, it is necessary to have a high beam stability. That's why a beam stability test was performed measuring the reaction rate of the $^{25}\mathrm{Mg(p,\gamma)^{26}Al}$ reaction fixing the beam energy exactly at the resonance energy. Because of the strong energy dependence of the cross section at the resonance, a change in reaction rate corresponds to a change in beam energy and thus it is possible to determine the long term stability of the beam. In figure (2) you can see the reaction rate of the $^{25}\mathrm{Mg(p,\gamma)^{26}Al}$ at the resonance energy ($E_b = 390$ keV) as a funcion of the time. During one hour the fluctuations of the beam energy was found to be 10 eV.

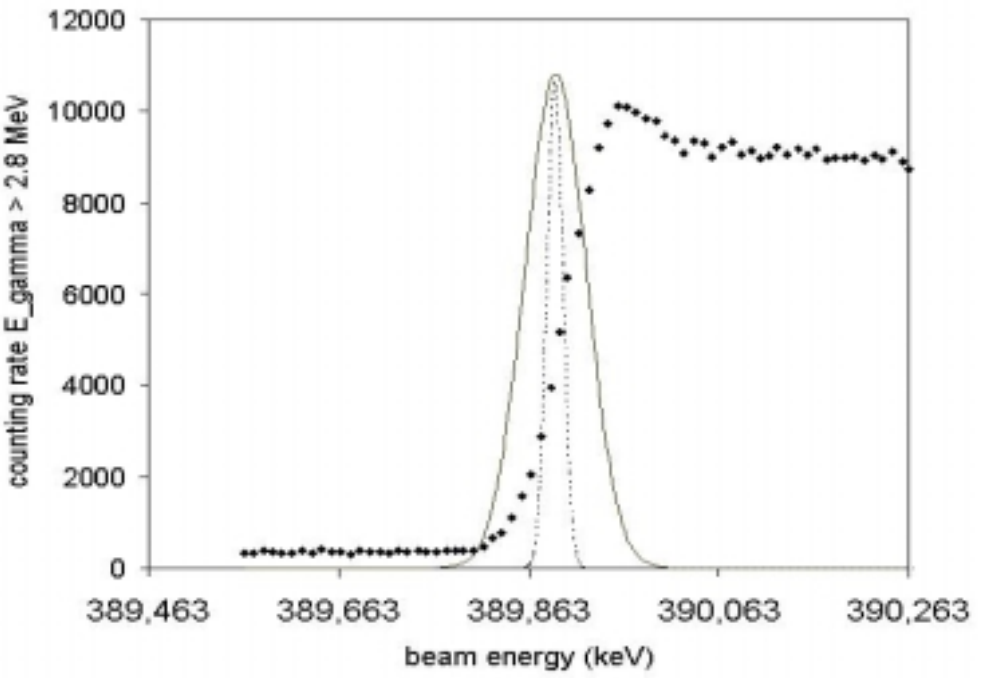

Figure 1: Beam energy spread study with nuclear resonance method. The points represents the measurements, the solid line the experimental Gaussian curve, the dotted line the resonance curve

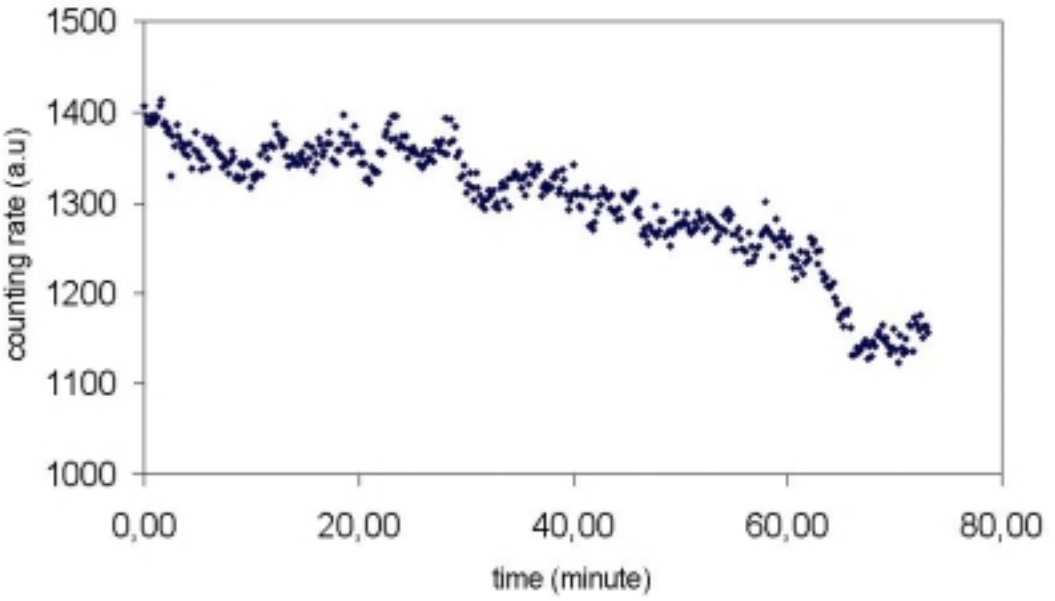

Figure 2: Beam stability test. The counting rate change corresponds to an energy fluctuation of 10 eV

Measurements of the equivalent X ray dose emitted by the accelerator have been performed recently. At a terminal voltage of 400 kV and a proton current of 420 μA the equivalent dose has been found to be less then 0.04 μSv/h at a distance of one meter from every point of the accelerator.

The first measurements to be carried out at the new accelerator will continue the research on the nuclear reaction relevant in the sun. At first the reaction $^{14}\mathrm{N}(\mathrm{p},\gamma)^{15}\mathrm{O}$ will be studied, which determines the velocity of the CNO cycle. Though the CNO cycle gives no significant contribution to the energy generation in the sun, it is important to know the neutrino flux produced by the decays of ^{15}O and ^{13}N in view of upcoming solar neutrino experiments like BOREXINO.

At solar energies the cross section of $^{14}\mathrm{N}(\mathrm{p},\gamma)^{15}\mathrm{O}$ is dominated by a subthreshold resonance at -504 keV. Recently some indirect measurements of this subthreshold resonance have been performed employing the Doppler shift method [4] and there are also some new calculations about its influence at solar energies [5]. Thus direct measurements of the $^{14}\mathrm{N}(\mathrm{p},\gamma)^{15}\mathrm{O}$ reaction at very low energies are needed.

2 The new BGO detector

The detectors used with the underground accelerators must provide high efficiency and low intrinsic activity. In addition they must provide the possibility of background recognition. This goal can be achieved by generating triggers based on coincidence conditions or on pulse shape analysis. A good resolution of the detector reduces dramatically the background in the detector. Extensive simulations have been carried out in order to design the new gas target and the new BGO detector.

The BGO-4π-summing detector consists of six optically separated segments, each of which is observed by two photomultipliers at either side of the same segment. The gas target is located inside the bore-hole of the BGO-detector. The six crystals of the BGO detector used have a length of 20 cm and are located at a distance of 4 cm from the beam axis. The bore-hole has a radius of 3 cm. The weight of the BGO detector is 83 kg. In this configuration the detector covers a solid angle of almost 4π and has an absolute efficiency of about 80 %. In figure 3 the gas target and detector setup is shown. The segmentation aims to collect information on angular distributions and branching ratios. The reactions take place inside the detector and thus all gammas generated are detected in coincidence. Signals generated by the two photomultipliers of the same segment are detected in coincidence in order to reduce the effect of the intrinsic noise of the photomultipliers. Unfortunately BGO detectors do not provide a good energy resolution, 11.3 % at 0.663 MeV (^{137}Cs peak), and about 8 % at 5.5 MeV (this value was obtained measuring the $\mathrm{D}(\mathrm{p},\gamma)^{3}\mathrm{He}$) reaction spectrum). In addition they have intrinsic background because of ^{207}Bi pollution. Since September 2000 the collaboration has performed different background measurements to test the capabilities of the new BGO detector. In figure (4) on the left a background spectrum of the summed energy is shown. The spectrum has been taken in the underground lab with an additional lead shielding. The measuring time is 12 days. On the right a background spectrum without any shielding measured in the underground lab is reported. The measuring time is 14 hours.

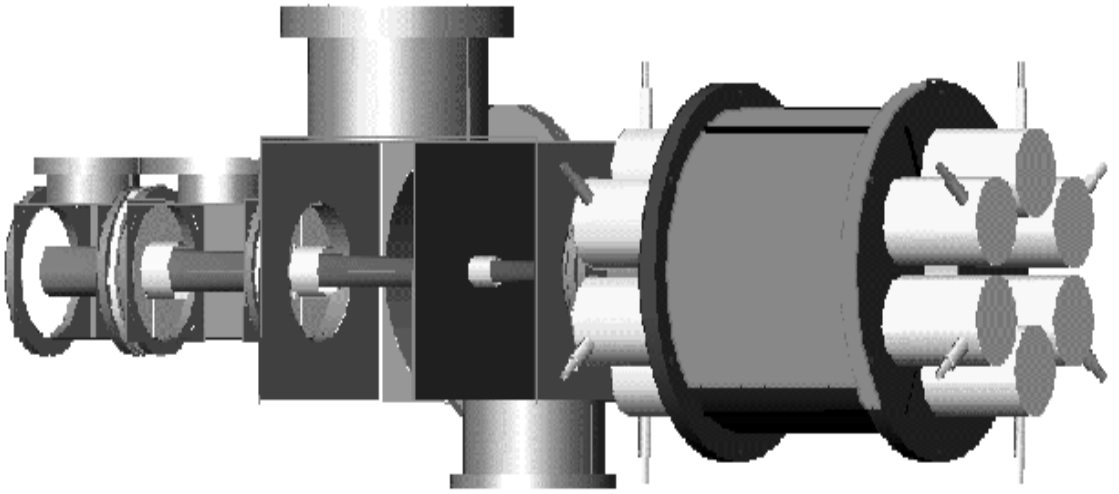

Figure 3: Bgo and gas target setup

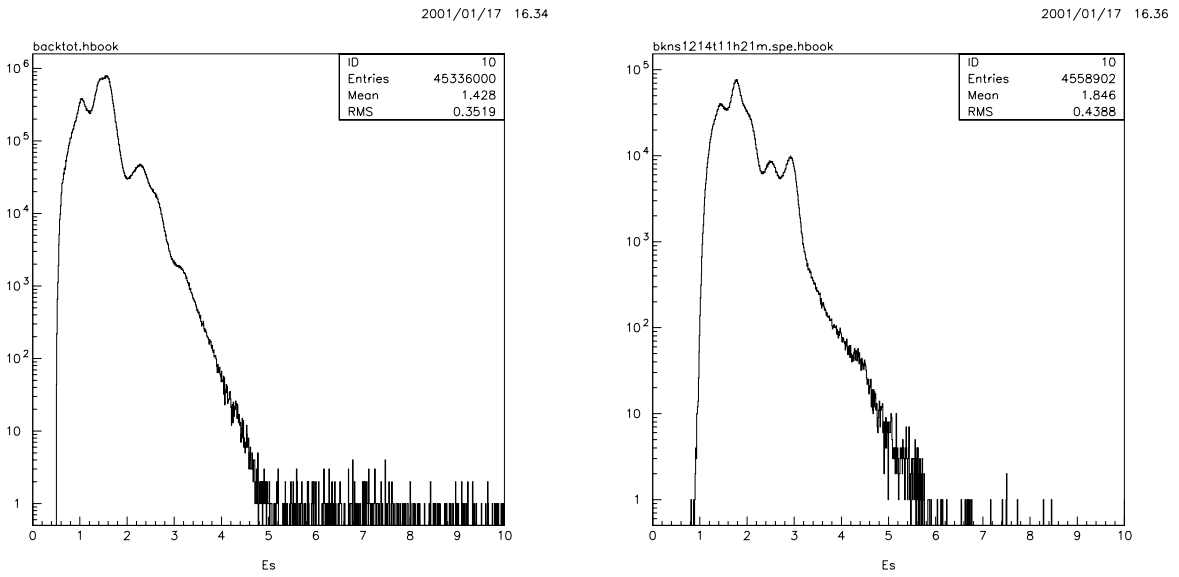

Figure 4: On the left lead shielded summed energy spectrum taken in the underground lab (measuring time 12 days). On the right summed energy spectrum taken in tha underground lab without any shielding (measuring time 14 hours)

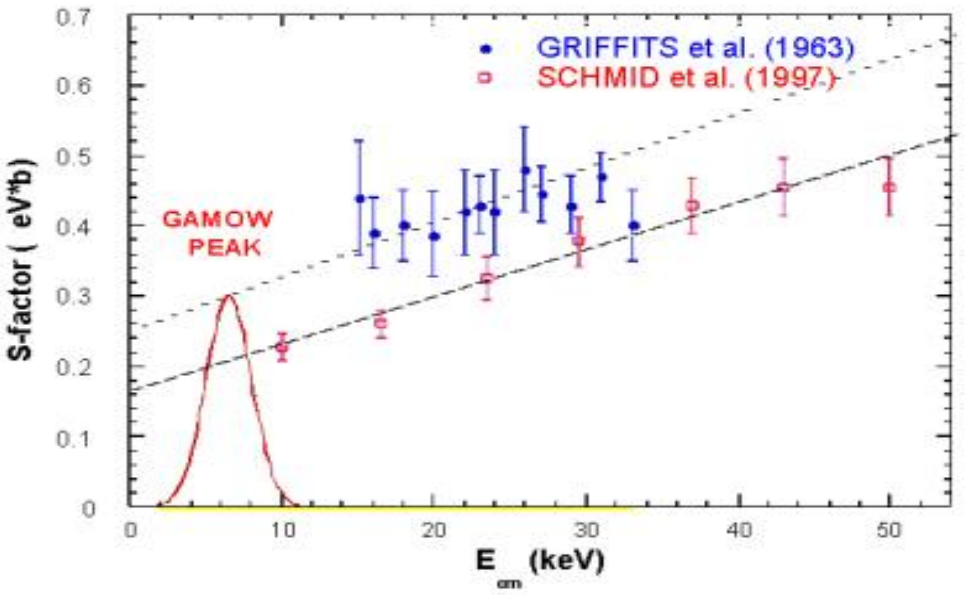

Figure 5: Discrepancy between the two existing data sets for the D(p, γ)^{3}He reaction. The full points are the Griffits data and the open points are the Schmid data.

3 The D(p,γ)^{3}He reaction

As for the 400 kV accelerator also for the other parts of the new equipment like the data acquisition system, BGO detector, gas target and calorimeter accurate testing is necessary. For this pourpous the LUNA collaboration decided to study the D(p, γ)^{3}He nuclear reaction at the old 50 kV accelerator facility. The D(p, γ)^{3}He is a direct capture reaction which emits a monoenergetic gamma and therefore it is a good test to study all the features of the BGO spectra. It is a reaction of the pp chain. With the low background reaction rate in the region near 5.5 MeV (Q-value), LUNA will be able to explore all the Gamow peak region at the energy of 6.5 keV. Very low energy measurements are required also because of the discrepacy between the two existing data sets (see figure 5) measured by Griffits [7] and Schmid [6].

4 Stopping power and electron screening effects in the D(^{3}He,p)^{4}He and ^{3}He(d,p)^{4}He fusion reactions

For absolute σ(E) measurements at subcoulomb energies, an accurate knowledge of the effective beam energy associated with the observed reaction yield is as important as the yield measurements themselves. In particular the bad knowledge of stopping power has been often claimed out as a possible explanation of measured screening potentials excess over theoretical expectations [8]. In the data analysis, in fact, the effective energy in the target involves always energy loss corrections, which are extracted from a standard compilation [9]. The compilation is based on experimental data down to energies around

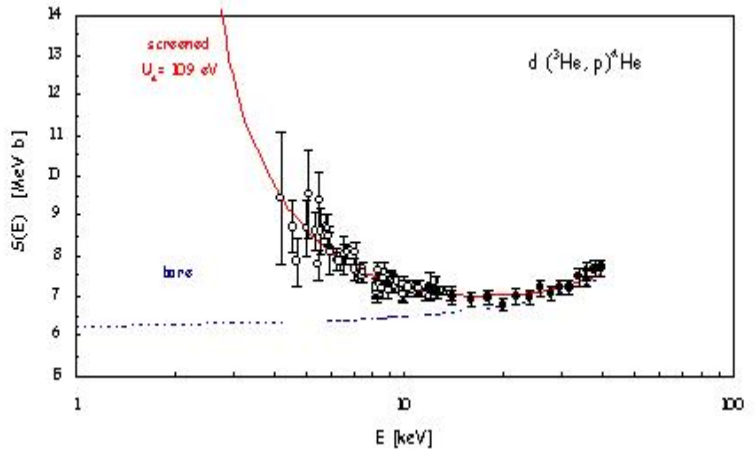

Figure 6: S(E) factor data for the d(^{3}He,p)^{4}He reaction (open points [12], filled points [13]), both obtained with the same LUNA setup. The errors shown represent only statistical and accidental uncertainties, which were used in the fits. The dashed curve represents the S(E) factor for bare nuclei and the solid curve that for screened nuclei with U_e=109 eV.

the Bragg peak, while at lower energies - relevant to nuclear astrophysics - the experimental data are extrapolated. Indeed experimental evidences of energy loss values lower than tabulated have been already reported [10]. For this reason the experimental study of electron screening effect has to be accomplished by a renewed evaluation of projectiles energy loss at the en ergies of interest. The D(^{3}He,p)^{4}He and ^{3}He(d,p)^{4}He cross sections have been measured at the center of mass energies E=4.2 keV to 60 keV and 10 keV to 40 keV, respectively, using the LUNA underground accelerator facility at LNGS and the 100 kV accelerator of the Ruhr-Universität Bochum (Germany) (for more details on experimental setup see [11, 12, 13]. The reaction yield dependence at a given beam energy for different gas target pressures has been used to evaluate the stopping power [14, 15].

The observed energy losses of ^{3}He ions in the D^2 target [12] came out in fair agreement with compilation: the measured S(E) astrophysical factor is shown in figure 6 [13]. These data lead to an electron screening potential Ue=109±9 eV [13] much larger than the expected value of 65 eV.

In the case of ^{3}He(d,p)^{4}He reaction, on the other side, a steep drop of stopping power below the theoretical values has been observed near E_d=18 keV (figure 8) [15]. This threshold behavior seems related to the minimum 1s→2s electron excitation of the ^{3}He target atoms (=19.8 eV, corresponding to E_d=18.2 keV) i.e. it is a quantum effect by which the atoms become nearly transparent for the ions. Using the measured stopping power the S(E) factor energy dependence shown in figure 7 has been found. It corresponds to a screening potential of U_e=219±7 eV [13] consistent with previous work [16] and much larger than the adiabatic limit.

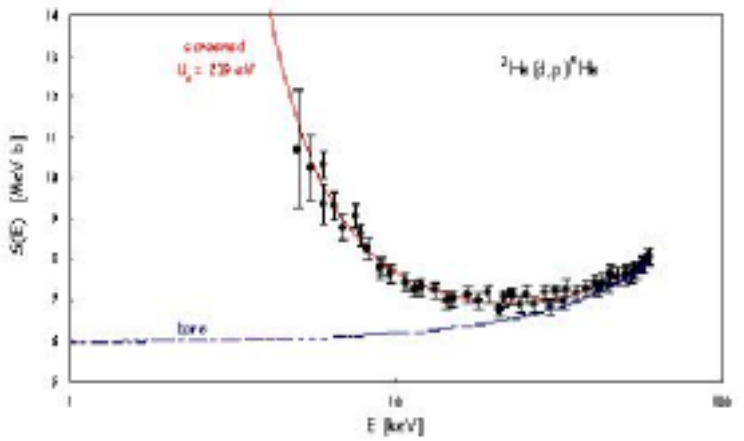

Figure 7: S(E) factor data for the ^{3}He(d,p)^{4}He reaction from the present work. The errors shown represent only statistical and accidental uncertainties, which were used in the fits. The dashed curve represents the S(E) factor for bare nuclei and the solid curve that for screened nuclei with U_e=219 eV.

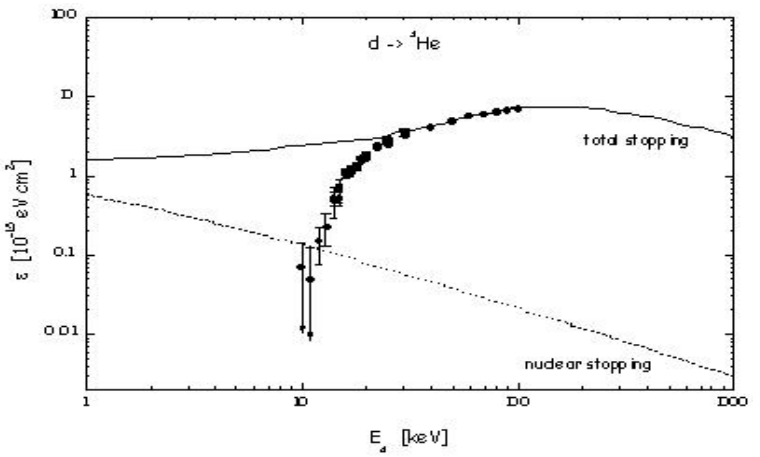

Figure 8: Deuterons stopping power in ^{3}He gas as function of deuteron energy. The total stopping power curve is obtained from the compilation [9] based on data above 80 keV. The nuclear stopping power curve is the prediction from [9]. The present data show a threshold effect in the stopping power near E_d=18 keV.

5 Pubblications and Conferences

1. A.Formicola et al., Eur. Phys. J. A8(2000)43.
2. H.Costantini et al., Phys. Lett. B482(2000)43.
3. F.Raiola et al., Submitted.
4. M.Aliotta et al.,Submitted.
5. R. Bonetti et al. "Recent results on cross section measurements of reaction of the hydrogen chain at solar energies", invited talk at the "International Conference on Nuclear Reaction Mechanism", Varenna, Italy, June 5-10, 2000.
6. P. Prati et al.,"Electron screening effects and astrophysical S(E) factor of D(^{3}He,p)^{4}H ", talk at the "VII Internationa Conference Nucleus-Nucleus collision", Strasburgh, France, July 3-7, 2000.
7. H. Costantini et al. "Status of the LUNA experiment at Gran Sasso", talk at the "17th Meeting between Astrophysicists and Physicists", Bruxelles, Belgium, December 11-12, 2000.
8. S. Zavatarelli, "Experimental study of the electron screening effect in the D(^{3}He,p)^{4}H fusion reaction", talk at the conference "Bologna 2000 on Structure of the Nucleus at the Down of the Century", Bologna Italy, May 29, 2000.
9. S. Zavatarelli, "The D(^{3}He,p)^4 fusion reaction: electron screening effects and astrophysical S(E) factor at low energies", Poster at the Conference "Nuclei in the Cosmos 2000", University of Arhus, Arhus, Denmark, June 27-July 1, 2000.
10. M.Junker, invited talk at "Nuclei in the Cosmos 2000", University of Arhus, Arthus, Denmark, 27 June-1 July, 2000.
11. M.Junker, invited talk at "TOURS 2000", Tours Symposium on Nuclear Physics IV, Tours, France, September 4-7, 2000.
12. M.Junker, invited talk at the "16th International Conference on the Application of Accelerators in Reserarch and Industry CARRI 2000", University of North Texas, Denton, USA, November 1-4 2000.
13. C.Rolfs, colloquium at Technische Universität München, January 10, 2000.
14. C.Rolfs, public talk at Museum Bochum, Bochum, Germany, January 16,2000.
15. M.Aliotta, F.Strieder, D.Rogalla, invited talk at Ringberg Winter School, March 20, 2000.
16. C.Rolfs, Public talk at Urania Berlin, April 4, 2000.
17. C.Rolfs, Public series at Universität Bochum, Bochum, Germany, April 25, 2000.

18. C.Rolfs, International Conference at Bologna, Bologna, Italy, May 29, 2000.
19. C.Rolfs, colloquium at Freie Universität Berlin, Berlin, Germany, July 13, 2000.
20. C.Rolfs, public talk at DESY, August 3, 2000.
21. C.Rolfs, survey talk at Erice International School, September 18, 2000.
22. C.Rolfs, Annual Meeting Of Portugese Physicists, September 29, 2000.
23. C.Rolfs, public Talk at Sternwarte Nordenham, November 2, 2000.
24. C.Rolfs, GSI colloquium, November 14, 2000.
25. C.Rolfs, International Colloquium at Bochum, Dicember 3, 2000.

References

[1] C. Rolfs and W.S. Rodney, Cauldrons in the cosmos (University of Chicago Press, 1988)

[2] G. Fiorentini, R. W. Kavanagh and C.Rolfs, Z.Phys. A350 (1995) 289

[3] U. Greife et al., Nucl. instr. Meth. A350(1994) 327

[4] A.E. Champagne,"14N(p,g)15O at low stellar temperatures" talk at 220th National ACS meeting, Nucleosynthesisi 2000, washington D.C. August 20-25 2000

[5] C. Angulo and P. Descouvemont, In print on nucl. phys. A

[6] G.J. Schmid et al., Phys. Rev. Lett. 76,17(1996)

[7] G.M. Griffits, M. Lal and C.D. Scarf, Can. J. Phys. Lett. 41,724 (1963)

[8] K. Langanke et al., Phys. Lett. B369(1996)211

[9] H.Andersen, J.F.Ziegler, The Stopping and Ranges of Ions in Matter (Pergamon, New York, 1977) and SRIM-2000

[10] R.Golser, D.Semrad, Phys.Rev.Lett. 66(1991)1831; Nucl.Instr.Meth. B69(1992)18

[11] M.Junker et al., Phys.Rev. C57(1998)2700

[12] H.Costantini et al., Phys.Lett. B482(2000)43

[13] M Aliotta et al., Submitted

[14] A.Formicola et al., Eur.Phys.J. A8(2000)443

[15] F. Raiola et al., Submitted

[16] P.Prati et al., Z.Phys. A350(1994)171

LVD. Large Volume Detector

M.Aglietta[14], E.D.Alyea[7], P.Antonioli[1], G.Badino[14], G.Bari[1], M.Basile[1], V.S.Berezinsky[9], F.Bersani[1], M.Bertaina[14], R.Bertoni[14], G.Bruni[1], G.Cara Romeo[1], C.Castagnoli[14], A.Castellina[14], A.Chiavassa[14], J.A.Chinellato[3], L.Cifarelli[1,†], F.Cindolo[1], A.Contin[1], V.L.Dadykin[9], L.G.Dos Santos[3], R.I.Enikeev[9], W.Fulgione[14], P.Galeotti[14], P.Ghia[14], P.Giusti[1], F.Gomez[14], F.Grianti[1], G.Iacobucci[1], E.Kemp[3], F.F.Khalchukov[9], E.V.Korolkova[9], P.V.Korchaguin[9], V.B.Korchaguin[9], V.A.Kudryavtsev[9], M.Luvisetto[1], A.S.Malguin[9], T.Massam[1], N.Mengotti Silva[3], C.Morello[14], R.Nania[1], G.Navarra[14], L.Periale[14], A.Pesci[1], P.Picchi[14], I.A.Pless[8], A.Romero[14], V.G.Ryasny[9], O.G.Ryazhskaya[9], O.Saavedra[14], K.Saitoh[13], G.Sartorelli[1], M.Selvi[1], N.Taborgna[5], N.Takahashi[12], V.P.Talochkin[9], G.C.Trinchero[14], S.Tsuji[10], A.Turtelli[3], P.Vallania[14], S.Vernetto[14], C.Vigorito[14], L.Votano[4], T.Wada[10], R.Weinstein[6], M.Widgoff[2], V.F.Yakushev[9], I.Yamamoto[11], G.T.Zatsepin[9], A.Zichichi[1,*]

[1] *University of Bologna and INFN-Bologna, Italy*
[2] *Brown University, Providence, USA*
[3] *University of Campinas, Campinas, Brazil*
[4] *INFN-LNF, Frascati, Italy*
[5] *INFN-LNGS, Assergi, Italy*
[6] *University of Houston, Houston, USA*
[7] *Indiana University, Bloomington, USA*
[8] *Massachusetts Institute of Technology, Cambridge, USA*
[9] *Institute for Nuclear Research, Russian Academy of Sciences, Moscow, Russia*
[10] *Okayama University, Okayama, Japan*
[11] *Okayama University of Science, Okayama, Japan*
[12] *Hirosaki University, Hirosaki, Japan*
[13] *Ashikaga Institute of Technology, Ashikaga, Japan*
[14] *Institute of Cosmo-Geophysics, CNR, Torino, University of Torino and INFN-Torino, Italy*
[†] *now at University of Salerno and INFN-Salerno, Italy*
[*] *Spokesperson*

Abstract

The Large Volume Detector (LVD) in the Gran Sasso Underground Laboratory is a ν observatory mainly designed to study low energy neutrinos from the gravitational collapse of galactic objects. The experiment is sensitive to collapses in our Galaxy since June 1992.

During 2000 the telescope continued the Galaxy monitoring searching for neutrino burst, with no positive results.

The third LVD tower has been completed, and tested. Since January 2001 the telescope is running with a scintillator mass $M = 1kton$, and a new, more reliable, DAQ system.

1 Introduction

The Large Volume Detector in the Gran Sasso underground Laboratory is a multipurpose detector consisting of a large volume of liquid scintillator interleaved with limited streamer tubes in a compact geometry.

A major purpose of the LVD experiment is to search for neutrinos from Gravitational Stellar Collapses (GSC) in our Galaxy [1].

Most theoretical models agree in predicting the total energy emitted as ν 's during the stellar collapse, the energy equipartition among the different ν flavours and the time duration of the ν burst. For any scintillator detector the bulk of events (about 90% of the total) is due to the capture reaction $\bar{\nu}_e p, e^+ n$. The e^+ spectrum is determined by the temperature of the $\bar{\nu}_e$ neutrino-sphere and therefore it is related to the equation of state of matter at the source.

Further, in LVD, about 5% of the events are due to neutral current interactions with ^{12}C which deexcites emitting a 15.1 MeV γ. Because μ and τ neutrino-spheres are located deeper in the collapsing stellar core, and because of the temperature gradient, their energy spectra have higher temperatures as compared with the electron neutrino spectra. As a consequence more then 90% of the n.c. interactions with Carbon nuclei are produced by ν_μ and ν_τ. Therefore the ratio between the number of n.c. interactions to the total is related to the ratio between μ, τ and e ν-sphere temperatures.

Only 3% of events in LVD, are due to elastic scattering of all neutrino flavours with electrons, and less then 1% to c.c. interactions of ν_e and $\bar{\nu}_e$ with ^{12}C nuclei. These reactions could easily be separated by subsequent β decay, but because of their relative high thresholds, they are few. It is worthwhile to note that if energetic μ and τ neutrinos oscillate into electron neutrinos, the $\bar{\nu}_e$ spectrum will be distorced and the number of c.c. interactions on carbon nuclei can increase.

Among all existing detectors of ν from gravitational collapse, LVD has some peculiarities:

- LVD can operate at very low energy thresholds.

  The detection of low energy neutrinos, of the order of a few MeV, gives the possibility to study objects emitting at low temperatures ν-sphere. When the collapsing star give up into a black hole, models predict a sharp, low energy neutrino bounch, due to the strong gravitational and Doppler red shift.

- LVD can identify interacting $\bar{\nu}_e$ by the strong signature of the dominant reaction $\bar{\nu}_e p, e^+ n$.

  The possibility to identify $\bar{\nu}_e$ interactions with protons by a stringent signature (and not simply by the absence of directionality as for light water Cherenkov detectors) gives us the chance to play with pure $\bar{\nu}_e$ energy spectrum and to separate the rare, but very interesting, charged and neutral current interactions with Carbon nuclei from the most common $\bar{\nu}_e$ interactions.

- LVD is highly modular.

  The modularity of LVD allows maintenance of part of the detector without stopping the whole telescope data taking. In fact in the last four years LVD has been observing the Galaxy searching for collapsing objects with an average duty cicle better than 97%. The monthly duty cicle of this period is shown in Fig.1. For the year 2000 the uptime efficiency reached 99.3%.

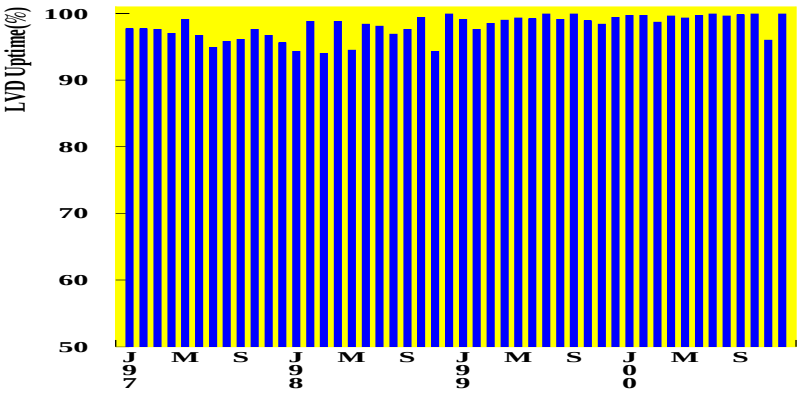

Figure 1: LVD monthly duty cicle

2 The LVD detector

The LVD detector, operating since June 1992, has a modular structure that consists of aligned towers of 35 modules each. In any tower the scintillator / tracking modules are stacked in five columns.

Every module contains 8 liquid scintillation counters of dimensions $1.5 \times 1 \times 1\ m^3$ seen by three photomultipliers. The density of the scintillator is about 0.8 g/cm^3 and the energy resolution is about 15% for a 10 MeV energy release, where, for electrons, it begins to be dominated by leakage effects in the counter.

The tracking system consists of L-shaped detectors for each module. Each element contains two staggered layers of 6.3 m long limited streamer tubes. The bidimensional read-out is made by means of 4 cm strips, parallel and perpendicular to the tubes, providing high detection efficiency and an angular resolution better than 4 milliradians.

In the search for ν bursts from GSC, the most important performances of LVD are the following:

- The information related to each signal is stored in a temporary memory buffer which is shared by 8 scintillator counters. Globally the whole experiment can store up to 5.4×10^4 pulses, which corresponds, following the most qualified models [2], to the signal from a supernova at a distance closer than 1 Kpc from the Earth.

- The total deadtime corresponds to a maximum detectable frequency (per counter) of 500 kHz and the read out procedure does not introduce any additional deadtime.

- The time of each signal, relative to the U.T. time ($\pm$ 1 μs from the Gran Sasso facility), is measured with an accuracy of $\pm$12.5 ns.

3 Detector completion and upgrade during 2000

3.1 Tower 3

The scintillator production (the liquid scintillator of the LVD third tower has been produced in the Gran Sasso Laboratory) was completed on February 2000. During March the last counters have been assembled in the structure, including the L-shaped hood of the tracking system. During the second half of the year the counters and their electronics have been tested and calibrated.

At present the full detector is in operation with an active scintillator mass $M = 1$ kt.

3.2 Shielding for top level counters

The counting rate of different counters depends on their exposure to the rock radioactivity. In particular, counters of the top level, which are less shielded than others against the tunnel walls, suffer of an higher background counting rate ($R_{top}/R_{ext} \sim 4$) and this entails a minor capability to tag $\bar{\nu}_e$ interactions for these counters.

In order to reduce that background it has been studied and realized an iron shielding (2 cm thick) and it is now partially assembled. For what concerns the neutron background it is foreseen an additional shield to be realized during the 2001.

3.3 Scintillator HV system

The upgrade of the whole HV system power supply for the scintillator photomultipliers has been realized during 2000. The new system (based on CAEN SY527) will allows a more complete remote control of every channel and more flexible configuration with respect to the old one.

3.4 DAQ upgrade

A complete upgrade of the DAQ system has been also completed during 2000. At tower level the new system is based on VME PowerPC CPUs Motorola 2700 running LynxOS. The CAMAC bus is read-out through the CBD 8210 (a standard VME-CAMAC adapter provided by CES). An AlphaStation 255/233 running Tru64 Unix complete the system for run control, boot-server and monitoring tasks.

On the basis of the experience of these years, particular care has been taken designing the new system to ensure high modularity of the DAQ configuration and possibility to insert/remove counters or electronic modules from the read-out for normal maintenance without stopping the data taking. Crate failures and bus errors handling has been implemented to ensure continuous data taking also. Excluding "catastrophic" events (long power supply black-out, CPU boot node failure, disk failure), hopefully we should no longer stop the run. We are also considering to add during year 2001 some redundancy to the system (mainly RAID controllers for disks and network apparata), to improve our fault tolerance capabilities.

The run control user interface is now completely WEB operated making easy remote maintenance.

The system has been firstly installed for tower 3 during late 1999. During February LVD LAN in Hall A has been fully upgraded to 100 Mbit and first counters data have been achieved at March. The new system was tested thoroughly during the year. Tower 2 migrates to the new DAQ during October and since December the whole LVD data acquisition is under the new system.

4 SNEWS

Since February 1999 the LVD joined the SNEWS (SuperNova Early Warning System) network[3]. This project, carried out by different neutrino telescopes searching for burst from SuperNova (AMANDA, LVD, SNO and SuperKamiokande are currently involved), developped an early alert system to the astronomers based on detection of ν burst candidates simultaneously from different experiments.

In order to build a redundant system and minimize network failures a second central server (the first one is in Kamioka) to collect the signals from different experiments has been setup and operated by LVD during 2000 also at LNGS and it is intended to be a facility at disposal of any LNGS experiment that will be interested in the future.

The project will move from a test phase to an operational one during 2001.

To simulate the detector response to a cluster of ν pulses as expected from the gravitational collapse of star in the Galaxy, a cluster generator producing light pulses (LED) on a number of counters of the telescope has been studied and realized, and it will be assembled in the first part of 2001. Moreover during 2001 a test of synchronism among the different telescopes of the SN Early Warning System has been planned.

5 Results

5.1 Search for gravitational collapse

During 2000 the LVD ν telescope continued the Galaxy monitoring in the search for neutrino bursts as expected from gravitational collapses of massive stars.

The time sequence of clustered single pulses is checked and compared with the expected one. Each cluster is defined by the multiplicity m and the time duration Δt ($\Delta t \leq 200\ s$). The corresponding Poisson probability is calculated on the basis of the current trigger rate and an imitation frequency (F_{im}) is obtained.

Since June 1992 no evidence for ν burst candidates has been found. On the basis of this data the upper limit at 90% c.l. on the rate of Gravitational Stellar Collapse in the Galaxy is 0.3 events $\cdot$ year^{-1}.

5.2 Upper limits to low energy $\bar{\nu}_e$ flux from GRB990705

On July 5^{th} 1999, 16:01:25 UT, a Gamma Ray Burst (GRB990705) has been detected by BeppoSAX from the direction of the outskirts of the Large Magellanic Clouds (GCN circular n.368). If the burst was indeed located in the LMC or its halo (or even closer), a search for a neutrino signal coincident with, or just prior to the GRB event, would be most interesting.

At the time of GRB990705 LVD was regularly taking data with an active scintillator mass $M = 573$ ton.

On July 19^{th} 1999, the result of a preliminary analysis of the data recorded during 48 hours of data taking around July 5^{th} was reported by the LVD collaboration (GCN circular n.390 [7]). The absence of a neutrino signal, as expected from a gravitational stellar collapse in the Galaxy or Magellanic Clouds, correlated to the GRB990705 was established. A more careful analysis has been performed to search for weaker signals even preceding GRB990705 [8].

Some models suggest that gamma ray bursts are related to Supernova explosions. In this scenario the neutrino emission should be associated to the cooling of the collapsed object while photons should be emitted by narrow ultra-relativistic jets streaming along the rotational axis. Therefore the time gap between the two signals depends on the time necessary to transfer energy

from the central engine, which emits thermal ν to the outer region transparent for high energy photons.

On the analogy of SN explosions modelling, where few hours are necessary to the shock to reach the star envelope and give rise to the sudden increase of luminosity, a similar time gap for the event under study has been assumed.

The search has been extended since 24 hours before the GRB time to 10 minutes after, for a total time $T = 1450\ min$ on three event classes, namely:

- class A: pulses with $E_d \geq 7MeV$ $(M = 573\ ton)$;
- class B: pulses with $E_d \geq 7MeV$ followed by at least one delayed low energy pulse in the same counter $(M = 573\ ton)$;
- class C: pulses detected by core scintillators $(E_d \geq 4MeV)$ followed by at least one delayed low energy pulse in the same counter $(M = 256\ ton)$.

The search for a signal in time coincidence with GRB990705 has been performed by comparing the number of observed signals inside time windows of different duration δt centered on the GRB time, with the average number of signals expected from background. On the other hand in the 24 hours search, the interval of interest has been divided into $N_{\delta t} = 2 \cdot \frac{T}{\delta t}$ intervals of duration δt, each one starting at the middle of the previous one. The multiplicity distributions of clusters (number of events within each interval of duration δt) have been studied for $\delta t = 1, 5, 10, 20, 50$ and 100 seconds and compared with expectations from pure Poissonian fluctuations of the background as calculated by using the average event rate in 24 hours.

The agreement between data and expectations allows to state that there is no evidence for any detectable ν signal during this period.

In the absence of any information on the distance of the source and the emission spectra, we can express the results of the search in terms of upper limits to the time integrated flux cross-section product at the Earth: $\int dt \int \frac{d^2\phi}{dEdt}\sigma dE$.
These limits, reported in Table 2 at 90% c.l. for various δt, are expressed in number of interactions per target proton.

	coincidence		24 hour preceding	
δt [s]	$\int_0^{\delta t} dt \int_5^{\infty} \frac{d^2\phi_\nu}{dEdt}\sigma(E)dE$	$\int_0^{\delta t} dt \int_8^{\infty} \frac{d^2\phi_\nu}{dEdt}\sigma(E)dE$	$\int_0^{\delta t} dt \int_5^{\infty} \frac{d^2\phi_\nu}{dEdt}\sigma(E)dE$	$\int_0^{\delta t} dt \int_8^{\infty} \frac{d^2\phi_\nu}{dEdt}\sigma(E)dE$
1	$1.7 \cdot 10^{-31}$	$4.3 \cdot 10^{-32}$	$5.9 \cdot 10^{-31}$	$1.9 \cdot 10^{-31}$
5	$1.7 \cdot 10^{-31}$	$4.3 \cdot 10^{-32}$	$5.9 \cdot 10^{-31}$	$2.4 \cdot 10^{-31}$
10	$1.7 \cdot 10^{-31}$	$4.3 \cdot 10^{-32}$	$7.4 \cdot 10^{-31}$	$2.8 \cdot 10^{-31}$
20	$1.7 \cdot 10^{-31}$	$7.5 \cdot 10^{-32}$	$8.1 \cdot 10^{-31}$	$3.5 \cdot 10^{-31}$
50	$1.7 \cdot 10^{-31}$	$8.6 \cdot 10^{-32}$	$9.6 \cdot 10^{-31}$	$5.2 \cdot 10^{-31}$
100	$2.9 \cdot 10^{-31}$	$8.6 \cdot 10^{-32}$	$1.1 \cdot 10^{-30}$	$6.0 \cdot 10^{-31}$

Tab.2: Upper limits (90% c.l.) to the $\bar{\nu}_e$ flux · cross-section, at the Earth, integrated over different time intervals.

Any hypothesis on the $\bar{\nu}_e$ spectrum leads to a limit to the time integrated $\bar{\nu}_e$ flux at the Earth. Assuming, on the analogy of ν emitted by SN, a thermal $\bar{\nu}_e$ spectrum, the time integrated $\bar{\nu}_e$ flux, for burst duration $\delta t \leq 10\ s$, is obtained as a function of the emission temperature $T[MeV]$ and the corresponding 90% *c.l.* upper limits are shown in fig. 2. These results have been accepted for publication on Astronomy and Astrophysics.

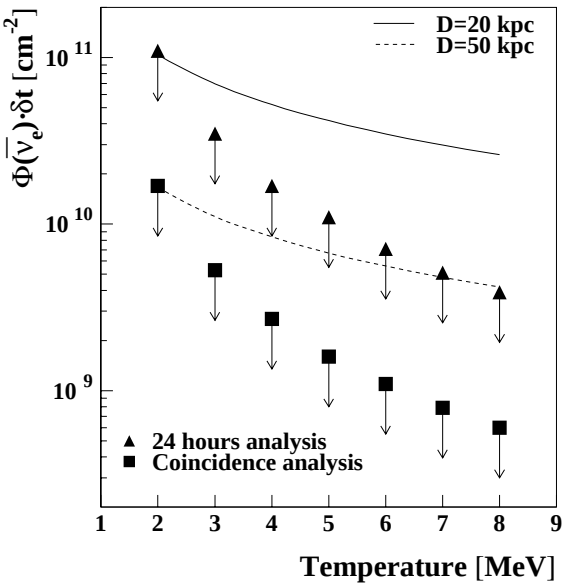

Figure 2: Upper limits (90% c.l.) to the time integrated $\bar{\nu}_e$ flux, at the Earth, for thermal $\bar{\nu}_e$ spectra and $\delta t \leq 10$ s, compared with expectations for different source distances.

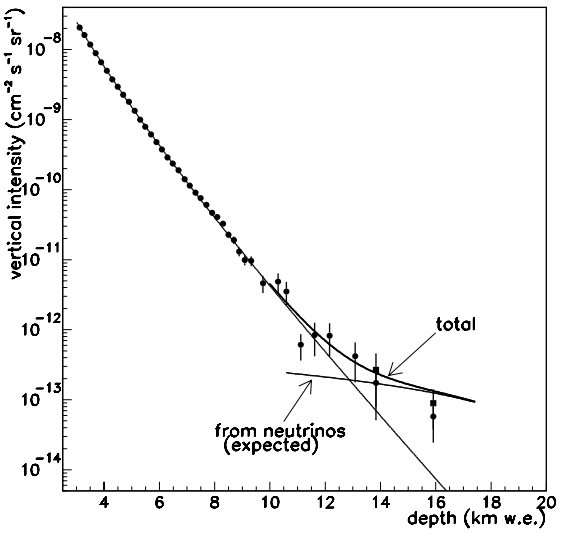

Figure 3: Muon depth-intensity measured at LVD up to 20 Km w.e. At depth > 14 km w.e. the squared point are computed with acceptance corrected for low energy muons, as expected for ν-induced.

5.3 Muon studies

Increasing statistics, the upgrade of existing or published analysis (see previous Annual Reports and [4, 5, 6]) is under way with particular interest for muon neutrino-induced at large depth and study of multiple muons events. During 2000, on tower 1 and 2 we collected and reconstructed more than 1.8 million of events with muon tracks.

A muon depth-intensity curve (not yet including the whole statistics) extending up to 20 km w.e. is shown in Fig. 3. The neutrino-induced component is clearly seen.

References

[1] LVD Collaboration, Il Nuovo Cimento, A105, 1793 (1992)

[2] A. Burrows et al., Phys.Rev. D, 45. 3361 (1992)

[3] http://hep.bu.edu/˜ snnet/

[4] The LVD Collaboration, Phys. Rev. D, 58, 2005 (1998)

[5] The LVD Collaboration, Phys. Rev. D, 60, 112001 (1999)

[6] The LVD Collaboration, 26th ICRC Proceedings, "Muon astronomy with LVD detector", SH 3.2.40, Vol. 7, 222 (Salt Lake City, USA, 1999)

[7] http://lheawww.gsfc.nasa.gov/docs/gamcosray/legr/bacodine/gcn3/390.gcn3

[8] LVD Collaboration, astro-ph/0011249 (November 2000), accepted for publication on Astronomy & Astrophysics

MACRO. Monopole Astrophysics Cosmic Ray Observatory

M. Ambrosio[12], R. Antolini[7], G. Auriemma[14,a], D. Bakari[2,17], A. Baldini[13], G. C. Barbarino[12], B. C. Barish[4], G. Battistoni[6,b], R. Bellotti[1], C. Bemporad[13], P. Bernardini[10], H. Bilokon[6], V. Bisi[16], C. Bloise[6], C. Bower[8], M. Brigida[1], S. Bussino[18], F. Cafagna[1], M. Calicchio[1], D. Campana[12], M. Carboni[6], S. Cecchini[2,c], F. Cei[13], V. Chiarella[6], B. C. Choudhary[4], S. Coutu[11,l], G. De Cataldo[1], H. Dekhissi[2,17], C. De Marzo[1], I. De Mitri[10], J. Derkaoui[2,17], M. De Vincenzi[18], A. Di Credico[7], O. Erriquez[1], C. Favuzzi[1], C. Forti[6], P. Fusco[1], G. Giacomelli[2], G. Giannini[13,e], N. Giglietto[1], M. Giorgini[2], M. Grassi[13], L. Gray[7], A. Grillo[7], F. Guarino[12], C. Gustavino[7], A. Habig[3], K. Hanson[11], R. Heinz[8], E. Iarocci[6,f], E. Katsavounidis[4], I. Katsavounidis[4], E. Kearns[3], H. Kim[4], S. Kyriazopoulou[4], E. Lamanna[14,m], C. Lane[5], D. S. Levin[11], P. Lipari[14], N. P. Longley[4,i], M. J. Longo[11], F. Loparco[1], F. Maaroufi[2,17], G. Mancarella[10], G. Mandrioli[2], S. Manzoor[2,o], A. Margiotta[2], A. Marini[6], D. Martello[10], A. Marzari-Chiesa[16], M. N. Mazziotta[1], D. G. Michael[4], S. Mikheyev[4,7,g], L. Miller[8,n], P. Monacelli[9], T. Montaruli[1], M. Monteno[16], S. Mufson[8], J. Musser[8], D. Nicolò[13,d], R. Nolty[4], C. Okada3, C. Orth[3], G. Osteria[12], M. Ouchrif[2,17], O. Palamara[7], V. Patera[6,f], L. Patrizii[2], R. Pazzi[13], C. W. Peck[4], L. Perrone[10], S. Petrera[9], P. Pistilli[18], V. Popa[2,h], A. Rainò[1], J. Reynoldson[7], F. Ronga[6], A. Rrhioua[2,17], C. Satriano[14,a], L. Satta[6,f], E. Scapparone[7], K. Scholberg[3], A. Sciubba[6,f], P. Serra[2], M. Sioli[2], G. Sirri[2], M. Sitta[16], P. Spinelli[1], M. Spinetti[6], M. Spurio[2], R. Steinberg[5], J. L. Stone[3], L. R. Sulak[3], A. Surdo[10], G. Tarlè [11], V. Togo[2], M. Vakili[15], E. Vilela[2], C. W. Walter[3,4] and R. Webb[15].

1. Dipartimento di Fisica dell'Università di Bari and INFN, 70126 Bari, Italy
2. Dipartimento di Fisica dell'Università di Bologna and INFN, 40126 Bologna, Italy
3. Physics Department, Boston University, Boston, MA 02215, USA
4. California Institute of Technology, Pasadena, CA 91125, USA
5. Department of Physics, Drexel University, Philadelphia, PA 19104, USA
6. Laboratori Nazionali di Frascati dell'INFN, 00044 Frascati (Roma), Italy
7. Laboratori Nazionali del Gran Sasso dell'INFN, 67010 Assergi (L'Aquila), Italy
8. Depts. of Physics and of Astronomy, Indiana University, Bloomington, IN 47405, USA
9. Dipartimento di Fisica dell'Università dell'Aquila and INFN, 67100 L'Aquila, Italy
10. Dipartimento di Fisica dell'Università di Lecce and INFN, 73100 Lecce, Italy
11. Department of Physics, University of Michigan, Ann Arbor, MI 48109, USA
12. Dipartimento di Fisica dell'Università di Napoli and INFN, 80125 Napoli, Italy
13. Dipartimento di Fisica dell'Università di Pisa and INFN, 56010 Pisa, Italy
14. Dipartimento di Fisica dell'Università di Roma "La Sapienza" and INFN, 00185 Roma, Italy
15. Physics Department, Texas A&M University, College Station, TX 77843, USA
16. Dipartimento di Fisica Sperimentale dell'Università di Torino and INFN, 10125 Torino, Italy
17. L.P.T.P., Faculty of Sciences, University Mohamed I, B.P. 524 Oujda, Morocco
18. Dipartimento di Fisica dell'Università di Roma Tre and INFN Sezione Roma Tre, 00146 Roma, Italy
a Also Università della Basilicata, 85100 Potenza, Italy
b Also INFN Milano, 20133 Milano, Italy
c Also Istituto TESRE/CNR, 40129 Bologna, Italy
d Also Scuola Normale Superiore di Pisa, 56010 Pisa, Italy
e Also Università di Trieste and INFN, 34100 Trieste, Italy
f Also Dipartimento di Energetica, Università di Roma, 00185 Roma, Italy
g Also Institute for Nuclear Research, Russian Academy of Science, 117312 Moscow, Russia
h Also Institute for Space Sciences, 76900 Bucharest, Romania
i The Colorado College, Colorado Springs, CO 80903, USA
l Also Department of Physics, Pennsylvania State University, University Park, PA 16801, USA
m Also Dipartimento di Fisica dell'Università della Calabria, Rende (Cosenza), Italy
n Also Department of Physics, James Madison University, Harrisonburg, VA 22807, USA
o Also RPD, PINSTECH, P.O. Nilore, Islamabad, Pakistan

Abstract

The status of the MACRO detector is described and experimental results are presented on atmospheric neutrinos and neutrino oscillations, high energy neutrino astronomy, searches for WIMPs, search for low energy stellar gravitational collapse neutrinos, searches for magnetic monopoles, nuclearites and lightly ionizing particles, high energy downgoing muons, primary cosmic ray composition and shadowing of primary cosmic rays by the moon and the sun.

1 Introduction

MACRO was a large area multipurpose underground detector designed to search for rare events in the cosmic radiation. It was optimized to look for the supermassive magnetic monopoles predicted by Grand Unified Theories (GUT) of the electroweak and strong interactions; it could also perform measurements in areas of astrophysics, nuclear, particle and cosmic ray physics. These include the study of atmospheric neutrinos and neutrino oscillations, high energy ($E_\nu \gtrsim 1$ GeV) neutrino astronomy, indirect searches for WIMPs, search for low energy ($E_\nu \gtrsim 7$ MeV) stellar collapse neutrinos, studies of various aspects of the high energy underground muon flux (which is an indirect tool to study the primary cosmic ray composition, origin and interactions), searches for fractionally charged particles and other rare particles that may exist in the cosmic radiation. The mean rock depth of the overburden is $\simeq$ 3700 m.w.e., while the minimum is 3150 m.w.e. This defines the minimum muon energy at the surface at ~ 1.3 TeV in order to reach MACRO. The average residual energy and the muon flux at the MACRO depth are ~ 310 GeV and ~ 1 m^{-2} h^{-1}, respectively. The detector was built and equipped with electronics during the years 1988$-$1995. It was completed in 1995 and it was running in its final configuration until December 19, 2000.

The highlights of the new results have been presented at the 2000 summer conferences (in particular at Neutrino 2000 and at the High Energy Conference in Japan); one of the main results is the evidence for anomalies in the atmospheric ν_μ flux, which are interpreted in terms of neutrino oscillations.

We are now preparing a technical paper and several papers with the final results of the experiment.

2 The Detector

The MACRO detector had a modular structure: it was divided into six sections referred to as supermodules. Each active part of one supermodule had a size of $12.6 \times 12 \times 9.3$ m^3 and had a separate mechanical structure and electronics readout. The full detector had global dimensions of $76.5 \times 12 \times 9.3$ m^3 and provided a total acceptance to an isotropic flux of particles of $\sim 10,000$ m^2 sr. The total mass was $\simeq$ 5300 t.

Redundancy and complementarity have been the primary goals in designing the experiment. Since no more than few magnetic monopoles could be expected, multiple signatures and ability to perform cross checks among various parts of the apparatus were important.

The detector was composed of three sub-detectors: liquid scintillation counters, limited streamer tubes and nuclear track detectors. Each one of them could be used in "stand-alone" and in "combined" mode. A general layout of the experiment is shown in Fig. 1.

Each supermodule contained 77 scintillation counters, divided into three horizontal planes (bottom, center, and top) and two vertical planes (east and west). The bottom and center horizontal planes, along with the lower seven scintillators of the east and west planes, occupied the lower section of each supermodule which was frequently referred to as the *lower* MACRO. The mass of the *lower* MACRO was $\simeq$ 4200 t, mainly in the form of

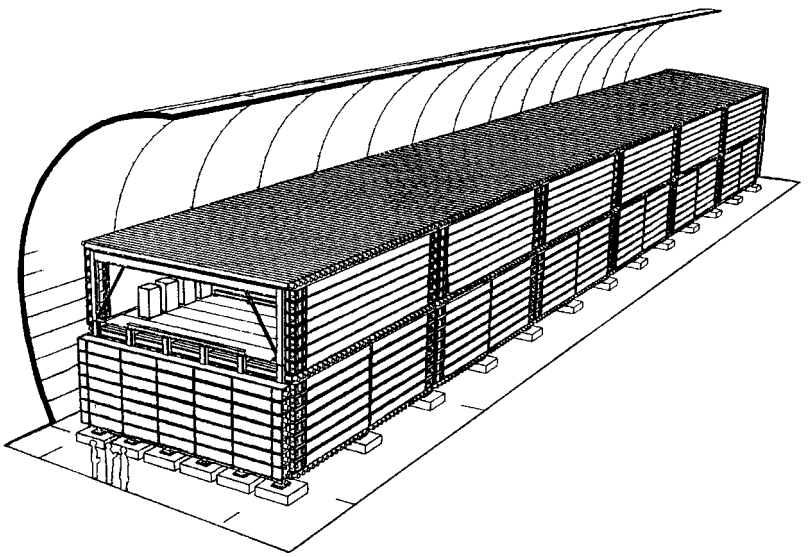

Figure 1: General layout of the MACRO detector which was installed in Hall B of the LNGS. Overall dimensions of the active part were $76.5 \times 12 \times 9.3$ m^3.

crushed Gran Sasso rock. The top plane and the upper seven scintillators of the east and west planes occupied the upper section of the detector, often referred to as the *Attico*. The lower part of the north and south faces of the detector were covered by vertical walls with seven scintillation counters each. The upper parts of these faces were left open in order to allow access to the readout electronics. The active volume of each horizontal scintillator counter was $11.2 \times 0.73 \times 0.19$ m^3, while the vertical ones measured $11.1 \times 0.22 \times 0.46$ m^3. All were filled with a mixture of mineral oil (96.4 %) and pseudocumene (3.6 %), with an additional 1.44 g/l of PPO and 1.44 mg/l of bis-MSB as wavelength shifters. The horizontal counters were seen by two 8″ phototubes (PMTs) and the vertical counters by one 8″ PMT at each end. Each PMT housing was equipped with a light collecting mirror. The total number of scintillators was 476 (294 horizontal and 182 vertical) with a total active mass of almost 600 tons. Minimum ionizing muons when crossing vertically the 19 cm of scintillator in a counter release $\simeq 34$ MeV of average energy and were measured with a timing and longitudinal position resolution of $\simeq 500$ ps and $\simeq 10$ cm, respectively.

The scintillation counters were equipped with specific triggers for rare particles, muons and low energy neutrinos from stellar gravitational collapses. The Slow Monopole Trigger (SMT) was sensitive to magnetic monopoles with velocities from about $10^{-4}c$ to $10^{-2}c$, the Fast Monopole Trigger (FMT) was sensitive to monopoles with velocities from about $5 \times 10^{-3}c$ to $5 \times 10^{-2}c$, the Lightly Ionizing Particle (LIP) trigger was sensitive to fractionally charged particles, the Energy Reconstruction Processor (ERP) and "CSPAM" were primarily muon triggers (but used also for relativistic monopoles) and the gravitational collapse neutrino triggers (the Pulse Height Recorder and Synchronous Encoder –PHRASE– and the ERP) were optimized to trigger on bursts of low energy events in the liquid scintillator. The scintillator system was complemented by a 200 MHz wave form digitizing (WFD) system used in rare particle searches but also on any occasion where knowledge of the PMT waveform was useful.

The lower part of the detector contained ten horizontal planes of limited streamer tubes, the middle eight of which were interleaved by seven rock absorbers (total thickness $\simeq 360$ g cm^{-2}). This sets a $\simeq 1$ GeV energy threshold for muons vertically crossing the lower part of the detector. In the *Attico* there were four horizontal streamer tube planes, two above and two below the top scintillator layer. On each lateral wall six streamer tube planes sandwiched the corresponding vertical scintillator plane (three streamer planes on each side). Each tube had a 3×3 cm^2 cross section and measured 12 m in length. The total number of tubes was 55, 200, all filled with a gas mixture of He (73 %) and n-pentane (27 %). They were equipped with 100 μ *Cu/Be* wires and stereo pickup strips at an angle of 26.5°. The intrinsic position and tracking resolutions of the streamer tube system were $\simeq 1$ cm and $\simeq 0.2°$, respectively. The overall angular resolution was limited to $\simeq 1°$ by the multiple scattering in the rock above the detector. The streamer tubes were read by 8-channel cards (one channel for each wire) which discriminated the signals and sent the analog information (time development and total charge) to an ADC/TDC system (the QTP). The signals were used to form two different chains (Fast and Slow) of TTL pulses, which were the inputs for the streamer tube Fast and Slow Particle Triggers.

The nuclear track detector was deployed in three planes, horizontally in the center of the lower section and vertically on the East and North faces. The detector was divided in 18126 individual modules, which could be individually extracted and changed upon need. Each module ($\sim 24.5 \times 24.5 \times 0.65$ cm^3 in size) was composed of three layers of CR39, three layers of Lexan and 1 mm Aluminium absorber to stop nuclear fragments.

In addition to these three detection elements, a Transition Radiation Detector (TRD) was installed in part of the *Attico*, right above the central horizontal scintillator plane of the main detector. It was composed of three individual modules (overall dimensions $6 \times 6 \times 2$ m^3) and it was made of 10 cm thick polyethylene foam radiators and proportional counters; each counter measured $6 \times 6 \times 600$ cm^3 and was filled with Ar (90 %) and CO_2 (10 %). The TRD provided a measurement of the muon energy in the range of 100 GeV $< E <$ 930 GeV; muons of higher energies could also be detected and counted.

3 Selected Physics Results

In year 2000 four papers were published on refereed journals; they concerned a search for nuclearites [M1], the study of low energy atmospheric muon neutrinos [M2], a search for Lightly Ionizing Particles [M3] and neutrino astronomy with the MACRO detector [M4]. Several results appeared in preliminary form in 22 paper contributions that were published in various physics conference proceedings [M5]-[M26]. They concerned the study of high and low energy atmospheric neutrinos, high energy muon neutrino astronomy, rare particle searches, the observation of the sun shadow of high energy primary cosmic rays and several aspects of "muon astronomy".

3.1 Neutrino-induced Upward Going Muons

Upward going muons are identified using the streamer tube system (for tracking) and the scintillator system (for time-of-flight measurement). A rejection factor of at least 10^7 is

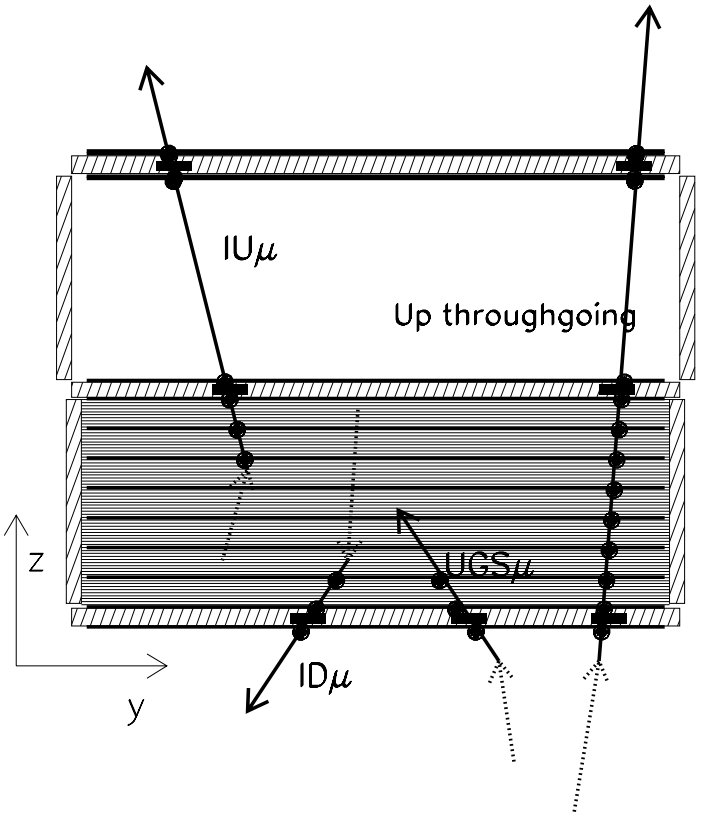

Figure 2: Sketch of different event topologies induced by ν_μ interactions in or around MACRO. The stars represent scintillator hits. The track directions are measured by the streamer tubes; the time-of-flight of the muons can be measured for *Up Semicontained* and *Up throughgoing* events.

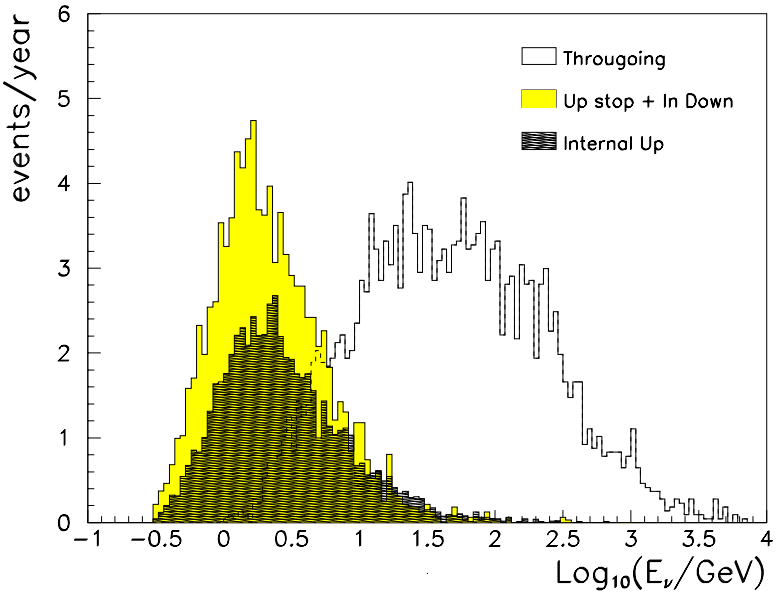

Figure 3: Distributions of the parent muon neutrino energy giving rise to the three different event topologies, upthroughgoing, up semicontained and upstopping plus down semicontained, with median neutrino energies of approximately 50, 4.2 and 3.5 GeV, respectively.

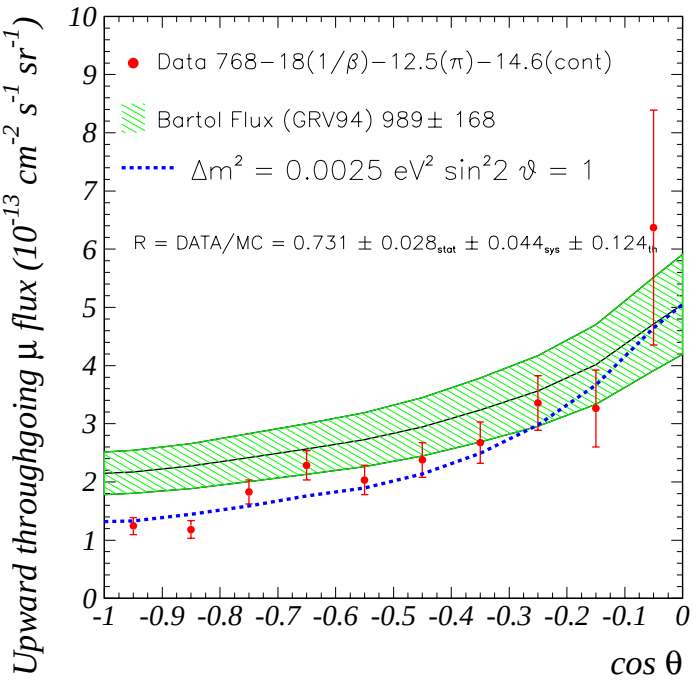

Figure 4: The black points are the measured flux of the up throughgoing muons with $E_\mu > 1$ GeV plotted vs. zenith angle θ. The solid line is the expectation for no oscillations (with 17 % scale uncertainty). The dashed line is the fit for an oscillated muon flux with maximum mixing and $\Delta m^2 = 0.0025$ eV^2.

needed in order to separate up-going muons from the large background coming from the down-going muons. Fig. 2 shows a sketch of the three different topologies of neutrino events analyzed: up throughgoing muons, semicontained upgoing muons and up stopping muons+semicontained downgoing muons. Fig. 3 shows the parent muon-neutrino energy spectra for the three event topologies, computed with Monte Carlo methods. The number of events measured and expected for the three topologies are given in Table 1.

The background on upgoing muons arising from downgoing muons interacting in the rock around MACRO and giving an upward going charged particle was studied in detail in [1]. This background is small at MACRO depths and when using a tracking system; it is large at lower depths and if no tracking system is present.

3.2 Upgoing μ fluxes. Neutrino oscillations

Up-throughgoing muons.

The *up throughgoing muons* come from ν_μ interactions in the rock below the detector; the ν_μ's have a median energy $\overline{E}_\nu \sim$ 50 GeV. The muons ($E_\mu > 1$ GeV) cross the whole detector. The time information provided by the scintillation counters allows the determination of the direction (versus) by the time-of-flight (T.o.F.) method. The data presented in Fig. 4 correspond to 5.0 live years with the full detector [M2, M5, M7, M9, M12, M15, M16, M17, M19, M23, M25], [2]. We studied a large number of possible systematic effects that could affect our measurements. We have shown that no significant systematic problems exist in the detector or in the data analyses. One of the most significant checks was performed using only the scintillator system with the PHRASE

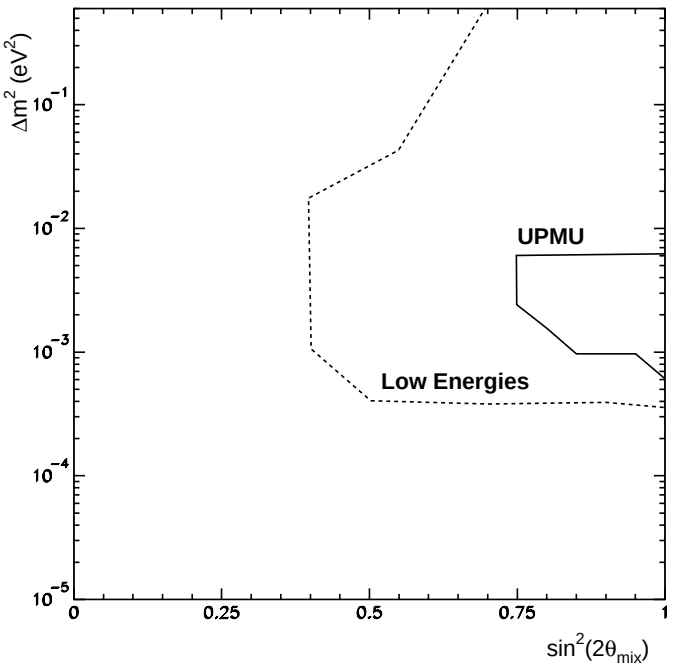

Figure 5: Allowed regions, at 90 % CL, for $\nu_\mu \to \nu_\tau$ oscillations from the two low energy samples and for the high energy up throughgoing sample.

Wave Form Digitizer, completely independent of the ERP system.

The measured data have been compared with Monte Carlo simulations. In the up throughgoing muon simulation the neutrino flux computed by the Bartol group is used. The cross sections for the neutrino interactions were calculated using the GRV94 parton distribution set. The propagation of muons to the detector was done using the energy loss calculation by Lohmann *et al.*. The total theoretical uncertainty on the expected muon flux, adding in quadrature the errors from neutrino flux, cross section and muon propagation, is 17 %. Fig. 4 shows the zenith angle distribution of the measured flux of up throughgoing muons with $E_\mu > 1$ GeV; the Monte Carlo expectation for no oscillations is shown as a dashed line, and for a $\nu_\mu \to \nu_\tau$ oscillated flux with $\sin^2 2\theta = 1$ and $\Delta m^2 = 0.0025$ eV^2 is shown by the solid line. The systematic uncertainty on the up throughgoing muon flux is mainly a scale error that doesn't change the shape of the angular distribution. The ratio of the observed number of events to the expectation without oscillations is 0.73.

To test oscillation hypotheses, the independent probabilities for obtaining the number of events observed and the angular distribution have been calculated for various parameter values. The value of Δm^2 suggested from the shape of the angular distribution is equal to the value needed to obtain the observed reduction in the number of events in the hypothesis of maximum mixing. For $\nu_\mu \to \nu_\tau$ oscillations the maximum probability is 57%; the best parameters are $\Delta m^2 = 0.0025$ eV^2, $\sin^2 2\theta = 1$. The probability for no-oscillations is 0.4 %. The probability for $\nu_\mu \to \nu_{sterile}$ oscillations is 14.5%; combining these probabilities with the measured ratio of horizontal/vertical muons (Fig. 6) we conclude that $\nu_\mu \to \nu_{sterile}$ oscillations are disfavoured compared to $\nu_\mu \to \nu_\tau$.

Fig. 5 shows the confidence regions for $\nu_\mu \to \nu_\tau$ computed according to ref. [3].

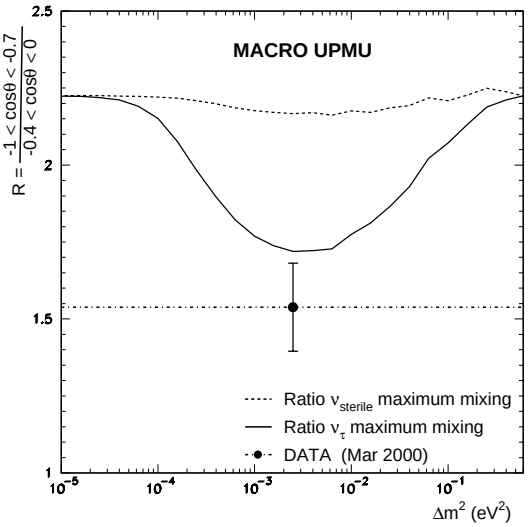

Figure 6: The ratio vertical/horizontal fluxes for upthroughgoing muons; the vertical flux is for $-1 < cos\theta < -0.7$, the horizontal one is for $-0.4 < cos\theta < 0$. The ratio is plotted at a Δm^2 around the minimum of the χ^2 for $\nu_\mu \rightarrow \nu_\tau$ oscillations.

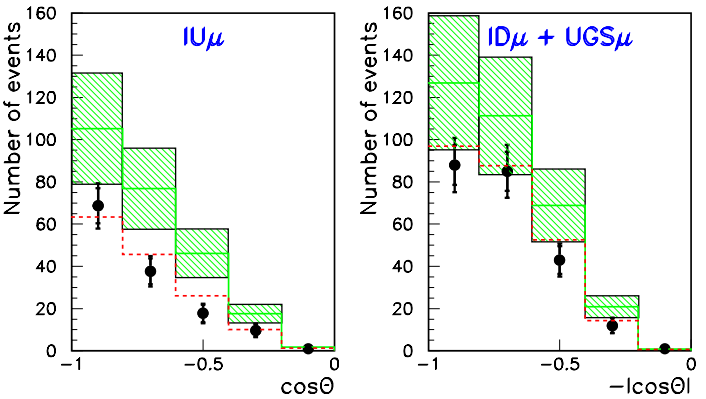

Figure 7: Measured and expected number of low energy muon neutrino events versus zenith angle; left: up semicontained events; right: up stopping plus down semicontained. The lines, with the $\pm 25\%$ scale errors, are the predictions without oscillations; the dashed lines are the predictions assuming neutrino oscillations with the parameters suggested by the Up throughgoing sample.

	Events selected	Predictions (Bartol flux) No oscillations	R = Data/MC
Up throughgoing	723	989	0.73
Internal Up	135	245	0.55
Up Stop + In Down	229	329	0.70

Table 1: Event summary for the MACRO neutrino flux analyses. The predicted numbers of events with oscillations are for maximum mixing and $\Delta m^2 = 0.0025$ eV^2. The ratios R = Data/MC are relative to MC expectations assuming no oscillations (column 4).

Low energy data.
The *upgoing semicontained muons* come from ν_μ interactions inside the lower apparatus. Since two scintillation counters are intercepted, the T.o.F. is applied to identify the upward going muons (Fig. 2). The average parent neutrino energy for these events is 4.2 GeV (see Fig. 3). If the atmospheric neutrino anomalies are the results of $\nu_\mu \rightarrow \nu_\tau$ oscillations with maximum mixing and Δm^2 between 10^{-3} and 10^{-2} eV^2 one expects a reduction of about a factor of two in the flux of these events, without any distortion in the shape of the angular distribution. This is what is observed in Fig. 7a.

The *up stopping muons* are due to external ν_μ interactions yielding upgoing muon tracks stopping in the detector; the *semicontained downgoing muons* are due to ν_μ induced downgoing tracks with vertex in the lower MACRO (Fig. 2). The events are found by means of topological criteria; the lack of time information prevents to distinguish the two sub samples. An almost equal number of up stopping and semicontained downgoing events is expected, and the average neutrino energy for these events is 3.5 GeV (Fig. 3). In case of oscillations with the quoted parameters, the flux of the up stopping events should be reduced by the same amount of the semicontained upgoing muons at $cos\theta \simeq -1$. No reduction is instead expected for the semicontained downgoing events (coming from neutrinos having path lengths of ~ 20 km).

MC simulations for the low energy data use the Bartol neutrino flux and the neutrino low energy cross sections of ref. [4]. The number of events and the angular distributions are compared with the predictions in Table 1 and Fig. 7. The low energy data show a uniform deficit of the measured number of events for the whole angular distribution with respect to predictions; there is good agreement with the predictions based on neutrino oscillations with the parameters obtained from up throughgoing muons.

Using the double ratio $R = (Data/MC)_{IU}/(Data/MC)_{ID+UGS}$ between data and MC of the two low energy data sets, the theoretical uncertainties on neutrino flux and cross sections almost disappear (a residual 5 % uncertainty remains due to the small differences between the energy spectra of the two samples). The systematic uncertainty is reduced to about 5 %. The average value of the double ratio over the measured zenith angle distribution is $R \simeq 0.79$ with 0.12 statistical uncertainty. $R = 1$ is expected in case of no oscillations.

Source	δ	Data 3^o	Backg 3^o	μ-Flux limit $cm^{-2}s^{-1}$	Prev. best μ limit $cm^{-2}s^{-1}$	ν-Flux limit $cm^{-2}s^{-1}$
SN1987A	-69.3^o	0	2.1	$0.14 \cdot 10^{-14}$	$1.1 \cdot 10^{-14}$B	$0.29 \cdot 10^{-6}$
Vela P	-45.2^o	1	1.7	$0.45 \cdot 10^{-14}$	$0.78 \cdot 10^{-14}$I	$0.84 \cdot 10^{-6}$
SN1006	-41.7^o	1	1.5	$0.50 \cdot 10^{-14}$	-	$0.92 \cdot 10^{-6}$
Gal. Cen.	-28.9^o	0	1.0	$0.30 \cdot 10^{-14}$	$0.95 \cdot 10^{-14}$B	$0.57 \cdot 10^{-6}$
Kep1604	-21.5^o	2	1.0	$1.02 \cdot 10^{-14}$	-	$1.92 \cdot 10^{-6}$
ScoXR-1	-15.6^o	1	1.0	$0.77 \cdot 10^{-14}$	$1.5 \cdot 10^{-14}$B	$1.45 \cdot 10^{-6}$
Geminga	18.3^o	0	0.5	$1.04 \cdot 10^{-14}$	$3.1 \cdot 10^{-14}$I	$1.95 \cdot 10^{-6}$
Crab	22.6^o	1	0.5	$2.30 \cdot 10^{-14}$	$2.6 \cdot 10^{-14}$B	$4.30 \cdot 10^{-6}$
MRK421	38.4^o	0	0.2	$4.57 \cdot 10^{-14}$	$3.3 \cdot 10^{-14}$I	$8.74 \cdot 10^{-6}$

Table 2: High energy neutrino astronomy: muon and neutrino flux limits (90 % c.l.) for selected sources calculated using the classical Poissonian method. Previous best limits: B is for Baksan, I is for IMB.

3.3 Energy separation of upthroughgoing muons

The upthroughgoing muon sample is induced by atmospheric ν_μ covering a large energy range (see Fig. 3). The event reduction due to $\nu_\mu \to \nu_\tau$ oscillations with the parameters quoted above should be about 50 % for $E_\mu < 10$ GeV and about 20 % for $E_\mu > 10$ GeV.

Muons traversing MACRO suffer multiple Coulomb scattering that leads to deviations of about few centimeters for energies $E_\mu \lesssim 10$ GeV when crossing the whole detector. We could thus separate the global upthroughgoing muon sample in a low ($\overline{E}_\mu \simeq 10$ GeV, $\overline{E}_\nu \simeq 20$ GeV) and in a high ($\overline{E}_\mu \simeq 50$ GeV, $\overline{E}_\nu \simeq 100$ GeV) energy samples. Ambiguous events are classified in an intermediate energy sample. Preliminary results are plotted in Fig. 8 as the ratios Data/MC; the graph includes also the point with all upthroughgoing muons and the point with the semicontained upgoing muons [M15]. The figure shows that lower energy events are more suppressed than higher energy ones, in agreement with the hypothesis of $\nu_\mu \to \nu_\tau$ oscillations with full mixing and $\Delta m^2 = 2.5 \cdot 10^{-3}$ eV^2. Note that the MC contains the systematic scale error of 17% for upthroughgoing events and 25% for semicontained events. The ratio of High energy muons / Low energy muons is not affected by this uncertainty.

3.4 Search for Astrophysical Point Sources (High Energy Muon Neutrino Astronomy)

The excellent angular resolution of the detector allowed a sensitive search for up-going muons produced by neutrinos coming from celestial sources, with a negligible atmospheric neutrino background. An excess of events was searched for around the positions of known sources in 3° (half width) angular bins. This value was chosen so as to take into account the angular smearing produced by the multiple scattering in the rock below the detector and by the energy-integrated angular distribution of the scattered muon, with respect to

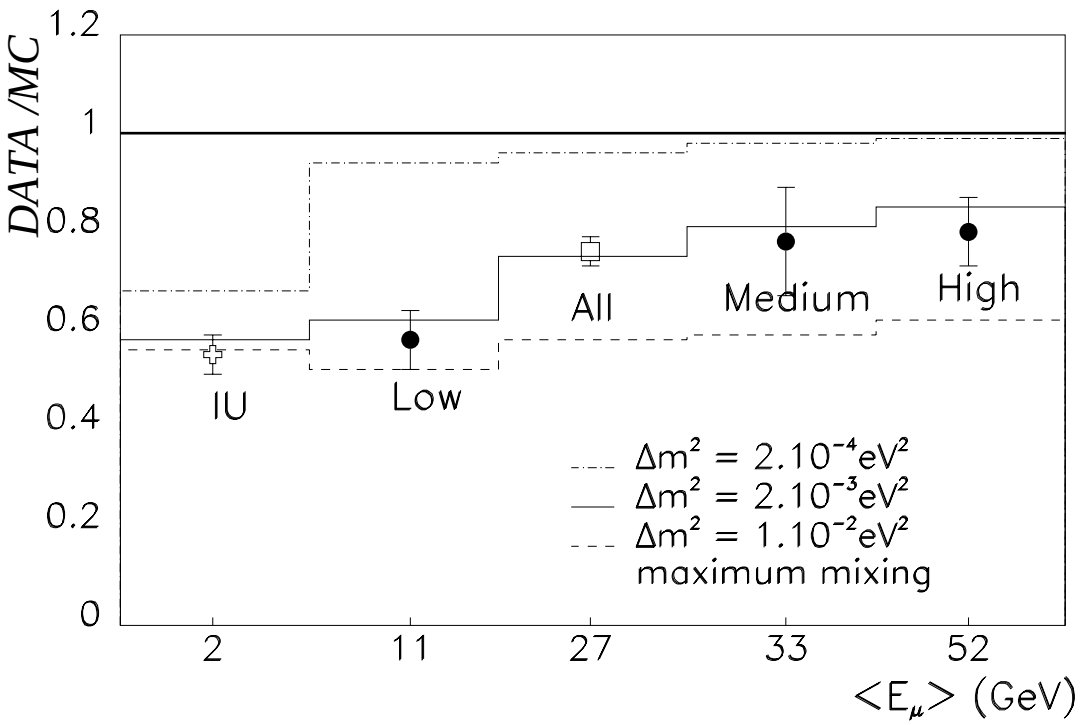

Figure 8: Ratio (Data/MC) vs. median muon energy for upthroughgoing muons separated by multiple scattering into High, Medium and Low energies; also the complete sample is plotted (All). The IU point is for the semicontained upgoing muons. In order to guide the eye the points are plotted with equal distances in abscissa. The solid line at (Data/MC) = 1 is expected for no oscillations; the other lines are the expectations for $\nu_\mu \rightarrow \nu_\tau$ oscillations with maximum mixing and three values of Δm^2. The data are in agreement with the $\Delta m^2 = 2.5 \cdot 10^{-3}\,\mathrm{eV}^2$ value. The ratios High/Low and High/Medium are affected by small systematic uncertainties.

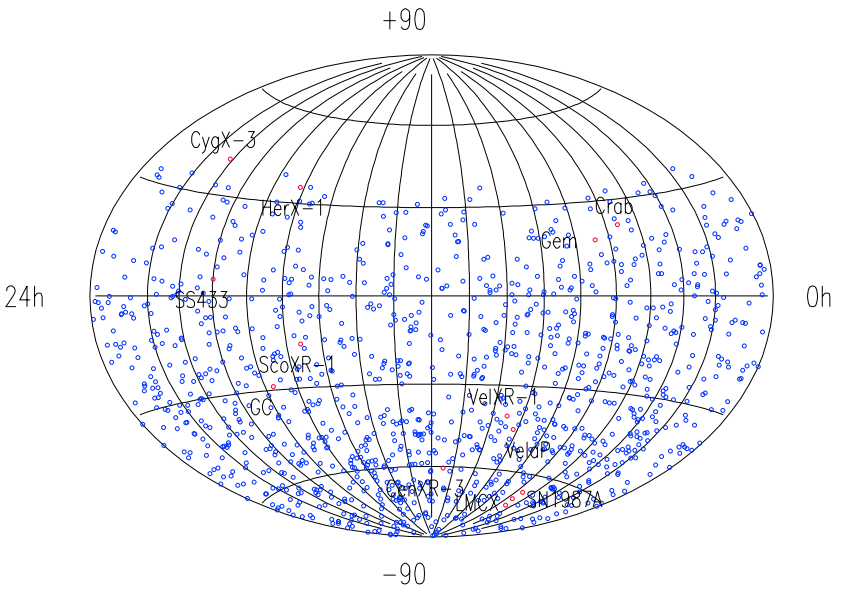

Figure 9: High energy neutrino astronomy. Upgoing muon distribution in equatorial coordinates (1197 events).

the neutrino direction. A total of 1197 events was used in this search, see Fig. 9. No excess was observed and the 90 % c.l. limits on the neutrino fluxes from specific celestial sources are about $\sim 10^{-14}$ cm^{-2} s^{-1}, see Table 2; preliminary data were reported at the 2000 conferences [M6, M8, M11, M25], [M4].

We searched for time coincidences of our upgoing muons with γ-ray bursts as given in the BATSE 3B and 4B catalogues, for the period from April 91 to December 99 [M4]. No statistically significant time correlation was found.

3.5 Indirect Searches for WIMPs

Weakly Interacting Massive Particles (WIMPs) could be part of the galactic dark matter; WIMPs could be intercepted by celestial bodies, slowed down and trapped in their centers. WIMPs and anti-WIMPs could annihilate and yield upthroughgoing muons. WIMPs annihilating in these celestial bodies would produce neutrinos of GeV or TeV energy, in small angular windows around their centers. The 90 % c.l. MACRO limit for the flux from the Earth center is $0.9 \cdot 10^{-14}$ cm^{-2} s^{-1} for a 15° cone around the vertical. For the same cone searched for around the Sun direction, the limit is $\sim 2.6 \times 10^{-14}$ cm^{-2} s^{-1} [7], [M11, M13]. If the WIMPs are identified with the smallest mass neutralino, the MACRO limit may be used to constrain the stable neutralino mass, following the models of Bottino et al. [5], see Figure 10.

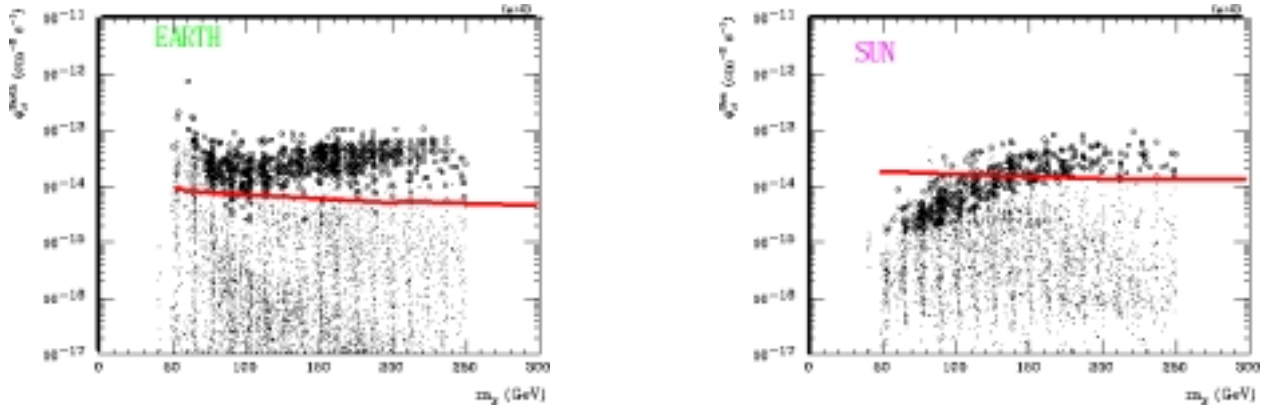

Figure 10: (a) Upward-going muon flux vs neutralino mass m_χ for ${E_\mu}^{th} = 1$ GeV from the Earth. Each dot is obtained varying model parameters. The solid line is the MACRO flux limit (90 % c.l.); the line for the no-oscillation hypothesis is essentially indistinguishable in the log scale from the one for the $\nu_\mu \to \nu_\tau$ oscillation hypothesis (it could be about two times lower). The open circles indicate models *excluded* by direct measurements (particularly the DAMA/NaI experiment [6]) and assume a local dark matter density of 0.5 GeV cm^{-3}. (b) The same as in (a) but for upward-going muons from the Sun [5].

3.6 Magnetic Monopoles and Nuclearites

The search for magnetic monopoles (MM) was one of the main objectives of the experiment. Supermassive ($m \sim 10^{17}$ GeV) GUT monopoles are expected to have typical galactic velocities, $\sim 10^{-3}c$, if trapped in our Galaxy. MMs trapped in our solar system or in the supercluster of galaxies may travel with typical velocities of the order of $\sim 10^{-4}c$ and $\sim 10^{-2}c$, respectively. Monopoles in the presence of strong magnetic fields may reach higher velocities; intermediate mass monopoles could reach relativistic velocities.

The reference sensitivity level for a significant MM search is the Parker bound, the maximum monopole flux compatible with the survival of the galactic magnetic field. This limit is $\Phi \lesssim 10^{-15}$ cm^{-2} s^{-1} sr^{-1}, but it could be reduced by almost an order of magnitude when considering the survival of a small galactic magnetic field seed [9]. Our experiment was designed to reach a flux sensitivity well below the Parker bound, in the MM velocity range of $4 \times 10^{-5} < \beta < 1$. The three MACRO sub-detectors have sensitivities in wide β-ranges, with overlapping regions; thus they allow multiple signatures of the same rare event candidate. No candidates were found in several years of data taking by any of the various subdetectors.

The limits set by different analyses were combined to obtain a global MACRO limit. For each β value, the global time integrated acceptance was computed as the sum of the independent portions of each analysis. Our limit is shown in Fig. 11 together with those set by other experiments [M14, M18, M20, M26] [9].

The searches based on the scintillator and on the nuclear track subdetectors were also used to set new limits on the flux of cosmic ray nuclearites (strange quark matter), see Fig. 12 [M20, M26]. Similar limits were obtained for Q-balls (agglomerates of squarks, sleptons and Higgs fields) [M26], [12].

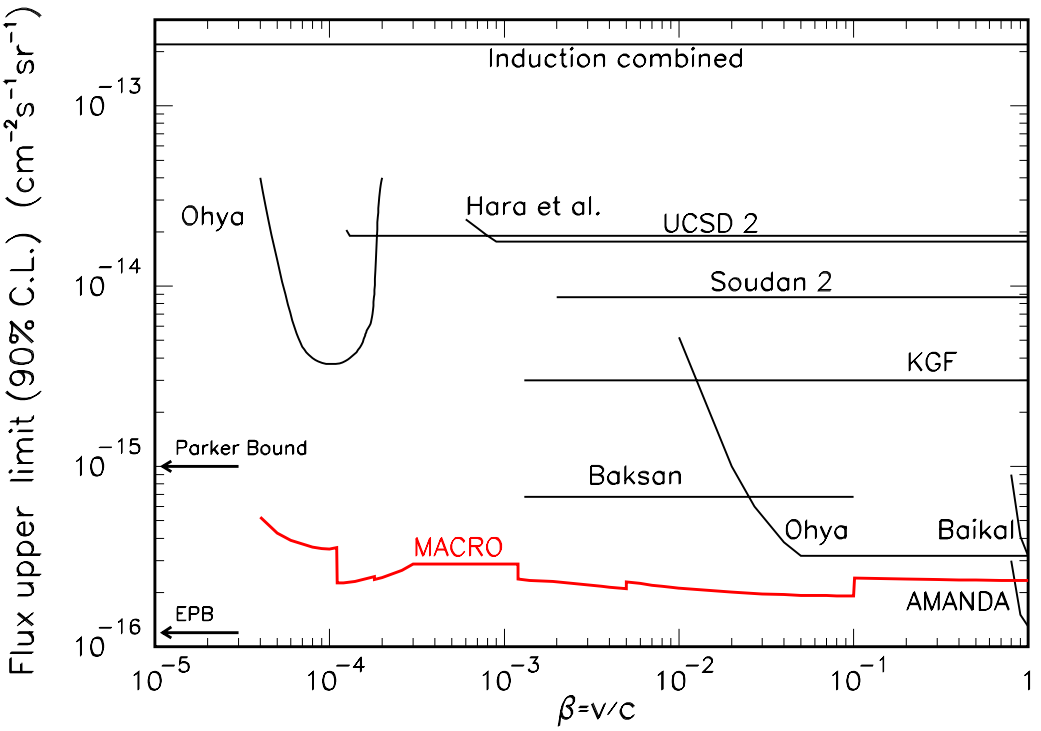

Figure 11: Magnetic monopole flux upper limits at the 90 % c.l. obtained by MACRO [M26] and other experiments [9, 10, 11]. The limits apply to singly charged ($g = g_D$) monopoles assuming that catalysis cross sections are smaller than a few mb.

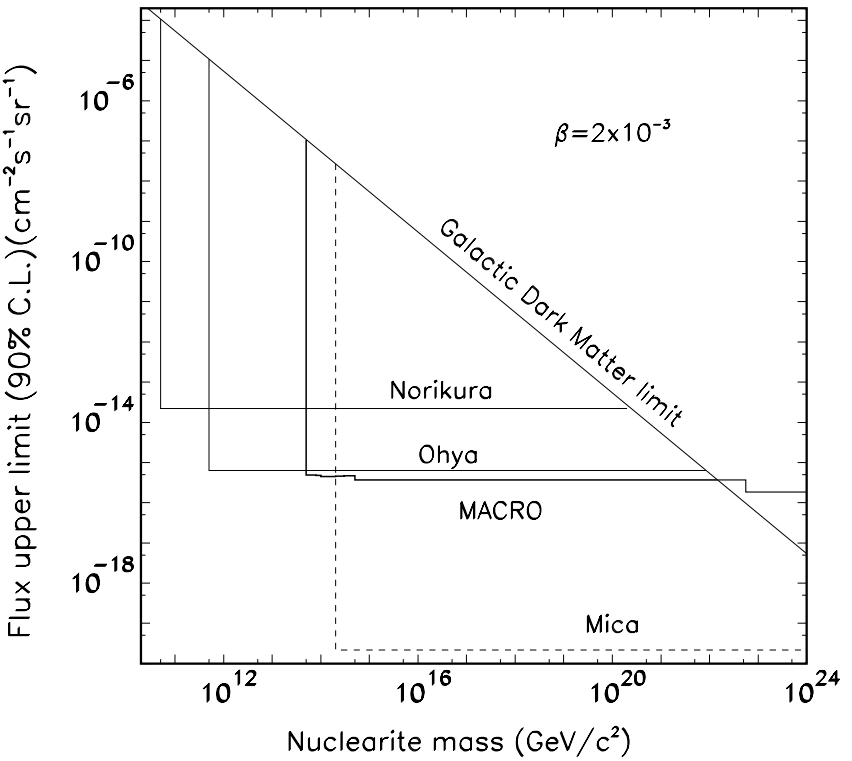

Figure 12: 90 % c.l. flux upper limits vs mass for nuclearites with $\beta = 2 \cdot 10^{-3}$ at ground level. Nuclearites of such velocity could have galactic or extragalactic origin. The MACRO direct limit (solid line) is shown along with the limits of Refs [11, 12] and the indirect mica limits of Refs. [14], [15] (dashed line). The limits for nuclearite masses larger than $5 \cdot 10^{22}$ GeV c^{-2} correspond to an isotropic flux.

Work is in progress in order to compute the energy losses of magnetic monopoles and dyons in the Earth and in the MACRO subdetectors for various particle masses and velocities [13]. This will allow a complete interpretation of all limits for monopoles of multiple charges, monopole composites as well as for monopoles of any given mass.

3.7 Neutrinos from Stellar Gravitational Collapses

A stellar gravitational collapse (GC) is expected to produce a large burst of all types of neutrinos and antineutrinos with energies of $7 - 30$ MeV and with a duration of ~ 10 s. The $\bar{\nu}_e$'s can be detected via the process $\bar{\nu}_e + p \rightarrow n + e^+$ in the liquid scintillator. About $100 \div 150$ $\bar{\nu}_e$ events should be detected in our scintillator for a stellar collapse at the center of our Galaxy.

We used two electronic systems for detecting $\bar{\nu}_e$'s from stellar gravitational collapses. The first system was based on the dedicated PHRASE trigger, the second one was based on the ERP trigger. Both systems had an energy threshold of ~ 7 MeV and recorded pulse shape, charge and timing informations. Immediately after a > 7 MeV trigger, the PHRASE system lowered its threshold to about 1 MeV, for a duration of 800 μs, in order to detect (with a $\simeq 25\,\%$ efficiency) the 2.2 MeV γ released in the reaction $n + p \rightarrow d + \gamma_{2.2\ \mathrm{MeV}}$ induced by the neutron produced in the primary process.

A redundant supernova alarm system was in operation, alerting immediately the physicists on shift. We defined a general procedure to alert the physics and astrophysics communities in case of an interesting alarm [16]. Finally, a procedure to link the various supernova observatories around the world was set up [16].

The MACRO active mass was ~ 580 t; the live-time fraction in the last four years was $\simeq 97.5\,\%$. No stellar gravitational collapses were observed in our Galaxy from the beginning of 1989 to the end of 2000.

3.8 Cosmic Ray Muons

The large area and acceptance ($\sim 10000\ m^2\,\mathrm{sr}$ for an isotropic flux) of our detector allows to study many aspects of physics and astrophysics of cosmic ray muons. We have recorded more than $\sim 6 \times 10^7$ single muons and $\sim 4 \times 10^6$ multiple muons at the rate of $\simeq 18,000$/day.

Muon intensity. The underground muon intensity vs. rock thickness provides information on the high energy ($E \gtrsim 1.3$ TeV) atmospheric muon flux and on the all-particle primary cosmic ray spectrum. The results can be used to constrain the models on cosmic ray production and interaction. The analysis performed in 1995 covered the overburden range $2200 \div 7000$ hg/cm^2 [17]; a new analysis is under development to extend the results to larger rock thicknesses.

Analysis of high multiplicity muon bundles. The study of high multiplicity muon bundles provides information on the primary composition model and on the hadronic interaction features in the high energy region of the primary spectrum. We analyzed events reconstructed in the wire view of the detector with a multiplicity $N_{wire} \geq 8$, corresponding to a primary energy $E_{primary} \geq 1000$ TeV (the region above the "knee"). We worked on a data sample consisting of 4893 events, for a total live time of 21622 h. A set of Monte Carlo

productions was done, using different hadronic interaction models (DPMJET, QGSJET, SIBYLL, HEMAS, HDPM) interfaced to the HEMAS and CORSIKA shower propagation codes. Each production was relative to 5528 h of MACRO live time. High multiplicity events were analyzed using two different methods [18, 19].

The first method is a study of muon correlations inside a bundle. We used the so called *correlation integral* analysis [20] to find out correlations of dynamical origin in the bundles. This tool is generally used in the study of physical systems with a multi-fractal behavior, e.g. systems generated by a cascade process. We found that the shower development in the atmosphere, being a typical cascade process, exhibits a self-similar behaviour. This feature was used to extract information on the primary composition model. In fact, since the cascade tree pattern in atmosphere is mainly determined by the number of "steps" in the tree formation, we expect a different behavior from light and heavy primaries originated cascades. For the same reason, the analysis should be less sensitive to the hadronic interaction model adopted in the simulations. The result of this analysis shows that, in the energy region above 1000 TeV, the composition model derived from the analysis of MACRO multiplicity distribution [18] is almost completely independent from the interaction model adopted.

The second method concerns the search for substructures ("clusters") inside muon bundles. This method of analysis, introduced in [21], has been extensively revised and improved. The search for clusters was performed by means of different software algorithms; the method is sensitive both to the hadronic interaction model and to the primary composition model. We proved that the dependence of the clustering from the composition model is a consequence of mathematical structure of the algorithm when applied to events with different average muon densities. On the other hand, the study of the muon clustering provided new information on the hadronic interaction model. When the primary composition model has been fixed (using the result of the first method), a particular choice of the bundle topology shows interesting connections with the early hadronic interaction features in the atmosphere: bundles with single muons well separated from the central core are produced with high probability in the fragmentation of hard partonic chains. The comparison between our data and Monte Carlo simulations allowed to place constraints on the reliability of the interaction models adopted. The same Monte Carlo study has shown that muon bundles with a central core and an isolated cluster with at least two muons are the result of random associations of peripheral muons. A combined analysis of this result with the study of the decoherence function for high multiplicity events has shown that the hadronic interaction model that better reproduces the underground observables is the QGSJET model.

Muon Astronomy. In the past, some experiments reported possible excesses of muons from the direction of known astrophysical sources, expecially Cyg X-3. Our data has not indicated any significant excess above the statistical background, both for steady dc fluxes and for modulated ac fluxes. For several sources (e.g. Cyg X-3, Vela Pulsar, etc.) our limits are the best existing. The data used for these analyses come from a long period of acquisition, from the february 1989 until the end of 1999 [M22] [22].

The MACRO pointing precision was checked via the shadow of the moon and the sun on primary cosmic rays, see below. The pointing resolution was checked with double muons, assuming they are parallel. The angle containing 68% of the events in a $\Delta\theta$ bin

is 0.8^o, which we take as our resolution.
All sky d.c. survey. The sky, in galactic coordinates, was divided into bins of equal solid angle, $\Delta\Omega = 2.1 \times 10^{-3} sr$, $\Delta\alpha = 3^o$, $\Delta sin\delta = 0.04$; they correspond to narrow cones of 1.5^o half angles. In order to remove edge effects, three other surveys were done, by shifting the map by one-half-bin in α (map 2), by one-half bin in sinδ (map 3) and with both α and sinδ shifted (map 4). For each solid angle bin we computed the deviation from the mean muon intensity after background subtraction in units of standard deviations

$$\sigma(i) = \frac{N_{obs}(i) - N_{exp}(i)}{\sqrt{N_{exp}(i)}} \qquad (1)$$

where $N_{obs}(i)$ is the observed number of events in bin i and N_{exp} is the number of events expected in that bin from the background simulation. No deviation was found and for the majority of the bins we obtain flux upper limits at the level of

$$\Phi_\mu{}^{steady}(95\%) \leq 5 \times 10^{-13} cm^{-2} s^{-1}. \qquad (2)$$

Specific point-like d.c. sources. For specific sources, Cyg X-3, Mrk421, Mrk501, we searched in a narrower cone (1^o half angle) around the source direction. We obtain flux limits at the level of $(2-4) \times 10^{-13} cm^{-2} s^{-1}$. There is a small excess at the level of 2.0 σ in the direction of Mrk501.
Modulated a.c. search from Cyg X-3 and Her X-1. No evidence for an excess was observed and the limits are $\Phi < 2 \times 10^{-13} cm^{-2} s^{-1}$.
Search for bursting episodes. Surface experiments reported high energy γ-bursts from celestial objects like Mrk421 and Mrk501. We made a search for pulsed muon signals in a narrow window (1^o half angle) around the location of these possible sources of very high energy photons. The bursting episodes of duration of $\sim$ 1 day were studied with two different methods. In the first method we searched for daily excesses of muons above the background, also plotting cumulative excesses day by day. In the second one we computed day by day the quantity $-lg_{10}P$ where P is the probability to observe a burst at least as large as N_{obs}. We find some possible excesses for Mrk421 on the days 7/1/93, 14/2/95, 27/8/97, 5/12/98. These deserve further studies.
Sidereal anisotropies. A search for sidereal anisotropies (modulations in arrival times introduced by the galaxy's rotational motion through the extragalactic cosmic rays) is in progress. The muon data are analyzed searching for periodic modulations. The amplitudes of the modulations are at the level of $\sim 0.2\,\%$. We are increasing the statistics and improving the systematics in order to obtain a significant result.
Seasonal variations. Underground muons are produced by mesons decaying in flight in the upper atmosphere. The muon flux thus depends on the ratio between the decay and the interaction probability of the parent mesons, which are sensitive to the atmospheric density and to the average temperature. The flux is expected to decrease in winter, when the temperature is lower and the atmosphere more dense, and to increase in summer. We found variations at the level of ± 2 % [23].
Solar daily variations are presently under study.

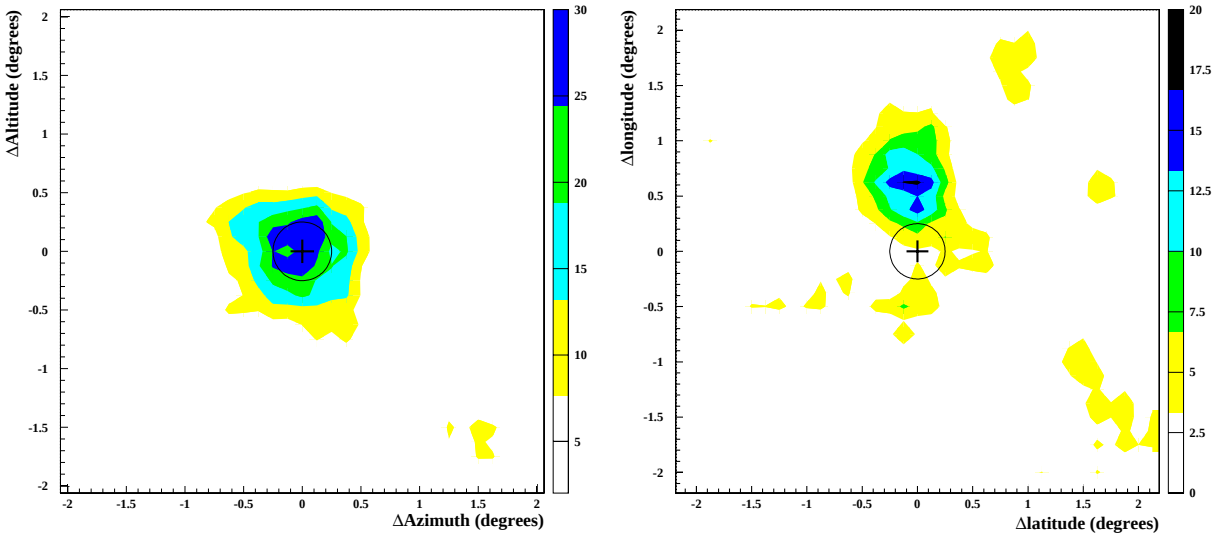

Figure 13: Moon and Sun shadows.(a) Two-dimensional distribution of the muon event density; the Moon is at (0,0). The various regions of increasing gray scale indicate various levels of deficit in percent. The darkest one corresponds to the maximum deficit. (b) Same analysis for the Sun direction.

Moon and Sun Shadows of primary cosmic rays. The pointing capability of MACRO was demonstrated by the observed "shadows" of the Moon and of the Sun, which produce a "shield" to the cosmic rays. We used a sample of 45×10^6 muons, looking at the bidimensional density of the events around the center of the Moon and of the Sun [24][M22]. In Fig. 13 we show two-dimensional plots of the of the muon deficits caused by the Moon and the Sun. For the Moon: we looked for events in a window $4.375^o \times 4.375^o$ centered on the Moon; the window was divided into 35×35 cells, each having dimensions of $0.125^o \times 0.125^o$ ($\Delta\Omega = 1.6 \times 10^{-2} deg^2$). The density of events is shown in a grey scale in a bidimensional plot in Fig. 13a. One observes a depletion of events with a statistical significance of 5.5 σ. The observed slight displacement of the maximum deficit is consistent with the displacement of the primary protons due to the geomagnetic field. We have repeated the same analysis for muons in the Sun window, Fig. 13b. The larger difference between the apparent Sun position and the observed muon density is due to the combined effect of the magnetic field of the Sun and of the geomagnetic field. The observed effect corresponds to a statistical significance of 4.5 σ.

3.9 Measurement of the Muon Energy with the TRD Detector

The underground differential energy spectrum of muons was measured with the TRD detector. The data were collected by the three TRD modules. We have analyzed two types of events: "single muons", i.e. single events in MACRO crossing a TRD module, and "double muons", i.e. double events in MACRO with only one muon crossing the TRD detector.The measurements refer to muons with energies $0.1 < E_\mu < 1$ TeV and for $E_\mu > 1$ TeV [25, M21]. In order to evaluate the local muon energy spectrum, we must

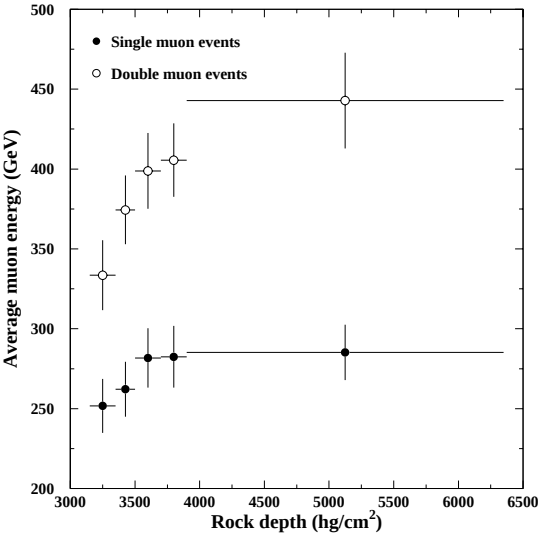

Figure 14: Average muon energy versus standard rock depth for single muons and for double muons [25, M21], see text.

take into account the TRD response function, which induces some distortion of the "true" muon spectrum distribution. The "true" distribution was extracted from the measured one by an unfolding procedure that yields good results only if the response of the detector is correctly understood. We have adopted an unfolding technique, developed according to Bayes' theorem. Fig. 14 shows the average muon energy versus standard rock thickness for single and double muons. Systematic uncertainties are included in the error bars (they arise mainly from energy calibration uncertainties). The corrected average single muon energy is 271 GeV, while for double muons it is 383 GeV. Double muons are more energetic than single muons; this is in agreement with the predictions of interaction models of primary cosmic rays with the atmosphere.

3.10 EAS-TOP/MACRO Coincidences

The coincidence data between EAS-TOP (which was located at Campo Imperatore) and MACRO includes the e.m. size in EAS-TOP and the TeV muons detected underground. Up to the end of 1999, EAS-TOP and MACRO collected 22531 events of this kind, in a time interval of 756.17 days of live-time. Analyses on part of these data have been published in [26]. The analysis of these events was not easy because of the difficulty of separating hadronic physics from primary composition effects and of understanding the role played by fluctuations intrinsic in the detection techniques.

We are trying to perform multicomponent observations of extensive air showers. The main principles of the method are discussed elsewhere [27].

We started to analyze data from the electromagnetic (N_e) and muon detectors ($N_\mu^{GeV} = N_\mu(E_\mu > 1\,\mathrm{GeV})$) of EAS-TOP and muons from the MACRO detector ($N_\mu^{TeV} = N_\mu(E_\mu >$

1.3 TeV)). These "3-fold" coincidence data are expected to provide a better discrimination of events produced by the heavy primary component, thus allowing a determination of the evolution of this fraction of primaries as a function of shower size.

Events which are candidates for being originated by "very heavy" (iron-like) primaries are selected from their characteristics in the EAS-TOP (N_e) and MACRO (N_μ^{TeV}). "Very heavy" primary candidates are selected from high TeV-muon multiplicities with a relatively low N_e. For these events, an analysis is then carried out using the $N_e - N_\mu^{GeV}$ data collected at the surface. The simulation has shown that, for fixed primary mass and energy, the fluctuations in the GeV and TeV muon numbers (N_μ^{GeV} and N_μ^{TeV}) are uncorrelated. Therefore, the measured correlation is not connected with the shower development but to the EAS primaries.

A simulation study has been started; it makes use of the CORSIKA code as event generator. We describe the primary spectrum as the combination of five primary groups (from protons to Fe nuclei), and different interaction models are applied. At present, we are considering the phenomenological model HDPM and the physical models QGSJET and DPMJET. The muon propagation in the rock is simulated by means of the MUSIC code, and the MACRO detector simulation is performed with GEANT. The full response of the detectors has been introduced.

The conversion from N_e to the primary energy E_0 is obtained from the same Monte-Carlo simulation giving:

$$E_0 = \left(\frac{N_e}{\alpha_{30^o}}\right)^{1/\beta} \qquad (3)$$

where both α and β depend on the mass number A and on the interaction model.

From the simulation we estimate the contribution to the high muon multiplicity region from each mass group. We are defining cuts to separate "light" (p, He) from "heavy" (N, Mg, Fe) primaries.

We started the analysis of the coincidence between muon events detected in MACRO and the Cherenkov signal detected by the EAS-TOP Cherenkov telescope. This analysis aims to study the dependence of TeV muon yield as a function of primary energy in a region (from few TeV to about 50 TeV) where protons largely dominate the primary spectrum. This will allow to place further constraints on the interaction models used in the Monte Carlo simulation.

4 Nuclear Track Detector Calibrations

We performed further calibrations of the nuclear track detector CR39 with both slow and fast ions. In all measurements we have seen no deviation of its response from the restricted energy loss (REL) model. To complete the calibration, nuclear track detector stacks made of CR39 and Lexan foils, placed before and after various targets, were exposed to 158 A GeV Pb^{82+} ions at the CERN-SPS and to 1 A GeV Fe^{26+} ions at the BNL-AGS. In traversing the target, the beam ions produce nuclear fragments with $Z < 82$ and $Z < 26$ for the lead and iron beams, respectively, thus allowing a measurement of the response of the detector in a Z regime most relevant to the detection of magnetic monopoles. We

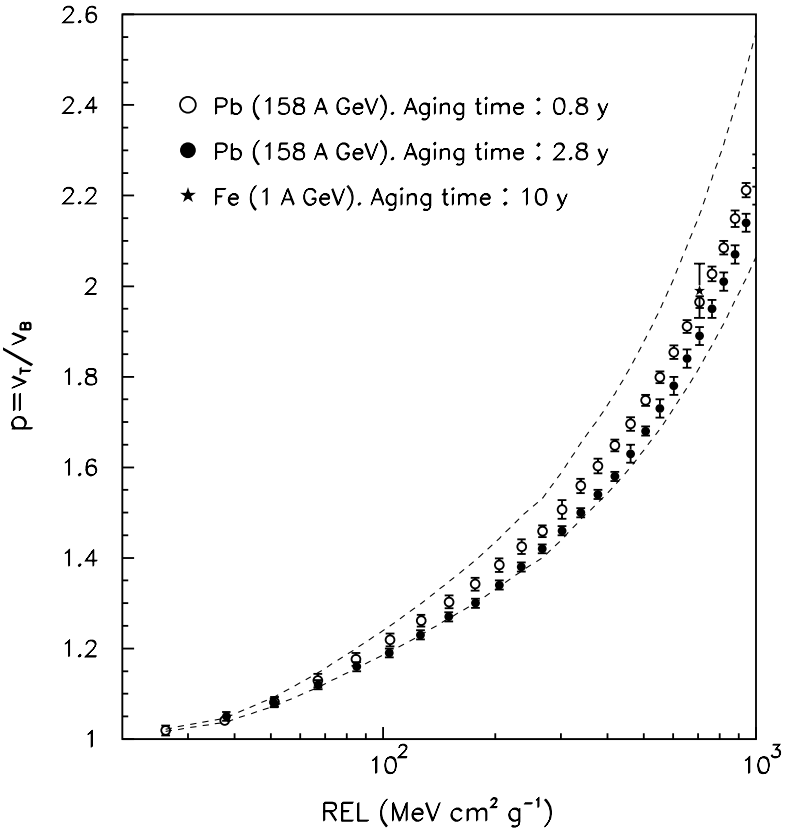

Figure 15: $p = v_T/v_B$ vs. REL for CR39 exposed to $^{207}Pb^{82+}$ ions of 158 A GeV and $^{56}Fe^{26+}$ ions of 1 A GeV at different times after production. This was done to estimate possible aging effects. The dashed lines indicate the systematic uncertainty arising mainly from fluctuations of the bulk etching rate v_B.

reported previously about the very good charge resolution of the detector in the range $72 < Z < 83$ (obtained by measurement of the etch-cone heights) and at lower Z (for $5 \leq Z < 50$) (by measurement of the cone base diameters).

Tests were made looking for a possible dependence of the CR39 response from its age, i.e. from the time elapsed between the date of production and the date of exposure ("aging effects"). Two sets of samples, 0.8 y and 2.5 y old, respectively, were exposed in November 1994 to 158 A GeV Pb^{82+} ions. For each detected nuclear fragment the reduced etch rate $p = v_T/v_B$ (v_T and v_B are the track and bulk etching rates, respectively) was computed and plotted in Fig. 15 vs REL. The lines represent the limits of the systematic uncertainties coming mainly from the uncertainty on v_B. A recent test was made by exposing CR39 samples 10y old to 1 A GeVFe^{26+} ions; the detector response is shown as a black star in Fig. 15. The results indicate that within experimental uncertainties, aging effects in the MACRO CR39 are negligible.

Until the end of december 2000, we etched and analyzed 530 m^2 of nuclear track detectors in the search for magnetic monopoles and nuclearites. The 90% c.l. limit for an isotropic flux of monopoles with $\beta > 0.1$ is now at the level of 2.4 10^{-16} $cm^{-2}s^{-1}sr^{-1}$ [28] [M24].

5 Conclusions

The MACRO detector, which has been running smoothly in year 2000, was turned off on 19 dec 2000. In 2000 we have extended most of our analyses and searches. We obtained important results on atmospheric neutrinos of high and low energies relevant to neutrino oscillations, more stringent limits on monopoles, nuclearites, WIMPs, astrophysical point sources, sidereal anisotropies, etc. Analyses sensitive to detector and Monte Carlo systematics have been refined and improved to yield solid results in many fields of high energy neutrino physics and astrophysics and of cosmic ray physics. No stellar gravitational collapse low energy neutrinos have been observed since 1989; our on-line monitor was integrated in a world supernova watch system.

6 List of MACRO publications, conference proceedings and memos MACRO/PUBs during 2000

[M1] MACRO Collaboration, M. Ambrosio et al., "Nuclearite search with the MACRO detector at Gran Sasso", Eur. Phys. J. C13(2000)453; hep-ex/9904031.

[M2] MACRO Collaboration, M. Ambrosio et al., "Low-energy atmospheric muon neutrinos in MACRO", Phys. Lett. B478(2000)5; hep-ex/0001044.

[M3] MACRO Collaboration, M. Ambrosio et al., "A search for lightly ionizing particles with the MACRO detector" Phys. Rev. D62(2000)052003; hep-ex/0002029.

[M4] MACRO Collaboration, M. Ambrosio et al., "Neutrino astronomy with the MACRO detector" Astrophys. J. 546(2001)1038; astro-ph/0002492.

[M5] A. Surdo for the MACRO Collaboration, "Atmospheric neutrinos and neutrino oscillations in the MACRO experiment", Vulcano Workshop 2000, 22-27 May 2000.

[M6] L. Perrone for the MACRO Collaboration, "Neutrino astronomy with MACRO at Gran Sasso", GIFCO, 24-26 May 2000, Lecce.

[M7] B. Barish for the MACRO Collaboration, "Atmospheric neutrinos with MACRO", Neutrino 2000 - XIX Int. Conf. on Neutrino Physics and Astrophysics, 16-21 June 2000, Sudbury, Ont, Canada.

[M8] T. Montaruli for the MACRO Collaboration, "Neutrino astronomy and Indirect search for WIMPs with MACRO", DARK2000, 10-15 July 2000, Heidelberg, Germany.

[M9] A. Surdo for the MACRO Collaboration, "Low and high energy atmospheric neutrinos with MACRO", 17th European Cosmic Ray Symposium, 23-28 July 2000, Lodz, Poland.

[M10] M. Sioli for the MACRO Collaboration, "New results in the study of multiple muon events with the MACRO experiment", ECRS 2000, 23-28 July 2000, Lodz, Poland.

[M11] G. Giacomelli, A. Margiotta for the MACRO Collaboration, "Neutrino physics and astrophysics with the MACRO detector", Chacaltaya Meeting on Cosmic Ray Physics, 23-27 July 2000, La Paz, Bolivia.

[M12] F. Ronga for the MACRO Collaboration, "Atmospheric neutrino results from MACRO", XXXth Int. Conf. on High Energy Physics, 27 July - 2 August 2000, Osaka, Japan.

[M13] D. Michael for the MACRO Collaboration, "Search for WIMPS with MACRO", Dark Matter 2000, 23-25 February 2000, Marina Del Rey, California.

[M14] L. Patrizii for the MACRO Collaboration, "Search for rare massive particles with the MACRO track-etch detector", 20th Int. Conf. Nuclear Track in Solids (ICNTS), 28 August-1 September 2000, Portoroz, Slovenia.

[M15] M. Spurio for the MACRO Collaboration, "Atmospheric neutrinos in MACRO", 3rd Int. Workshop on New Worlds in Astroparticle Physics, 1-3 September 2000, Faro, Portugal.

[M16] D. Michael for the MACRO Collaboration, "Neutrino Induced Upgoing Muons in MACRO", DPF 2000, 9-12 September 2000, Columbus, Ohio.

[M17] B. Nolty for the MACRO Collaboration, "Semi-Contained Neutrino Events in MACRO", DPF 2000, 9-12 September 2000, Columbus, Ohio.

[M18] M. Sitta for the MACRO Collaboration, "Search for Magnetic Monopoles with the MACRO Detector", DPF 2000, 9-12 September 2000, Columbus, Ohio.

[M19] F. Ronga for the MACRO Collaboration, "New atmospheric neutrino results from Soudan 2 and MACRO", Europhysics Neutrino Oscillation Workshop, 9-16 September 2000, Otranto, Italy.

[M20] I. De Mitri for the MACRO Collaboration, "Search for magnetic monopoles and other massive particles with MACRO", European Research Conference on "Frontiers in Particle Astrophysics and Cosmology", 30 September - 5 October 2000, San Feliu de Guixols, Spain.

[M21] F. Loparco for the MACRO Collaboration, "Misura dell'energia dei muoni sotterranei mediante il TRD dell'esperimento MACRO", LXXXVI Congresso Nazionale Societa' Italiana Fisica, 6-11 October 2000, Palermo, Italy.

[M22] M. Brigida for the MACRO Collaboration, "Ricerca di sorgenti localizzate di raggi cosmici tramite l'apparato MACRO", LXXXVI Congresso Nazionale Societa' Italiana Fisica, 6-11 October 2000, Palermo, Italy.

[M23] M. Spurio for the MACRO Collaboration, "Studio dei neutrini atmosferici in MACRO", LXXXVI Congresso Nazionale Societa' Italiana Fisica, 6-11 October 2000, Palermo, Italy.

[M24] M. Giorgini for the MACRO Collaboration, "Ricerca di monopoli magnetici con rivelatori nucleari a tracce", LXXXVI Congresso Nazionale Societa' Italiana Fisica, 6-11 October 2000, Palermo, Italy.

[M25] T. Montaruli for the MACRO Collaboration, "Astrofisica dei neutrini di alta energia", LXXXVI Congresso Nazionale Societa' Italiana Fisica, 6-11 October 2000, Palermo, Italy.

[M26] MACRO Collaboration, M. Ambrosio et al., "Search for massive rare particles with MACRO", hep-ex/0009002.

7 References

[1] MACRO Collaboration, M. Ambrosio et al., Astropart. Phys. 9(1998)105, hep-ex/9807032.

[2] MACRO Collaboration, M. Ambrosio et al., "Measurement of the atmospheric neutrino-induced upgoing muon flux using MACRO", Phys. Lett. **B434** (1998) 451, hep-ex/9807005; MACRO Collaboration, M. Ambrosio et al., "Atmospheric neutrino flux measurements using upgoing muons", Phys. Lett. **B357** (1995) 481.

[3] G. Feldman and R. Cousins, Phys. Rev. **D57** (1998) 3873.

[4] P. Lipari et al., Phys. Rev. Lett. **74** (1995) 384.

[5] A. Bottino, N. Fornengo, F. Donato and S. Scopel (private communication). N. Fornengo, in Proceedings of the Ringberg Euroconference "New Trends in Neutrino Physics", Ringberg Castle, Tegernsee, Germany, May 1998, edited by B. Kniel, World Scientific, Singapore.

[6] R. Bernabei et al., Phys. Lett. B **389** (1996)757.

[7] MACRO Collaboration, M. Ambrosio et al., "Limits on dark matter WIMPs using upward-going muons in the MACRO detector", Phys. Rev. **D60** (1999)082002; hep-ex/9812020.

[8] MACRO Collaboration, M. Ambrosio et al., "Magnetic monopole search with the MACRO detector at Gran Sasso", Phys. Lett. **B406**(1997) 249.

[9] G. Giacomelli and L. Patrizii, "Magnetic monopoles", Lecture at the Fifth School on Particle Astrophysics, Trieste 29 June-10 July 1998, hep-ex/0002032, DFUB 98/30.

[10] S. Nakamura et al., Phys. Lett. **B263** (1991) 529.

[11] S. Orito et al., Phys. Rev. Lett. **66** (1991) 1951.

[12] D. Bakari et al., "Magnetic monopoles, nuclearites, Q-balls: a qualitative picture", hep-ex/0004019.

[13] J. Derkaoui et al., Astropart. Phys. **9** (1998) 173; "Energy losses of magnetic monopoles and dyons in scintillators, streamer tubes and nuclear track detectors", Astrop. Phys. **10** (1999)339.

[14] P. B. Price, Phys. Rev. **D38** (1988) 3813.

[15] D. Ghosh and S. Chatterjea, Europhys. Lett. **12** (1990) 25.

[16] MACRO Collaboration, M. Ambrosio et al., "Real time supernova neutrino burst detection with MACRO", Astropart. Phys. 8 (1998) 123.

[17] MACRO Collaboration, M. Ambrosio et al., "Vertical muon intensity measured with MACRO at the Gran Sasso laboratory", Phys. Rev. **D52** (1995) 3793.

[18] MACRO Collaboration, M. Ambrosio *et al.*, Phys. Rev. **D56** (1997)1407; 1418.

[19] M. Sioli, "A new approach to the study of high energy muon bundles with the MACRO detector at Gran Sasso", Tesi di Dottorato, Universitá di Bologna (2000).

[20] P. Lipa, P. Carruthers, H.C. Eggers and B. Buschbeck, Phys. Lett. **285B** (1992) 300.

[21] G. Battistoni *et al.*, LNGS-95-09 (1995); Proceedings of the XXIV Int. Cosmic Ray Conf., Roma, Italy, 1995, ed. N. Iucci *et al.*, Arti Grafiche Editoriali, Urbino, (1995), Vol. 1, p. 508.

[22] MACRO Collaboration, S. Ahlen et al., "Muon astronomy with the MACRO detector", Astroph. J. 412(1993)301.

[23] MACRO Collaboration, M. Ambrosio et al., "Seasonal variations in the underground muon intensity as seen by MACRO", Astropart. Phys. 7(1997)109.

[24] MACRO Collaboration, M. Ambrosio et al., "Observation of the shadowing of cosmic rays by the moon using a deep underground detector", Phys. Rev. **D59** (1999)012003.

[25] MACRO Collaboration, M. Ambrosio et al., "Measurement of the energy spectrum of underground muons at Gran Sasso with a transition radiation detector", Astropart. Phys. 10 (1999) 11.

[26] EAS-TOP and MACRO Collaborations, Nucl. Phys. B35(1994) 257; Nucl. Phys. B48(1996)450.

[27] EAS-TOP Collaboration, Nucl. Phys. B54B(1997)263.

[28] P. Serra et al., "Total charge changing cross section of 158 A GeV *Pb* ions in different targets with nuclear track detectors", proceedings of the XXV ICRC Conference, Durban (South Africa), 28 july - 8 August 1997 and DFUB **10/97** (1997).

MIBETA and CUORICINO. Cryogenic experiments on double beta decay and search for rare events

A. Alessandrello[a], C. Brofferio[a], C. Bucci[b], O. Cremonesi[a], E. Fiorini[a], A. Giuliani[a], A. Nucciotti[a], M. Pavan[a], G. Pessina[a], S. Pirro[a], C. Pobes[b], E. Previtali[a], M. Vanzini[a], L. Zanotti[a]

[a] Dipartimento di Fisica G. Occhialini dell'Università di Milano-Bicocca e Sezione di Milano dell'INFN, via Celoria 16, I-20133 Milan, Italy

[b] Laboratori Nazionali del Gran Sasso, I-67010, Assergi (AQ), Italy

Abstract

This report describes the progress achieved in 2000 by the MIBETA and CUORICINO experiments at Laboratori Nazionali del Gran Sasso

1 The experimental apparatus

The experimental apparatuses and the searches reported here refer both to the presently running experiment MIBETA and to the strictly connected research and development for the already approved experiment CUORICINO, in view of a larger experiment CUORE to be proposed next March. The apparatus used for both of these experiments consists of two dilution refrigerators operating in Hall A and C.

The former has a power of 1000 μW at 100 mK, the second a power of 200 μW at the same temperature. Both have been made with previously tested low radioactivity materials and are equipped with helium liquefier, which provides a substantial recovery of the Helium and also prevents Helium contamination in the tunnel atmosphere. In addition the group is carrying on continuous measurements of radioactive contamination in the Low Radioactivity Laboratory, where two of the large Ge detectors have been installed by the group itself.

The dilution refrigerator operating in Hall A contains an array of 20 crystals of TeO_2 of $3 \times 3 \times 6$ cm^3 each for a total mass of almost 7 kg, by far the largest cryogenic mass operating underground. After summer of 2000 we have decided to improve substantially the background and resolution of this setup not only to reach more stringent results on double beta decay, but also to test some new ideas in view of CUORICINO and possibly CUORE. The dilution refrigerator in Hall C is substantially used for Research

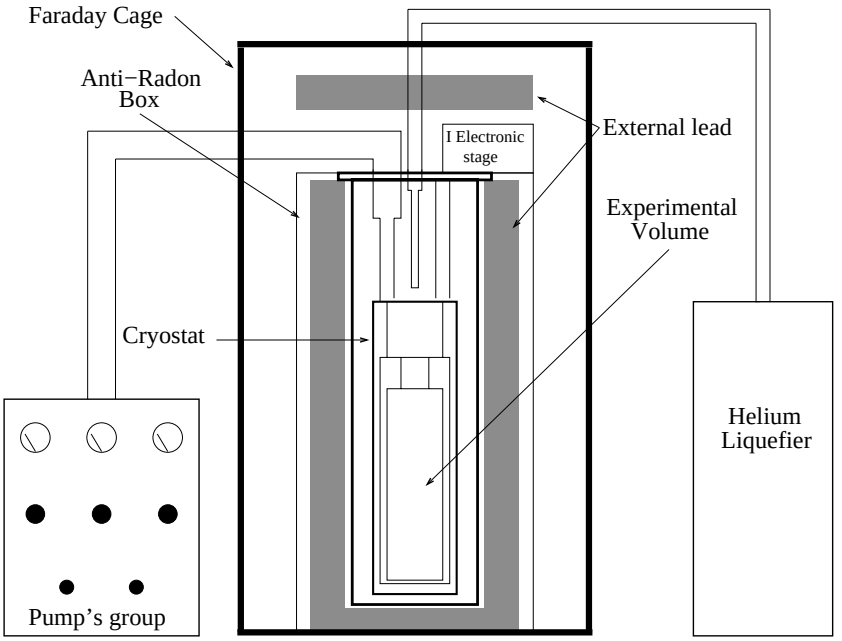

Figure 1: The cryogenic setup.

and Development for CUORICINO. It has been run with various arrays of the same crystals operating in Hall A and also of crystals of $5 \times 5 \times 5$ cm^3 each, which, with a mass of about 760 g each represent the largest thermal detector operated underground. They are the same as those to be used in CUORICINO.

2 Aim of the MIBETA experiment

One of the main objects of this experiment is the search for double beta decay of ^{130}Te both in the lepton conserving two neutrino and in the lepton non-conserving neutrinoless channel. The former one is allowed by the standard model of weak interactions, but a direct result on its lifetime would solve a long standing problem arising from the data provided by geochemical experiments, which yield lifetimes in strong disagreement among themselves. For this reason two crystals of $^{130}TeO_2$ and two crystals of $^{128}TeO_2$ have been installed in the dilution refrigerator operating in Hall A, together with crystals of natural tellurium. Most of the interest of the group is however addressed to the neutrinoless double beta decay channel which would imply lepton number non-conservation and, indirectly, a non-zero neutrino mass. The Grand Unified Theories of fundamental interaction predict both these facts. The interest of the group is also addressed to search for other rare events, like those produced by direct interaction of WIMPS. We have in fact proved that the efficiency (Quenching Factor) for nuclear recoils in our detector is constantly equal to one for energies ranging from 20 to 200 keV.

3 Results obtained in 2000 with the MIBETA experiment

The dilution refrigerator contains an array of 20 crystals of TeO_2 of $3 \times 3 \times 6$ cm^3 with a mass of 340 grams each (fig.2).

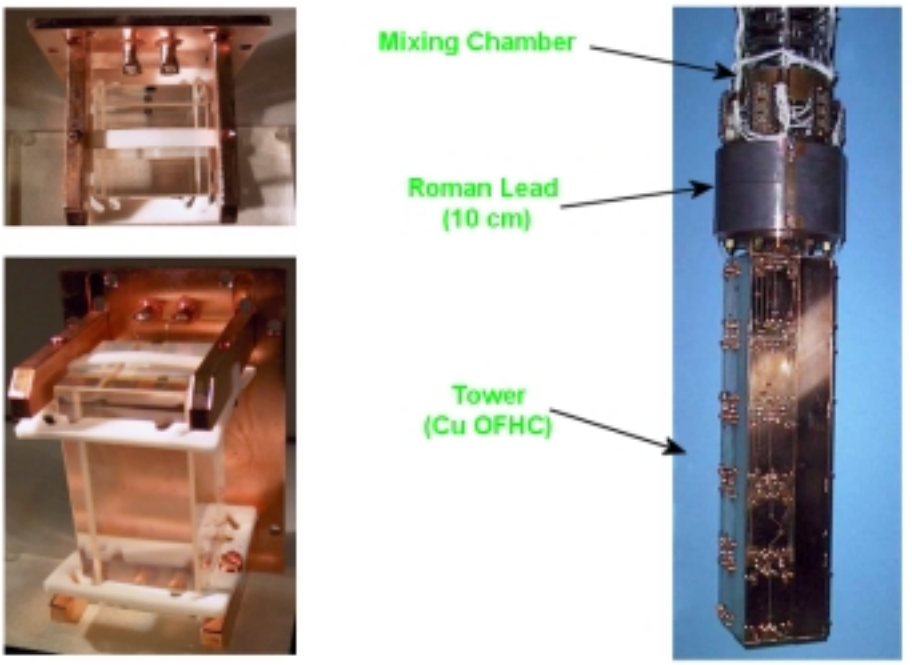

Figure 2: The 20 crystal array tower and the single module.

Neutron Transmutation doped (NTD) thermistors glued on these crystals were used to read-out the thermal signal. Also glued on each crystal was a doped Si resistor used as heater to generate a reference pulse in order to control "on line" the stability of the gain of each bolometer.

The readout was accomplished with a room temperature low noise differential voltage-sensitive preamplifier, an amplifier and an antialiasing Bessel filter. Pulses were then sent to an 8 channel (multiplexed to 32) 16bit ADC embedded in a VXI acquisition system. The Si heaters were connected to a remote programmable pulse generator.

As shown in Fig.1, the array is shielded with an internal layer of Roman lead of 1 cm minimum thickness, while the thermal shields provide a 2 cm minimum thickness of electrolytic copper. The dilution refrigerator is shielded with two layers of lead of 10 cm minimum thickness. The outer layer is of common low radioactivity lead, while the internal one is made with special lead with a ^{210}Pb contamination of 16 ± 4 Bq/kg. In order to shield against the unavoidable radioactive contamination due to some fundamental components of the dilution refrigerator (as the silver powder and stainless steel tubes) a layer of 10 cm Roman lead was placed above the tower of the array inside the cryostat. A similar layer, also inside the cryostat, was placed below the tower. A further layer of Roman lead of 1 cm minimum thickness is installed inside the dilution refrigerator.

The external lead shield was surrounded by a radon box and by a Faraday cage to suppress electromagnetic interference. Each run starts with cooling of the cryostat and with the stabilization of its temperature. The bias of each detector is then optimized. The detector is then calibrated with an exposure, lasting about 3 days, with mixed U and Th sources placed at the two opposite side of the 20 crystal tower.

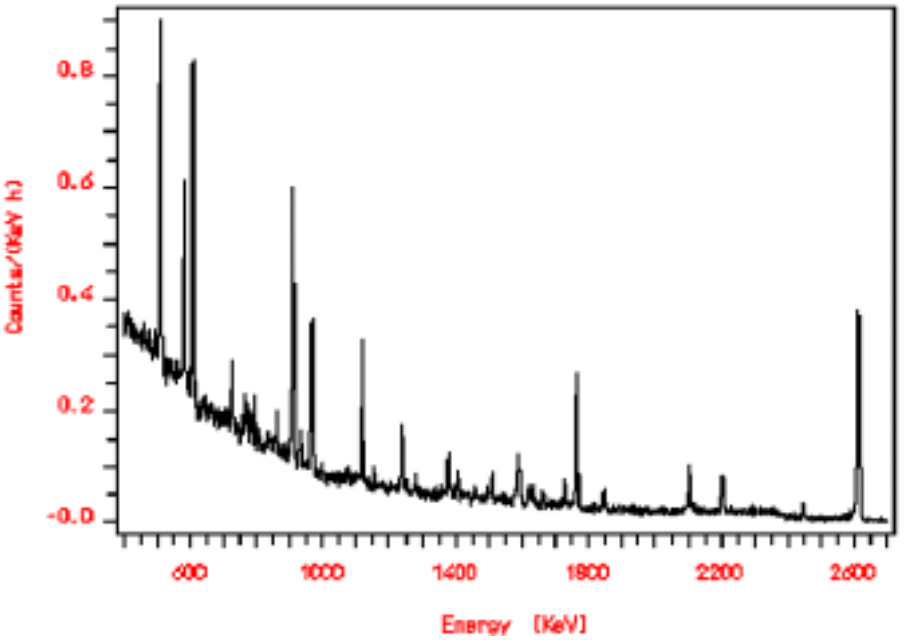

Figure 3: Sum of the ^{238}U and ^{232}Th calibration spectra of the 20 detectors.

The excellent reproducibility of each detector is shown in Fig. 3 where the total calibration spectrum obtained by adding the pulses from all 20 crystals is presented. A second calibration is carried out at the end of each run, which lasts about 15-20 days unless there is a forced interruption as those of water or power supply. The apparatus has been operated in total for 100,000 hours x crystal of effective running time.

^{130}Te		
Process	Counts	Limit on Half-Life [years] at 95% c.l.
$0^+ \to 0^+ \ (0\nu)$	$6.3^{+7.6}_{-5.5}$	1.6×10^{23}
$0^+ \to 2^+ \ (0\nu)$	$8.1^{+15.1}_{-7.3}$	1.1×10^{23}
$0^+ \to 0^+ \ (2\nu)$	-	4.4×10^{20}
$0^+ \to 0^+ \ (1\chi)$	-	1.5×10^{21}
$0^+ \to 0^+ \ (2\chi)$	-	8.4×10^{20}
^{128}Te		
$0^+ \to 0^+ \ (0\nu)$	$18.1^{+12.9}_{-17.3}$	9.8×10^{22}

Table 1: Limits obtained on double beta decay of ^{130}Te and ^{128}Te.

No evidence appears in the region of neutrinoless double beta decay, as indicated in Fig.4, where the peaks due to the 2615 and 2447 keV due to ^{208}Tl and ^{214}Bi can be easily seen.

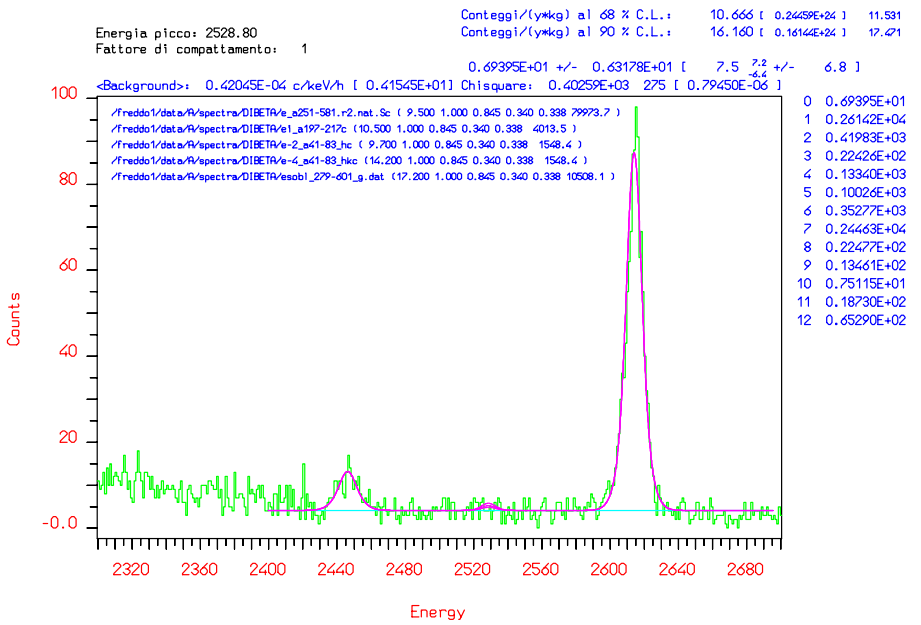

Figure 4: Region of the ^{130}Te neutrinoless double beta decay.

The data set is saved for the off-line analysis based on all useful information contained in the signal like channel number, trigger time, baseline, pulse amplitude and pulse shape parameters. These are rise and decay time and parameters determined by comparing the signal with the expected response function.

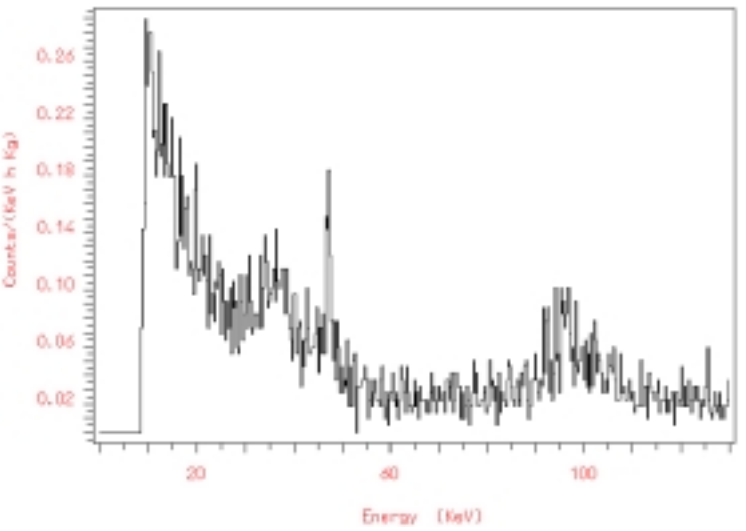

Figure 5: Low energy spectrum.

The Si heater mentioned before allows to produce every 300 seconds a reference pulse on each detector This allow to correct gain instabilities due to temperature fluctuations which range from 10 to 100 microkelvin on a 1 day scale.

No evidence have been found for double beta decay to the 2^+ excited state at 536 keV of ^{130}Xe, for neutrinoless double beta decay of ^{128}Te, and for the decays of ^{130}Te with the emission of two neutrinos or one or two majorons. The corresponding limits are reported in Table I.

We would like to note that our limits on the lepton non conserving channels are the most restrictive in the literature after those obtained in double beta decay experiments with ^{76}Ge. Our limit on lifetime restricts the average neutrino mass to values ranging from 1 to 2 eV, according to most theoretical calculation. Our limits on the two neutrino double beta decay of ^{130}Te are already near to those obtained in geochemical experiments and clearly indicate that the possibility of a large escape of ^{130}Xe experiments can be excluded. The counting rates at low energy have been considerably reduced, mainly by suppression of electromagnetic noise end interference a shown in Fig. 5.

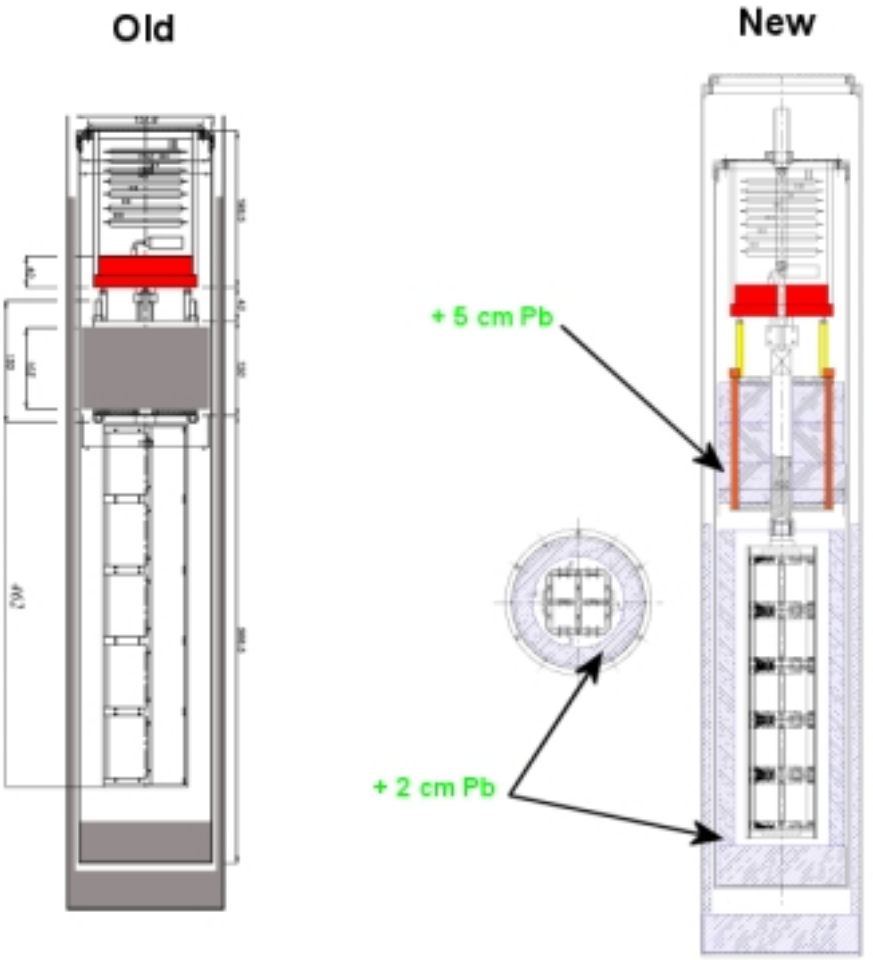

Figure 6: Old and new set-up of the 20 crystal array.

The clear peak at 46 keV due to the decay of ^{210}Pb and the bump due to nuclear

recoils can be easily seen. We would like to note that the counting rate in this region has been strongly reduced and that, taking into account the quenching factor, the sensitivity of our experiment in the search for direct interaction of WIMPs is already near to those of dedicated experiment like, e.g. HMDM.

Our measurements in the MIBETA experiment together with the results of the R&D activity carried out in Hall C, have prompted us to modify substantially the 20 crystal set-up, lapping the crystals, electropolishing the entire frame and adding 2 cm of Roman lead to the internal shield. This new system, which is presently being mounted is shown in Fig.6.

4 Aims of the R & D activity carried out in Hall C in view of the experiment CUORICINO

After the approval by the Gran Sasso Scientific Committee and by the funding authorities of the experiment CUORICINO, we have carried out an intense activity in Hall C for the preparation of this experiment. The setup, to be installed in Hall A in the same dilution refrigerator presently housing the twenty crystal array, will consist in an array of 56 cubic crystals of natural TeO_2 of $5 \times 5 \times 5$ *cm* side with the total mass of about 42 chilograms.

Figure 7: Two 4-crystal arrays are mounted simultaneously in Hall C test facility

This setup will make possible not only an improved search for neutrinoless double beta decay, but also a more sensitive experiment on direct interactions of WIMPS via the seasonal variation of their interaction rate. We also plan to investigate a possible subdiurnal modulation of the signal induced in this detector by electromagnetic interactions of axions coming from the sun. This electromagnetic signal would in fact be enhanced

when the position of a crystal plane of our crystals will be under the Bragg angle with respect to the direction of these incoming particles. The tetragonal structure of our crystals makes this search very attractive. Our efforts have been addressed to the reduction of microphonics with the aim to improve the resolution and in a systematic search to reduce the background of spurious counting. For this reason we have performed measurements with various arrays, of which the final one is shown in Fig.7.

It consists in two arrays of 4 crystals each. The upper one (Fig.8) is made by crystals of $3\times3\times6$ cm^3, the same as those of the twenty crystal array, and is being used to test the radioactive contamination and to try to reduce it. The lower one is made by four crystals of $5 \times 5 \times 5$ cm^3, as those to be used by CUORICINO, and is intended to optimize the resolution of these bolometers.

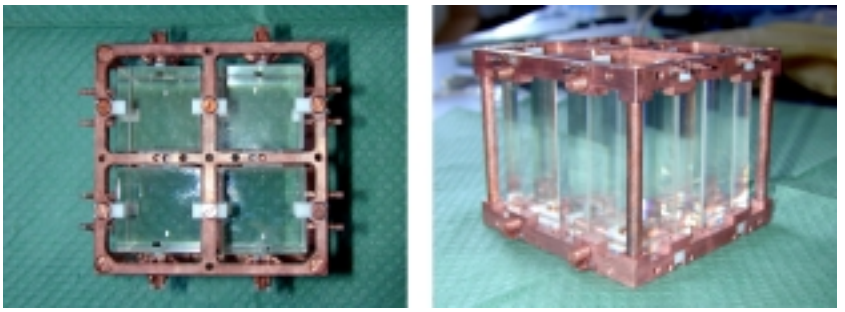

Figure 8: Copper holder of the array of 4 crystals $3 \times 3 \times 6$ cm^3.

A crucial improvement in the resolution has been obtained by suspending the entire array with a spring damped with teflon (Fig.7). As a consequence we have obtained an energy resolution with the $5 \times 5 \times 5$ crystal better than with those of the twenty crystal array.

5 Results obtained in the R & D for CUORICINO

The results obtained using the above mentioned spring are shown in Fig. 9.

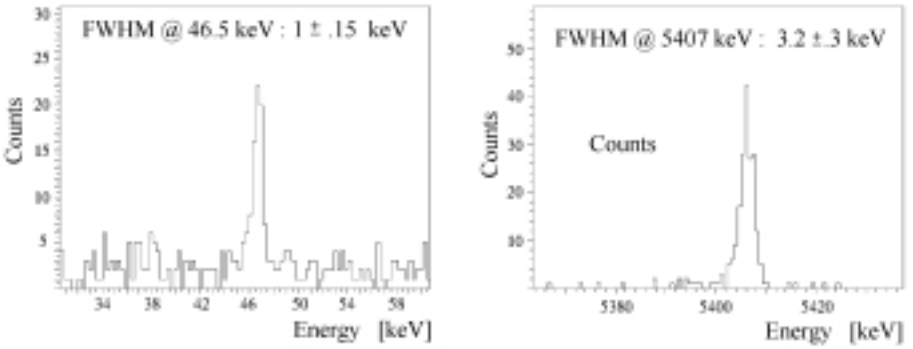

Figure 9: Energy resolution in the low and high energy region

We would like to note that the resolution obtained at low energy is similar to that of Ge diodes, while the resolution for the ^{210}Po α particles is by far the best obtained with any type of detector.

Considerable reduction of the background was obtained by lapping the crystals with grinding powder previously tested for its low content of radioactive contamination. The peaks due to α particles were reduced by an order of magnitude, while the continuum in the region of neutrinoless double beta decay was reduced by a factor of two. We have presently mounted the crystals of the array in a copper frame electrocleaned with a special procedure by the group of dr. Vincenzo Palmieri at the Laboratori Nazionali di Legnaro. The result is shown in Fig.10 and has to be compared with Fig.7. This procedure seems to produce a further reduction of the background.

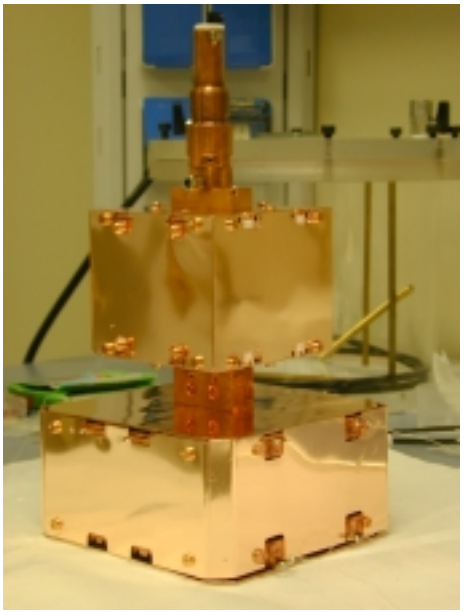

Figure 10: Electropolished copper holder.

The group is presently preparing the project for the experiment CUORE based on an array of one thousand crystals of TeO_2 of $5 \times 5 \times 5$ cm^3 to be proposed to the Scientific Committee of the Gran Sasso Laboratory next march. The new cryogenic scheme of CUORE is shown in Fig.11. The detector will be substantantially a cube made by 25 vertical towers of 10 "floors" of four crystal each, as those presently operated in Hall C.

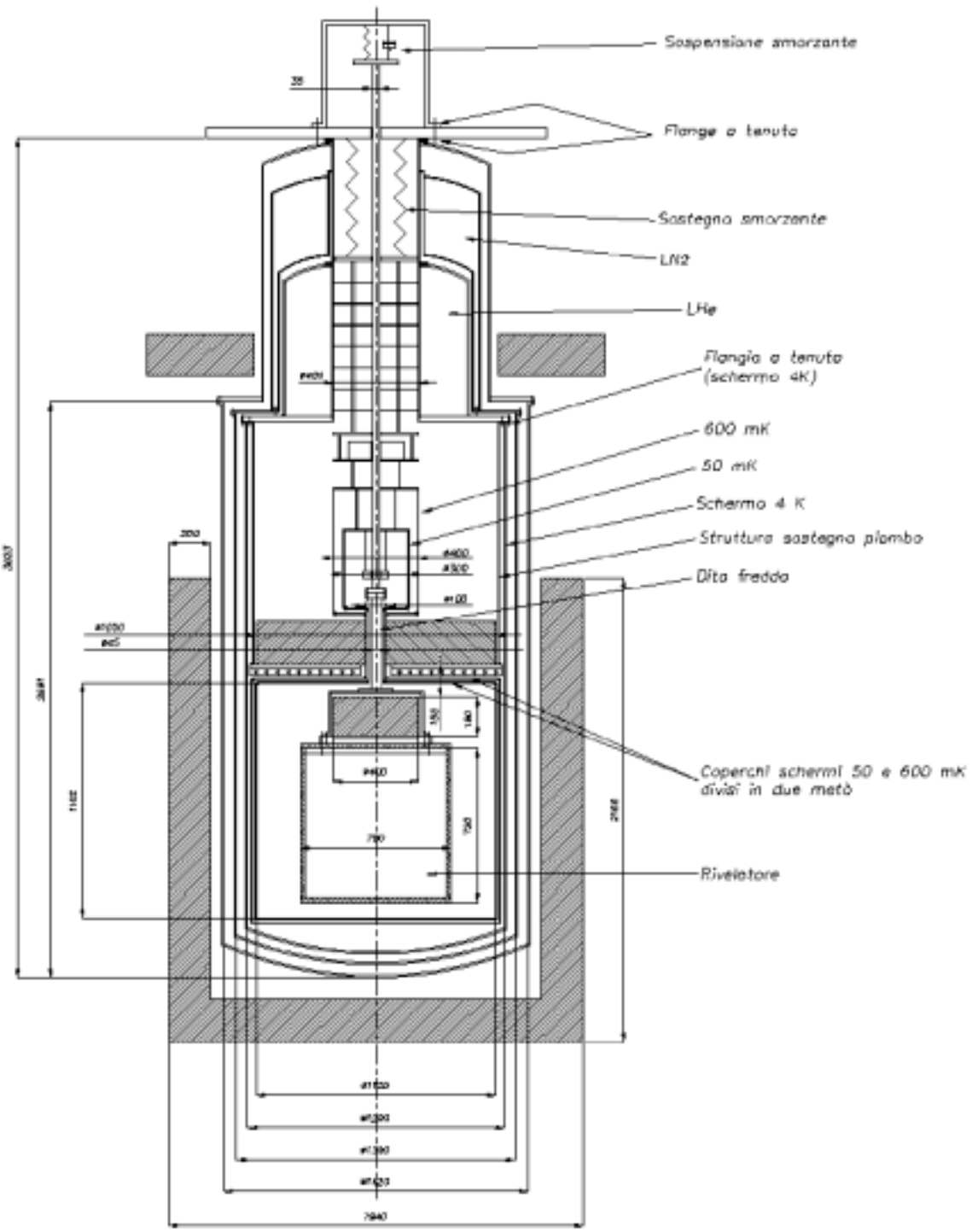

Figure 11: Cryogenic setup of CUORE.

6 List of Publications

1. E. Fiorini: Weak interaction searches with cryogenic detectors, Invited Talk to LTD8, Dalfsen (The Netherlands), August 16-20, 1999, NIM A 444 (2000) 65

2. A. Alessandrello et al. : A massive thermal detector for alpha and gamma spectroscopy, NIM A 440 (2000) 397

3. E. Fiorini: CUORE and CUORICINO, Nuclear Phys. B. (in the press)

4. A. Alessandrello et al.: New experimental results on double beta decay of ^{130}Te, Physics Letters B, Vol. 486 (1-2) (2000) pp. 13-21

5. E. Fiorini: Double Beta Decay: the Future, Review Talk to "Neutrino 2000", Intern. Conf. On Neutrino Physics and Astrophysics, Subdury (Canada) , June 16-21, 2000, Nucl.Phys.B (Proc.Suppl.) in the press

6. A. Alessandrello et al.: CUORICINO, a thermal detector array to search for rare events, Nucl. Phys. B (Proc. Suppl.) 87 (2000) 78

THEORETICAL GROUP

R. Aloisio [b], Z. Berezhiani [b], V.Berezinsky, P. Chardonnet [c], Delepine[1], G. Di Carlo [a], A. F. Grillo, A. Galante [b], M. Gianotti [b], M.P. Lombardo[2], M. Marchesini [d] , F. Vissani

[a] on leave from Laboratori Nazionali di Frascati, Italy
[c] LAPP, Annecy, France
[d] Bologna University, Italy
[b] Physics Department, University of L' Aquila, Italy
[1] From September 2000; [2] until August 2000

Abstract

The activity of the group has concerned research in three main areas: Astroparticle Physics and Cosmology, Particle Phenomenology, and Lattice Gauge Theory.

1 Astroparticle Physics

The Astroparticle group of LNGS in 2000 included V.Berezinsky, P.Chardonnet (LAPP, France), M.Marchesini, F.Vissani and visitors B.Hnatyk (Lviv University, Ukraine) and S.Grigorieva (Institute for Nuclear Research, Moscow). The group worked in close collaboration with A.Vilenkin (Tufts University, USA), M.Kachelriess (CERN) and P.Blasi (Fermilab).

Scientific work

The main field of the work is astroparticle physics, including solar neutrinos, physics in underground detectors, massive neutrinos, ultra high energy cosmic rays, topological defects, relativistic astrophysics. From several works finished in 2000 two following results can be emphasized.

V.Berezinsky, A.Vilenkin and B.Hnatyk have demonstrated that cusps of superconducting cosmic strings can be the Gamma Ray Burst (GRB) engines. The short pulse of low-frequency e-m radiation, emerged during cusp event. It produces the beam of accelerated particles, which plays a role of fireball in GRB. This model has essentially only one free parameter and successfully explains the range of observed fluences, rate of

GRB, rate-fluence dependence, and the range of durations. The short wave-length perturbations, wiggles, naturally explains the short-time structure of GRBs (astro-ph/0001213).

V.Berezinsky and M.Kachelriess created the Monte-Carlo simulation for jet fragmentation at very high primary energy with the detailed account of supersymmetry effects. The initial energy can reach GUT scale, while in the existing MC simulations this energy cannot be higher than 10^6 GeV. This high initial energy became possible due to the new method of describing the parton hadronization. This Monte-Carlo simulation was applied for calculation of hadron spectra from the decay of superheavy particles (hep-ph/0009053).

Participation in conferences

V. Berezinsky and F.Vissani presented invited talks at the conference "Physics of Particles, Astrophysics and Cosmology" (LNGS, October 22-24 2000). F. Vissani presented invited talks at the Vulcano 2000 Workshop "Frontier Objects in Astroparticle and Particle Physics" (Vulcano, 22-27 May 2000); at the "9^{th} Marcell Grossmann Meeting" (Rome, 2-9 Jul 2000); at the "3^{rd} International Conference on Dark Matter in Astro and Particle Physics (DARK 2000)" (Heidelberg, 10-15 Jul 2000). F.Vissani presented a talk at the "Europhysics Neutrino Oscillation Workshop (NOW 2000)" (Conca Specchiulla, Otranto, 9-16 Sep 2000); and attended the "19^{th} International Conference on Neutrino Physics and Astrophysics (Neutrino 2000)" (Sudbury, Canada, 16-21 Jun 2000).

Journal and Proceedings publications of 2000

1. V.Berezinsky, G.Fiorentini, and M.Lissia,
"Vacuum oscillations and excess of high energy solar neutrino events observed in Superkamiokande"
Astroparticle Physics, 12, 299, 2000.

2. V.Berezinsky,
"Ultra High Energy Cosmic Rays"
Nucl. Phys. B (Proc. Suppl.) 81, 311, 2000.

3. V.Berezinsky,
"Ultra High Energy Cosmic Rays from cosmological relics"
Nucl. Phys. B (Proc. Suppl.) 87, 387, 2000.

4. V.Berezinsky and A.Vilenkin,
"Ultra-high energy neutrinos from hidden-sector topological defects"
Phys. Rev. D 62, 083512, 2000.

5. F. Vissani,
"Aspects of CP Violation in the leptonic sector"
In Frascati Physics Series XVI, 337, 2000

6. A. Datta, B. Mukhopadhyaya and F. Vissani,
"Tevatron signatures of an R parity violating supersymmetric theory"
Phys. Lett. B, 492, 324, 2000

Preprints of 2000

1. V.Berezinsky, B.Hnatyk and A.Vilenkin,
"Superconducting cosmic strings as Gamma Ray Burst Engines"
astro-ph/0001213

2. V.Berezinsky (in EASTOP collaboration),
"Upper limit on electron antineutrino flux from GRB 990705"
astro-ph/0011249

3. V.S.Berezinsky and V.I.Dokuchaev,
"Hidden source of high energy neutrinos in collapsing galactic nucleus"
astro-ph/0002274.

4. F. Vissani,
"Charm production by cosmic muons"
hep-ph/0004073

5. F. Vissani (in The SUSY Working Group),
"The SUSY Working Group: Summary report"
hep-ph/0005142

6. F. Vissani,
"What is the standard model of elementary particles and why we have to modify it"
hep-ph/0007040

7. F. Vissani,
"Non-oscillation searches of neutrino mass in the age of oscillations"
hep-ph/0012018

During 2000 R. Aloisio, P. Blasi (FermiLab), P.L. Ghia (Torino and LNGS) and A. F. Grillo started a systematic analysis on the bounds that VHE and UHE cosmic ray experiments can put on the parameters of possible violations of Lorentz invariance which can be possibly expected in some quantum gravity theories. It turns out that the observation of absorption cutoffs (like the GZK one) on the spectra of VHE γ and UHE protons can put very stringent limits on violation parameters. This analysis has been presented by A. F. Grillo at various Workshops and by P. L. Ghia at the Gamma 2000 Conference.

1. R. Aloisio, P. Blasi, P.L. Ghia e A.F. Grillo,
"Probing The Structure of Space-Time with Cosmic Rays", Phys. Rev. **D62** (2000) 053010.
2. R. Aloisio e A.F. Grillo
"Cosmic Rays and the Structure of Space-Time", Proceedings of the Workshop 'Frontier Objects in Astrophysics and Particle Physics', Vulcano (Italia), May 22-27 2000, *preprint* astro-ph/0008491.

2 Particle Phenomenology

The particle phenomenology group including Z. Berezhiani, D. Delepine and M. Giannotti worked in close collaboration with A. Rossi (Padova), D. Comelli, A. Drago, F. Villante (Ferrara), L. Bento, G. Branco (Lisbon) and W. Buchmuller (DESY).

Scientific work

The main field of the groups activity is the particle phenomenology, including supersymmetry and grand unification, flavour problem, CP violation, neutrino physics, and its applications in astrophysics and cosmology. ¿From several works finished in 2000 the following results are to be mentioned.

Z. Berezhiani and A. Rossi have studied the fermion mass and mixing structure in grand unified theories with the flavour symmetry $SU(3)_H$ between families. The presented models explain the origin of the fermion mass and mixing hierachy and provide fermion mass textures with high precission predictions in confront of the experimental situation concerning the quark and lepton mixing angles and CP-violation parameters.

Z. Berezhiani and A. Drago have suggested a new mechanism for the Gamma Ray Bursts (GRB) via emission of axion-like particle with mass order 1 MeV and decay constant order 10^6 GeV. This mechanism can power the fireball formation with the huge energetics and large Lorentz factor from the collapsing objects like the neutron star merger or the collapsar, and can explain association of some GRB with the supernovae type 1b,c. Such an axion-like particle can be tested with future reactor or beam dump experiments.

Z. Berezhiani, D. Comelli and F. Villante have studied a cosmological evolution of the mirror universe, an identical copy of the observed particle world interacting with the latter only gravitationally. Its existence can be motivated in the context of string or brane world theories. The primordial nucleosynthesis bounds demand that at the Big Bang the mirror particle sector is born with at least factor two lower temperature than the ordinary one. In this case mirror baryogenesis should be more effective than ordinary one, and the mirror baryons can constitute dark matter of the universe, with strong implications for the large scale and galactic halo structures, CMBR angular anisotropies, microlensing, etc.

Participation in conferences

Z. Berezhiani presented invited talks at the Europhysics Conf. Planck'2000 "Physics from Planck Scale to Electroweak Scale" (Castelvecchio Pascoli, Italy, 15-20 April 2000); at the Int. Conf. "Beyond 4 Dimensions" (Trieste, Italy, 2-6 July 2000); at the Int. Workshop "New Trends in Astroparticle Physics" (Faro, Portugal, 1-3 Sept. 2000); at the Int. Workshop "30 Years of Supersymmetry" (Minneapolis, USA, 22-29 Oct. 2000), and at the Euro-GDR Meeting on Supersymmetry (Paris, France, 29 Nov.- 2 Dec. 2000). M. Giannotti presented an invited talk at the Int. Conf. "Quarks 2000" (Pushkin, St. Petersburg, Russia, 14-22 May 2000), and a talk at the Gran Sasso Summer Institute "Supersymmetry and Dark Matter" (LNGS, Italy, 8-21 July 2000).

Publications

1. Zurab Berezhiani, Alessandro Drago,
"Gamma Ray Bursts via emission of axion-like particles"
Phys. Lett. B 473, 281, 2000.

2. Luis Bento, Zurab Berezhiani,
"Classical Nambu-Goldstone fields",
Phys. Rev. D 62, 055003, 2000.

3. Zurab Berezhiani, Anna Rossi,
"Towards a grand unified picture for neutrino and quark mixings",
Nucl. Phys. B 81 (Proc.Suppl.), 346, 2000.

4. Zurab Berezhiani, Anna Rossi,
"Predictive grand unified textures for quark and neutrino masses and mixings"
Nucl. Phys. B 594, 113, 2001, hep-ph/0003084.

5. W. Buchmuller, L. Covi, D. Delepine,
"Inflation and supersymmetry breaking",
Phys. Lett. B 491, 183, 2000.

6. W. Buchmuller, D. Delepine, L.T. Handoko,
"Neutrino masses and flavor changing processes",
Nucl. Phys. B 576, 445, 2000

7. Zurab Berezhiani, Denis Comelli, Francesco L. Villante,
"The early mirror universe: inflation, baryogenesis, nucleosynthesis and dark matter",
hep-ph/0008105, accepted for publication in Phys. Lett. B (in press)

8. Zurab Berezhiani, Leonida Gianfagna, Maurizio Giannotti,
"Strong CP-problem and mirror world: the Weinberg-Wilczek axion revisited",
hep-ph/0009290, accepted for publication at Phys. Lett. B (in press).

9. G. Branco, D. Delepine, R. Gonzalez-Felipe,
"Dynamical CP violation and flavour-changing processes",
Preprint FISIST/01-2001/CFIF, January 2001.

3 Lattice Gauge Theories

The activity has concerned the study of QCD-like theories at non zero density and of QCD with a theta vacuum

QCD-like theories at nonzero density

R. Aloisio, G. Di Carlo, A. Galante, A.F. Grillo, in collaboration with V. Azcoiti (University of Zaragoza).

The study of the properties of Quantum ChromoDynamics (QCD), in particular at non zero baryonic density, can provide in principle an ab initio calculation of nuclear and particle properties and processes of relevance to Cosmology, Astrophysics and to Heavy Ions experiments. such as the equation of state of nuclear matter and the relevant critical properties. This kind of study is extremely difficult from a numerical point of view, due to the complex nature of the fermionic action in SU(3) that does not allow the use of standard simulation techniques. Owing to these difficulties the interest has been focused on the study of a class of theories or models that share some fundamental properties with QCD, or QCD itself in nonphysical limits, more affordable from a numerical point of view.

The current situation of the results of three colors theory in the infinite gauge coupling limit [1,6], has been critically re-examined, raising strong doubts on the robusteness of the signal of strong first order phase transition obtained, in 1989, using the MDP (Monomer-Dimer-Polymer) algorithm. The existence of this transition could be considered as one of the few universally accepted results of numerical simulations of finite density QCD up to now, and the MDP as the only algorithm effective, in the strong coupling regime, to produce sensible results. In heavy quark limit signals of a deconfining (first order) phase transition at small density and near to the zero density critical temperature have been obtained [2]. This transition, expected on general grounds within phenomenological models, has never been seen before; previous results, instead, obtained using approximations or simplified models, casted doubts on its real existance.

Another important case is two color QCD, in which the gauge group is reduced to SU(2). We have studied, in light quark regime [1,3,4,7] the diquark condensate formation at high density and zero temperature. This phenomenon, similar to the standard description of the superconducting phase of ordinary matter (BCS), has been studied in the strong coupling limit using two techniques formerly developed for the analysis of chiral transition in noncompact QED. The first one, via the study of susceptibility, allows to avoid any extrapolations procedure, making particularly clear the numerical analysis of the formation of the condensate [3]. The second one, based on the probability distribution function of the order parameter, allows the determination of the order parameter itself at zero external source [4,7]. The results are in quite good agreement with the predictions of Low Energy Lagrangians, and state the existence of a phase of diquark condensation for a chemical potential larger than half the pion mass.

QCD with a theta-vacuum term

A. Galante in collaboration with V. Azcoiti and V. Laliena (University of Zaragoza).

A study of the effects induced by a topological term in QCD Lagrangian has been developed. The main result is the following theorem: "If there is a non-trivial dependence of the properties of the vacuum of QCD on the θ angle then there must be a non-analytic=

ity between $\theta = 3D0$ and $\theta = 3D\pi$" [5]. This theorem allows us to put in evidence the limits of approximated schemes used up to now to look at the theta dependence of QCD. Moreover, using a gaussian form for the probability distribution function of topological charge density, we have derived a results recently obtained by E. Witten in the contest of duality relations between string theories and SU(N) in the large N limit [5,8].

In addition to the above, the LNGS and in particular Andrea Donati, Aurelio Grillo, Giuseppe Di Carlo, in collaboration with Emanuele Panizzi (L'Aquila) and Alberto Petricola (L'Aquila-LNGS) have be= en involved in an interdisciplinary activity supported by Consorzio Ricerca del Gran Sasso.

Publications

1. R. Aloisio, V. Azcoiti, G. Di Carlo, A. Galante, A.F. Grillo; "Three and Two Colours Finite Density QCD at Strong Coupling: A New Look"
Nucl. Phys. B564 (2000) 489.

2. R. Aloisio, V. Azcoiti, G. Di Carlo, A. Galante, A.F. Grillo; "Finite density Fat QCD"
Phys. Rev. D61 (2000) 111501R.

3. R. Aloisio, V. Azcoiti, G. Di Carlo, A. Galante, A.F. Grillo; "Fermion condensates in two colours finite density QCD at strong coupling"
Phys. Lett. B493 (2000) 189.

4. R. Aloisio, V. Azcoiti, G. Di Carlo, A. Galante, A.F. Grillo; "Probability distribution function of the diquark condensate in two colours QCD"
hep-lat/0011079, submitted to Nucl. Phys. .

5. V. Azcoiti, A. Galante, V. Laliena; "Theta dependence in QCD"
in preparation.

Proceedings

6. R. Aloisio, V. Azcoiti, G. Di Carlo, A. Galante, A.F. Grillo; "Strongly Coupled QCD at Finite Baryon Density"
LATTICE99, Nucl. Phys. (Proc. Suppl.) 83 (2000) 351.

7. R. Aloisio, V. Azcoiti, G. Di Carlo, A. Galante, A.F. Grillo; "Diquark condensation in two colours QCD"
International Workshop on Non-Perturbative Methods and Lattice QCD, Guangzhou, China, 15-21 May 2000 hep-lat/0007045.

8. V. Azcoiti, A. Galante, V. Laliena; "QCD with a theta-vacuum term: a complex system with a simple complex action"
International Workshop on Non-Perturbative Methods and Lattice QCD, Guangzhou, China, 15-21 May 2000 hep-lat/0007045.

TRIS

E. Battistelli[a], G.Boella[a], F.Cavaliere[b], A. De Lucia[a],
M.Gervasi[a], A.Passerini[a], D. Restifo[b], G.Sironi[a]
M.Zannoni[a]

[a] University of Milano-Bicocca
Physics Dept. "G. Occhialini"
P.le delle Scienze, 3 20126 Milano - Italy
[b] University of Milano
Physics Dept.
via Celoria, 16 20133 Milano - Italy

Abstract

TRIS is a set of three radiometers which have been built to study the diffuse background and look for deviations from a pure planckian distribution in the frequency spectrum of the 3K Cosmic Background Radiation, Relic of the Big Bang, at frequencies close to 1 GHz. The system is installed at Campo Imperatore (2000 m a.s.l.). In December 2000 observations were concluded. We are now reducing the data.

1 Introduction

Spectral distortions, spatial anisotropies and residual polarization are fine features of the Cosmic Background Radiation (CBR), Relic of the Big Bang, currently used by cosmologists to probe the Universe up to red shifts Z close to 10^6, when the Universe was extremely young and matter condensations did not exist. Studies of the condensed objects we see today on the sky do not allow to go back so far. In fact no object with Z greater than about 6 has been discovered so far and theory tells us that stable matter condensations could form only when Z became smaller than 10^3 and the Universe was at least a million years old (for a general discussions see for instance Partridge 1995 [1]).

1.1 The experiment

TRIS is a set of three absolute radiometers (see fig.1) we built and installed at Campo Imperatore (2000 m a.s.l.) with the aim of studying the diffuse background radiation of celestial origin at 0.6, 0.82 and 2.5 GHz and get the spectrum of the CBR at frequencies close to 1 GHz. Here in fact models of the Universe (e.g. C. Burigana & al. 1991 [2]) show that deviations from a Planck distribution are expected. Amplitude and frequency

of that distortion depend on, and can be used to evaluate, the universal abundance of barionic matter.

Figure 1: The Tris Experiment at Campo Imperatore: from left to right the 0.6, 0.82 and 2.5 GHz radiometers are shown.

2 TRIS Activities in year 2000

A complete description of TRIS and its program of observation can be found elsewhere (Zannoni 1999 & al. [3] and references therein and previous LNGS Annual Reports). In spite of bad weather and external activities at the site which forced us to turn off TRIS for three months in year 2000 we:

- collected data sufficient to prepare accurate profiles of the variations of the sky temperature at declination +42° versus the right ascension,
- measured the absolute temperature of the sky at various points along the above profiles,

- got auxiliary data (ground, atmospheric and interference contributions to the signals collected by the radiometer antennae).

In December 2000 the program of observations planned for TRIS was completed. New kinds of observations would be possible with TRIS. Unfortunately the site at Campo Imperatore has to be cleared therefore, as soon as the road to Campo Imperatore will reopen at the end of the winter season, we will move antennae and radiometers at a new site.

3 Conclusions

At present we are busy in reducing th data collected by TRIS. Subtraction from the measured signals of the contributions produced by human activity (interferences), ground emission, atmospheric emission and solar emission is the first step. Then the three sets of clean data measured at 0.6, 0.82 and 2.5 GHz at at declination $+42°$ and right ascension ranging between $0h$ and $24h$ are introduced in a mathematical model which describes the diffuse radiation as a combination of three components (Cosmic Background Radiation (CBR), Galactic (synchrotron) Radiation, blend of unresolved extragalactic sources). Solving the system of equations allow to work out the temperature of the CBR at the three frequencies of TRIS (Sironi & al. 1993 [5]). Finally these values of CBR temperature are compared among them and with data at other frequencies in literature looking for deviation from a flat (planckian) distribution. An important intermediate step in this analysis is the evaluation of the spectral index of the frequency power law which describes the galactic components (see fig.2). Results on this point have been already obtained and partially published (Zannoni & al. 2000 [4]).

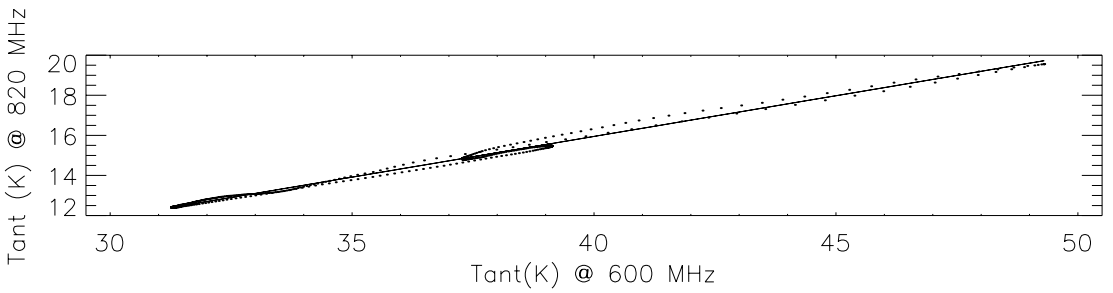

Figure 2: T-T plot of the sky temperature measured at 820 MHz versus the sky temperature measured at 600 MHz. The solid line is the linear regression of the scatter plot. The resulting Spectral Index γ is 2.92 ± 0.09.

The analysis of the full set of TRIS data will be completed by July 2001. The expected final accuracy on the absolute temperature of the CBR in the GHz region is about 200 mK, to be compared with an accuracy of the data presently available at the same frequencies definitely worse (for a discussion see Sironi & al. 1993 [5], Zannoni & al. 1999 [3]).

4 List of Publications

1. M. Zannoni, M. Gervasi, G. Boella, G. Sironi:*The Spectral Index of the Galactic foreground affecting CMB measurements* - IAU General Assembly Proc. Symp. 201, in press.

2. M. Zannoni, E. Battistelli, G. Boella, F. Cavaliere, M. Gervasi, A. Passerini and G. Sironi:*TRIS experiment: recent measurements of spectral index of the Galactic diffuse emission* - SIF Conf. Proc. 68:179, **2000**

3. D. Restifo:*Stima del contributo galattico alla radiazione diffusa celeste* - Laurea Thesis University of Milano November 2000 not published.

References

[1] R.B. Patrtridge: *3K: The Cosmic Microwave Background Radiation* Cambridge University Press, Cambridge (UK) **1995**.

[2] C. Burigana, G. De Zotti and L. Danese, *ApJ*, 379:1-5, **1991**.

[3] M. Zannoni & al., *AIP Conf. Proc.*, 476:165, **1999**.

[4] M. Zannoni & al., *IAU General Assembly Proc. Symp. 201*, in press.

[5] G. Sironi & al., *ASP Conf. Proc.*, 51:541, **1993**.

GIGS. The Interferometric Station at LNGS

Antonella Amoruso[a,c], Luca Crescentini[b,d], Roberto Scarpa[a,c]

[a] Dip.to di Fisica Univ. dell'Aquila, L'Aquila - Italy
[b] Dip.to di Scienze della Terra Univ. di Camerino, Camerino (MC) - Italy
[c] INFN - Gruppo collegato dell'Aquila, L'Aquila - Italy
[d] INFN - LNGS, L'Aquila - Italy

Abstract

From a technical point of view, during 2000 the experimental apparatus has been improved, substituting data acquisition PCs and adding remote control of the experiment. Work is still in progress toward a full understanding of the seismological implications of the slow activity recorded during 1997 and toward identification of the source(s) of the events.

1 Introduction

The interferometric station at LNGS consists of two laser interferometers for geophysical purposes. They measure the extension of two 90m-long baselines, approximately parallel and perpendicular to the average direction of the Apennines. The instruments have very high sensitivity ($\approx 3 \times 10^{-12}$), large dynamic range (unbounded in principle), and good reliability. The experiment has been planned for a better knowledge of crustal deformation processes, related to a wide range of phenomena (strain accumulation and release, aseismic slips, coseismic steps, slow earthquakes, earth tides).

2 Research Activity

The main scientific results obtained till now are the observation of several clustered slow earthquakes in 1997, the consequent stating of an unusual scaling law between the amplitude and the rise time of the events and its preliminary interpretation in terms of fault friction [1]. We are still working to understand the seismological implications of the slow activity and to identify the source(s) of the events, also taking into account different kind of data and the main features of the Gran Sasso massif. We have performed some simulations to compare the slow signals with what expected for extensional seismic mechanisms usually retrieved for regular earthquakes in Central Apennines. We have modified the AXITRA code (freely available), which is able to compute the full field (near-, intermediate-,

and far-fields) of the seismic waves, in order to take into account the unusual time features of slow earthquakes. We have generated synthetic straingrams expected for different sources at different distances and azimuthal angles from the recording straimeter. Typical synthetic straingrams are shown below for 20-km and 7-km source distance from the interferometer.

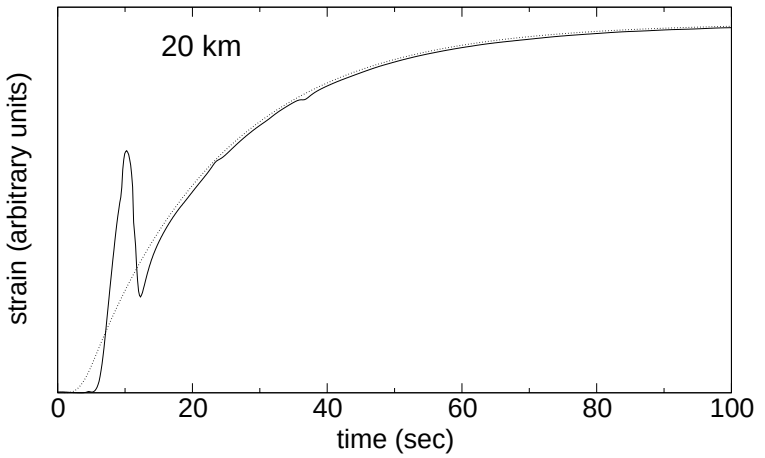

Figure 1: Typical source at 20-km distance from the strainmeter.

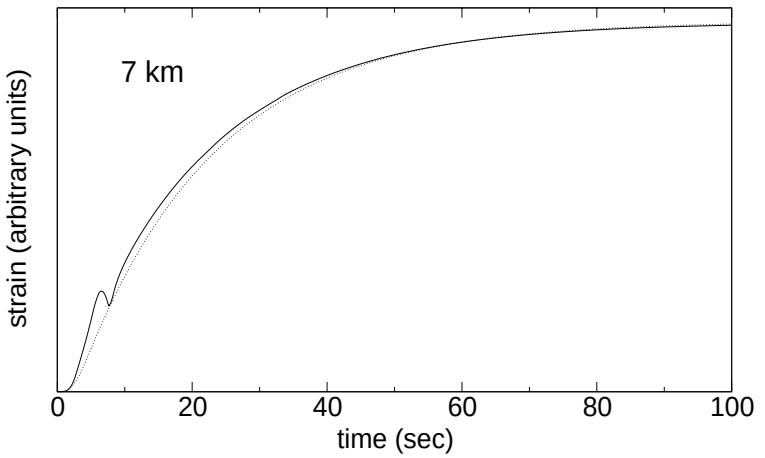

Figure 2: Typical source at 7-km distance from the strainmeter.

Location of the source(s) of the slow events can not be determined uniquely, but constraints can be given considering the shape of the signals and the records of the very-broadband seismographic station (AQU-MEDNET) located in L'Aquila (about 18 km SW of the interferometer). Records by the seismographic station during the occurrence of the slow events show no detectable signal. The transfer function of the seismograph and the scaling law between amplitude and rise time of the slow events indicate that the highest signal-to-noise ratio is achieved for the shortest slow events (about 20 s).

We have computed synthetic seismograms that should have been recorded by the very-broadband seismograph e.g. for a typical source 5-km South of the interferometer, with the source time history and a seismic moment consistent with the signals recorded by the interferometer.

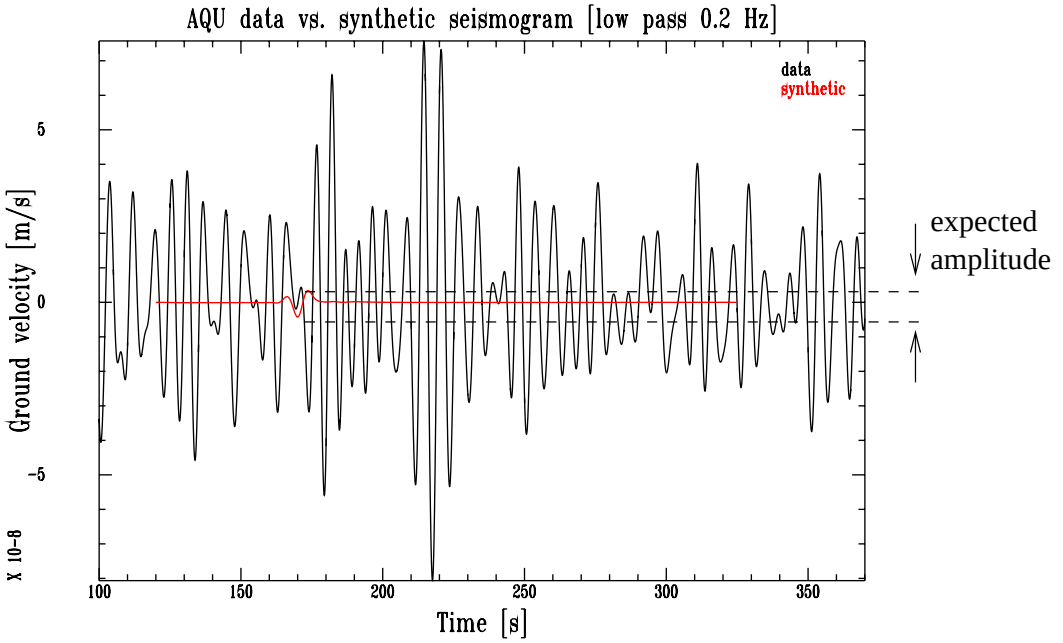

Figure 3: Comparison of synthetic seismogram as expected at AQU-MEDNET station and recorded data.

The results are in agreement with the lack of detection by the seismograph. The close proximity of the slow earthquake source(s) to the interferometer has thus been confirmed. Further simulations are in progress. We are trying to draw a consistent picture of what happened in 1997, also taking into account various features of the Gran Sasso massif (e.g. fault locations and fault gouges) and possible implications of the Ph anomaly observed by the LSS group in the groundwater collected close to the interferometer [2]. If successful, this attempt could enlighten the role of slow earthquakes in accomodating tectonic stress.

We are preliminarly analyzing data recorded during 2000, in particular at tidal frequencies, taking into account both solid tides and ocean loading.

3 List of Publications

1. Amoruso, A., L. Crescentini, A. Morelli, W. Plastino, F. Bella, and R. Scarpa, Strain data, groundwater chemistry, and seismic records during a slow earthquake sequence in Central Italy in 1997, AGU Fall Meeting, San Francisco (USA), 2000.

References

[1] L. Crescentini, A. Amoruso, and R. Scarpa, Constraints on Slow Earthquakes Dynamics from a Swarm in Central Italy, Science, **286**, 2132-2134, 1999.

[2] F. Bella and W. Plastino, LSS. Liquid Scintillation Spectrometry - Radon time series analysis at LNGS , I, INFN-LNGS Annual Report 1999, 193-198, 2000.

Tectonic deformation events and local seismicity in the Gran Sasso area of the central Apennines

Vittorio Sgrigna[a]

[a] Dipartimento di Fisica "E. Amaldi", Università degli Studi di Roma "Roma Tre"

Abstract

Geophysical investigations carried out at LNGS during 2000 concerning deformation phenomena of seismotectonic interest are described. In particular, ground tilt results associated with the main shocks of the Umbria-Marches seismic sequence occurred in 1997 are reported. Preseismic creep strains were observed before the occurence of such earthquakes.

1 Introduction

Investigations concerning deformation events of tectonic interest, detected at three sites of the LNGS are carried out and correlated to earthquakes. Observations deal with the possibility to study the time and space of earthquake occurrence by the study of rock microfracturing process which takes place in the preparation focal area during the preseismic period.

Such process gives rise to a nonelastic rock behaviour (dilatancy) in which volumetric strain increases relative to what would be expected from the elasticity. At the LNGS, the intermediate-term volumetric strain increase, involved in the thrust and deep fault systems of the Gran Sasso chain, is studied by continuous ground tilt measurements.

Tiltmeters are also installed at the Gran Sasso area, outside the LNGS, for a better investigation of the above-mentioned phenomena of tectonic interest.

2 Results

Results obtained at LNGS and in the surrounding area during 2000, are summarized in the following sections.

2.1 Investigations in the Gran Sasso area

In the 1999 scientific report it was shown that seismological data from the Latium-Abruzzi carbonate platform, including the Gran Sasso chain, fit a block tectonic modelling previously proposed for this area on the basis of structural and paleomagnetic evidences [1]. A migration of earthquake foci was also observed. Velocity values were similar to those obtained in other seismic regions ($\approx 0.1 cm/s$), demostrating the slow propagation of a stress-strain field in such areas [2].

Finally, an aquifer-induced seismicity effect was also observed in the Gran Sasso area [3]. In particular, a sudden increase in the groundwater level changes, superimposed to the normal seasonal cyclic variations, triggered small earthquakes of the region.

During 2000, geostructural and geophysical mesaurements for the seismic hazard assessment and prediction have also been carried out in the Caucasus [7]. This area shows some similiarity with the central Apennines Region which includes the Gran Sasso chain. In order to monitor ground deformation processes, it is necessary to place strainmeters close to the tiltmeters already installed in the area under study. The experimental apparatus in the LNGS includes such instruments (three tiltmeters and an interferometric strainmeter), even if they are used by two different research teams. On the contrary, strainmeters need to complete the instrumental network installed in the Gran Sasso surrounding area. For this purpose, an original two-frequency electromagnetic strainmeter for ground field measurements has been realized [8]. The main peculiarities of this new instrument are the possibility to carry out a continuous monitoring of ground strain variations with a sensitivity grater than 10^{-8} for base length from some ten meters to some ten kilometers.

2.2 Investigations in the LNGS

2.2.1 Experimental apparatus

The experimental apparatus consists of three tiltmeters realised at the Department of Physics of our University [4]. Tilt sensors consist of two-component-horizontal-pendulum tiltmeters with Zöllner bifilar suspension. They have been made using super Invar. The analog detecting system is constituted by an infrared laser beam and a 1024 photodiodes linear array of 0.5 inch long. The resolution is of $0.05 \mu rad$. A digital aquisition system allows the tilt data to be collected hourly.

2.2.2 Ground tilt

A 2-D model for slow crust movements, including creep-related tilt and strain precursors of earthquakes, has been proposed [2]. The model describes the earthquake preparation through the rheological properties of viscoelastic fault gouge (separating rigid crustal blocks) studied by constitutive equations of Standard Linear Solid.

Ground tilt variations have been correlated to the Umbria-Marches seismic sequence of 1997-1998. An aseismic creep strain was observed at LNGS. It revealed to be precursor of the above-mentioned seismic sequence. Results of similar quality was obtained at Peschiera and L'Aquila tilt sites. No preseismic signals were detected in the Stiffe cave

tilt site located at greater distance where preseismic creep amplitudes are of the same order of the signal background, according to theoretical models based on dislocation or dilatancy theories.
Such creep strains resulted also to be shifted in time between them, indicating a possible slow propagation ($\approx 1cm/s$) of the preseismic tilt field generated in the Umbria preparation focal area. A best fitting of the same experimental creep curves was carried out on the basis of viscoelastic models, as follows:

Kelvin-Voigt model

$$\sigma = \mu\varepsilon + \eta\frac{\partial\varepsilon}{\partial t} \tag{1}$$

Zener (SLS) model

$$\sigma + \frac{\partial\sigma}{\partial t}\tau_\sigma = M_R(\varepsilon + \frac{\partial\varepsilon}{\partial t}\tau_\varepsilon) \tag{2}$$

Burgers model

$$\eta_1\frac{\partial^2\varepsilon}{\partial t^2} + \mu_1\frac{\partial\varepsilon}{\partial t} = \frac{\eta_1}{\mu_2}\frac{\partial^2\sigma}{\partial t^2} + (1 + \frac{\mu_1}{\mu_2} + \frac{\eta_1}{\eta_2})\frac{\partial\sigma}{\partial t} + \frac{\mu_1}{\eta_2}\sigma \tag{3}$$

Maxwell model generalized by M. Caputo

$$\mu\nu\frac{\partial^z\varepsilon}{\partial t^z} = \mu\sigma + \nu\frac{\partial^z\sigma}{\partial t^z} \qquad with\ 0 < z < 1 \tag{4}$$

where σ, ε, μ, η are stress, strain, rigidity and Newtonian viscosity, respectively. τ_σ, τ_ε, and M_R are characteristic parameters of the model. In equation (4) the anelastic properties are represented by ν (with dimensions $gcm^{-1}\,s^{-2+z}$) and z.
The creep functions corresponding to the above mentioned constitutive equations are as follow:

$$c(t) = \frac{1}{2\mu}(1 - e^{-(\mu/\eta)\,t}) \tag{5}$$

$$c(t) = \frac{1}{M_R}[1 - (1 - \frac{\tau_\sigma}{\tau_\varepsilon})e^{-t/\tau_\varepsilon}] \tag{6}$$

$$c(t) = \frac{t}{2\eta_2} + \frac{1}{2\mu_2} + \frac{1}{2\mu_1}(1 - e^{-(\mu_1/\eta_1)t} \tag{7}$$

$$c(t) = \frac{1}{2\mu} + \frac{t^z}{2\nu\Gamma(z+1)} \tag{8}$$

All these results have been reported to the 1999 AGU Fall Meeting of the American Geophysical Union [5], [6].
Theoretical investigations concerning the study of the seismicity patterns, earthquake nucleation in an interacting fault system, and mechanisms of rupture processes have also been carried out [9], [10], [11].

3 Conclusions

Experimental and theoretical results at LNGS obtained during 2000, as well as the ongoing investigations, confirm a good agreement between geodynamic, rheological, and seismological data. These correlations are also confirmed by similar investigations carried out in the Gran sasso area of the carbonate platform and in particular in the Peschiera, Stiffe and L'Aquila tilt sites. The theoretical modelling also corroborate such results.

4 List of Publications

1. Bella, F., P.F. Biagi, M. Caputo, E. Cozzi, G. Della Monica, A. Ermini, W. Plastino, V. Sgrigna, D. Zilpimiani, 1997. *Helium content in the Caucasus as earthquake precursor*, in: Rare Gas Geochemistry, Guru Nanak Dev University, Amritsar-143005 (India), *Proc.* 3^{rd}*ICRGG*, pp. 158-166.

References

[1] Bella, F., M. Caputo, G. Della Monica, A. Lisi, W. Plastino, R. Scandone, and V. Sgrigna, 1998. *Crustal blocks and seismicity in the central Apennines*, Nuovo Cimento, **21C**, 597-607.

[2] Bella, F., M. Caputo, G. Della Monica, W. Plastino, V. Sgrigna, Yu. P. Vaveluk, and T.B. Yanovskaya, 1998.*A 2-D model for tilt and strain fields associated to earthquakes in crustal block structures*, Phys. Earth and Planet. Int., **106**, 155-164.

[3] Bella, F., P.F. Biagi, M. Caputo, E. Cozzi, G. Della Monica, A. Ermini, W. Plastino, and V. Sgrigna, 1998. *Aquifer-induced seismicity in the central Apennines (Italy)*, Pure Appl. Geophys., **153**, 179-194.

[4] Bella, F., P.F. Biagi, G. Della Monica, A. Ermini, and V. Sgrigna, 1998. *A horizontal pendulum tiltmeter with digital recording system*, Nuovo Cimento, **12C**, 799-809.

[5] Malvezzi, V., F. Bella, G. Della Monica, D. Zilpimiani, and V. Sgrigna, 1999. *Creep-related tilt precursors and rheological behavior of crustal block boundaries*, EOS Trans. T12B-10, AGU vol. **80**, n.46, pag. F934.

[6] Sgrigna, V., M. Caputo, V. Malvezzi, T. B. Yanovskaya, 1999. *A numerical 2-D model for crustal block dynamics in seismic regions*, EOS Trans. T12B-09, AGU vol. **80**, n. 46, pag. F934.

[7] Caputo, M., I. Gamkrelidze, V. Malvezzi, V. Sgrigna, G. Shengelaia, D. Zilpimiani, 2000. *Geostructural basis and Recent Geophysical Investigation for the Seismic Hazard Assessment and Prediction in the Caucasus*, Nuovo Cimento,**23C**, 191-214.

[8] Sgrigna, V., V. Malvezzi, D. Zilpimiani, 2000. *A Two-Frequency Electromagnetic Strainmeter for Ground Field Measurements*, Geophys. Res. Lett.,submitted.

[9] Caputo, M., G. Della Monica, F. Fattori Speranza, S. Reseda, V. Sgrigna, 2000. *Earthquakes in a Fault System Imbedded in an Elastic Body Subject to an Increasing Shear Stress*, Nuovo Cimento, **23C**, 293-313.

[10] Console, R., F. Fattori Speranza, V. Sgrigna, 2000. *A Modelling for Earthquake Nucleation in an Interacting Fault System*, Tectonophys., submitted.

[11] Manjavidze, J., V. Sgrigna, D. Zilpimiani, 2000. *Phenomenology of Rupture Processes in Homogeneous Isotropic Media*, Nuovo Cimento, **23C**, 165-175.

Radiocarbon and radon analysis for geophysical monitoring of Gran Sasso aquifer

Francesco Bella[a] and Wolfango Plastino[a,b]

[a]Department of Physics, University of Roma Tre, via della Vasca Navale, 84, I-00146, Rome (Italy)

[b]INFN, Section Rome III, via della Vasca Navale, 84, I-00146, Rome (Italy)

Abstract

From 1996, geophysical and geochemical investigations with an automatic multiparametric equipment [1] have being performed to study the properties of the Gran Sasso aquifer and the possible correlations with deformation events of tectonic interest and local seismicity. The hydrological system is $MgCa(CO_3)_2$-CO_2-H_2O with an high dynamics behaviour due to high permeability of cretaceous limestones. During these years some *anomalies* in geophysical and geochemical groundwater parameters have been recorded emphasizing an high correlation with tectonic deformation processes and local seismicity [2].

Also, we have completed the 1220 Quantulus^{TM} ultra low level background scintillation spectrometer setup. The aim of this research actvitiy is to perform high precision measurements of natural radioisotopes (radiocarbon and tritium) in groundwater to better define the hydrological properties of the Gran Sasso aquifer.

1 Introduction

The radon groundwater monitoring is a useful tool to study the correlations between the possible radon variations with the deformation processes of tectonic interest. Temporal variations of this radioisotope have been justified with the stress variations in rock associated with the seismicity supposing crustal gas-fluxes along active faults or the radon transport from its origin to the surface through microfractures [3]. Moreover, radon diffusive processes are related to groundwater geochemistry and nontectonic environmentals factors [1],[4]. Also, groundwater dynamics must be taken into account to discriminate the radon variations related with Darcian groundwater velocity.

Then, we have scheduled another monitoring activity with radiocarbon and tritium analysis by liquid scintillation spectrometry to better define the hydrological properties of the Gran Sasso aquifer and radon variations source(s).

2 Radiocarbon analysis with liquid scintillation spectrometry

The 1220 Quantulus^{TM} ultra low background liquid scintillation spectrometer setup started in 1999 with radiocarbon measurements performed at underground laboratory of Gran Sasso and the Radiocarbon Laboratory of ENEA-Bologna to study the efficiency and background variations related to measurements sites has been completed [5].

For the background two sets of three teflon vials with benzene volumes ranging from 1 ml to 5 ml filled with pure analytical benzene were used. For the modern standards two sets of three teflon vials with the same benzene volumes filled with pure analytical benzene enriched with radiocarbon to give the same activity as the standard sucrose ANU (sucrose ANU/modern=1.0866) were used. The scintillation cocktail comprised 15 mg butyl-PBD / ml benzene [6]. For each of these standards, spectra were obtained for forty one hour periods [7].

The count rate of the two sets (A, B) of teflon vials with benzene volumes of 1, 3 and 5 ml related to surface and underground laboratories is shown in tables 1 and 2. The data are related to optimized soft window in channels 5-540 and PAC equal to 200. Also the modern activity, the efficiency (Eff), the figure of merit (FM), the factor of merit for radiocarbon dating (fM) and the maximum determinable age (Tmax) for a 2σ detection criterion and a counting time of 4742 minutes are shown in tables 1 and 2.

Sample	Count rate cpm	Count error cpm	Modern activity dpm	Modern activity error dpm	Eff %	FM	fM	T_{max} BP
L1A	**0.278**	**0.022**						
H1A	**12.949**	**0.148**	**8.853**	**0.088**	**80.93**	**25531.503**	**17**	**48200**
L1A	***0.059***	***0.010***						
H1A	***12.282***	***0.144***	***8.540***	***0.094***	***76.76***	***99734.000***	***35***	***54000***
L3A	**0.398**	**0.026**						
H3A	**39.140**	**0.257**	**27.068**	**0.161**	**83.28**	**17419.104**	**43**	**55900**
L3A	***0.150***	***0.016***						
H3A	***38.235***	***0.254***	***26.609***	***0.166***	***81.35***	***44052.587***	***69***	***59600***
L5A	**0.655**	**0.033**						
H5A	**65.206**	**0.332**	**45.101**	**0.209**	**83.60**	**10676.865**	**57**	**58000**
L5A	***0.235***	***0.020***						
H5A	***63.874***	***0.328***	***44.464***	***0.215***	***81.89***	***28580.867***	***92***	***61900***

table 1. The count rate of the set A of teflon vials with benzene volumes of 1, 3 and 5 ml related to surface (bold) and underground (bold italic) laboratories. The labels L and H indicate background and modern standards, respectively.

Sample	Count rate cpm	Count error cpm	Modern activity dpm	Modern activity error dpm	Eff %	FM	fM	T_{max} BP
L1B	**0.273**	**0.021**						
H1B	**12.646**	**0.146**	**8.645**	**0.087**	**79.03**	**22856.284**	**17**	**48100**
L1B	***0.096***	***0.013***						
H1B	***12.020***	***0.142***	***8.331***	***0.090***	***75.13***	***58659.673***	***27***	***51900***
L3B	**0.442**	**0.027**						
H3B	**38.463**	**0.255**	**25.565**	**0.159**	**81.84**	**15152.806**	**40**	**55300**
L3B	***0.157***	***0.016***						
H3B	***38.181***	***0.254***	***26.567***	***0.166***	***81.24***	***42038.809***	***67***	***59400***
L5B	**0.590**	**0.032**						
H5B	**64.470**	**0.330**	**44.628**	**0.208**	**82.65**	**11570.346**	**59**	**58300**
L5B	***0.230***	***0.020***						
H5B	***64.176***	***0.329***	***44.678***	***0.216***	***82.28***	***29488.245***	***94***	***62100***

table 2. The count rate of the set B of teflon vials with benzene volumes of 1, 3 and 5 ml related to surface (bold) and underground (bold italic) laboratories. The labels L and H indicate background and modern standards, respectively.

The guard count rate which is in anticoincidence and coincidence with coincident sample events recorded at surface and underground laboratories is shown in figures 1 and 2 respectively [7].

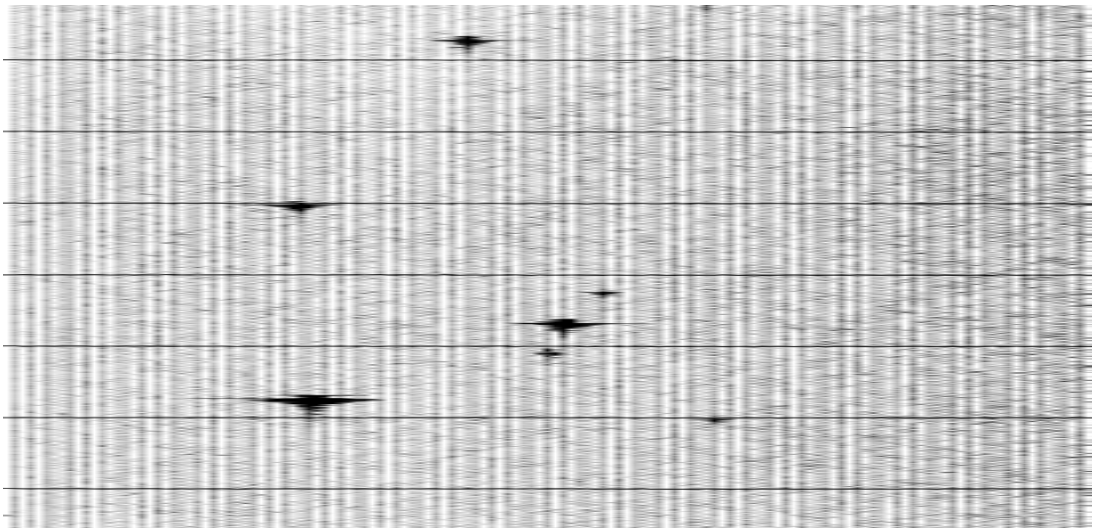

fig. 1. The guard count rate which is in anticoincidence with coincident sample events recorded at surface (a) and underground (b) laboratories.

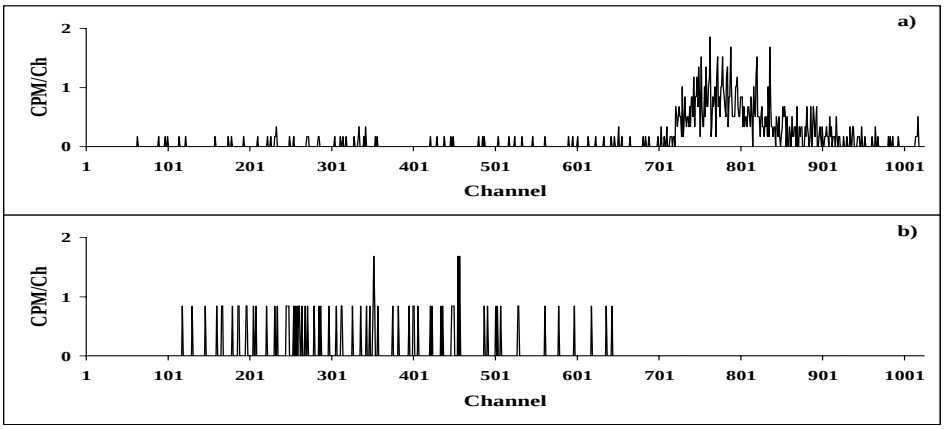

fig. 2. The guard count rate which is in coincidence with coincident sample events recorded at surface (a) and underground (b) laboratories. To a better graphical representation the CPM/Ch of surface (a) and underground (b) laboratories are multiplied by factors 10^1 and 10^3 respectively.

From the spectra shown in figure 1 may be observed that the cosmic muon flux is missing at underground laboratory (0.071 cpm) compared to surface one (414 cpm). The anticoincident Compton continuum spectrum shows 669 and 161 cpm at surface and underground laboratories, respectively. This part of guard spectrum reflects the flux of the environmental gamma photons and secondary cosmic particles. The remaining Compton signal in Gran Sasso is from the guard phototubes which are fully embedded in the scintillating cocktail filling the guard. The guard count rate which is in coincidence with coincident sample events shows at surface laboratory a cosmic muon flux of 10.9 cpm and Compton continuum spectrum shows 1.06 cpm while at underground laboratory we have recorded 0.0 cpm and 0.063 cpm, respectively. The coincident guard events are active background reducing events. The data indicates a background reduction of approximately 65% at the underground laboratory compared to surface one, with no differences in the efficiency particularly for the 3 and 5 ml benzene volumes of set B. This background reduction results from the low environmental radiation flux in Gran Sasso [7].

3 Radon groundwater geochemistry

The trends of the geochemical parameters monitored during the period from May, 1996 to December, 2000 are shown in figure 3.

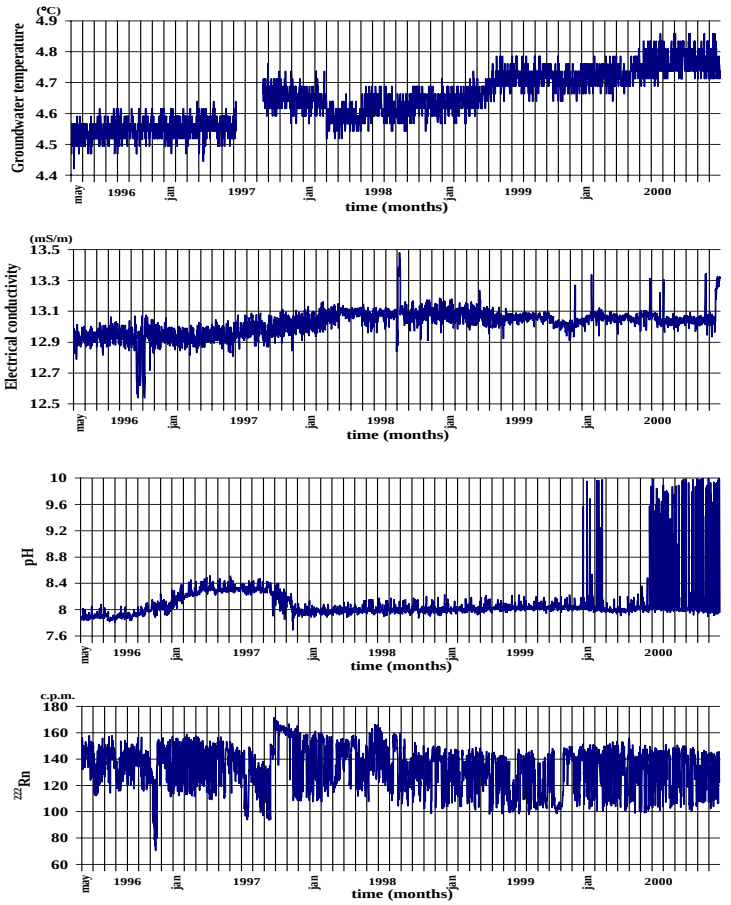

fig. 3. The trends of the geochemical parameters monitored during the period from May, 1996 to December, 2000.

The data of the groundwater temperature sensor from July, 1997 to September, 1997 are not supplied for the breakdown between the thermocouple output and the analogic input channel.

The time series analysis shown strong *anomalies* in pH, radon and pressure of solved gases highly correlate with the Umbria-Marche seismic sequence (1997-1998) and due to the occurrence of transient compression phase producing a change of the carbon dioxide content in groundwater. Also, electrical conductivity spike-like *anomalies* correlates with local seismic events emphasizing variations in groundwater dynamics [2].

In particular, during the period from January, 2000 to February, 2000 and from July, 2000 till now pH *anomalies* have been point out. This phenomenology is probably due to mixing of groundwater through the tectonic discontinuities which separate dolomitic limestones from sileceous limestones emphasizing a local deformation process. Also, electrical conductivity spike-like *anomalies* have been point out during the above mentioned periods and a long term variation started 15^{th} December, 2000 is still active. The ground-

water temperature shown during the period from June, 1998 to December, 2000 a rise trend with a maximum excursion of 0.2°C .

The trends of the setting parameters monitored during the period from May, 1996 to December, 2000 are shown in figure 4.

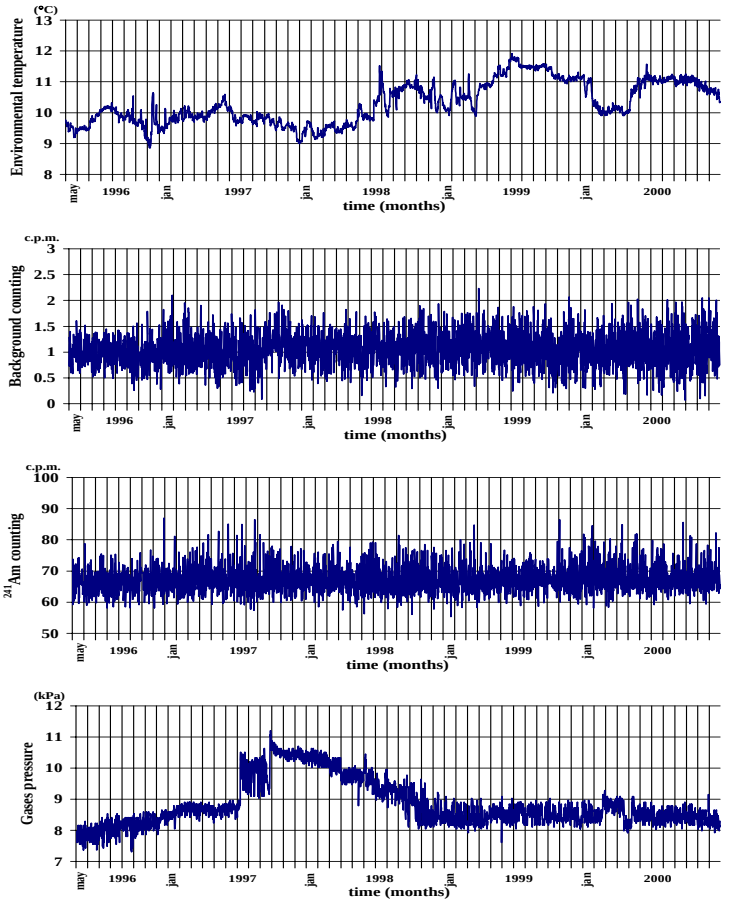

fig. 4. The trends of the setting parameters monitored during the period from May, 1996 to December, 2000.

An autoregeressive linear model to describe the residual time series normalized to zero mean and unit variance and estimate the occurence probability of hydrogeochemical *anomalies* is selected [2],[8].

The ε Dobrovolsky's parameter [9] is computed by means of the seismic events of INGV (National Institute for Geophysics and Volcanology) catalogue recorded within a distance of 100 km from the measurement site and available from May, 1996 to December, 2000 [10]. We have considered an inferior limit of ε equal to $0.1 \cdot 10^{-8}$.

The residual time series of the electrical conductivity, pH, ^{222}Rn and ε Dobrovolsky's parameter during the above mentioned period are shown in figure 5.

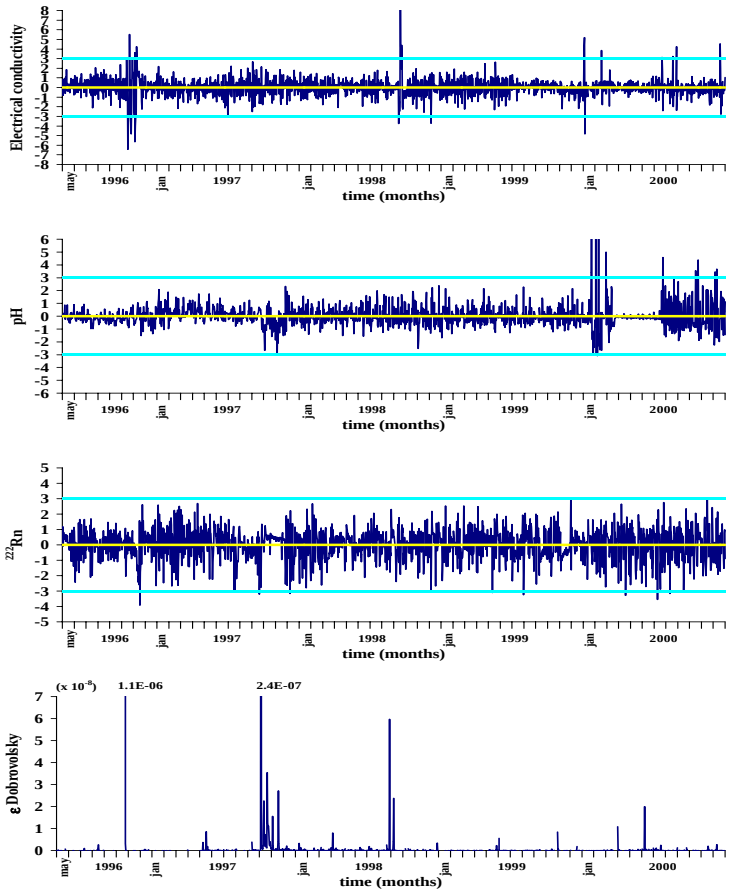

fig. 5. The residual time series of electrical conductivity, pH, ^{222}Rn and ε Dobrovolsky's parameter during the period from May, 1996 to December, 2000.

Using the εDobrovolsky's parameter two seismic sequence probably related to detected *anomalies* have been identified: a) 11^{st} March, 2000, M_D=4.3, d=56 km; b) 17^{th} May, 2000, M_D=2.6, d=6.4 km. Also, the occurrence probability of the *anomalies* during the period from May, 1996 to December, 1999 have been justified [2].

4 Conclusion

The measurements carried out between surface and underground laboratories with the ultra low background liquid scintillation spectrometers have emphasized a background reduction of 65% at underground laboratory. Then, the characteristics of the underground laboratory of Gran Sasso makes it possible to perform high precision radiocarbon measurements and to improve fM by 60% and to extend the dating limit from 58000 to 62000

BP (5 ml-3 days counting).

During the last year, the time series analysis of the geochemical parameters has emphasized *anomalies* in pH and electrical conductivity probably related to mixing of the groundwater through mylonitized faults. The occurrence of this new phenomenology may be justified by local deformation process producing rock permeability variations. Actually, the above mentioned *anomalies* have being recorded.

Acknwoledgments The authors wish to thank Prof. Alessandro Bettini for the his kind collaboration and the Dr. Raffaele Adinolfi Falcone, Dr. Alfredo Fulgenzi, Mr. Massimiliano De Deo, Mr. Nicola Massimiani, Mr. Nando Polidoro, Mr. Fabrizio Torelli of the LNGS and Mr. Fabio Basti, Mr. Antonio Miriametro of the University of Rome "La Sapienza" for the useful and precious assistance. The authors are grateful to Dr. Rita Di Giovambattista for the seismological data and Dr. Domenico Giambuzzi and Mr. Maurizio Faragalli of the Azienda Speciale Acquedotto del Ruzzo for tha data provided.

References

[1] Plastino, W. and Bella, F., *Radon groundwater monitoring at underground laboratories of Gran Sasso (Italy)*, submitted to Geophysical Research Letters.

[2] Bella, F. and Plastino, W., 1999, *Radon time series analysis at LNGS, I*, LNGS Annual Report 1999, INFN, 193-198.

[3] Hauksson, E., 1981, *Radon content of groundwater as an earthquake precursor: evaluation of worldwide data and physical basis*, J. Geophys. Res., 86, 9397-9410.

[4] Shapiro, M.H., Rice, A., Mendenhall, M.H., Melvin, D. and T.A. Tombrello, 1984/1985, *Recognition of environmentally caused variations in radon time series*, Pure and Appl. Geophys., 122, 309-326.

[5] Bella, F., Bartolomei, P. and Plastino, W., 1999, *Radiocarbon measurements by liquid scintillation spectrometry*, LNGS Annual Report 1999, INFN, 204-207.

[6] Gupta, S.K. and Polach, H.A., 1985, *Radiocarbon Dating Practices at ANU*, Canberra, Radiocarbon Laboratory, Research School of Pacific Studies, ANU: 72-75.

[7] Plastino, W., Kaihola, L., Bartolomei, P. and Bella, F., *Cosmic background reduction in the radiocarbon measurements by liquid scintillation spectrometry at the underground laboratory of Gran Sasso*, Radiocarbon, in press.

[8] Box, G.E.P. and Jenkins, G.M., 1976, *Time series analysis forecasting and control*, Holden Day, Oakland, California.

[9] Dobrovolsky, I.P., Zubkov, S.I and Miachkin, 1979, *Estimation of the size of earthquake preparation zones*, Pure and Appl. Geophys., 117, 1025-1044.

[10] INGV, Istituto Nazionale di Geofisica e Vulcanologia, 1996-2000, *Seismological Bulletins*, Roma.

LNGS-EXP 20/99
Measurement of the Radon concentration in the water from the Gran Sasso fault

D. Barbaresi[a], A. Bassignani[b], G. Colombo[b], L. Degli Esposti[a], R. Fresca Fantoni[b], G. Giacomelli[a], G. Maltoni[a], G. Mandrioli[a], F. Materazzi[b], L. Patrizii[a] and G. Sirri[a]

[a] Dipartimento di Fisica dell'Università di Bologna and INFN, Bologna
[b] Eni S.p.A. Agip Division, Radiation Protection Department, San Donato Milanese

Abstract

Since 1999 the groundwater Rn concentration has been monitored near the fault in the interferometric tunnel of the underground Gran Sasso Laboratory. The main goal of the experiment is the search for possible correlations between changes of radon in water and earthquakes.

Water is directly collected from the fractured rock and radon gas is extracted by nitrogen bubbling from samples of water. The detector is a silver activated zinc sulfide scintillator located in an electrostatic chamber. The apparatus is remotely controlled via Internet; tests and measurements may be displayed on web pages.

1 Introduction

Radon contents in groundwaters and in air are being monitored by several experiments with the aim of studying possible correlations between radon concentration variations and seismic phenomena [1-5].

We developed and implemented an automatic instrument for monitoring the radon concentration in groundwater. Since the middle of 1999 this apparatus is collecting test data in the interferometric tunnel of the underground Gran Sasso laboratory, near the fault. The fault is one of the most important features of the Gran Sasso Massif.

The apparatus may be considered to complement other instruments that are monitoring seismic activities in the underground laboratory: a geodetic interferometer [6], tiltmeters and the apparatus for groundwater analysis of the University of Roma Tre [7].

During year 2000 measurements with a sampling rate of 2 measurements per day were made.

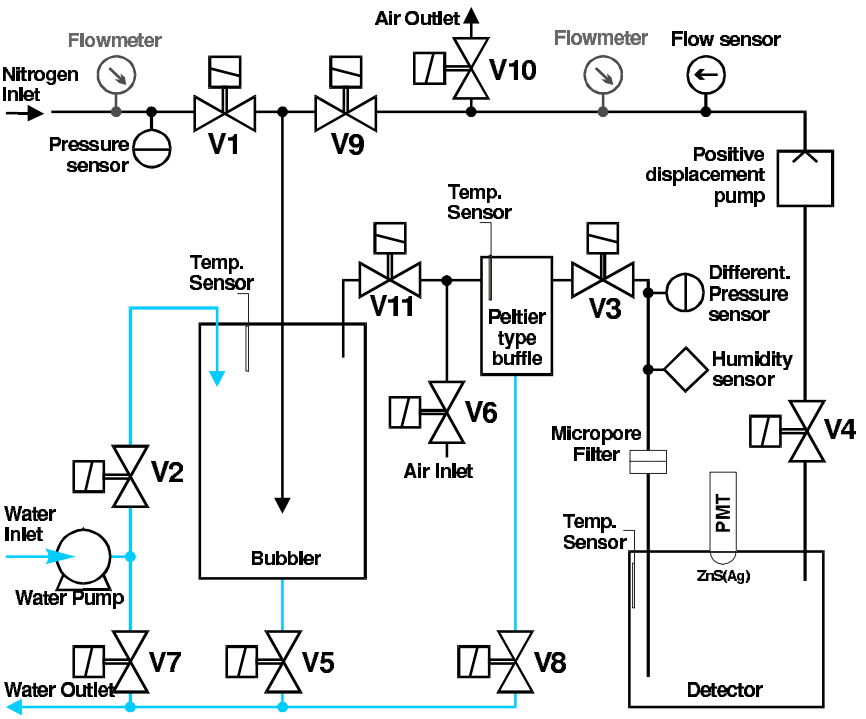

Figure 1: Layout of the radon extraction system.

2 The apparatus

The apparatus consists of three sections: the system for the extraction of radon from water, the detecting system and the data acquisition and control system.

2.1 Radon extraction system

The layout of the extraction system is shown in Fig. 1.

The process starts by flushing the radon extraction system with nitrogen gas (at this time the valves V1, V11, V3, V4, V10 are opened); immediately after background counting begins. Then a sample of 1.9 liters of water collected directly from the rock fault is pumped into the bubbler.

Radon gas is then extracted from water by nitrogen bubbling. The bubbling circuit includes the bubbler, the drying system, the detector chamber, the air flow sensor, the air pump and the valves V3, V4, V9, V11.

After radon extraction all the valves are closed and radon counting starts. At the end of each counting run, the water is pumped out, and the process restarts.

2.2 Detection system

The detector is a Pylon mod. PMT-EL, which is a silver activated zinc sulfide scintillator ZnS(Ag) located in a 5 litre electrostatic chamber.

The scintillator is covered by an aluminized mylar foil that acts as cathode of the

electrostatic chamber and collects the positively charged radon daughters. A power supply polarizes the chamber creating a potential difference of about 1000 Volts.

^{222}Rn in the nitrogen gas pumped inside the detector decays in ^{218}Po and is attracted to the negatively charged aluminium cathode. ^{218}Po decays in ^{214}Bi , which in turn decays in ^{214}Pb and then in ^{214}Po with the following half-lives ($t_{1/2}$):

$$\underset{}{^{222}\mathrm{Rn}} \overset{\alpha}{\Longrightarrow} \underset{3.82\ \mathrm{d}}{^{218}\mathrm{Po}} \overset{\alpha}{\Longrightarrow} \underset{3.05\ \mathrm{min}}{^{214}\mathrm{Pb}} \overset{\beta}{\longrightarrow} \underset{26.8\ \mathrm{min}}{^{214}\mathrm{Bi}} \overset{\beta}{\longrightarrow} \underset{19.7\ \mathrm{min}}{^{214}\mathrm{Po}} \overset{\alpha}{\Longrightarrow} \underset{164\ \mu\mathrm{s}}{^{210}\mathrm{Pb}}$$

^{222}Rn , ^{218}Po and ^{214}Po emit alpha particles and a fraction of these particles impacts the scintillator producing light pulses that are transmitted through the light pipe to the photomultiplier (PMT).

2.3 Data acquisition system

Control processes and data acquisition are performed by a PC with a Pentium processor and two I/O interface boards. The temperatures of the devices, the pressure and air flow in the circuit, the water level and the environmental temperature and pressure are monitored. The computer is remotely controlled via Internet; the tests and the measurements may be displayed on web pages.

3 Results

An example of background measurements and of radon concentration measurements performed over a 12 hour period are shown in Fig. 2.

A plot of the radon concentration and of the background in the period July-Dec 2000 is shown in Fig. 3.

4 Conclusions

An apparatus for monitoring radon concentration in the water from the Gran Sasso fault has been designed and implemented. The extraction technique and the detector system allow to have a good reproducibility and good count ratio between radon and background.

Several improvements are in progress. In order to improve the stability of radon extraction and of the detection efficiency, a new air-conditioning system has been installed in the hut. A new system for collecting water is being designed in order to minimize radon exchange phenomena between air and water. Finally monitoring of other important parameters such as pH and electric conductivity of the water are being implemented.

References

[1] M. Noguchi and H. Wakita, A method for Continous Measurement of Radon in Groundwater for Earthquake Prediction, Jou. Geoph. Res. 82 (1977) 1353.

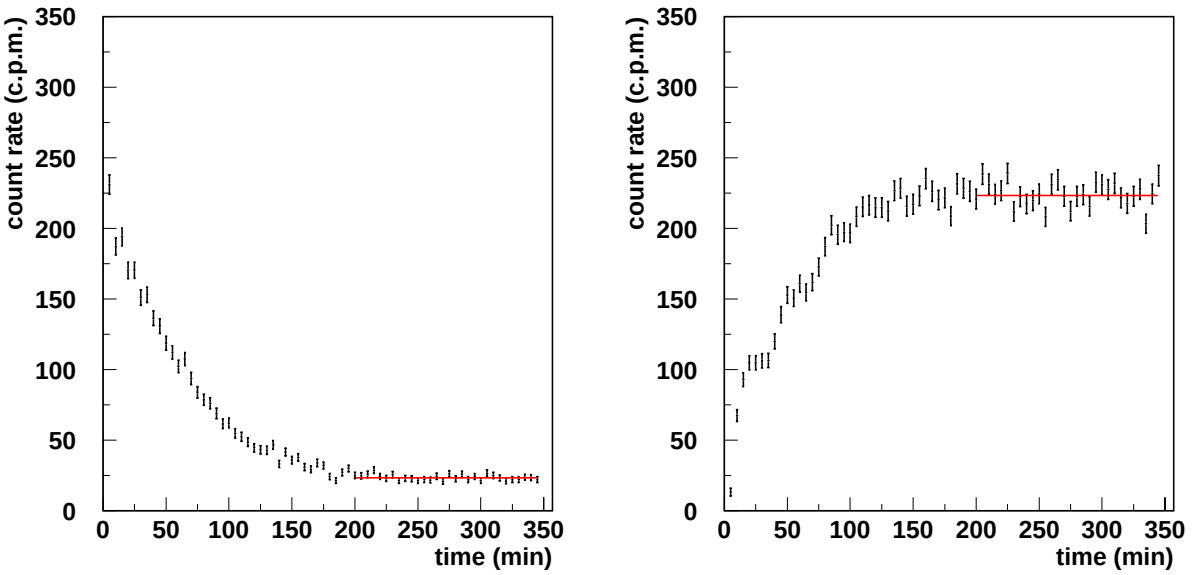

(a) (b)

Figure 2: Example of a measurement of the background (a) and of the radon concentration (b). Final counting rates may be obtained from a fit of the data over 300 minutes or simply by taking the average rates from 180' to 350', as indicated by the solid lines.

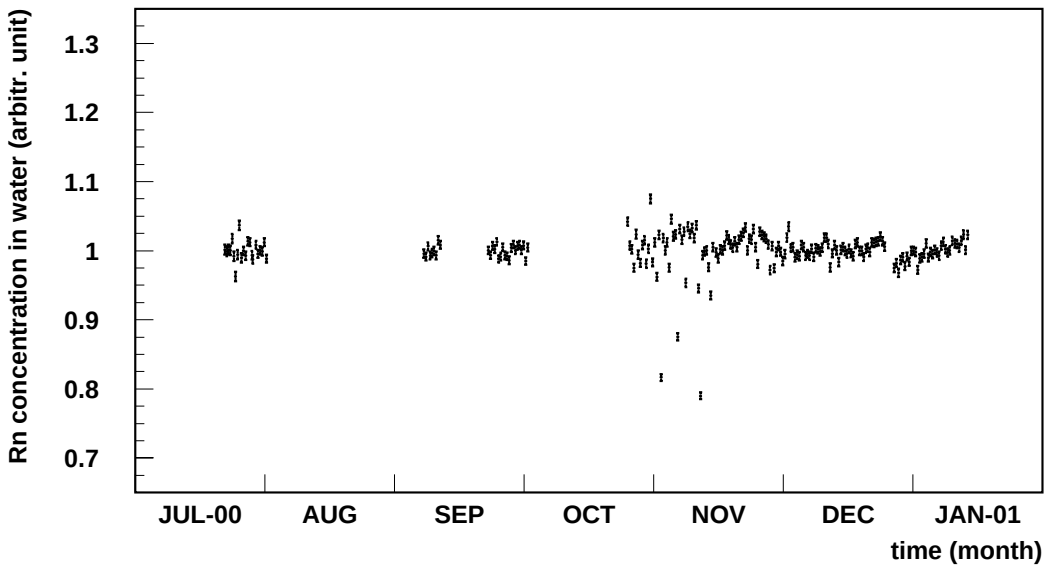

Figure 3: Corrected radon measurements made during the period July 2000 - Jan 2001.

[2] Chi-Yu King, Radon monitoring for Earthquake Prediction in China, Earthq. Predict. Res. 3 (1985) 47.

[3] A.A. Qureshi et al., Radon measurements for use in earthquake prediction and location of geological faults in Pakistan, Proc. of 2nd Workshop on Radon Monitoring in Radioprotection, Trieste (1991) 532.

[4] N. Matsumoto, Regression Analysis for anomalous changes of ground water level due to earthquakes, Geoph. Res. Lett. 19 (1992) 1193.

[5] U. Facchini et al. , Study on Radon Emission in a fault located in the Bergamasc Prealps, Atti Colloquio scientifico sulla protezione sismica (1993).

[6] A. Amoruso et al., GIGS, the Geophysical Interferometer at Gran Sasso, LNGS Annual Report 1997 and 1998.

[7] F. Bella et al., Tectonic deformation events and local seismicity in the Gran Sasso area of the Central Apennines, LNGS Annual Report 1997 and 1998.

For more references, see:

[8] M.M. Monnin and J.L. Seidel, Physical models related to radon emission in connection with dynamic manifestations in the upper terrestrial crust: a review, Radiation Measurements 28 (1997) 703.

[9] M. Singh et al. , Radon in ground water related to seismic events, Radiation Measurements 30 (1999) 465.

PULEX-2
Biological Experiment

F. Amicarelli[d], F. Antonelli[a], C. Ara[d], M. Balata[e], M. Belli[a,c], M.P. Cerú[d], S. Colafarina[d], L. Conti Devirgliis[d], A. De Marco[d], A. Falgiani[e], S. Nisi[e], O. Sapora[b,c], L. Satta[f], G. Simone[a,c], E. Sorrentino[a,c], M.A. Tabocchini[a,c]

[a] Physics Laboratory, Istituto Superiore di Sanità
[b] Comparative Toxicology and Ecotoxycology Laboratory, Istituto Superiore di Sanità
[c] INFN-Gr.coll.Sanità
[d] Department of Basic and Applied Biology, L'Aquila University
[e] Service of Chemistry,
Cryogenic and Chemical plants of the INFN-Gran Sasso National Laboratory
[f] Energetics Department, Rome University "La Sapienza"

Abstract

The PULEX-2 experiment represents an interdisciplinary research that exploit the unique opportunity offered by the Gran Sasso National Laboratory of a well equipped low background radiation environment. Mammalian cells were cultured in parallel at the LNGS underground Laboratory, where a cell culture facility has been especially set up, and at the Istituto Superiore di Sanità, in the presence of standard radiation background. Both cultures were periodically tested to check for the onset of metabolic changes and different sensitivity to genotoxic damage caused by ionizing and UV radiation, as well as by chemical agents. These tests include measurements of enzyme activities protecting from oxidative cell damage, induction of apoptosis and mutation. After about 600 generations the first phase of the experiment is completed and we report on the preliminary results.

1 Introduction

The Gran Sasso National Laboratory (LNGS) which is an excellent shielding against cosmic rays and neutrons, offers a unique opportunity for investigating the effects of a low background radiation environment on living organisms.
It is well known that the background radiation represents an important factor involved in biological evolution. Natural selection has promoted the development and the maintenance of biochemical/biological defense mechanisms against damage by radiation as well

as other genotoxic agents. In the last fifteen years adaptive response has been reported for different organisms and different biological end-points showing that cells pre-exposed to low doses of radiation or chemical mutagenic agents can acquire resistance to subsequent exposure to moderate or high doses of the same agents [1]. In this framework, scarce data concern the adaptive effects after "cronic" exposure to very low doses and low dose rates such as those given by the natural radiation background.
The interest in this kind of studies is twofold: for a better understanding of the basic mechanisms involved in the radio-adaptive response and for their relevance in radiation protection. For the latter purpose, the present regulations are based on the so-called linear-no-threshold theory, implying the additivity of the effects due to the exposures taken during the life span. The adaptive response casts doubts on the validity of such a model implying a non-linear dose-response relationship.
Few years ago a first experiment (PULEX) performed on yeast cells cultured in the underground laboratory of the LNGS indicated that cells grown in a low background environment are less protected from DNA damage induced by methyl-methane sulfonate than cells grown in a "standard" environment, such that found at the Rome University [2]. At the present, a new experiment (PULEX-2) performed in the framework of a collaboration among LNGS, Università di Roma, Università dell' Aquila and Istituto Superiore di Sanità, is in progress to extend the previous observations to cultured mammalian cells. This time the "standard" environment was that found at the Physics Laboratory of the Istituto Superiore di Sanita', were the reference culture was maintained.
In the year 2000, after about 9 months of cell conditioning, corresponding to about 600 generations, the exploratory phase of the experiment has been completed. It has proven doable, and the experimental procedure has been defined. At the end of this period there is a pool of cells frozen in liquid nitrogen at different conditioning times. These cells are kept either to perform new tests on the onset of adaptive response, or to verify already obtained results.

2 Materials and Methods

A cell culture laboratory has been set up at the LNGS, in the gallery connecting the main experimental halls for underground physics (low background radiation).
This laboratory is arranged in a new barrack of 240cm $\times$ 700cm $\times$ 260cm(high) dimensions. The barrack is equipped with all the basic uses (electrical power, water, telephone, heating, etc).
A laminar flow hood for biologic purposes, an incubator with CO_2 atmosphere (placed in a metallic shield: further protection against radioactive background), a microscope, a cryogenic dewar for keeping the cells and some other minor devices are the equipment being used for performing the underground activities of the experiment. In the barrack another shielding container is available in case it were desired to use an additional incubator.
A ventilation piping supplies continuously fresh air in the room, so that the radon level is kept always at its minimum level. This underground laboratory was set up with the financial and manpower support of the LNGS.

The background radiation has been continuously monitored, in the LNGS and in the ISS. The fluence ratios between low and standard background radiation environments are 10^{-6} for cosmic rays and 10^{-3} for neutrons. For the low energy gamma ray dose, measured with Harshaw calcium fluoride thermoluminescent dosimeters, the ratio is $5x10^{-2}$. Furthermore a radon measuring instrument records the radon concentration in the laboratory as a function of time. The radon concentration is about one order of magnitude lower in the LNGS then in the ISS.
V79 Chinese hamster fibroblasts were grown in E-MEM medium supplemented with antibiotics and foetal calf serum [3]. To minimise the sources of variability, all reagents and chemicals used throughout the entire experiment were from the same batches.
Measurements of enzyme activities [4], apoptosis [5], gene expression [6] and mutation induction [3] were periodically performed on both cultures.

3 Results and Discussion

The aim of the experiment was to investigate if the environmental radiation background might contribute to the maintenance or induction of mechanisms involved either in protection or in repair against the induction of DNA damage or in the expression of gene(s) known to be involved in apoptosis (programmed cell death). To this purpose, V79 cells deriving from the same culture, were grown in parallel at the ISS (standard background radiation) and at the LNGS (low background radiation), and periodically tested to check for the onset of changes in enzyme activities protecting from oxidative cell damage and for different sensitivity to genotoxic agents.

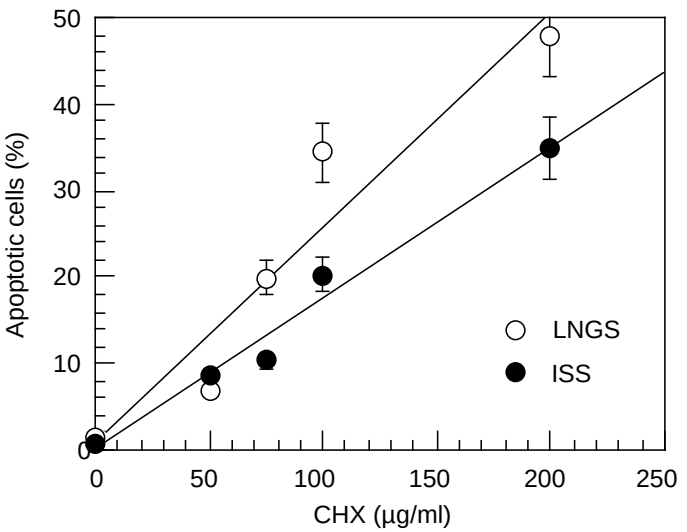

Figure 1: Apoptotic activity as a function of CHX concentration after 9 month conditioning in low/standard background radiation.

Measurements of enzyme activities were performed for superoxide dismutase (SOD),

catalase (CAT), Se-dependent and independent glutathione peroxidase, reductase and transferase (GSH-PX, GSSG-RX, GST).
Cell response to genotoxic damage was studied after treatment with chemical and physical agents. Cycloheximide, a protein synthesis inhibitor, was used to induce apoptosis and for monitoring the expression of p53 and c-myc genes.
Gamma rays and UV radiation, that induce different types of DNA damage, were used for studying mutation induction at the X-linked hypoxantine-guanine phosphorybosil transferase locus (hprt).
The results obtained show that after about 600 generations conditioning in low/standard background radiation environment some changes occur for the activities of some tested enzymes (CAT and GSSG-RX).
Moreover, cells grown in low radiation environment show an increased apoptotic activity after induction with cycloheximide compared to those grown in standard radiation environment (Fig.1). With regard to the expression of c-myc and p53 genes, it seems to be decreased after CHX treatment although it is not dose-dependent and appears similar in both cell cultures. On the other hand, the basal level in the control is slightly reduced in cells cultured at the LNGS (low background radiation).

For hprt mutation, cells cultured in the low radiation environment seem to be more

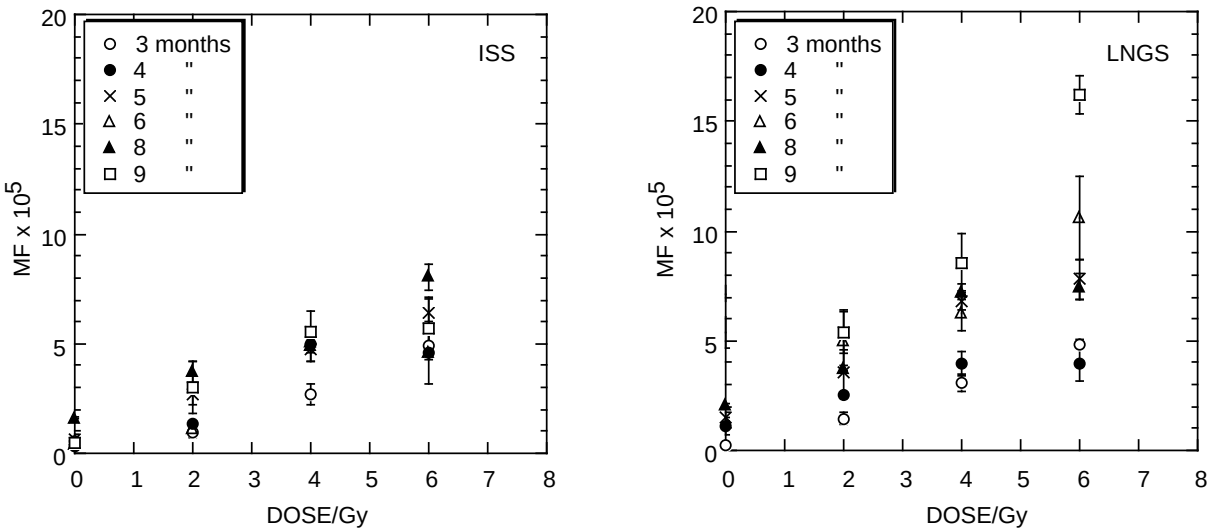

Figure 2: hprt mutation frequency after gamma irradiation of V79 cells grown in low/standard background radiation for different conditioning time.

sensitive to mutation induction (Fig.2).
These results suggest that a significant reduction in the background exposure can affect the susceptibility to acute exposures of genotoxic agents.

4 List of Publications

1. F.Antonelli, M.Belli, O.Sapora, G.Simone, E.Sorrentino, M.A.Tabocchini, F.Amicarelli, C.Ara, M.P.Cerú, S.Colafarina, L.Conti-Devirgiliis, A.De Marco, B.Pruiti, M.Balata, A.Falgian, S.Nisi, L.Satta. Radiation biophysics at the Gran Sasso Laboratory: influence of a low background radiation environment on the adaptive response of living cells. 6th International Workshop on Topics in Astroparticle and Underground Physics (TAUP), Paris, France, September 6-10, 1999. Nuclear Physics (in press)

2. F. Antonelli, M. Belli, G. Simone, E. Sorrentino, M.A. Tabocchini, O. Sapora, L. Conti Devirgiliis, M.P. Cerú, F. Amicarelli, C. Ara, B. Pruiti, M. Balata, A. Falgiani, S. Nisi, L. Satta. Influence of a low background radiation environment on the cell response to physical and chemical agents: the Pulex-2 experiment at the LNGS. VII Congresso Annuale della Società Italiana di Mutagenesi Ambientale (SIMA), Cortona, 6 - 8 ottobre 1999

3. F. Antonelli, M. Belli, G. Simone, E. Sorrentino, M.A. Tabocchini, O. Sapora, L. Conti Devirgiliis, M.P. Ceru, F. Amicarelli, C. Ara, S.Colafarina, M. Balata, A. Falgiani, S. Nisi, L. Satta. Influenza del basso fondo di radiazione sulla risposta cellulare ad agenti fisici e chimici: la risposta adattativa delle cellule viventi. X Convegno Nazionale della Societá Italiana per le Ricerche sulle Radiazioni (SIRR), Frascati, 19-22 novembre 2000

References

[1] United Nations Scientific Committee on the Effects of Atomic Radiation, Sources and Effects of Ionizing Radiation, Annex B. Adaptive responses to radiation in cells and organisms, UNSCEAR 1994.

[2] L. Satta et al., Mut. Res., 347 (1995) 129

[3] M. Belli et al., Int. J. Rad. Biol., 74 (1998) 501

[4] F.Amicarelli et al., BBA, Mol. Basis Dis., 1453/1 (1999) 105

[5] E.B. Thompson, Ann. Rev. Physiol., 60 (1998) 575

[6] J. Galea-Lauri, J. Immunol., 157 (1996) 4109